# The Metabolic Fate and Bioactivity of Anthocyanins in Humans

A Thesis Presented to

**Norwich Medical School**

**University of East Anglia**

In Fulfilment of the Requirements for the Degree of

**Doctor of Philosophy**

By

**Rachel M. de Ferrars**

(B.Sc. Hons)

May 2014

*© This copy of the thesis has been supplied on condition that anyone who consults it is understood to recognise that its copyright rests with the author and that use of any information derived there from must be in accordance with current UK Copyright Law. In addition, any quotation or extract must include full attribution.*

Rachel M. de Ferrars © 2014

# Abstract

The Metabolic Fate and Bioactivity of Anthocyanins in Humans

Rachel M. de Ferrars

Anthocyanins, the class of flavonoid responsible for giving a red hue to many berries, have been associated with a decreased risk of cardiovascular disease. However, numerous intervention studies feeding anthocyanin-rich foods report limited (<1%) bioavailability of the parent anthocyanins *in vivo*. Due to the instability of anthocyanins at neutral pH, it is postulated that degradation products and metabolites of anthocyanins may be responsible for the perceived bioactive effects. The aims of the present thesis were: (1) To model and establish analytical methods for the extraction and quantification of putative anthocyanin metabolites in urine, serum and faecal samples. (2) To identify and explore the pharmacokinetics of anthocyanin metabolites via the analysis of urine, serum and faecal samples from two human interventions, feeding either (a) 500 mg of isotopically ($^{13}C_5$) labelled anthocyanin or (b) 500 mg elderberry anthocyanins for 12 wks. (3) To explore the impact of acute (500 mg) versus chronic (500 mg/day for 12 wks) anthocyanin consumption on their metabolism and (4) To investigate the anti-inflammatory activity of six anthocyanin metabolites at physiologically relevant concentrations (0.01 µM to 10 µM) using human umbilical vein endothelial cells (HUVECs). Following the consumption of 500 mg elderberry anthocyanins, 28 anthocyanin metabolites were identified in urine and 21 in plasma, with the phenolic metabolites within plasma identified at 45 fold higher levels than their parent compounds. Similar results were observed within the $^{13}$C-labelled anthocyanin intervention, where 17 $^{13}$C-labelled compounds were identified in serum and 31 in urine. However, chronic consumption of anthocyanins had no impact on the formation of the metabolites. The cardiovascular bioactivity of anthocyanins may be linked to the anti-inflammatory activity of their metabolites. IL-6 and VCAM-1 are cytokines and adhesion molecules integral to the initiation and progression of inflammation. *In vitro,* anthocyanin metabolites reduced CD40L and TNF-α stimulated expression of the inflammatory markers, sVCAM-1 and IL-6, indicating that the anti-inflammatory effects of anthocyanins are likely attributed to their metabolites. In conclusion, the present thesis provides a new understanding into the metabolism and bioactivity of anthocyanins, which should provide an informative insight into how the consumption of higher intakes of anthocyanins may contribute to optimising human health.

# Table of Contents

# Table of Figures

# Table of Tables

# Acknowledgements

In writing my Ph.D. thesis, I have received support from many people, some of whom deserve a special mention. First, I would like to express my gratitude to my supervisors, Dr. Colin D. Kay and Professor Aedín Cassidy from whom I have learnt a lot in many ways. I especially thank Colin Kay, my primary supervisor, for his advice, feedback, encouragement and patience during all stages of the research process. I also thank my fellow colleagues, Hiren Amin, Michael Edwards and Charles Czank for their valuable input into this thesis, for the interesting debates concerning anthocyanins and for the many memorable moments and the other members of the Department of Nutrition in general, for their assistance and encouragement over the past three years. I would also like to thank my examiners, Professor Alan Crozier and Professor William Fraser for all their feedback and comments, which have been gratefully incorporated into the present thesis. Finally, I would like to thank my family in Cornwall and my boyfriend Frederick Wandschneider for their love and support throughout my studies,

# Chapter 1. Anthocyanins: Review of the scientific literature

## 1.1. Introduction

In recent years, polyphenols have become a major focus of many epidemiological and bioavailability studies. Initially the focal reason for this interest was the identification of their potential antioxidant properties. Whilst this concept is no longer accepted, evidence suggests they may have several properties, which make them potentially important compounds for the prevention of multiple diseases (cardiovascular, neurodegenerative, obesity and cancer) (Baur *et al.*, 2006; de Pascual-Teresa *et al.*, 2010; Feng *et al.*, 2007; Hooper *et al.*, 2008; Ramassamy, 2006; Vauzour *et al.*, 2008; Wallace, 2011). Polyphenols can be divided into three main groups: tannins, lignins and flavonoids. Flavonoids comprise the largest and most renowned division of polyphenols and consist of several thousand compounds, consumed as part of an everyday plant-rich diet. Flavonoids can be classified into six main subgroups based on the variation in their heterocyclic C-ring: anthocyanidins, flavan-3-ols, flavonols, flavones, flavanones and isoflavonoids (Hollman, 2004; Zamora-Ros *et al.*, 2010) (**Figure 1.1**)**.** The following review summarises the current literature pertaining to the metabolism, degradation, bioavailability and bioactivity of anthocyanidins, which in plants are found as glycosylated structures termed ‘anthocyanins’.

**Figure 1.1** General structures of common dietary flavonoids.

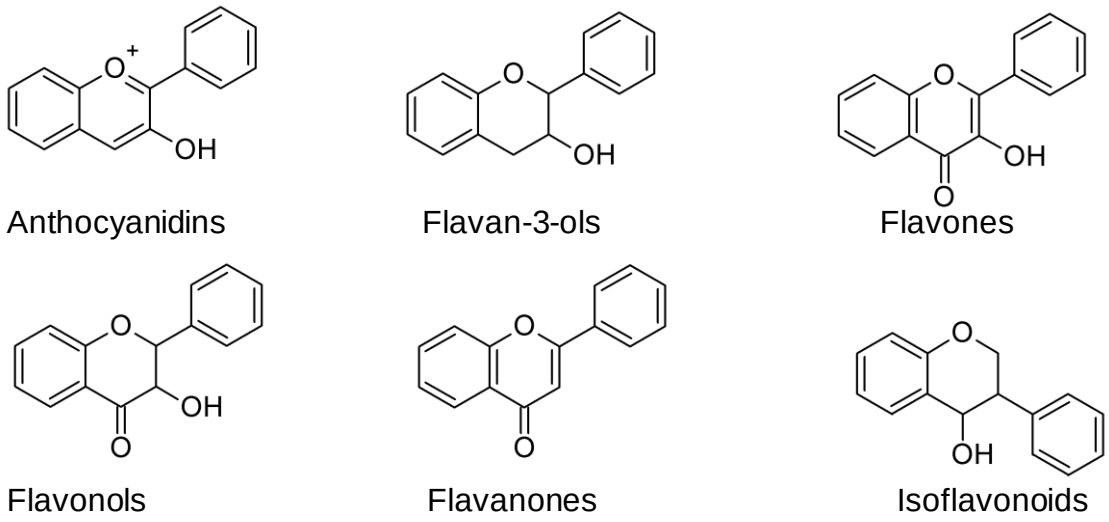


Adapted from (Hollman, 2004; Zamora-Ros *et al.*, 2010).

Anthocyanins (Greek; *anthos*=flower, *kyanos*=blue) are common water-soluble pigments, widely distributed in plant tissues, found in the leaves, flowers and fruits, and are partially responsible for giving many plants a characteristic red to purple hue (Chalker-Scott, 1999). Anthocyanins have a number of properties, which may produce health benefits. They have been shown to reduce risk factors of cardiovascular and inflammatory diseases (de Pascual-Teresa *et al.*, 2010; Hooper *et al.*, 2008; Wallace, 2011), neurodegenerative diseases such as Alzheimer's and Parkinson's disease and cognitive function (Tarozzi *et al.*, 2007), cancer (Feng *et al.*, 2007) and obesity (Sasaki *et al.*, 2007). For example, a 14 year follow-up study of 157,000 people, found an increase in anthocyanin intake from 6 mg/day to 19 mg/day was associated with an 8% reduction in the relative risk of hypertension (Cassidy *et al.*, 2011) and an increase in anthocyanin intake from 8 to 24 mg/day was associated with a 3 mm Hg reduction in central systolic blood pressure (Jennings *et al.*, 2012). The present work focuses on the bioactivity and the beneficial properties of anthocyanin metabolites against cardiovascular disease (CVD).

## 1.2. Anthocyanin chemistry

The basic structure of anthocyanins is based on the flavylium ion (2-phenylchromenylium) and consists of cationic oxygen-containing heterocycle pyran with a fused benzene ring. There are six predominant anthocyanidins (cyanidin, delphinidin, pelargonidin, peonidin, petunidin and malvidin) found in plants, which account for over 90% of the 625 anthocyanins currently identified (Wallace, 2011). Anthocyanins differ according to their types of glycosylation and acylation and the number and position of hydroxyl- and methoxy-groups on their B-ring (Wu *et al.*, 2006) (**Figure 1.2**). Glycosylation commonly occurs with glucose, galactose, rhamnose, arabinose and xylose, with anthocyanins most frequently forming 3-monosides, 3-biosides (disaccharides), 3-triosides and 3,5-diglycosides of these sugars (Castañeda-Ovando *et al.*, 2009; McGhieandWalton, 2007). Cyanidin-3-glucoside is the most common anthocyanin within the UK diet, with cyanidin accounting for 50% of anthocyanidins in fruit and vegetables (Figure 1.2). Anthocyanins have a maximum absorbance in the visible range, between 465 and 550 nm, with a second maxima between 270 and 280 nm.

## 1.3. Anthocyanins in plants

The synthesis of an anthocyanin from its precursors, 4-coumaroyl-CoA and malonyl-CoA, requires over seven enzymes and a monosaccharide molecule (Gould, 2004; Shirley, 1996). Anthocyanins play a vital role in a plant's survival. The red colour of anthocyanins plays a

role in attracting and repelling various animals, and can protect photosynthetic apparatus from photoinhibition resulting from overloading of the photosynthetic electron transport chain in strong light (Gould, 2004). Furthermore, the induction of anthocyanins in cold temperatures can reduce the risk of photo-oxidative damage to leaves as they senesce in autumn, which would otherwise decrease the efficiency of nutrient retrieval (Feild *et al.*, 2001). Similarly, a high anthocyanin content in leaves increases the osmotic potential, thereby delaying freezing to protect the leaf from a late frost, or minimising evapotranspiration to increase the plants hardiness to drought (Chalker-Scott, 1999).

**Figure 1.2** Structural identification of anthocyanidins and their approximate distribution in nature.

| Anthocyanidin | $R_1$ | $R_2$ | Distribution |
|---|---|---|---|
| Cyanidin | -OH | -H | 50% |
| Delphinidin | -OH | -OH | 12% |
| Pelargonidin | -H | -H | 12% |
| Peonidin | $-OCH_3$ | -H | 12% |
| Petunidin | -OH | $-OCH_3$ | 7% |
| Malvidin | $-OCH_3$ | $-OCH_3$ | 7% |

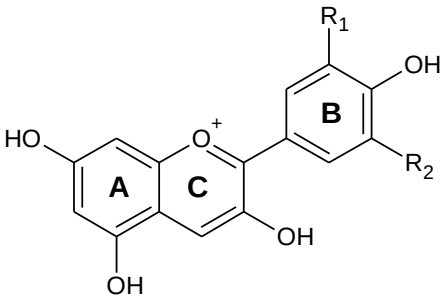


$R_1$ and $R_2$ represent functional groups. Adapted from (Castañeda-Ovando *et al.*, 2009; Wu *et al.*, 2006).

## 1.4. Dietary consumption of anthocyanins

Anthocyanins are naturally abundant constituents within our diets, regularly consumed in red vegetables and berries (Neveu *et al.*, 2010). Typical anthocyanin concentrations within berries range from 72 to 500 mg/100 g fresh fruit, but in some berries, can reach concentrations of 1300 mg/100 g fresh fruit (Neveu *et al.*, 2010) (**Table 1.1**). Anthocyanin content varies considerably between species and are highly dependent upon many factors such as environmental conditions, ripeness, cultivar, cultivation site, processing and storage (Del Rio *et al.*, 2010). Furthermore, anthocyanin intake varies considerably depending on socio-demographic and lifestyle factors (Chun *et al.*, 2007) and can range several-fold depending on individual dietary patterns (Burton-Freeman, 2010).

Estimates of habitual anthocyanin intake are poorly established, principally due to a lack of available data in food composition databases and variations of estimated intake between method of dietary assessment (Manach *et al.*, 2005). However, estimates range from 3 to 47 mg/day [3.1 mg/day, United States (Chun *et al.*, 2007); 12.5 mg/day, United States (Wu *et al.*, 2006); 18 mg/day, Spain (Zamora-Ros *et al.*, 2010) and 47 mg/day, Finland (Ovaskainen

*et al.*, 2008)]. In addition, large doses (> 500 mg) of anthocyanins can be obtained from single servings of some anthocyanin rich berries, vegetables and juices (Table 1.1).

**Table 1.1** Anthocyanin content within common foods.

| Food | Mean Content (mg) per 100 g FW | | | | | | |
|---|---|---|---|---|---|---|---|
| | **Cy** | **Pel** | **Peo** | **Del** | **Pet** | **Mal** | **Total** |
| Black elderberry | 1315 | 2 | - | - | - | - | 1317 |
| Blackberry | 173 | - | - | - | - | - | 173 |
| Blackcurrant | 187 | 2 | 1 | 392 | 10 | - | 592 |
| Highbush blueberry | 10 | - | 2 | 46 | 29 | 48 | 134 |
| Black grape | 1 | - | 6 | 3 | 3 | 59 | 72 |
| Strawberry | 5 | 68 | - | - | - | - | 73 |
| Red Onion | 3 | - | - | 7 | - | - | 9 |

Numbers represent total of all glycoslated forms of anthocyanins. Cy, cyanidin; Pel, pelargonidin; peo, peonidin; del, delphinidin; pet, petunidin; mal, malvidin. Data derived from (Neveu *et al.*, 2010).

## 1.5. Anthocyanin stability

Isolated anthocyanidins are unstable and are susceptible to factors including light, pH, temperature and oxygen (Fossen *et al.*, 1998). Anthocyanidins can form several different pH-dependent structural isoforms depending on the pH of the solution (Manach *et al.*, 2005). The pH dependent transformation of anthocyanidins can be observed through the dramatic colour change, which is caused by their unique positive charge and chromophore giving them their characteristic pH dependent colour. The relative abundance of each isoform at equilibrium varies with pH and the structure of the anthocyanidin (MazzaandBrouillard, 1987), however in general, the red-blue coloured flavylium cation is the predominate species at pH 1 (**Figure 1.3A**). As the pH increases to pH 2-4, the blue coloured quinoidal species can be observed (Figure 1.3B-D). At pH 5-6, a colourless carbinol pseudobase forms (Figure 1.3E) followed by a pale yellow chalcone (Figure 1.3F), and a highly reactive α-diketone, formed when the C-ring structure of the carbinol pseudobase opens (Fossen *et al.*, 1998).

Within plants, warm climates result in lower anthocyanin content. This is best observed within red wines, where hot regions, such as California, do not produce grapes containing the same anthocyanin content as those produced in cooler regions, due to decreased synthesis and increased catabolism of the anthocyanins at higher temperatures (Shaked-Sachray *et al.*, 2002). Within a laboratory setting, the temperature stability of anthocyanins is of importance as it can affect the identification and recovery of anthocyanins and the consistency of data during processing and storage. At constant pH, the degradation of

anthocyanins increases within increasing temperature (Kırca *et al.*, 2007; Patras *et al.*, 2010). This has been observed during sample processing, and during storage. For example, black carrot anthocyanins stored at pH 4.3 demonstrated a half-life of 71.8 weeks at 4 ºC, 4.1 weeks at 37 ºC, 17 h at 70 ºC and 4.5 h at 60 ºC (Kırca *et al.*, 2007).

The stability of glycosylated anthocyanins is greatly increased over anthocyanidin aglycones; in a degradation study, 100% loss in anthocyanidins aglycones was observed for samples stored in buffer at 37 °C, pH 7 for 2 h, in contrast, the anthocyanin glycosides demonstrated a loss of 20 to 100% over a 12 h period (Woodward *et al.*, 2009). The stability of anthocyanins is also influenced by their B-ring moieties; *in vitro* pelargonidin-3-glucoside, cyanidin-3-glucoside and delphinidin-3-glucoside demonstrated a loss of 20%, 40% and 100% respectively over 12 h (Woodward *et al.*, 2009). Therefore, whilst the presence of a sugar moiety infers increased stability, this is also influenced by the B-ring moieties, with the presence of additional hydroxyl and methoxy groups appearing to decrease the molecules stability (Fossen *et al.*, 1998; Woodward *et al.*, 2009).

**Figure 1.3** Anthocyanins pH dependent chemical structures.

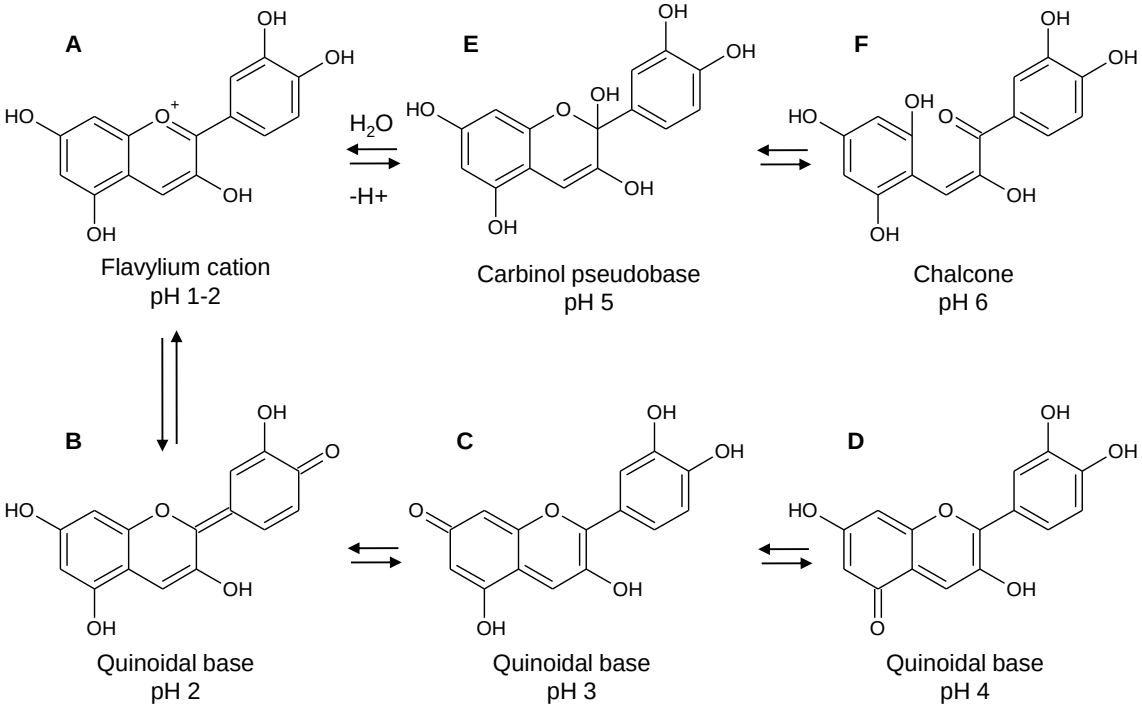


Adapted from (Castañeda-Ovando *et al.*, 2009).

Following exposure to neutral pH, temperature or enzymes (β-glucosidase) anthocyanins degrade to form phenolic acid and phloroglucinaldehyde components *in vitro* (Kay *et al.*, 2009; Piffaut *et al.*, 1994; Seeram *et al.*, 2001; Woodward *et al.*, 2009). Due to variations in their B-ring, cyanidin degrades to form protocatechuic acid whilst peonidin forms vanillic

acid **(Figure 1.4)**. These results suggest that due to the warm, basic physiochemical conditions found in the gastrointestinal tract (GIT) (Fallingborg, 1999), a large proportion of ingested anthocyanins may also be degraded into phenolic acids and aldehyde. Yet there is still considerable uncertainty as to what occurs *in vivo*. In one paper, protocatechuic acid was reported to be a major metabolite of cyanidin glycoside in humans (Vitaglione *et al.*, 2007), yet subsequent papers have failed to detect protocatechuic acid in rat blood plasma, stating protocatechuic acid is not a major intestinal metabolites of cyanidin glycosides (Ichiyanagi *et al.*, 2007). Reasons for these discrepancies may be due to substantial degradation reactions within the small intestine and colon and further conjugation reactions occurring in the intestine, kidneys or liver.

**Figure 1.4** Degradation of anthocyanidins into reactive α-diketone and monomeric phenolic acids and aldehyde.

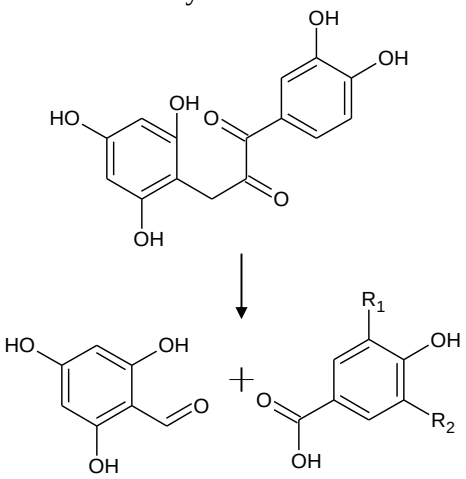


| Anthocyanidin | Phenolic acid | $R_1$ | $R_2$ |
|---|---|---|---|
| Cyanidin | Protocatechuic acid | -OH | -H |
| Delphinidin | Gallic acid | -OH | -OH |
| Pelargonidin | 4-Hydroxybenzoic acid | -H | -H |
| Peonidin | Vanillic acid | $-OCH_3$ | -H |
| Petunidin | 3-Methylgallic acid | -OH | $-OCH_3$ |
| Malvidin | Syringic acid | $-OCH_3$ | $-OCH_3$ |

$R_1$ and $R_2$ represent functional groups. Adapted from (Fleschhut *et al.*, 2006; KepplerandHumpf, 2005; Woodward *et al.*, 2009).

The pH of urine is also of significance, as it can affect the elimination of an analytes. The pH of urine is typically acidic, but can range from pH 4.5 to 8, depending on fluid ingestion and diet, with more acidic urine caused by the consumption of acidic fruits such as cranberries (Freudenthaler *et al.*, 1998; Hertrampf *et al.*, 1991; Miller *et al.*, 2009; Roy *et al.*, 1987). For example, the renal excretion of salicylate is highly dependent upon pH, and in order to treat an aspirin overdose, urine is alkalinised in order to enhance the elimination of salicylate (Miller *et al.*, 2009; Proudfoot *et al.*, 2003). In brief, this may occur because the ionisation of weak acids, such as salicyclic acid, is increased in an alkali environment, this results in a decrease in their reabsorption with increasing pH, following filtration at the glomeruli (Proudfoot *et al.*, 2003)

## 1.6. Anthocyanin bioavailability

In contrast to flavanones and flavanols such as epicatechin, which can reach micromolar concentrations, anthocyanins are present at nanomolar concentrations in plasma (Manach *et al.*, 2005; WilliamsonandManach, 2005). Anthocyanins are rapidly absorbed and reach maximum plasma concentration within 30 min to 4 h in humans depending on the contents of the stomach and the compounds ingested (**Table 1.2**). In a study feeding 400 mL red grape juice containing 284 mg anthocyanins, anthocyanins reached maximal plasma concentrations of 223 nM, 0.5 h following consumption (Bitsch *et al.*, 2004a). Similarly, a study feeding blackcurrant concentrate containing 2380 mg anthocyanins detected maximal plasma concentrations of 147 nM, 1.5 h following consumption (Matsumoto *et al.*, 2001).

The recovery of anthocyanins and anthocyanin metabolites in urine has also been low, typically ranging from 0.004 to 0.11% of the ingested dose (Bub *et al.*, 2001; Kay *et al.*, 2005; Manach *et al.*, 2005). Whilst a few studies have measured levels of anthocyanin excretion up to 5% after strawberry, red wine and cranberry consumption (Felgines *et al.*, 2003; Lapidot *et al.*, 1998; Ohnishi *et al.*, 2006), these cases are exceptions, and still only comprise a small proportion of total anthocyanin ingested (Table 1.2).

**Table 1.2** Summary of key pharmacokinetic data derived from selected human anthocyanins bioavailability studies.

| Food consumed | Anthocyanin dose (mg) | Study duration (h) | Plasma $C_{max}$ (nM) | Plasma $T_{max}$ (h) | Urinary excretion (%) | Reference |
|---|---|---|---|---|---|---|
| Red wine | 68 | 6 | 1 | 0.3 | 0.03 | (Bub *et al.*, 2001) |
| Red wine | 95 | 24 | 4 | 1.8 | 0.05 | (Garcia-Alonso *et al.*, 2009) |
| Strawberry | 179 | 24 | - | - | 1.80 | (Felgines *et al.*, 2003) |
| Strawberry | 222 | 24 | 274 | 1.1 | 0.75 | (Mullen *et al.*, 2008a) |
| Red grape | 284 | 7 | 223 | 0.5 | 0.23 | (Bitsch *et al.*, 2004a) |
| Purple sweet potato | 311 | 24 | 2 | 1.5 | 0.02 | (Harada *et al.*, 2004) |
| Purple carrots | 416 | 24 | 6 | 2.0 | 0.03 | (Kurilich *et al.*, 2005) |
| Cranberry | 651 | 24 | - | - | 5.00 | (Ohnishi *et al.*, 2006) |
| Elderberry | 720 | 24 | 97 | 1.2 | 0.05 | (Cao *et al.*, 2001) |
| Chokeberry | 721 | 24 | 96 | 2.8 | 0.15 | (Kay *et al.*, 2005) |
| Elderberry | 722 | 7 | 95 | 1.0 | 0.04 | (Netzel *et al.*, 2005) |
| Blueberry | 1200 | 4 | 29 | 4.0 | 0.003 | (Mazza *et al.*, 2002) |
| Chokeberry | 1300 | 24 | 351 | 2.0 | - | (Kay *et al.*, 2004) |
| Blackcurrant | 2380 | 8 | 147 | 1.5 | 0.11 | (Matsumoto *et al.*, 2001) |

$C_{max,}$ maximum concentration; $T_{msx}$, time of maximum concentration.

As of yet, no conclusive explanation has been given for the low anthocyanin recovery observed within these studies. It is possible that due to their unstable nature, the anthocyanins are present as degradation products, intermediates or metabolites, which

remain undetected. This remains a possibility despite the best efforts of many researchers, due to numerous potential structures, the complex profiles formed following conjugation and a lack of analytical standards. It is also probable that plasma and urine samples may give an inaccurate assessment of anthocyanin bioavailability due to the rapid removal of anthocyanins from the bloodstream or the requisition of anthocyanins by body tissues (Crozier *et al.*, 2010). The large number of structures present in food sources and the ability of anthocyanin metabolism to convert their form (i.e 3'-methylation of cyanidin results in the formation of peonidin) further complicates the elucidation of the bioavailability of anthocyanins (Del Rio *et al.*, 2010).

## 1.7. Anthocyanin metabolism and absorption

In order for anthocyanins to elicit biological effects *in vivo*, sufficiently high concentrations of the bioactive molecule must be present within the circulation for a sufficient length of time. However, there are considerable gaps in our knowledge concerning the metabolism of anthocyanins. Following consumption, anthocyanins enter the stomach, followed by the small intestine and colon, where they may undergo extensive degradation, metabolism and catabolism. This may be followed by absorption and subsequent phase I and II metabolism (Levsen *et al.*, 2005; WangandHo, 2009) within body tissues such as the liver and kidneys (Wang *et al.*, 2009), before excretion through the bilary or urinary routes.

### 1.7.1. Anthocyanin stability and absorption in the stomach.

The acidic condition of the gastric content provides a favourable environment for anthocyanins (He *et al.*, 2009; Hollman *et al.*, 1995; McDougall *et al.*, 2005a; McDougall *et al.*, 2005b), which have a structure which is highly influenced by pH (Miyazawa *et al.*, 1999). In simulated gastrointestinal digestion studies, where red wine (McDougall *et al.*, 2005b), raspberry (McDougall *et al.*, 2005a), chokeberry (Bermúdez-Soto *et al.*, 2007) and red cabbage (McDougall *et al.*, 2007) anthocyanins were incubated with pepsin and hydrochloric acid for 2 h at 37 °C, total anthocyanin content remained stable. However, as *in vitro* digestion simulations cannot mimic possible uptake of anthocyanins via active transport processes, a number of investigations on the fate of anthocyanins in the stomach in murines have been conducted (Passamonti *et al.*, 2003; Talavéra *et al.*, 2003). A study injecting the stomach (with a ligated pylorus) of fasted (24 h) and anesthetised rats with a physiologic buffer containing 14 µM anthocyanin extract found a high proportion (19-37% depending on anthocyanin structure) of anthocyanin mono-glycosides were absorbed intact, based on analysis of stomach contents and plasma after 30 min (Talavéra *et al.*, 2003). Similar results were obtained, with anthocyanins detected in the plasma within 6 min, when

1 mM grape anthocyanins were introduced into the sealed stomach of rats through a tube entering via the duodenum (Passamonti *et al.*, 2003).

A proposed method for the uptake of anthocyanins within the stomach is via the bilitranslocase transporter (Passamonti *et al.*, 2003), an anion carrier located within the liver and gastric mucosa, as anthocyanins have been shown to inhibit its activity (Passamonti *et al.*, 2002). Absorption of anthocyanins within the stomach would explain the intact and rapid absorbance of anthocyanins in plasma, which can appear within a few minutes of oral administration in murines (He *et al.*, 2009; Matsumoto *et al.*, 2001; Tsuda *et al.*, 1999) and within 60 min in humans (Bub *et al.*, 2001; Matsumoto *et al.*, 2001), yet the plausibility of this theory is uncertain. Anthocyanins are present as cations in gastric conditions, the absorbance of nutrients from the stomach is unusual and the rapid appearance of anthocyanins within the circulatory system in humans may solely result from absorbance in the upper small intestine, particularly considering most studies dose fasted volunteers with liquid solutions of anthocyanins. Rat studies which have directly measured anthocyanin absorbance within the stomach, were carried out under exceptionally unnatural conditions, with high concentrations of aqueous anthocyanins administered directly to the sealed stomachs of fasted and anaesthetised murines by intubation (Passamonti *et al.*, 2003) or injection (Talavéra *et al.*, 2003). It is therefore uncertain as to how relevant these studies are when looking at anthocyanin metabolism in humans.

### 1.7.2. Anthocyanin absorption in the small intestine.

Upon entry into the small intestine, anthocyanins are subjected to an increased pH and a gradually increasing array of bacteria (Berg, 1996). Within humans, absorption studies conducted using ileostomy volunteers provide the clearest picture of the passage of anthocyanins prior to reaching the colon. A study feeding 300 g raspberries to patients who had an ileostomy obtained an average recovery of 40% of the ingested dose within the ileal fluid. However, this ranged from 6% for cyanidin-3-glucoside to 75% recovery for pelargonidin-3-glucoside (González-Barrio *et al.*, 2010), thereby emphasising the impact additional hydroxyl groups have on the molecules stability *in vivo*. Similar results were obtained from a study feeding volunteers with an end ileostomy 300 g blueberries, where recoveries of the ingested anthocyanins included 28% for cyanidin-3-glucoside, 45% for cyanidin-3-arabinoside and 85% for malvidin-3-arabinoside (Kahle *et al.*, 2006). These results indicate that anthocyanins containing few hydroxyl or methoxy groups within their B-ring and attached to complex sugar moieties likely remain intact until the large intestine; however, in the case of anthocyanins such as cyanidin-3-glucoside, a high proportion of the degradation, metabolism and/or absorption appears to occur before the large intestine.

Nevertheless, there are limitations involved with these studies; ileostomy patients often have an increased gut permeability, electrolyte imbalance, lower production of urine and the terminal gut often develops its own microflora (WilliamsonandClifford, 2010). In addition, the fate of the anthocyanins remains unknown, as only their disappearance from the small intestine is monitored.

In contrast to other flavonoids, such as quercetin which require deglycoslation prior to absorption, the absorption of intact anthocyanin glycosides has been confirmed through the presence of low concentrations of anthocyanins identified in the plasma of rats and humans (McGhie *et al.*, 2003; Milbury *et al.*, 2002; Miyazawa *et al.*, 1999; Mülleder *et al.*, 2002; Wu *et al.*, 2002). Furthermore, a study which continually perfused the intestinal lumen of anesthetised rats with physiological buffer (pH 6.6) containing 10 μM anthocyanins for 45 min noted an absorption of 11 to 22% of the perfused dose (Talavéra *et al.*, 2004). The mechanism of absorption for anthocyanins through the epithelial cells of the intestinal lumen is uncertain, but may be aided by lactase phlorizin hydrolase (LPH), sodium dependent glucose transporter (SGLT1) or glucose transporters 2 (GLUT2) (Crozier *et al.*, 2009; Del Rio *et al.*, 2010).

LPH, a β-glycosidase enzyme found on the brush border of the intestinal epithelial cells, is thought to hydrolyse a range of flavonoid glycosides, including the structurally similar flavonol, quercetin (Day *et al.*, 2000). The hydrolysis of quercetin glycosides releases the more lipophilic aglycone form, which may subsequently enter the endothelial cells by passive diffusion **(Figure 1.5)** (Crozier *et al.*, 2009; Day *et al.*, 2000; Del Rio *et al.*, 2010). The hydrolysis of anthocyanins by LPH is probable, as anthocyanidin aglycones have been reported within rat jejunum (Tsuda *et al.*, 1999), although not in plasma. As the aglycone structures are unstable at neutral pH, the anthocyanidins likely subsequently degrade to form phenolic acid and aldehyde. Alternatively, glycosides may be actively transported into the epithelial cells and subsequently hydrolysed by cytosolic β-glucosidase (CβG). SGLT1 has been proposed to play a role in the active transport of flavonoid glycosides (Gee *et al.*, 2000; Gee *et al.*, 1998; Hollman *et al.*, 1999). Quercetin glycosides have been found to interact with intestinal glucose transporters in rat jejunum (Gee *et al.*, 1998) and studies on the absorption of quercetin-4'-glucoside and quercetin-3'-glucoside demonstrated a reduction in flavonoid transport when glucose or phlorizin (SGLT1 inhibitors) were present, thus suggesting SGLT1 may have a role in mucosal uptake of the flavonoids (Walgren *et al.*, 2000; Wolffram *et al.*, 2002). However, there have been a number of contradictory studies attesting to the role of SGLT1 in the transport of flavonoids. The reduction in flavonoid

transport in the presence of SGLT1 inhibitors may be caused by the flavonoids interacting with, rather than being transported by SGLT1, especially considering sequential studies using *Xenopus* oocytes expressing human SGLT1 found none of the tested flavonoids were transported by SGLT1 (Arts *et al.*, 2002; KottraandDaniel, 2007).

Another possible mechanism for the absorption of anthocyanins through intestinal epithelial is via glucose transporters 2 (GLUT2) (Del Rio *et al.*, 2013; Faria *et al.*, 2009; ManzanoandWilliamson, 2010). An experiment conducted using caco-2 cells found that anthocyanin transport across cells pretreated with anthocyanins was increased compared to control cells, and the expression of GLUT2 expression was significantly increased in these cells (Faria *et al.*, 2009). Following absorption into the epithelial cell, anthocyanins and anthocyanin metabolites may enter the portal circulation via diffusion, or via a transporter such as GLUT2. The use of the GLUT2 transporter is supported by evidence which shows polyphenols inhibiting GLUT2 facilitated glucose efflux on the basolateral side of cells (Manzano *et al.*, 2010) (Figure 1.5). Alternatively, flavonoid conjugates formed in the intestinal mucosa may be secreted back into the gut lumen using the multiresistant protein 2 (MRP2) transporter and P-glycoproteins (Figure 1.5) (Crozier *et al.*, 2009; Del Rio *et al.*, 2010; Del Rio *et al.*, 2013).

**Figure 1.5** Potential mechanisms for anthocyanin absorption

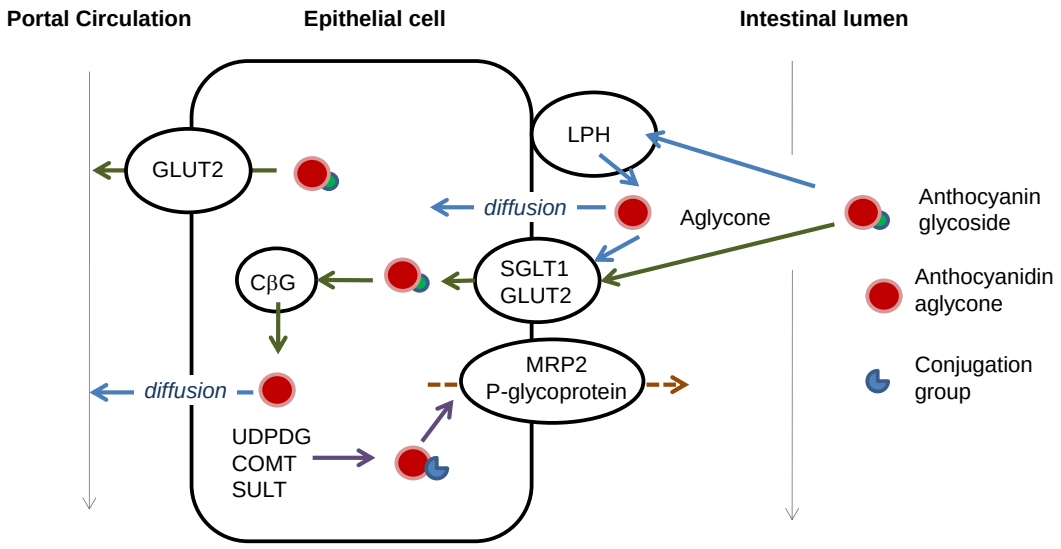


CβG, cytosolic β-glucosidase; GLUT2, glucose transporters 2; LPH, lactase phlorizin hydrolase; MRP2, multiresistant protein 2; SGLT1, sodium dependent glucose transporter; SULT, sulfotransferase; UDPDG, uridine-5'-diphospho-glucuronosyltransferase. Adapted from (Day *et al.*, 2000; Gee *et al.*, 2000; McGhie *et al.*, 2007; Walgren *et al.*, 2000).

### 1.7.3. Anthocyanin metabolism and absorption in the colon

Anthocyanins not absorbed, degraded or metabolised within the small intestine reach the large intestine, where they are exposed to a large array of microflora; over 400 species and $10^{10} – 10^{11}$ microbes per gram intestinal contents are predicted to be present (Arumugam *et al.*, 2011; Berg, 1996; Qin *et al.*, 2010), with *Bacteroides species*, *Clostridium species* and *Eubacterium species* making up the majority of the microflora within the intestines (WilliamsonandClifford, 2010). *Ex vivo* faecal fermentation studies of anthocyanins have reported the deglycosylation of anthocyanins and the appearance of their aglycones, phloroglucinaldehyde and their corresponding B-ring degradation products following incubation with a human faecal suspension within an anaerobic chamber (Aura *et al.*, 2005; Fleschhut *et al.*, 2006; González-Barrio *et al.*, 2010; Hassimotto *et al.*, 2008; Keppler *et al.*, 2005). Only a slight decrease in the anthocyanin content was observed in the heat-inactivated faecal suspension, indicating the bacteria were primarily responsible for the disappearance of anthocyanins (Fleschhut *et al.*, 2006).

In addition to the parent anthocyanins, the microbial metabolism of the phenolic degradation products has also been investigated. A faecal fermentation study, which incubated phenolic acids and phloroglucinaldehyde in sterilised caecum inoculum from pigs found phenolic acids were stable within the sterilised samples whilst phloroglucinaldehyde was degraded extensively, with only small amounts remaining detectable after 24 h. The possible reactions involved in the degradation of aldehydes include condensation with free amine ($NH_2$) groups of amino acids or proteins or the formation of an imine (Keppler *et al.*, 2005).

Despite the detection of B-ring degradation product in a number of *in vitro* fermentation studies, the measured amounts of phenolic degradation products formed do not account for the entire starting concentration of anthocyanin, therefore, it is likely that further unknown anthocyanin intermediates are present or that further microbial metabolism takes place (Keppler *et al.*, 2005). In addition to the *O*deglycosylation and degradation of anthocyanins, the microflora are capable of *C*-deglycosylation, hydrolysis of esters and deglucuronidation. The resulting aglycones are susceptible to aromatic dehydroxlation, demethoxylation and demethylation, hydrogenation, and α- and β-oxidation of the aliphatic elements generated following the rupture of the heterocyclic oxygen ring (WilliamsonandClifford, 2010). The dehydroxylation of *ortho*-dihydroxy substrates, such as protocatechuic acid, can occur either at a *meta* (3-OH) or *para* (4-OH) position, however dehydroxylation at the *meta* position is less efficiently removed, so *meta* hydroxyl catabolites often predominate (WilliamsonandClifford, 2010). Demethylation of anthocyanin degradation products has

been reported *in vitro,* with a pig faecal fermentation study observing the demethylation of vanillic acid and sinapic acid to from gallic acid and protocatechuic acid respectively (Keppler *et al.,* 2005). Therefore, the degradation and transformation of anthocyanins by colonic microflora can result in the formation of a complex range of phenolic structures.

Comparatively few of the bacterial enzymes responsible for the transformation of phenolic compounds within the GIT have been characterised. However, hydroxylation of the flavonoid A-ring has been demonstrated with *Pseudomonas* species and *Eubacterium* species are known to degrade flavonoids anaerobically via deglycosylation and cleaving the C-ring (WilliamsonandClifford, 2010).

### 1.7.4. Phase II metabolism of anthocyanins.

Prior to passage into the portal circulation from the small intestine, anthocyanins may undergo metabolism, forming glucuronidated, sulfated and methylated metabolites, through the action of uridine-5'-diphospho-glucuronosyltransferase (UDPDG), sulfotransferase (SULT) and catechol-*O*-methyltransferase (COMT) enzymes respectively (Crozier *et al.*, 2009; PiskulaandTerao, 1998; Tsuda *et al.*, 1999), which are abundant within the gastrointestinal tract (Riches *et al.*, 2009; Zhang *et al.*, 2007). Within the portal circulation, anthocyanin metabolites may be subjected to further phase II metabolism by UDPDG, SULT and COMT enzymes within the liver, and following entry into the systemic circulation, may be further metabolised within tissues such as the kidneys and lungs (Talavéra *et al.*, 2005)**.** Following administration of anthocyanins to humans, glucuronidated, sulfated and methylated metabolites of anthocyanins have been found within urine and plasma (Azzini *et al.*, 2010; Bitsch *et al.*, 2004b; Carkeet *et al.*, 2008; Felgines *et al.*, 2003; Felgines *et al.*, 2005; Hollands *et al.*, 2008; Kay *et al.*, 2005; Mullen *et al.*, 2008a). In general, the formation of glucuronide conjugates is considered the most common phase II metabolic route for water-soluble metabolites, and accounts for the majority of conjugated metabolites found in the urine and bile.

A study feeding 200 g strawberries identified four conjugated anthocyanin metabolites, including three mono-glucuronides and one sulfoconjugate of pelargonidin within urine. The glucuronide conjugates were excreted at concentrations up to 2675 nM/24 h, whilst the sulfate conjugate reached 134 nM/24 h (Felgines *et al.*, 2003). Animals studies have observed similar results (Talavéra *et al.*, 2005; Talavéra *et al.*, 2004). In a study which perfused the intestinal lumen of anesthetised rats with high concentrations of blackberry anthocyanins, they observed the methylation of cyanidin-3-glucoside to peonidin-3-glucoside, and glucuronidation to cyanidin and peonidin monoglucuronide in urine and

plasma (Talavéra *et al.*, 2004). Similarly, a study feeding chokeberry to weanling pigs observed methylation and glucuronidation of cyanidin-3-glucoside (Wu *et al.*, 2005).

Alternatively prior to conjugation, anthocyanins may be degraded into their phenolic acid and aldehyde within the small intestine lumen or epithelial cells or by microflora within the colon (Pérez-Vicente *et al.*, 2002). A study feeding cyanidin-3-glucoside to rats identified higher concentrations of protocatechuic acid than the parent anthocyanin within plasma (Tsuda *et al.*, 1999) and a study in caco-2 cells found protocatechuic acid and phloroglucinaldehyde were metabolised to glucuronide and sulfate conjugates (Kay *et al.*, 2009).

In addition to methylation, sulfation and glucuronidation, anthocyanins are speculated to undergo conjugation with glutathione (GSH), a tripeptide present in millimolar concentrations within intracellular fluid (**Figure 1.6**). The formation of GSH conjugates of quercetin has been observed within murine hepatic suspensions, and GSH related metabolites of quercetin degradation products have been observed in human urine (HongandMitchell, 2006). Furthermore, a quercetin GSH adduct has been putatively identified within human plasma (Lee *et al.*, 2012). GSH has a nucleophilic cysteinyl thiol group, which allows it to be added to activated double bonds, such as those found at the *ortho*-position of a phenolic group or aromatic ring (Levsen *et al.*, 2005), therefore such anthocyanins are also probable candidates for GSH conjugation.

### 1.7.1. Enterohepatic circulation and urinary excretion

Following their absorption and metabolism, anthocyanins may be eliminated through the urinary (Felgines *et al.*, 2003) or biliary routes (Ichiyanagi *et al.*, 2006; Talavéra *et al.*, 2003; Talavéra *et al.*, 2004). Compounds eliminated within bile are generally large (>375 Da) and lipophilic (Millburn *et al.*, 1967). Therefore conjugates formed through phase II metabolism are more likely to be enter the enterohepatic circulation, to be modified, secreted back into the small intestine, and possibly reabsorbed, whereas smaller, polar conjugates follow the urinary route. Analysis of bile samples from rats with high concentrations of anthocyanins injected into their intestinal lumen, found anthocyanins and methylated anthocyanins present within the bile within 20 min (Ichiyanagi *et al.*, 2006; Talavéra *et al.*, 2003; Talavéra *et al.*, 2004).

**Figure 1.6** Structure of glutathione

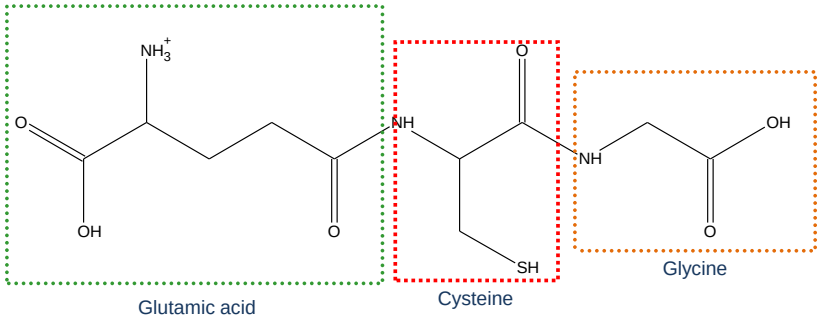


### 1.7.2. Distribution of anthocyanins

The use of radioactive [such as carbon-14 ($^{14}$C)] or stable isotopes [such as carbon-13 ($^{13}$C) and deuterium ($^{2}$H)] can facilitate the elucidation of metabolite structures *in vivo* (Mutlib, 2008). Radiolabeled analogues are widely used to provide a qualitative and quantitative assessment of a drugs' distribution and excretion patterns in humans and animals, whilst stable isotopes can facilitate the elucidation of a metabolites structure using HPLC-MS/MS by separating the molecular weight of the labelled and unlabelled analogues by a couple of mass units (Mutlib, 2008). However to date, few studies have used isotopically labelled anthocyanins to determine the absorption, metabolism, distribution and elimination (ADME) of anthocyanins in humans. Previously, a flavonol intervention study administered 4-$^{14}$C-quercetin either orally (100 mg) or intravenously (0.3 mg) to human volunteers (Walle *et al.*, 2001). The dose was predominantly recovered in the form of $CO_2$, which is likely primarily due to the position of the $^{14}$C label on the C=O bond, at the 4-position in the C-ring. In contrast, a 2-$^{14}$C-quercetin-4'-glucoside study, containing the labelled carbon at the 2-position in the C-ring, detected minimal radioactivity outside of the gastrointestinal tract in rats, with the majority of the compound absorbed within the colon and rapidly removed from the circulation by the kidneys or excreted within faeces (Mullen *et al.*, 2008b). An anthocyanin labelled study which fed $^{14}$C-cyanidin-3-glucoside with the labelling on the six carbons within the B-ring, by direct stomach intubation to mice, obtained 92% recovery of the label in mice which were sacrificed after 3 h. The majority of the label was within the gastrointestinal tract, suggesting cyandin-3-glucoside is poorly absorbed in mice and that anthocyanins have a limited systemic bioavailability (Felgines *et al.*, 2010).

## 1.8. Anthocyanins and cardiovascular disease

CVD is responsible for an estimated 17.3 million deaths worldwide every year (WHO, 2013) and is caused by disorders of the heart and blood vessels, and includes coronary heart disease, cerebrovascular disease and peripheral artery disease. Whilst the evidence for the

protective effects of anthocyanin rich diets on cardiovascular protection is mixed, a significant amount of epidemiological studies (Cassidy *et al.*, 2013; Cassidy *et al.*, 2011; McCullough *et al.*, 2012; Mink *et al.*, 2007; Rissanen *et al.*, 2003; Sesso *et al.*, 2007) and randomised control trials (Basu *et al.*, 2010; Rodriguez-Mateos *et al.*, 2013; Zhu *et al.*, 2013) generally support the concept that high intakes of anthocyanins are associated with a decreased risk of cardiovascular disease. A study of 157,000 people, with 14 years of follow up found that a high anthocyanin intake was associated with an 8% reduction in the relative risk of hypertension (Cassidy *et al.*, 2011), similarly a prospective study of 93,600 women, with 18 years follow up, found an association between a higher anthocyanin intake and a decreased risk of death due to CVD (Cassidy *et al.*, 2013). Mechanistic studies suggest that the benefits of high anthocyanin intake may be due to their effects on endothelial dysfunction and inflammation (BellandGochenaur, 2006; García-Lafuente *et al.*, 2009; Heiss *et al.*, 2010; Libby *et al.*, 2002; Xu *et al.*, 2004a; Xu *et al.*, 2004b).

### 1.8.1. Endothelial Dysfunction

Many anthocyanin bioactivity studies have focused on the protective effects of anthocyanins against endothelial dysfunction. Endothelial dysfunction can be broadly defined as the imbalance of vasodilating and vasoconstricting substances within the endothelium (Bell *et al.*, 2006; Heiss *et al.*, 2010; Xu *et al.*, 2004a; Xu *et al.*, 2004b). Nitric oxide (NO) is a powerful vasodilator and cellular signalling molecule responsible for maintaining endothelium homeostasis; within the endothelium it is produced by endothelial nitric oxide synthase (eNOS), which uses L-arginine, oxygen and reduced nicotinamide-adenine-dinucleotide phosphate (NADPH) as co-substrates (FörstermannandSessa, 2012). The bioavailability of NO is reduced by increased superoxide ($O_2^{\bullet-}$) production, as $O_2^{\bullet-}$ reacts with NO to produce peroxynitrite ($ONOO^-$). A major source of $O_2^{\bullet-}$ in the endothelium is NADPH oxidase 2 (NOX2), which belongs to the family of enzymes capable of generating $O_2^{\bullet-}$ by transferring electrons from NADPH. NO and $O2^{\bullet-}$ can react to form $ONOO^-$, which can oxidise the essential cofactor of eNOS, tetrahydrobiopterin ($BH_4$), to form $BH_3\bullet$ and $BH_2$, which lead to the uncoupling of eNOS (**Figure 1.7**). Functional, NO generating eNOS is converted into a dysfunctional, $O_2^{\bullet-}$ generating enzyme that contributes to vascular oxidative stress (Förstermann *et al.*, 2012). Therefore, impairment of NO or eNOS, in conjunction with increased levels of reactive oxygen species (ROS) is a significant step towards the development of endothelium dysfunction and ultimately CVD (Bell *et al.*, 2006).

**Figure 1.7** Potential mechanisms by which cardiovascular risk factors lead to eNOS uncoupling and oxidative stress.

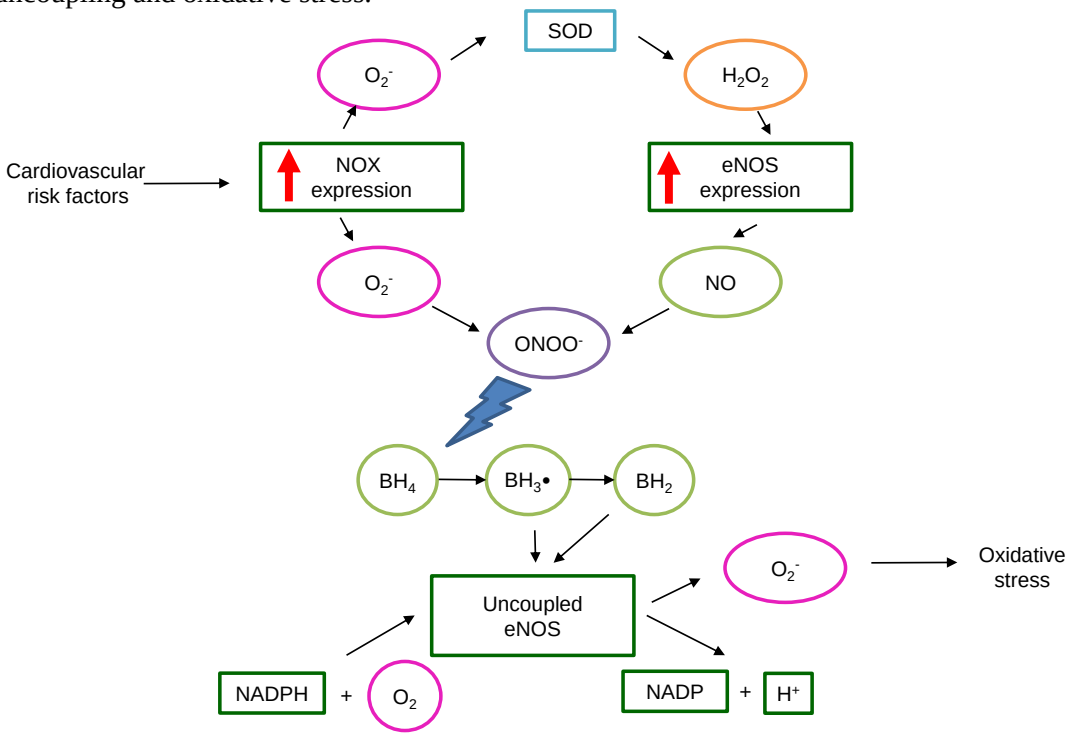


$BH_4$, tetrahydrobiopterin; eNOS, endothelial nitric oxide synthase; NOX, NADPH oxidase; SOD, superoxide dismutase. Adapted from (Förstermann *et al.*, 2012).

One of the mechanisms by which anthocyanins are thought to help prevent the progress of CVD is by up-regulating the activity of eNOS, resulting in an increased presence of bioavailable NO (Wallace, 2011; Xu *et al.*, 2004b). A significant increase in flow mediated dilation (FMD), a technique that measures NO mediated brachial artery dilation in hypercholesterolemic individuals, was detected in a randomised, double blind, placebo controlled crossover study, following a 12-week intervention feeding 320 mg berry anthocyanins, thus demonstrating an improved vasodilatory response from anthocyanin consumption (Zhu *et al.*, 2011). Similarly, an *ex vivo* study conducted using porcine coronary arterial rings found berry anthocyanins using concentrations of 0.005 mg/L to 5 mg/L induced dose responsive endothelium-dependent vasorelaxation, which was prevented by the application of $NO_2$-L-arginine, a known inhibitor of eNOS (Bell *et al.*, 2006). This suggests the endothelial NO system is involved in the relaxation response to anthocyanins. Cellular evidence has also supported this hypothesis; 0.1 µM cyanidin-3-glucoside applied to bovine artery endothelial cells for 8 h was found to up-regulate eNOS, inducing a two-fold increase in NO production (Xu *et al.*, 2004a; Xu *et al.*, 2004b).

### 1.8.2. Inflammation

Inflammation is a defence mechanism whereby leukocytes migrate into damaged tissues, to destroy agents which may potentially cause further tissue damage (García-Lafuente *et al.*, 2009). Acute inflammation is a limited, generally beneficial response whilst chronic inflammation is more persistent, and is involved in the development of many diseases, including arteriosclerosis, diabetes and cancer (García-Lafuente *et al.*, 2009). Inflammation drives the formation, and progression of atherosclerotic plaques through initiating the expression of adhesion molecules and cytokines, which leads to the recruitment and aggregation of leukocytes (Libby *et al.*, 2002). Several mechanisms explaining the link between a decrease in risk factors associated with inflammation and anthocyanins have been described. These include modulation of inducible nitric oxide synthase (iNOS), modulation and regulation of pro-inflammatory molecules such as adhesion molecules and cytokines and modulation of arachidonic acid related enzymes (García-Lafuente *et al.*, 2009).

**Modulation of iNOS**

In contrast to eNOS which is constitutively expressed in most cells, iNOS is regulated at the transcriptional level, and highly activated by inflammatory stimuli such as lipopolysaccharide (LPS) and inflammatory cytokines, in cells such as macrophages and is responsible for the overproduction of NO during inflammation. Damage to healthy cells, as well as invading microbes can be caused by the NO radical, or by the interaction of NO with superoxide leading to the formation of peroxynitrite. Excessive NO production by iNOS can lead to arteriolar vasodilation, microvascular damage and septic shock (García-Lafuente *et al.*, 2009). Therefore, compounds which can reduce NO production through interacting with iNOS without affecting eNOS can be important in regulating inflammation (García-Lafuente *et al.*, 2009). Anthocyanins, including blackberry extract, cyanidin-3-glucoside and pelargonidin-3-glucoside, have been reported to inhibit iNOS protein and mRNA expression in a dose-dependent manner in macrophages (Hämäläinen *et al.*, 2007; Pergola *et al.*, 2006; Wang *et al.*, 2008) and microglia (Jeong *et al.*, 2013) exposed to the inflammatory stimulus LPS.

**Modulation of adhesion molecules**

The recruitment of adhesion molecules responsible for the arrest, adherence, transmigration and accumulation of leukocytes is one of the earliest events in the initiation of atherosclerosis, and occurs at arterial sites following pro-atherogenic stimuli such as oxidised LDL (oxLDL) or free radicles (EpsteinandRoss, 1999; García-Lafuente *et al.*, 2009). The endothelium reacts to proatherogenic stimuli by expressing two classes of

adhesion molecule, selectins and cell adhesion molecules (Fotis *et al.*, 2012). Selectins participate in the early stages of leukocyte recruitment, rolling and tethering at the endothelial surface by interacting with their ligands to create weak bonds between activated endothelial cells (P- and E-selectins) and leukocytes (L-selectins) (Blankenberg *et al.*, 2003), whilst cell adhesion molecules aid the arrest and extravasation of leukocytes. Intercellular adhesion molecules (ICAM) bind to multiple β2 integrins, platelet endothelial cellular adhesion molecule-1 (PECAM-1) are dense at junctions between endothelial cells and participate in homophilic binding and vascular cell adhesion molecule-1 (VCAM-1) is transcriptionally induced on endothelial cells and participates in the firm adhesion of leukocytes to the endothelium. VCAM-1 also interacts with integrin α4β1, which induces signals within endothelial cells, including the activation of NADPH oxidase to catalyse the production of ROS, thus triggering endothelial shape change and allowing leukocyte emigration (**Figure 1.8**) (Matheny *et al.*, 2000). Anthocyanins have been reported to modulate the expression of VCAM-1 (Chao *et al.*, 2013; Kim *et al.*, 2006; Miyazaki *et al.*, 2008; Nizamutdinova *et al.*, 2009; Xia *et al.*, 2009). Humans fed 320 mg/day anthocyanins for 24 weeks (Zhu *et al.*, 2013) and mice fed purple sweet potato for four weeks (Miyazaki *et al.*, 2008) had significantly lower plasma VCAM-1 levels. Similarly, *in vitro*, pre-treatment of TNF-α challenged endothelial cells with black soybean anthocyanins (Chao *et al.*, 2013; Kim *et al.*, 2006; Nizamutdinova *et al.*, 2009) and grape seed extract (SenandBagchi, 2001) has been shown to reduce VCAM-1 expression.

**Modulation of cytokines and chemokines**

Cytokines and chemokines are mediators of local and intercellular communications required for the response to a wide range of stimuli in immune and inflammatory processes (Wallace, 2011). Several cytokines, such as tumour necrosis factor-α (TNF-α), interleukin (IL)-6 and IL-1β, and chemokines such as monocyte chemoattractant protein-1 (MCP-1), are predominately produced by activated macrophages, dendritic cells and T-cells, and are strongly associated with the chronic inflammatory response (BaudandKarin, 2001; García-Lafuente *et al.*, 2009). These pro-inflammatory molecules contribute to atherogenesis by triggering attachment and transendothelial migration of leukocytes into the endothelium and by maintaining the inflammation inside atherosclerotic lesions and promoting the proliferation and migration of smooth muscle cells (García-Lafuente *et al.*, 2009). Moreover, in target cells, cytokines interact with their receptor protein to stimulate the activation of pro-inflammatory signalling pathways such as the mitogen activated protein kinases (MAPK) and nuclear factor-κB (NF-κB) pathways (Baud *et al.*, 2001; García-Lafuente *et al.*, 2009).

**Figure 1.8** Schematic diagram of the leukocyte-endothelial interactions and the roles of selectins and adhesion molecules in the early stages of atherosclerosis.

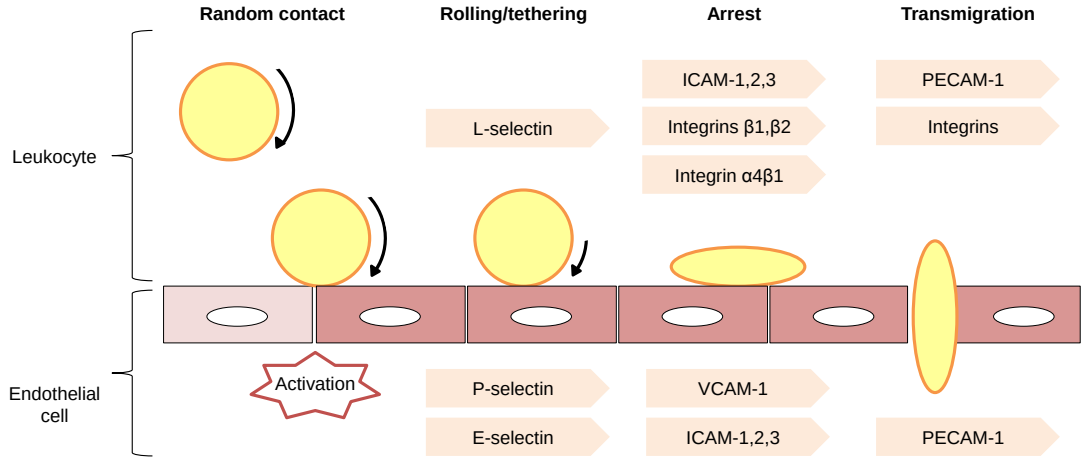


ICAM, intercellular adhesion; PECAM-1platelet endothelial cellular adhesion molecule-1; VCAM-1, vascular cell adhesion molecule-1. Adapted from (Blankenberg *et al.*, 2003; Fotis *et al.*, 2012).

NF-κB is activated by numerous pro-inflammatory stimuli and controls the expression of numerous genes involved in inflammatory response and secretion of cytokines and chemokines (BremnerandHeinrich, 2002). It is generally represented by subunits p65 and p50 and in its inactive form resides in the cytoplasm bound to the inhibitory protein, NF-κB inhibitory protein (IκB) (Min *et al.*, 2010). The up-regulation of effector proteins by NF-κB is initiated by upstream signalling cascades, such as the TNF-α or CD40L signalling cascades. CD40L or TNF-α released from macrophages, bind with their receptors (CD40 and TNFR1), thus activating the recruitment of multiple protein kinases, leading to the activation of the IkB kinase (IKK) complex (Bremner *et al.*, 2002). The IKK complex triggers the phosphorylation of IκB, which is recognised by an ubiquitin protein ligase and undergoes poly-ubiquitination, which targets the protein from rapid degradation (**Figure 1.9**). The free NF-κB is translocated into the nucleus where NFκB binding sites are found in the promoter regions of cell adhesion molecules and cytokines including IL-1, IL-6, IL-8 and TNF-α (Bremner *et al.*, 2002). One of the mechanism by which anthocyanins and their degradation products are thought to reduce inflammation is through the inhibition of the activation of NF-κB (Karlsen *et al.*, 2007; Wang *et al.*, 2010). Anthocyanins have been shown to suppress LPS and CD40L stimulated NF-κB activation through inhibiting IκBα phosphorylation and the translocation of NF-κB (p65) into the nucleus (Min *et al.*, 2010; Xia *et al.*, 2009).

**Figure 1.9** Activation of NF-κB and MAPK signalling pathways by CD40-CD40L and TNF-α.

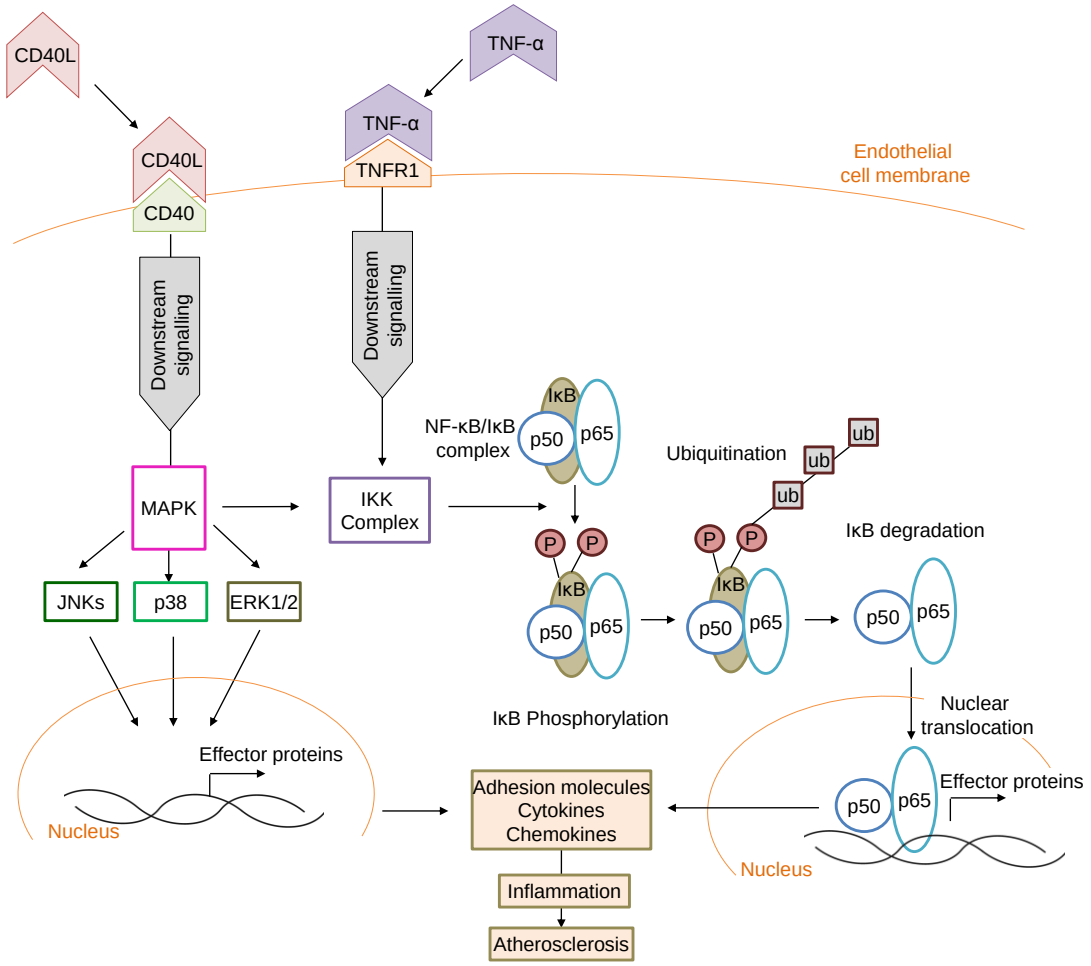


CD40L, Cluster of differentiation 40 ligand; ERK, extracellular-signal-regulated kinases; IKK, inhibitory-κB kinase; JNK, c-Jun N-terminal kinases; MAPK, mitogen-activated protein kinase complex; NF-κB, nuclear factor-κB; P, phosphate; p38, mitogen-activated protein kinase; p50, NF-κB p50 subunit; p65, NF-κB p65 subunit; TNF-α, tumour necrosis factor-α; TNFR1, TNF receptor-1; ub, ubiquitination. Adapted from (Bremner *et al.*, 2002; Pamukcu *et al.*, 2011).

The MAPK family consists of three members: extracellular signal regulated kinase (ERK), p38 and c-jun NH2-terminal kinase (JNK), and its activation can lead to the degradation of the IκB-α protein and subsequent activation of NF-κB (Figure 1.9) (Hirano *et al.*, 1996). Endothelial cells pre-treated with anthocyanins have been shown to reduce CD40L induced production of pro-inflammatory molecules and decreased the activation of JNK and p38 (Xia *et al.*, 2009) and protocatechuic acid has also been shown to reduce the LPS stimulated production of inflammatory cytokines through inhibiting the activation of JNK, ERK and p38 in macrophages (Min *et al.*, 2010).

## 1.9. Summary

Anthocyanins can constitute major dietary components of phytochemical intake, with intake in excess of 500 mg being feasible for those who follow a diet rich in berries, red vegetables and red wine (Del Rio *et al.*, 2013). Moreover, a high intake of anthocyanins has been linked to a decrease in risk factors associated with CVD (Cassidy *et al.*, 2013; Cassidy *et al.*, 2011; McCullough *et al.*, 2012; Mink *et al.*, 2007; Rissanen *et al.*, 2003; Sesso *et al.*, 2007). However, anthocyanins have an exceptionally low bioavailability, with intervention studies identifying low nanomolar concentrations present within the systemic circulation, which rarely equates to more than 1% of the ingested dose (Felgines *et al.*, 2005; Garcia-Alonso *et al.*, 2009; Kay *et al.*, 2005; Kay *et al.*, 2004). Due to their unstable nature at physiological pH, it has been proposed that anthocyanins are likely present in the circulation, as unidentified degradation products and metabolic intermediates (Kay, 2010), and that these metabolites may be responsible for the perceived bioactivity of anthocyanins against CVD. The foregoing review therefore highlighted the gaps in our current understanding of anthocyanins, particularly their absorption, metabolism and ultimately their bioactivity *in vivo.*

The key to establishing the bioactivity of anthocyanins *in vivo* is to first gain a complete understanding their absorption, distribution and metabolism, and subsequently incorporate this understanding into establishing their bioactivity. Since anthocyanins are unstable at physiological pH, attention must turn to the possible bioactivity of unknown anthocyanin degradation products and metabolites. To date, few studies have search for anthocyanin degradants and those that have, generally had difficulties separating anthocyanin degradation products from phenolics present within the bolus. The reason the metabolic pathway of anthocyanin remains elusive, may in part be due to the lack of studies using pure or labelled anthocyanins and in part due to the lack of intrinsic methods developed for the detection of anthocyanin degradation products and metabolites. Therefore, the current thesis set out to:

1. Develop methods for the detection of anthocyanin metabolites.
2. Identify novel anthocyanin metabolites in human biological samples from anthocyanin intervention trials.
3. Establish the bioactivity of identified metabolites *in vitro*, with a specific focus on inflammation.

As initial data from our lab suggests that the metabolites of anthocyanins are not bioactive against biomarkers for vascular activity, such as eNOS and NO (unpublished data), the

present thesis focused on the anti-inflammatory activity of anthocyanins metabolites on the production of VCAM-1 and IL-6 in human umbilical vein endothelial cells (HUVECs) following stimulation with either CD40L or TNF-α. VCAM-1 and IL-6 were selected for analysis as they play key roles in the progression of inflammation, VCAM-1 aids leukocyte attachment and transmigration (Blankenberg *et al.*, 2003), and IL-6 is responsible for the recruitment of multiple pro-inflammatory molecules, and in combination with its receptor can dictate the transition from acute to chronic inflammation (Gabay, 2006). Therefore, strategies targeting these molecules can lead to an effective prevention of chronic inflammatory diseases.

# Chapter 2. Methods for isolating, identifying and quantifying known and predicted anthocyanin metabolites in clinical samples

## 2.1. Introduction

Epidemiological evidence suggests an association between the consumption of fruits and vegetables rich in anthocyanins and a decreased risk of cardiovascular disease (Cassidy *et al.*, 2011; McCullough *et al.*, 2012; Mink *et al.*, 2007). However, there is a distinct lack of information regarding the bioavailability and metabolic fate of anthocyanins in humans, which is predominantly due to anthocyanin bioavailability studies demonstrating extremely low recoveries of anthocyanins post ingestion (Kay *et al.*, 2005; Manach *et al.*, 2005; Williamson *et al.*, 2005). This low recovery of anthocyanins led to the notion that anthocyanin may degrade and be extensively metabolised (via phase I and II metabolism or bacterial catabolism) *in vivo*, and it is postulated that these products of anthocyanin degradation are likely to be responsible for their associated health-promoting properties (Del Rio *et al.*, 2010; Tsuda, 2011; WilliamsonandClifford, 2010).

A limited number of previous *in vitro* studies have reported the degradation of anthocyanins into phenolic acids and aldehydes (Kay *et al.*, 2009; Woodward *et al.*, 2009) and their subsequent methyl, glucuronide and sulfate conjugation (Woodward *et al.*, 2011). This has been observed *in vivo*, with a few studies reporting the presence of the phenolic acid degradation products in serum and urine (Azzini *et al.*, 2010; Czank *et al.*, 2013; Hassimotto *et al.*, 2008; Ichiyanagi *et al.*, 2007; Nurmi *et al.*, 2009; Vitaglione *et al.*, 2007). However, there are still conflicting reports in the literature regarding the identity and prevalence of the major metabolites present following the consumption of anthocyanin-rich foods and until these are realised, the mechanisms associated with their health effects will remain undefined.

The major challenges associated with the recovery and detection of anthocyanins relate to their instability under neutral pH (Fossen *et al.*, 1998) and heat (Fleschhut *et al.*, 2006; Keppler *et al.*, 2005; Woodward *et al.*, 2009), their extensive metabolic conjugation *in vivo* (Mullen *et al.*, 2008a) and their probable catabolism by intestinal microflora (WilliamsonandClifford, 2010). It is therefore likely that after consumption of anthocyanin rich foods, a complex mixture of intact anthocyanins, phenolic degradation products, phase II metabolic conjugates and colonic metabolites exist in tissues and biological fluids (Czank *et al.*, 2013). Whilst a number of methods have been developed for the analysis of flavonoids

and flavonoid derived phenolics (Kylli *et al.*, 2010; Plazonić *et al.*, 2009; ZhangandZuo, 2004), the vast majority of reported methods for anthocyanin analysis (in particular) have concentrated on quantification of parent/precursor forms or their respective metabolic conjugates (methyl, glucuronide and sulfate derivatives of anthocyanins). There are limited reports where quantitative analytical methods have been optimised for the analysis of anthocyanins and their phenolic acid and aldehyde degradation products and metabolites together (Kay, 2010; Nurmi *et al.*, 2009; WilliamsonandClifford, 2010).

Developing an appropriate method for this purpose presents many challenges, as there is an extremely large diversity of metabolic by-products, whose structures and physicochemical properties make extraction and quantification in complex matrices problematic. In addition, many phase II conjugates of phenolic acids are not commercially available for use as reference standards for method development. In order to facilitate the development of a suitable method, in-house synthesis is therefore often necessary. The objective of the present chapter was firstly to model the putative metabolites formed from the metabolism of anthocyanins and secondly to develop and validate extraction and detection methods suitable for determining the absorption, distribution, metabolism and elimination (ADME) of anthocyanins, including their degradation products and metabolites, in clinical samples. HPLC and MS variables such as organic modifier, ionic modifier concentration, mobile phase gradient, flow rate, column, ion source and multiple reaction monitoring (MRM) parameters were assessed to optimise analytical performance. Analytical methods were validated for the 45 analytes and four internal standards and confirmed using clinically derived urine and serum samples, for linearity, precision and accuracy using the U.S. Department of Health and Human Services Food and Drug Administration (FDA) guidance for industry bioanalytical methods validation (FDA, 2001).

When working with biological samples, it is often necessary to isolate the analytes of interest from their matrices. This allows the analyte to be detected within a 'clean' chromatogram by reducing the signal to noise ratio, thus improving the detection of analytes present in low concentrations. In addition, extracted samples can be concentrated, further increasing the detection limits of the analytes of interest. Typically, individual classes of (poly)phenolic compounds can be extracted from human matrices using either protein precipitation (Marks *et al.*, 2009; Mullen *et al.*, 2009; Stalmach *et al.*, 2009a; Stalmach *et al.*, 2009b), liquid-liquid extraction (LLE) (Graf *et al.*, 2006; Mullen *et al.*, 2002) or solid phase extraction (SPE) (Kay *et al.*, 2005; Kay *et al.*, 2004; Mazza *et al.*, 2002; Woodward *et al.*, 2009). The present study will focus on developing and validating a method for SPE of urine, serum and faecal samples, as it allows sample concentration and the removal of ion suppressing solutes

such as salts, urea and proteins, whilst retaining the analytes of interest, anthocyanins and phenolic acids (Kraemer-Schafhalter *et al.*, 1998; Mazza *et al.*, 2004). The analytes explored in the present chapter include anthocyanins (cyanidin-3-glucoside, C3G; pelargonidin-3-glucoside, P3G), their degradation products (protocatechuic acid, PCA; 4-hydroxybenzoic acid; phloroglucinaldehyde, PGA), phase II conjugates (protocatechuic acid-3-glucuronide, protocatechuic acid-4-glucuronide, vanillic acid-4-glucuronide, benzoic acid-4-glucuronide, isovanillic acid-3-glucuronide, protocatechuic acid-3-sulfate, protocatechuic acid-4-sulfate, vanillic acid-4-sulfate, isovanillic acid-3-sulfate and benzoic acid-4-sulfate) and probable colonic metabolites (2-hydroxybenzoic acid, 3-hydroxybenzoic acid, 4-hydroxybenzoic acid, 2,3-dihydroxybenzoic acid, 2,4-dihydroxybenzoic acid, protocatechuic acid, 3,5-dihydroxybenzoic acid, gallic acid, 2-methoxybenzoic acid, 4-methoxysalicylic acid, 6-methoxysalicyclic acid, vanillic acid, isovanillic acid, syringic acid, 3-methylgallic acid, methyl-3,4-dihydroxybenzoate, methyl-3,4-dimethoxybenzoate, methyl vanillate, methyl gallate, 4-hydroxybenzyl alcohol, *p*-coumaric acid, caffeic acid, ferulic acid, sinapic acid, phloroglucinaldehyde, 4-hydroxybenzaldehyde, 3,4-dihydroxybenzaldehyde, 4-hydroxyphenylacetic acid, homoprotocatechuic acid, homovanillic acid, hippuric acid, 3-methylhippuric acid, 4-methylhippuric acid) and four internal standards (scopoletin, phloridzin, taxifolin and 7,8-dihydroxycourmarin). The present chapter therefore describes methods for the identification and quantification of an extensive series of anthocyanin metabolites for use in future clinical intervention studies.

## 2.2. Materials and Methods

### 2.2.1. Chemicals

Cyanidin-3-glucoside, pelargonidin-3-glycoside, peonidin-3-glucoside, cyanidin-3-sambubioside, cyanidin-3-rutinoside and cyanidin-3,5-diglucoside were obtained from Extrasynthese (Genay, France). Phase II conjugates of phenolic acids (protocatechuic acid-3-glucuronide, protocatechuic acid-4-glucuronide, vanillic acid-4-glucuronide, benzoic acid-4-glucuronide, isovanillic acid-3-glucuronide, protocatechuic acid-3-sulfate, protocatechuic acid-4-sulfate, vanillic acid-4-sulfate, isovanillic acid-3-sulfate and benzoic acid-4-sulfate) were synthesised were synthesised at St Andrews University as part of a BBSRC collaborative project, via recently published methods (Zhang *et al.*, 2012). Formic acid, hydrochloric acid and the remaining compounds (2-hydroxybenzoic acid, 3-hydroxybenzoic acid, 4-hydroxybenzoic acid, 2,3-dihydroxybenzoic acid, 2,4-dihydroxybenzoic acid, protocatechuic acid, 3,5-dihydroxybenzoic acid, gallic acid, 2-methoxybenzoic acid, 4-methoxysalicylic acid, 6-methoxysalicyclic acid, vanillic acid, isovanillic acid, syringic acid,

3-methylgallic acid, methyl-3,4-dihydroxybenzoate, methyl-3,4-dimethoxybenzoate, methyl vanillate, methyl gallate, 4-hydroxybenzyl alcohol, *p*-coumaric acid, caffeic acid, ferulic acid, sinapic acid, phloroglucinaldehyde, 4-hydroxybenzaldehyde, 3,4-dihydroxybenzaldehyde, 4-hydroxyphenyl-acetic acid, homoprotocatechuic acid, homovanillic acid, hippuric acid, 3-methyl hippuric acid, 4-methyl hippuric acid, phloridzin, scopoletin, taxifolin and 7,8-dihydroxycourmarin) were purchased from Sigma-Aldrich (Dorset, UK). HPLC grade methanol, acetonitrile and ethyl acetate were purchased from Fisher Scientific (Loughborough, UK). All water utilised was of Milli-Q grade (18.2 MΩ $cm^{-1}$).

### 2.2.2. Materials

Strata-X™ SPE columns (6 mL, 500 mg, 88 Å), HPLC columns [Kinetex pentafluorophenol (PFP) reverse phase (RP) (2.6 µm, 100 × 4.6 mm, 100 Å), Synergi Max RP (4 µm, 250 × 4.6 mm, 80 Å), Luna C18 (2) RP (4 µm, 250 × 4.6 mm, 100 Å), Synergi Polar RP (4 µm, 250 × 4.6 mm, 80 Å)] and SecurityGuard® cartridges (PFP and C18, 4 × 2.0 mm) were purchased from Phenomenex (Macclesfield, UK). Bond Elute C18 SPE columns (20 mL, 5 g, 70 Å) and Eclipse XDB-C18 HPLC (5 µm, 150 × 4.6 mm, 80 Å) columns were from Agilent (Wokingham, UK). Sterile filtered human male serum from AB plasma, Discovery® DSC-18 SPE columns (6 mL, 1 g), Acrodisc PTFE syringe filters (13 mm, 0.45 µm) were purchased from Sigma-Aldrich (Dorset, UK). Human faeces and urine were collected following internal protocols, approved by the Norfolk Research Ethics Committee (Norfolk, UK).

### 2.2.3. Metabolite Modelling

To identify target compounds for method development, a model of the putative metabolism of anthocyanins was developed in ACD ChemSketch 2.0 (ACD Labs, UK) based on published and predicted phase I, phase II and colonic metabolites for anthocyanins, their derived phenolic acids and as well as other common flavonoid metabolites (Aura *et al.*, 2005; CheminatandBrouillard, 1986; Donovan *et al.*, 1999; Donovan *et al.*, 2002; Fernandes *et al.*, 2008; Mazza *et al.*, 1987; Mazza *et al.*, 2002; Moridani *et al.*, 2001; Williamson *et al.*, 2010).

### 2.2.4. Stock Standards

Stock solutions of pure standards were prepared at 5 mg/mL in dimethyl sulfoxide (DMSO) and used to produce a mixture of standards diluted to the appropriate concentration in 0.1% formic acid in methanol.

### 2.2.5. HPLC-ESI-MS/MS conditions

HPLC-ESI-MS/MS analysis was carried out on an Agilent (Wokingham, UK) 1200 series HPLC with the inclusion of an ABSciex (Warrington, UK) 3200 series Q-trap MS/MS, attached to a Turbo V electrospray ionisation (ESI) source. The column temperature was set at 37 °C with a 5 µL injection volume and absorbance was recorded at 265, 280, 300, 320, 360 and 525 nm. The following variables were further evaluated: column type [Eclipse XDB-C18 (5 µm, 150 × 4.6 mm, 80 Å), Kinetex PFP (2.6 µm, 100 × 4.6 mm, 100 Å), Synergi Max (4 µm, 250 × 4.6 mm, 80 Å), Luna C18 (2) (4 µm, 250 × 4.6 mm, 100 Å) and Synergi Polar (4 µm, 250 × 4.6 mm, 80 Å)], organic modifier (acetonitrile or methanol), ionic modifier (0.1 to 1.0% formic acid), flow rate (0.5 to 1.5 mL/min), HPLC mobile phase gradient elution and MS source and multiple reaction monitoring (MRM) related parameters.

Source parameters were manually optimised for flow rates of 1.5 mL/min using flow assisted syringe infusion; the HPLC flow gradient was set to 10% mobile phase B and the syringe infusion of the analyte (50 µM in 0.1% formic acid/methanol) was set to 10 µL/min. The source parameters were optimised based on the conditions which resulted in the most intense ion, and optimised parameters include temperature (200 to 750 °C), nebulizer gas (0 to 90 psi) and auxiliary gas (0 to 90 psi), curtain gas (CUR; 10 to 50 psi) and ion spray voltage (IS; -1000 to -4500 V; +1000 to +5500 V). The optimised method for HPLC-ESI-MS/MS analysis utilised a PFP column and guard cartridge with the mobile phase consisting of 0.1% formic acid (v/v) in water (mobile phase A) and 0.1% formic acid (v/v) in acetonitrile (mobile phase B) at a flow rate of 1.5 mL/min at 0 min, 1 mL/min at 7 to 14 min and 1.5 mL/min at 14 to 28 min. The gradient consisted of 1% B at 0 min, 7.5% B at 7 min, 7.6% B at 14 min, 10% B at 17 min, 12% B at 18.5 min, 12.5% B at 20 min, 30% B at 24 min, 90% B at 25 to 28 min, 1% B at 29 to 32 min. Optimal MS/MS source parameters included curtain gas 40, ion spray voltage (IS) -4000 V (or IS +5500 V), temperature 700 °C and nebulizer and auxiliary gas 60 psi.

MRM mode was used to identify and quantify analytes. MRM related parameters, including declustering potential (DP), entrance potential (EP), collision energy (CE) and collision exit potential (CXP), were individually optimised for each compound via direct syringe infusion using a Hamilton syringe pump (Bonaduz, Switzerland). Individual standards (50 µM in 0.1% formic acid/methanol) were injected at a constant flow rate of 10 µL/min. The ions in MRM mode were produced by collision-activated dissociation (CAD) of the selected precursor ions in the collision cell. The optimum CAD ($N_2$) was 3 arbitrary units. MRM analysis of mixed standards at 50 µM was used to verify the final method in positive and

negative mode and MRM related parameters were considered optimised when MRM intensities were above $5.0 \times 10^4$ counts per second.

### 2.2.6. Extraction chromatography

The SPE procedure was based on previously published methods (Woodward *et al.*, 2009) and optimised at the Institute of Food Research (Norwich, UK) for the following variables: SPE sorbent bed material (DSC-18 or Strata-X™), addition of preservative (with or without 10% ascorbate w/v in 10 mM ethylenediaminetetraacetic acid [EDTA]), acid modifier (formic acid or HCl), elution volume (1 to 9 mL) and final concentration [i.e. complete or incomplete (≈ 50 µL remaining) evaporation]. The final SPE method for urine and serum consisted of the samples being diluted 2:1 with 1% formic acid in milliQ water (pH 2.4) and loaded onto either DSC-18 (6 mL, 1 g, urine) or Strata-X™ (6 mL, 500 mg, serum) SPE columns. The columns had previously been conditioned with one column volume of 1% formic acid in methanol followed by one column volume of 1% formic acid in water (pH 2.4). After the samples were loaded, the columns were washed with two column volumes of 1% formic acid in water, dried under vacuum for 30 min and 'soaked' in one third of a column volume of 1% formic acid in methanol for 10 min. Extracts were eluted under gravity with 7 mL of 1% formic acid in methanol, concentrated to approximately 50 µL using a Speedvac® centrifugal evaporator and reconstituted with 200 µL 1% formic acid in water. A post-extraction volume marker (5 µL of 1 mM scopoletin) was added and used to accurately calculate volume.

Faecal samples were extracted using an identical process, except samples were first prepared, which included autoclaving at 121 °C for 30 min, lyophilisation and rehydration at 20% wet weight/volume as previously described (Graf *et al.*, 2006). Samples were then extracted via a two-stage methanol extraction (30 min vortex of 1:1 sample-to-solvent ratio) and evaporated to 2 mL, using a Speedvac® centrifugal evaporator. Samples were then loaded onto a conditioned Bond Elute C18 (20 mL, 5 g) SPE column, washed with two column volumes of acidified water (pH 2.4), eluted with 20 mL 1% formic acid in methanol and concentrated to approximately 1 mL using a Speedvac® centrifugal evaporator.

In order to establish the extraction efficiencies of the SPE methods, baseline urine, serum and faecal homogenates were spiked with the analytes of interest at 50 µM and allowed to stand for 20 min prior to extraction. All samples were syringe filtered [Acrodisc PTFE syringe filters (13 mm, 0.45 µm)] and stored at -80 °C prior to analysis. Extractions were conducted in triplicate.

### 2.2.7. Methods validation

Validation of the HPLC-MS/MS method was carried out in terms of the linearity, precision and accuracy of compounds spiked into mobile phase, using the guidelines set out by the Food and Drug Administration for Bioanalytical Methods Validation (2001) (FDA, 2001). Six-point calibration curves (0 to 20 µM) were prepared, by diluting the stock solutions to the appropriate concentration with mobile phase. The method was validated based on the mean, standard deviation and coefficient of variation (CV) of the slope after each concentration was injected six times.

The limit of detection (LOD) of an analytical method represents the lowest concentration of the test compound that remains acceptably detectable. LODs were established by calculating the concentration of analyte yielding a peak height signal-to-noise ratio of 3:1 (signal-to-noise method) when the analyte was spiked into urine, serum and faecal matrices at concentrations of 0.34 µM to 4 µM post extraction. Where the analytes of interest were endogenously present in the baseline matrix, peak heights were corrected for baseline concentrations.

The extraction methods were validated by calculating the extraction efficiencies of the compounds of interest spiked into baseline urine, serum and faecal homogenates prior to SPE, relative to matrix-matched (urine, serum, faeces) control samples spiked with the same mixture of the standards post SPE. Five-point calibration curves (25 µM to 400 µM) were constructed for each analyte within a matched-matrix, with coefficient of determination ($r^2$) established as linear ($r^2 \geq 0.99$). Extraction efficiency data are given as mean ± SD of three replicates and where stated, statistical comparisons were undertaken using t-tests ($p \leq 0.05$, $n = 3$) in SPSS 18 (IBM, UK).

The final urine and serum methods were applied to the analysis of anthocyanin metabolites in samples derived from a previous clinical intervention trial feeding participants (n=15) a 500 mg bolus of elderberry derived anthocyanins, where samples were collected for 3 h post bolus (Curtis *et al.*, 2009). The faecal method was applied to samples derived from a study feeding participants (n = 8) 500 mg $^{13}$C-labelled cyanidin-3-glucoside, where samples were collected for 48 h post bolus (Czank *et al.*, 2013). The analytes were quantified using the optimised extraction and detection methods and the lowest and highest urinary, plasma concentrations identified are presented.

## 2.3. Results

### 2.3.1. Metabolite modelling

Target compounds for method development were chosen based on previously published studies (Aura *et al.*, 2005; Cheminat *et al.*, 1986; Czank *et al.*, 2013; Donovan *et al.*, 1999; Donovan *et al.*, 2002; Fernandes *et al.*, 2008; Mazza *et al.*, 1987; Mazza *et al.*, 2002; Moridani *et al.*, 2001; Williamson *et al.*, 2010) and putative metabolites were modelled *in silico* using ACD ChemSketch 2.0 (ACD Labs, UK), based on known phase I and II conjugation pathways and colonic metabolism of other similarly structured flavonoids. For example, post consumption of a bilberry-lingonberry purée, a metabolism study identified benzoic acids including protocatechuic acid, syringic acid and vanillic acid, phenylacetic acids including homovanillic acid and homoprotocatechuic acid, and cinnamic acids including caffeic acid, ferulic acid and *p*-courmaric acid (Nurmi *et al.*, 2009). Therefore, these metabolites, and also phase II conjugates of these metabolites, such as methyl-3,4-dihydroxybenzoate, the methylated conjugated of vanillic acid, and 3-hydroxybenzoic acid, the dehydroxylated conjugated of protocatechuic acid, were included.

This approach yielded a total of 112 putative metabolites, including the parent structure (cyanidin-3-glucoside), its aglycone (cyanidin), two degradation products (protocatechuic acid and phloroglucinaldehyde), 97 phase I (oxidation, reduction and hydrolysis) and phase II (sulfation, glucuronidation, methylation and cysteine and glutathione conjugation) metabolites and 11 possible colonic metabolites based on microbiota degradation and conjugation reactions from the literature, including *ex vivo* (ForesterandWaterhouse, 2008) and i*n vitro* fermentation studies (Aura *et al.*, 2005; González-Barrio *et al.*, 2010). From these, 45 of the most probable metabolites were selected for method validation and utilised in the present study; 34 compounds were commercially available and purchased from Sigma-Aldrich, and ten were synthetically produced (sulfated and glucuronidated conjugates of protocatechuic acid, 4-hydroxybenzoic acid, vanillic acid and isovanillic acid) at St Andrews University (Zhang *et al.*, 2012) (**Table 2.1**).

**Table 2.1** Structures of the optimised anthocyanins, degradation products and putative metabolites.

| Structure | Common Name | IUPAC Name | Configuration[a] |
|---|---|---|---|
| Anthocyanin 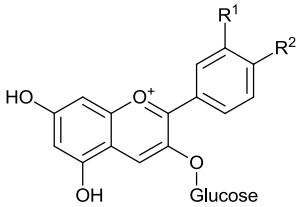 | Cyanidin-3-glucoside | (*2S,3R,4S,5R,6R*)-2-[2-(3,4-Dihydroxyphenyl)-5,7-dihydroxy-chromen-3-yl]oxy-6-(hydroxymethyl)oxane-3,4,5-triol | $R^1$,$R^2$ = OH |
| | Pelargonidin-3-glucoside | (2*S,3R,4S,5R,6R*)-2-[5,7-Dihydroxy-2-(4-hydroxyphenyl)chromen-3-yl]oxy-6-(hydroxymethyl)oxane-3,4,5-triol | $R^2$ = OH |
| | Peonidin-3-glucoside | (2S,3R,4S,5S,6R)-2-[5,7-dihydroxy-2-(4-hydroxy-3-methoxyphenyl)chromenylium-3-yl]oxy-6-(hydroxymethyl)oxane-3,4,5-triol | $R^1$=$OCH_3$, $R^2$=OH, |
| Benzoic acids 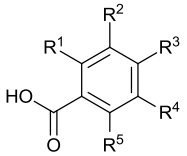 | 2-Hydroxybenzoic acid | 2-Hydroxybenzoic acid | $R^1$ = OH |
| | 3-Hydroxybenzoic acid | 3-Hydroxybenzoic acid | $R^2$ = OH |
| | 4-Hydroxybenzoic acid | 4-Hydroxybenzoic acid | $R^3$ = OH |
| | 2,3-Dihydroxybenzoic acid | 2,3-Dihydroxybenzoic acid | $R^1$,$R^2$ = OH |
| | 2,4-Dihydroxybenzoic acid | 2,4-Dihydroxybenzoic acid | $R^1$,$R^3$ = OH |
| | Protocatechuic acid | 3,4-Dihydroxybenzoic acid | $R^2$,$R^3$ = OH |
| | Protocatechuic acid-3-glucuronide | 6-(5-Carboxy-2-hydroxyphenoxy)-3,4,5-trihydroxytetrahydro-2*H*-pyran-2-carboxylic acid | $R^2$ = O-GlcA, $R^3$ = OH |
| | Protocatechuic acid-4-glucuronide | 6-(4-Carboxy-2-hydroxyphenoxy)-3,4,5-trihydroxytetrahydro-2*H*-pyran-2-carboxylic acid | $R^2$ = OH, $R^3$ = O-GlcA |
| | Protocatechuic acid-3-sulfate | 5-Carboxy-2-hydroxyphenyl sulfate | $R^2$ = $OSO_3^-$, $R^3$ = OH |
| | Protocatechuic acid-4-sulfate | 4-Carboxy-2-hydroxyphenyl sulfate | $R^2$ = OH, $R^3$ = $OSO_3^-$ |
| | 3,5-Dihydroxybenzoic acid | 3,5-Dihydroxybenzoic acid | $R^2$, $R^4$ = OH |
| | Gallic acid | 3,4,5-Trihydroxybenzoic acid | $R^2$,$R^3$,$R^4$ = OH |
| | 2-Methoxybenzoic acid | 2-Methoxybenzoic acid | $R^1$ = $OCH_3$ |
| | 3-Methoxybenzoic acid | 3-Methoxybenzoic acid | $R^2$ = $OCH_3$ |
| | 4-Methoxybenzoic acid | 4-Methoxybenzoic acid | $R^3$ = $OCH_3$ |
| | 4-Methoxysalicyclic acid | 2-Hydroxy-4-methoxybenzoic acid | $R^1$=OH, $R^3$=$OCH_3$ |
| | 6-Methoxysalicyclic acid | 2-Hydroxy-6-methoxybenzoic acid | $R^1$ = OH, $R^5$ = $OCH_3$ |
| | Vanillic acid | 4-Hydroxy-3-methoxybenzoic acid | $R^2$ = $OCH_3$, $R^3$ = OH |
| | Vanillic acid-4-glucuronide | 6-(4-Carboxy-2-methoxyphenoxy)-3,4,5-trihydroxytetrahydro-2*H*-pyran-2-carboxylic acid | $R^2$ = $OCH_3$, $R^3$ = O-GlcA |

| | | | |
|---|---|---|---|
| | Vanillic acid-4-sulfate | 4-Carboxy-2-methoxyphenyl sulfate | $R^2 = OCH_3$, $R^3 = OSO_3^-$ |
| | Isovanillic acid | 3-Hydroxy-4-methoxybenzoic acid | $R^2 = OH$, $R^3 = OCH_3$ |
| | Isovanillic acid-3-glucuronide | 6-(5-Carboxy-2-methoxyphenoxy)-3,4,5-trihydroxytetrahydro-2*H*-Pyran-2-carboxylic acid | $R^2$ = O-GlcA, $R^3 = OCH_3$ |
| | Isovanillic acid-3-sulfate | 5-Carboxy-2-methoxyphenyl sulfate | $R^2 = OSO_3^-$, $R^3 = OCH_3$ |
| | Syringic acid | 4-Hydroxy-3,5-dimethoxybenzoic acid | $R^2$,$R^4 = OCH_3$, $R^3$ = OH |
| | 3-Methylgallic acid | 3,5-Dihydroxy-4-methoxybenzoic acid | $R^3$,$R^5$ = OH, $R^4 = OCH_3$ |
| | Benzoic acid-4-glucuronide | 6-(4-Carboxyphenoxy)-3,4,5-trihydroxytetrahydro-2*H*-pyran-2-carboxylic acid | $R^3$ = O-GlcA |
| | Benzoic acid-4-sulfate | 4-Carboxyphenyl sulfate | $R^3 = OSO_3^-$ |
| Benzoates 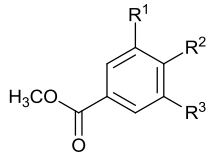 | Methyl-3,4-dihydroxybenzoate | Methyl 3,4-dihydroxybenzoate | $R^1$,$R^2$ = OH |
| | Methyl-3,4-dimethoxybenzoate | Methyl 3,4-dimethoxybenzoate | $R^1$,$R^2 = OCH_3$ |
| | Methyl vanillate | Methyl 4-hydroxy-3-methoxybenzoate | $R^1 = OCH_3$, $R^2$ = OH |
| | Methyl gallate | Methyl 3,4,5-trihydroxybenzoate | $R^1$,$R^2$,$R^3$ = OH |
| Benzyl alcohol 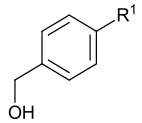 | 4-Hydroxybenzyl alcohol | (4-Acetyloxyphenyl)methyl acetate | $R^1$ = OH |
| Phenylpropenoic acids 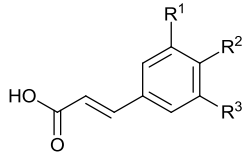 | *p*-Coumaric acid | 3-(4-Hydroxyphenyl)prop-2-enoic acid | $R^2$ = OH |
| | Caffeic acid | 3-(3,4-Dihydroxyphenyl)prop-2-enoic acid | $R^1$,$R^2$ = OH |
| | Ferulic acid | 3-(4-Hydroxy-3-methoxyphenyl)-prop-2-enoic acid | $R^1 = OCH_3$, $R^2$ = OH |
| | Sinapic acid | 3-(4-Hydroxy-3,5-dimethoxyphenyl)prop-2-enoic acid | $R^1$, $R^3 = OCH_3$, $R^2$ = OH |

| | | | |
|---|---|---|---|
| Benzaldehydes 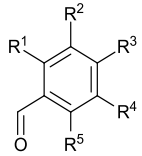 | Phloroglucinaldehyde | 2,4,6-Trihydroxybenzaldehyde | $R^1$,$R^3$,$R^5$ = OH |
| | 4-Hydroxybenzaldehyde | 4-Hydroxybenzaldehyde | $R^3$ = OH |
| | 3,4-Dihydroxybenzaldehyde | 3,4-Dihydroxybenzaldehyde | $R^2$,$R^3$ = OH |
| | Vanillin | 4-Hydroxy-3-methoxybenzalehyde | $R^2$ = $OCH_3$, $R^3$ = OH |
| Phenylacetic acids 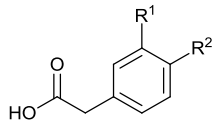 | 4-Hydroxyphenylacetic acid | 2-(4-Hydroxyphenyl)acetic acid | $R^2$ = OH |
| | Homoprotocatechuic acid | 2-(3,4-Dihydroxyphenyl)acetic acid | $R^1$,$R^2$ = OH |
| | Homovanillic acid | 2-(4-Hydroxy-3-methoxy-phenyl)acetic acid | $R^1$ = OH, $R^2$ = $OCH_3$ |
| Hippuric acids 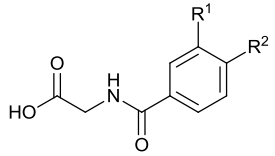 | Hippuric acid | 2-Benzamidoacetic acid | $R^1$,$R^2$ =H |
| | 3-Methylhippuric acid | 3-Methylhippuric acid | $R^1$ = $CH_3$ |
| | 4-Methylhippuric acid | 4-Methylhippuric acid | $R^2$ = $CH_3$ |

$R^1$-$R^5$ represents hydrogen (H) or position of [a]functional group. OH, hydroxyl; $OCH_3$, methoxy; $CH_3$, methyl; O-GlcA, O-glucuronide; $OSO_3^-$, sulfate.

### 2.3.2. HPLC-ESI-MS/MS

To obtain the optimal separation of the analytes of interest by HPLC-UV/vis, system conditions including column type, flow rate, acid modifier and organic modifier were investigated. Five HPLC columns commonly utilised in flavonoid analysis (Eclipse XDB C18, Kinetex PFP, Synergi Max, Luna C18 and Synergi Polar RP) were selected to establish the chromatographic separation of the target compounds. The PFP column resulted in 29 ± 14% to 45 ± 15% reduction in peak width (**Figure 2.1A**) and 42 ± 22% to 77 ± 45% increase in peak height (Figure 2.1B) compared to the Eclipse C18, Synergi Max, Luna C18 and Synergi Polar RP columns. The PFP column thereby yielded the highest selectivity for aromatic and polar compounds, giving the best separation of the structurally similar aromatic compounds. This was particularly evident for the sulfated compounds; the Eclipse and Luna C18 columns resulted in very poor resolution and separation of the sulfated compounds, the Synergi Max and Polar RP columns resulted in improved resolution, however, the PFP column provided the greatest resolution, with two to tenfold improvement in peak intensity relative to the other stationary phases (**Figure 2.2**). No column tested was capable of sufficiently separating the isomers of protocatechuic acid-sulfate under the explored conditions.

**Figure 2.1** HPLC column optimisation

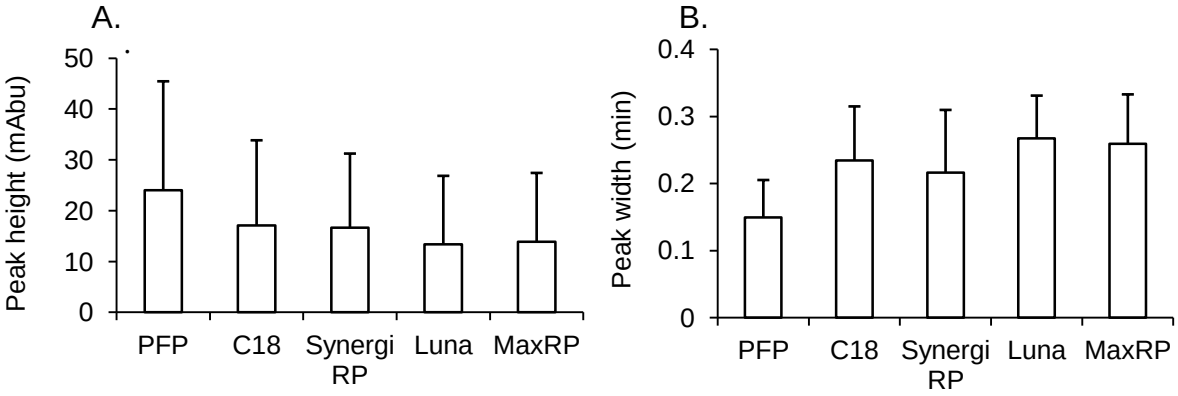


(A) Peak width relative to column type, (B) peak height relative to column type. Graphs are depicted as mean +SD of n=10 compounds (cyanidin-3-glucoside, pelargonidin-3-glucoside, scopoletin, *p*-courmaric acid, phloroglucinaldehyde, ferulic acid, benzoic acid-4-glucuronide, sinapic acid, isovanillic acid and gallic acid).

**Figure 2.2** MRM chromatograms of sulfated metabolites using Eclipse C18, Luna C18, Synergi max RP, Synergi Polar RP and Kinetex PFP HPLC columns.

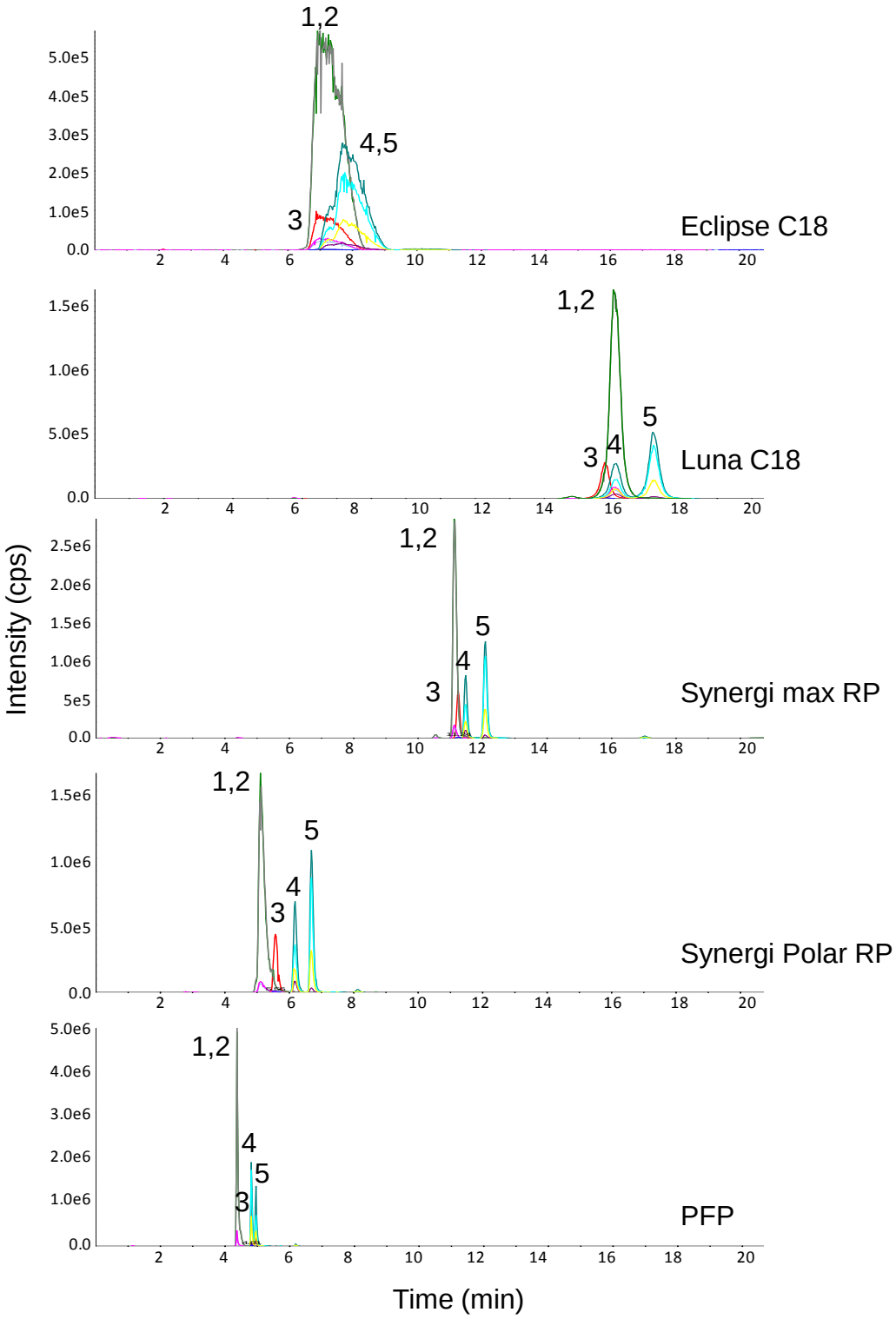


Flow rate: 1 mL/min; Solvent A: 0.1% formic acid in water (v/v); Solvent B: 0.1% formic acid in acetonitrile (v/v); gradient: 1-15% B at 0 minutes, 15% B at 15 minutes; 99% B at 17 to 20 minutes. [1]PCA-4-sulfate; [2]PCA-3-sulfate; [3]benzoic acid-4-glucuronide; [4]vanillic acid-4-glucuronide; [5]isovanillic acid-3-glucuronide.

Flow rates between 1.0 mL/min and 1.5 mL/min were tested on the PFP column, to establish the optimal flow rate for the separation and resolution of the analytes of interest. The maximum flow rate (1.5 mL/min) within the systems pressure limits (400 bar) was selected as it provided optimal peak resolution (reduced peak broadening), resulting in a 40% reduced peak width relative to 1 mL/min (**Figure 2.3**). A flow rate of 1.5 mL/min decreasing to 1 mL/min from 7 to 14 min was necessary to achieve optimal separation while staying within the pressure limitations of the HPLC system utilised.

**Figure 2.3** HPLC flow rate optimisation

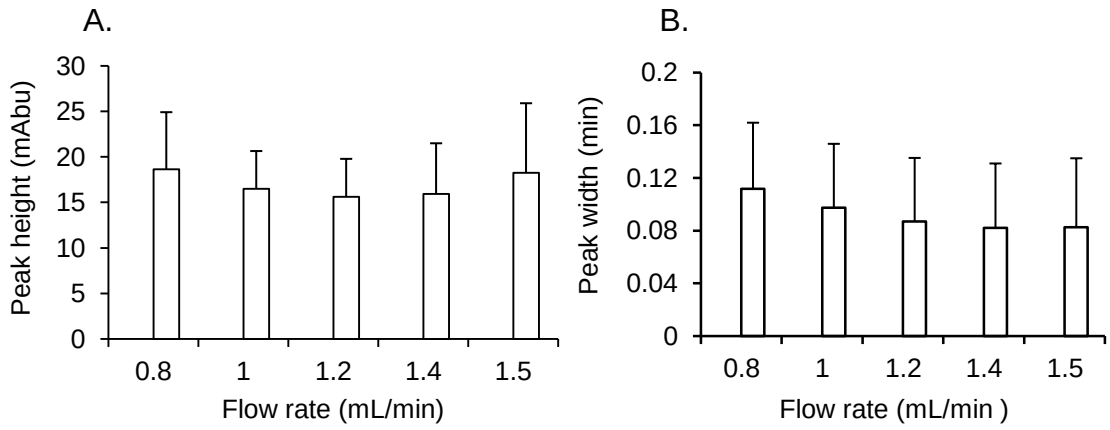


(A) Peak height and (B) peak width of n=10 compounds (cyanidin-3-glucoside, pelargonidin-3-glucoside, scopoletin, p-courmaric acid, phloroglucinaldehyde, ferulic acid, benzoic acid-4-glucuronide, sinapic acid, isovanillic acid and gallic acid) with flow rates of 0.8 mL/min to 1.5 mL/min. Graphs are depicted as mean +SD.

Acid modifier concentration of 0%, 0.1%, 0.5% and 1% formic acid were tested on the PFP column, to establish the optimal flow rate for the separation and resolution of the analytes of interest. The peak intensities and the peak widths of the phenolic analytes decreased with increasing formic acid within the mobile phase; 0.1% formic acid resulted in a 389 ± 530% increase in peak height relative to 1% formic acid (**Figure 2.4A**). Furthermore, a lower increase in peak width (i.e. decrease in peak resolution) was observed using 0.1% formic acid (144 ± 44% increase relative to 1% formic acid) compared to 0% formic acid (216 ± 87% increase relative to 1% formic acid) (Figure 2.4C). A similar effect was observed for the anthocyanins peak width, which demonstrated a significantly lower increase in peak width (i.e. decrease in peak resolution) using 0.1% formic acid (213 ± 23% increase relative to 1% formic acid) compared to 0% formic acid (1150 ± 60% increase relative to 1% formic acid) (Figure 2.4E). In contrast, the anthocyanin peak intensities (Figure 2.4B) decreased with decreasing formic acid (Figure 2.4D). In the current study, 0.1% formic acid was

selected for HPLC-ESI-MS/MS analysis as it provided overall the optimal resolution for phenolic analytes and anthocyanins.

**Figure 2.4** HPLC optimisation of acid modifier in mobile phase

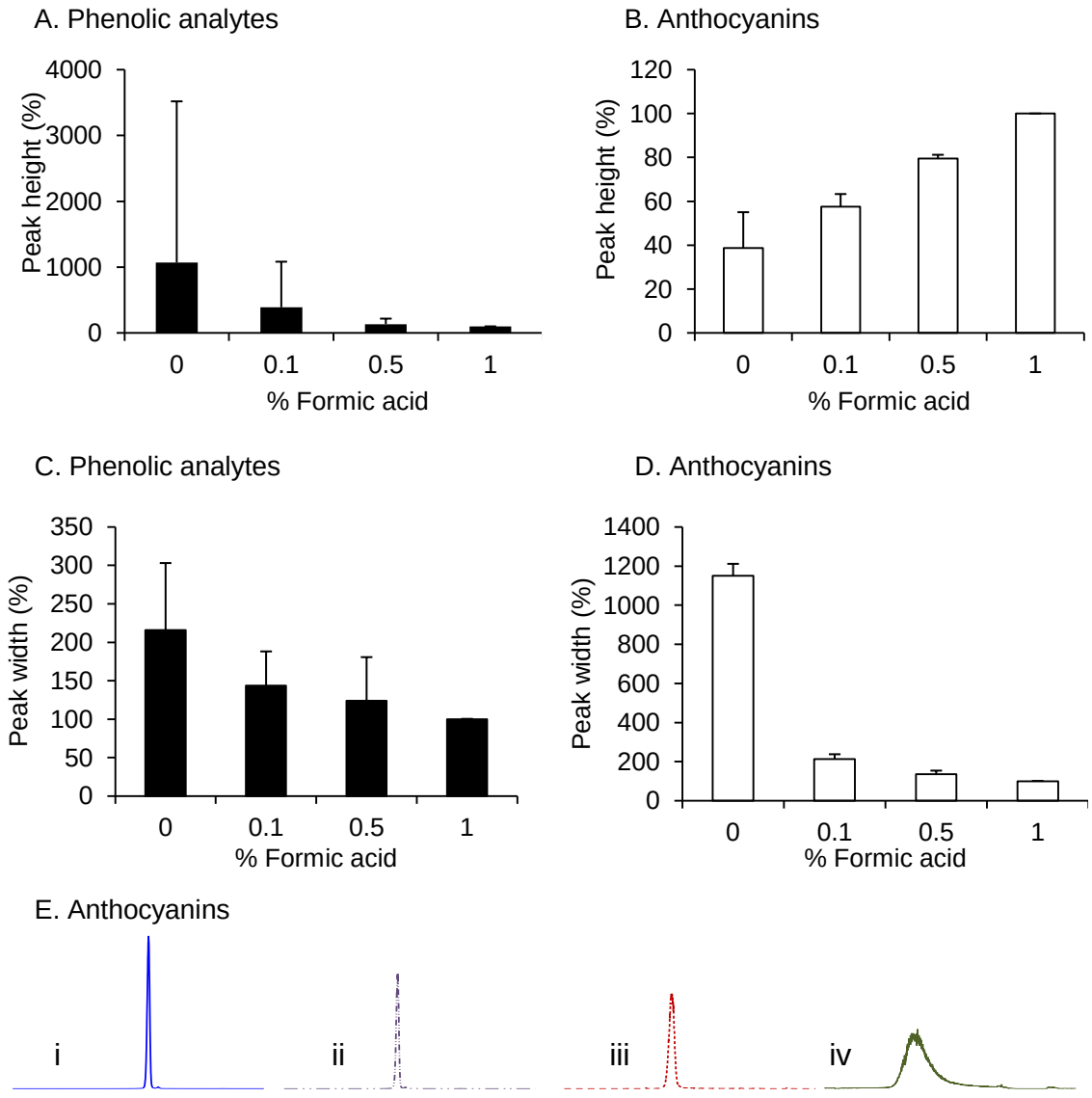


Peak height of (A) phenolic analytes and (B) anthocyanins, and peak widths of (C) phenolic analytes and (D) anthocyanins with 0%, 0.1%, 0.5% and 1% formic acid within the mobile phase. Flow rate: 1 mL min-1; gradient: 1-15% B at 0 minutes, 15% B at 15 minutes; 99% B at 17 to 20 minutes. Values are represented as mean % change relative to 1% formic acid +SD [phenolic analytes, n=19: protocatechuic acid (PCA), vanillic acid (VA), PCA-4-sulfate, VA-4-sulfate, benzoic acid (BA)-4-glucuronide (GlcA), PCA-4-GlcA, VA-4-GlcA, BA-4-sulfate, Methyl-3,4-dihydroxybenzoate, homoPCA, caffeic acid, hippuric acid, ferulic acid, phloroglucinaldehyde, *p*-courmaric acid, 4-hydroxyBA, 3,4-dihydroxybenzaldehyde, gallic acid and phloridzin; anthocyanins, n=3: cyanidin-3-glucoside, cyanidin-3-rutinoside, pelargonidin-3-glucoside]. (E) Extracted MRM chromatograms for cyanidin-3-glucoside with i) 1%, ii) 0.5, iii) 0.1% and iv) 0% formic acid in the mobile phase.

The organic modifiers, methanol and acetonitrile were compared for their suitability for use with anthocyanin and putative anthocyanin metabolites. Acetonitrile provided a 138 ± 78% increase in peak intensity (**Figure 2.5A**) and a 20 ± 31% decrease in peak width (Figure 2.5C) for the phenolic analytes compared to methanol. However, the opposite effect was observed for the anthocyanins tested, with a 78 ± 83% increase in peak intensities (Figure 2.5C) and (81 ± 25%) decrease in peak widths (Figure 2.5D) observed with methanol compared to acetonitrile. Acetonitrile was selected as the optimal organic modifiers, as it was optimal for the separation and detection of the phenolic analytes.

**Figure 2.5** HPLC optimisation of organic modifier in mobile phase

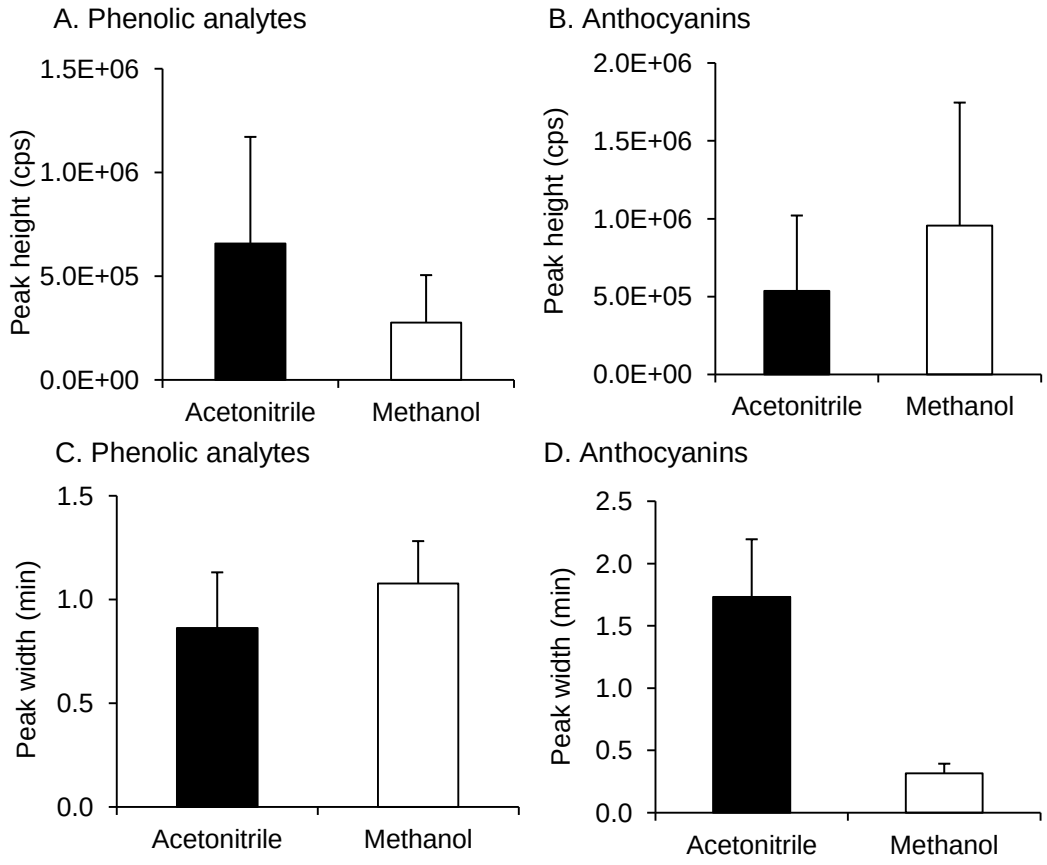


Peak height of (A) phenolic analytes and (B) anthocyanins and peak widths of (C) phenolic analytes and (D) anthocyanins with the mobile phase containing 0.1% formic acid in acetonitrile or methanol. [Phenolic metabolites, n=19: protocatechuic acid (PCA), vanillic acid (VA), PCA-4-sulfate, VA-4-sulfate, benzoic acid (BA)-4-glucuronide (GlcA), PCA-4-GlcA, VA-4-GlcA, BA-4-sulfate, Methyl-3,4-dihydroxybenzoate, homoPCA, caffeic acid, hippuric acid, ferulic acid, phloroglucinaldehyde, *p*-courmaric acid, 4-hydroxyBA, 3,4-dihydroxybenzaldehyde, gallic acid and phloridzin; anthocyanins, n=3: cyanidin-3-glucoside, cyanidin-3-rutinoside, pelargonidin-3-glucoside]. Values are represented as mean +SD.

The source parameters for the electrospray ionisation (ESI) Turbo V source were manually optimised to provide the optimal nebulisation, evaporation and ionisation for a flow rate of 7% acetonitrile at 1.5 mL/min using flow assisted syringe infusion (FIA). Optimised source parameters were established as a CUR of 40 psi, which prevented solvent entering the orifice, a temperature of 700 °C, which ensured evaporation at 1.5 mL/min and gas flows of 60 psi (nebulizer and auxiliary gas) for optimal nebulisation of the solvent. The position of the ionisation needle was optimised to give the highest ion intensity at x=5, y=5.

The MRM related parameters, consisting of declustering potential (DP), entrance potential (EP), collision energy (CE) and collision exit potential (CXP), were optimised for each individual compound separately in positive or negative mode in order to select the most abundant ion pairs and the optimal declustering and entrance potentials and collision energies for fragmenting and focusing the ions through the quadruples. Compound parameters were optimised for the three most intense ion transitions (**Table 2.2**) and MRM analysis of a 50 µM mixed standard of the 45 analytes was used to verify the final method in positive and negative mode (**Figure 2.6**).

### 2.3.3. HPLC-ESI-MS/MS method validation

The final HPLC-MS/MS method was validated across 45 analytes for linearity, precision and accuracy using six-point calibration curves in mobile phase following six repeat injections. All calibration curves were linear over the concentration ranges (1.25 to 20 µM), with correlation coefficients ($r^2$) ranging from 0.991 to 1.000 (CV, 0.2%) (Table 2.2). The CV of the slope ranged from 1.4% for vanillic acid-4-sulfate to 9.6% for pelargonidin-3-glucoside. The sensitivity of the method was established using baseline serum, urine and faecal samples derived from previously conducted anthocyanin intervention trials (Czank *et al.*, 2013; de Ferrars *et al.*, 2013; de Ferrars *et al.*, 2014), which were spiked post extraction. The HPLC-ESI-MS/MS LODs ranged from 1 nM for phloridzin to 2604 nM for homovanillic acid in urine, 0.3 nM for phloridzin to 2340 nM for homovanillic acid in serum and 1 nM for phloridzin to 2238 nM for 4-hydroxyphenylacetic acid in faeces (**Table 2.3**).

**Table 2.2** Optimised multiple reaction monitoring (MRM) transitions and parameters of target analytes[a]

| Analyte | MRM mode | λmax (nm) | Rt (min) | MW | Precursor ion (*m/z*)[b] | $MS^2$ Fragments (m/z) | CE (V) | DP (V) | EP (V) | CXP (V) |
|---|---|---|---|---|---|---|---|---|---|---|
| **Anthocyanins** | | | | | | | | | | |
| Cyanidin-3-glucoside | + | 514 | 11.7 | 449.4 | 449 | 287[c],241,213,137 | 30,70,70,70 | 60 | 5 | 2 |
| Pelargonidin-3-glucoside | + | 502 | 14.6 | 433.3 | 433 | 271[c],197,121,65 | 30,70,70,120 | 50 | 5 | 2 |
| Peonidin-3-glucoside | + | 518 | 16.9 | 463.4 | 463 | 301[c] | 10 | 30 | 5 | 2.5 |
| Cyandin-3-sambubioside | + | 516 | 12.0 | 581.5 | 581 | 287[c] | 10 | 30 | 5 | 2.5 |
| Cyanidin-3-rutinoside | + | 518 | 13.32 | 595.5 | 595 | 287[c] | 10 | 30 | 5 | 2.5 |
| Cyanidin-3,5-diglucoside | + | 512 | 7.18 | 611.5 | 611 | 287[c] | 10 | 30 | 5 | 2.5 |
| **Benzoic acids** | | | | | | | | | | |
| 2-Hydroxybenzoic acid | - | 300 | 19.0 | 138.1 | 137 | 93[c],75,65 | -25,-50,-40 | -30 | -7 | -2 |
| 3-Hydroxybenzoic acid | - | 298 | 8.6 | 138.1 | 137 | 93[c],65 | -18,-16 | -40 | -9 | 0 |
| 4-Hydroxybenzoic acid | - | 258 | 6.8 | 138.1 | 137 | 93[c],65 | -20,-22 | -35 | -5 | 0 |
| 2,3-Dihydroxybenzoic acid | - | 315 | 9.3 | 154.1 | 153 | 109[c],91 | -22,-32 | -60 | -2 | 0 |
| 2,4-Dihydroxybenzoic acid | - | 258 | 10.1 | 154.1 | 153 | 109,65[c] | -22,-26 | -35 | -5 | 0 |
| Protocatechuic acid (PCA) | - | 260 | 4.5 | 154.1 | 153 | 108[c],91,81 | -31,-31,-31 | -42 | -10 | 0 |
| PCA-3-glucuronide | - | 256 | 4.2 | 330.2 | 329 | 175,153[c],113,109 | -21,-25,-25,-50 | -45 | -5 | -3 |
| PCA-4-glucuronide | - | 252 | 3.1 | 330.2 | 329 | 175,153[c],113,109 | -21,-25,-25,-50 | -45 | -5 | -3 |
| PCA-3 and 4-sulfate | - | 256 | 5.0 | 233.0 | 231 | 189,153,109[c],97 | -15,-25,-40,-30 | -38 | -3 | -2 |
| 3,5-Dihydroxybenzoic acid | - | 250 | 4.5 | 154.1 | 153 | 109[c],67,65, | -16, -16,-18 | -35 | -9 | 0 |
| Gallic acid | - | 276 | 2.5 | 170.1 | 169 | 125[c],107,79 | -15,-15,-15 | -50 | -7 | 0 |
| 2-Methoxybenzoic acid | + | 296 | 13.4 | 152.1 | 153 | 135[c],92,77,63 | 16,35,30,70 | 40 | 7 | 6 |
| 4-Methoxysalicylic acid | - | 256 | 21.8 | 168.1 | 167 | 123,108[c],80 | -15,-25,-35 | -34 | -3 | -2 |
| 6-Methoxysalicyclic acid | - | 254 | 23.7 | 168.1 | 167 | 123[c],109 | -20,-30 | -21 | -8 | -2 |
| Vanillic acid | - | 262 | 9.6 | 168.1 | 167 | 152[c],123,108 | -20,-14,-20 | -30 | -2 | 0 |
| Vanillic acid-4-glucuronide | - | 254 | 4.5 | 344.3 | 343 | 175,167,152,113[c],108 | -15,-20,-40,-20,-55 | -60 | -4 | -2 |
| Vanillic acid-4-sulfate | - | 252 | 7.4 | 247.0 | 245 | 167[c],152,123,108 | -20,-25,-30,-30 | -33 | -4 | -2 |
| Isovanillic acid | + | 260 | 9.8 | 168.1 | 169 | 151[c],125,93,65 | 19,12,19,34 | 27 | 6 | 6 |
| Isovanillic acid-3-glucuronide | - | 260 | 5.8 | 344.3 | 343 | 175,167,152,113[c],108 | -15,-30,-40,-20,-55 | -66 | -4 | -2 |

| | | | | | | | | | | |
|---|---|---|---|---|---|---|---|---|---|---|
| Isovanillic acid-3-sulfate | - | 254 | 6.8 | 233.0 | 231 | 167[c],152,108,80 | -25,-30,-40,-45 | -33 | -4 | -2 |
| Syringic acid | + | 274 | 12.2 | 198.2 | 199 | 155,140[c],125,77 | 13,21,39,35 | 34 | 5 | 6 |
| 3-Methylgallic acid | - | 272 | 7.5 | 184.1 | 183 | 168[c],139 | -16,-16 | -36 | -3 | -5 |
| Benzoic acid-4-glucuronide | - | 248 | 2.7 | 314.2 | 313 | 175,137,113,93[c] | -15,-20,-20,-54 | -54 | -7 | -2 |
| Benzoic acid-4-sulfate | - | 248 | 6.4 | 217.0 | 217 | 173,137[c] | -10,-21 | -31 | -3 | -2 |
| **Benzoates** | | | | | | | | | | |
| Methyl 3,4-dihydroxybenzoate | - | 260 | 13.9 | 168.1 | 167 | 108[c],91 | -28,-30 | -45 | -8 | 0 |
| Methyl 3,4-dimethoxybenzoate | + | 260 | 24.7 | 196.2 | 197 | 165,153,138[c] | 17,15,15 | 36 | 9 | 4 |
| Methyl vanillate | + | 262 | 21.2 | 182.2 | 183 | 151[c],124,107,77 | 18,20,40,40 | 38 | 6 | 2 |
| Methyl gallate | - | 272 | 7.9 | 184.1 | 183 | 124[c],106,78 | -28,-38,-42 | -45 | -4 | 0 |
| **Benzyl alcohols** | | | | | | | | | | |
| 4-Hydroxybenzyl alcohol | - | 276 | 5.1 | 124.1 | 123 | 105,77[c] | -15,-20 | -24 | -10 | -2 |
| **Phenylpropenoic acids** | | | | | | | | | | |
| *p*-Coumaric acid | - | 310 | 15.5 | 164.2 | 163 | 119[c],117,93 | -20,-42,-40 | -30 | -10 | 0 |
| Caffeic acid | - | 324 | 10.6 | 180.2 | 179 | 135[c],106,89 | -20,-40,-40 | -45 | -6 | -2 |
| Ferulic acid | - | 320 | 18.9 | 194.2 | 193 | 178,149,134[c] | -20,-20,-20 | -30 | -6 | -2 |
| Sinapic acid | - | 322 | 20.4 | 224.2 | 223 | 208[c],193,164,149,121 | -18,-28,-22,-28,-40 | -38 | -2 | -2 |
| **Benzaldehydes** | | | | | | | | | | |
| Phloroglucinaldehyde | - | 292 | 18.2 | 154.1 | 153 | 151[c],125,107,83 | -20,-20,-20,-20 | -88 | -7 | -2 |
| 4-Hydroxybenzaldehyde | - | 285 | 9.4 | 122.1 | 121 | 108[c],92,65 | -31,-34,-35 | -47 | -7 | -10 |
| 3,4-Dihydroxybenzaldehyde | - | 280 | 6.5 | 138.1 | 137 | 108[c],92,81 | -30,-30,-26 | -40 | -10 | 0 |
| Vanillin | - | 280 | 12.6 | 152.2 | 151 | 136[c],108,92 | -20,-30,-30 | -25 | -6 | 0 |
| **Phenylacetic acids** | | | | | | | | | | |
| 4-Hydroxyphenylacetic acid | - | 275 | 7.4 | 152.1 | 151 | 123,107[c],93,79 | -25,-17,-25,-25 | -50 | -7 | -2 |
| Homoprotocatechuic acid | - | 280 | 5.1 | 168.1 | 167 | 123[c],108,95 | -20,-30,-40 | -20 | -8 | -2 |
| Homovanillic acid | - | 280 | 10.1 | 182.2 | 181 | 137[c],122 | -10,-20 | -43 | -2 | -4 |
| **Hippuric acids** | | | | | | | | | | |
| Hippuric acid | - | 246 | 6.9 | 179.2 | 178 | 134[c],132,77 | -18,-22,-22 | -40 | -3 | 0 |
| 3-Methylhippuric acid | - | 246 | 14.1 | 193.2 | 192 | 148[c],146,91 | -16,-22,-26 | -35 | -10 | 0 |
| 4-Methylhippuric acid | - | 246 | 13.8 | 193.2 | 192 | 148[c],146,91 | -16,-22,-26 | -35 | -5 | 0 |
| **Internal Standards** | | | | | | | | | | |
| Phloridzin | - | 286 | 24.2 | 436.4 | 435 | 273[c],167,123,81 | -26,-40,-50,-80 | -40 | -4 | -2 |

| | | | | | | | | | | |
|---|---|---|---|---|---|---|---|---|---|---|
| Scopoletin | - | 350 | 19.1 | 192.2 | 192 | 148,120,104[c] | -32,-28,-34 | -35 | -10 | 0 |
| Scopoletin | + | 350 | 19.1 | 192.2 | 193 | 133[c],122,94 | 27,37,43 | 56 | 4 | 4 |
| Taxifolin | - | 288 | 20.8 | 304.2 | 303 | 285,151,125[c] | -17,-30,-30 | -50 | -5 | 0 |
| 7,8-Dihydroxycourmarin | - | 322 | 10.6 | 178.1 | 177 | 121[c],105,93 | -30,-26,-32 | -50 | -8 | 0 |

[a]A dwell time of 50 ms was used across all transitions; [b]Precursor and [c]daughter transition used for MRM quantitation. Rt, retention time; CE, collision energy corresponding to $MS^2$ fragment; DP, declustering potential; MW, molecular weight; V, Volts;

**Figure 2.6** Multiple reaction monitoring (MRM) chromatogram showing the ion pairs used for quantification for the optimised negative (A) and positive (B) HPLC-MS/MS methods.

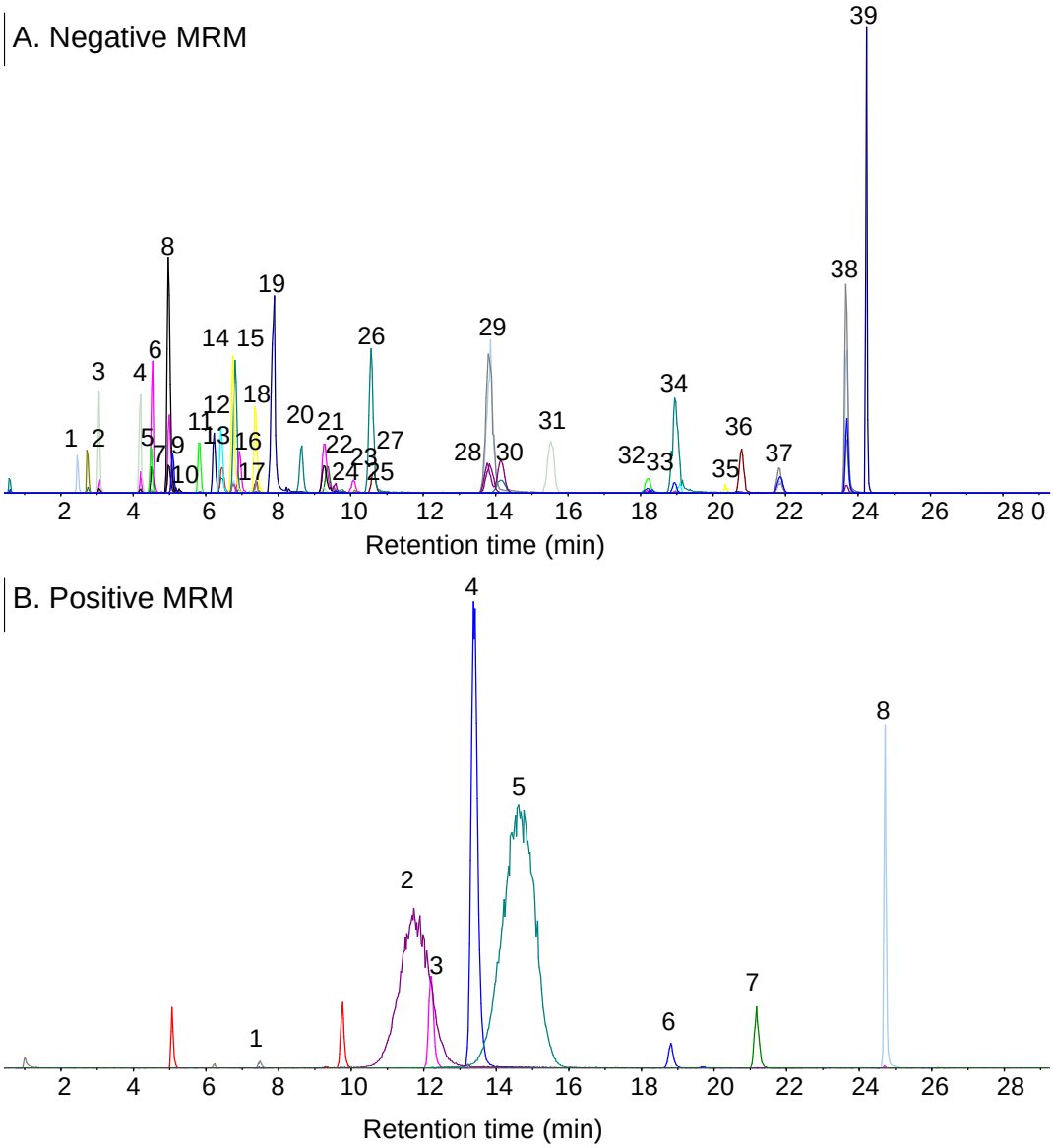


(A) [1]Gallic acid, [2]benzoic acid (BA)-4-glucuronide, [3]protocatechuic acid (PCA)-4-glucuronide, [4]PCA-3-glucuronide, [5]vanillic acid (VA)-4-glucuronide, [6]PCA, [7]3,5-dihydroxy BA, [8]PCA-3 and 4-sulfate, [9]4-hydroxybenzyl alcohol, [10]homoPCA, [11]isoVA-3-glucuronide, [12] BA-4-sulfate, [13]3,4-dihydroxybenzaldehyde, [14]isoVA-3-sulfate, [15]4-hydroxyBA, [16]hippuric acid, [17]4-hydroxyphenylacetic acid, [18]VA-4-sulfate, [19]methyl gallate, [20]3-hydroxyBA, [21]2,3-dihydroxyBA, [22]4-hydroxybenzaldehyde, [23]VA, [24]2,4-dihydroxyBA, [25]homoVA, [26]caffeic acid, [27]7,8-dihydroxycourmarin, [28]4-methylhippuric acid, [29]methyl-3,4-dihydroxybenzoate, [30]3-methylhippuric acid, [31]*p*-coumaric acid, [32]phloroglucinaldehyde, [33]ferulic acid, [34]2-hydroxyBA, [35]sinapic acid, [36]taxifolin, [37]4-methoxysalicylic acid, [38]6-methoxysalicyclic acid, [39]phloridzin. (B) [1]3-methylgallic acid, [2]cyanidin-3-glucoside, [3]isoVA, [4]syringic acid, [5]pelargonidin-3-glucoside, [5]2-methoxyBA, [7]methyl vanillate, [8]methyl-3,4-dimethoxybenzoate.

**Table 2.3** Validation of HPLC-MS/MS methods within urine, serum and faecal matrices.

| Analyte | Slope (a)[a] Mean ± SD | CV (%) | $R^2$ | LOD (nM) Urine | Serum | Faeces |
|---|---|---|---|---|---|---|
| **Anthocyanins** | | | | | | |
| Cyanidin-3-glucoside | 594,473 ± 39,888 | 6.71 | 0.998 | 2 | 4 | 4 |
| Pelargonidin-3-glucoside | 1,034,231 ± 98,822 | 9.56 | 0.996 | 2 | 1 | 2 |
| **Benzoic acids** | | | | | | |
| 2-Hydroxybenzoic acid | 189,231 ± 4,334 | 2.29 | 0.998 | 116 | 86 | 136 |
| 3-Hydroxybenzoic acid | 60,138 ± 2,698 | 4.49 | 0.999 | 173 | 191 | 214 |
| 4-Hydroxybenzoic acid | 167,981 ± 7,078 | 4.21 | 0.995 | 139 | 74 | 86 |
| 2,3-Dihydroxybenzoic acid | 78,108 ± 1,819 | 2.33 | 0.999 | 92 | 29 | 126 |
| 2,4-Dihydroxybenzoic acid | 19,681 ± 746 | 3.79 | 0.999 | 98 | 68 | 112 |
| Protocatechuic acid (PCA) | 15,128 ± 760 | 5.02 | 0.997 | 41 | 1 | 9 |
| PCA-3-glucuronide | 174,408 ± 5711 | 3.27 | 0.999 | 6 | 1 | 4 |
| PCA-4-glucuronide | 102,003 ± 4,943 | 4.85 | 0.999 | 5 | 2 | 4 |
| PCA-3 and 4-sulfate | 378,495 ± 13,989 | 3.70 | 0.998 | 1 | 2 | 1 |
| 3,5-Dihydroxybenzoic acid | 234,649 ± 8,897 | 3.79 | 0.996 | 24 | 31 | 150 |
| Gallic acid | 34,012 ± 907 | 2.67 | 0.997 | 15 | 29 | 20 |
| 2-Methoxybenzoic acid | 400,431 ± 20,139 | 5.03 | 0.996 | 16 | 23 | 22 |
| 4-Methoxysalicylic acid | 300,116 ± 9,224 | 3.07 | 0.998 | 23 | 29 | 375 |
| 6-Methoxysalicyclic acid | 15,687 ± 583 | 3.72 | 0.999 | 116 | 25 | 333 |
| Vanillic acid | 11,322 ± 337 | 2.97 | 0.999 | 53 | 16 | 45 |
| Vanillic acid-4-glucuronide | 56,069 ± 2,416 | 4.31 | 0.999 | 37 | 6 | 11 |
| Vanillic acid-4-sulfate | 214,295 ± 3,041 | 1.42 | 0.999 | 2 | 3 | 3 |
| Isovanillic acid | 30,715 ± 1,362 | 4.44 | 0.998 | 47 | 77 | 94 |
| Isovanillic acid-3-glucuronide | 67,871 ± 3,294 | 4.85 | 1.000 | 9 | 5 | 9 |
| Isovanillic acid-3-sulfate | 308,646 ± 7,864 | 2.55 | 0.999 | 2 | 3 | 3 |
| Syringic acid | 61,287 ± 2,709 | 4.42 | 0.998 | 16 | 45 | 21 |
| 3-Methylgallic acid | 1,584 ± 69 | 4.37 | 0.997 | 360 | 121 | 400 |
| Benzoic acid-4-glucuronide | 66,978 ± 2,529 | 3.78 | 0.998 | 4 | 10 | 21 |
| Benzoic acid-4-sulfate | 143,079 ± 4,552 | 3.18 | 0.998 | 1 | 4 | 2 |
| **Benzoates** | | | | | | |
| Methyl 3,4-dihydroxybenzoate | 230,527 ± 10,659 | 4.62 | 0.996 | 2 | 3 | 6 |
| Methyl 3,4-dimethoxybenzoate | 93,306 ± 5,946 | 6.37 | 0.999 | 8 | 23 | 22 |
| Methyl vanillate | 33,814 ± 3,204 | 9.47 | 0.999 | 43 | 68 | 36 |
| Methyl gallate | 257,934 ± 19,070 | 7.39 | 1.000 | 1 | 2 | 3 |
| **Benzyl alcohols** | | | | | | |
| 4-Hydroxybenzyl alcohol | 963 ± 40 | 4.16 | 0.995 | 62 | 246 | 424 |

| | | | | | | |
|---|---|---|---|---|---|---|
| **Phenylpropenoic acids** | | | | | | |
| *p*-Coumaric acid | 111,853 ± 8,169 | 7.30 | 0.994 | 46 | 51 | 30 |
| Caffeic acid | 333,099 ± 8,610 | 2.58 | 0.992 | 67 | 122 | 100 |
| Ferulic acid | 40,588 ± 1,939 | 4.78 | 1.000 | 14 | 9 | 67 |
| Sinapic acid | 7,806 ± 638 | 8.17 | 0.999 | 39 | 7 | 20 |
| **Phenylaldehydes** | | | | | | |
| Phloroglucinaldehyde | 23,907 ± 1,126 | 4.71 | 0.992 | 13 | 5 | 40 |
| 4-Hydroxybenzaldehyde | 1,235 ± 63 | 5.11 | 0.998 | 25 | 40 | 14 |
| 3,4-Dihydroxybenzaldehyde | 43,960 ± 1,288 | 2.93 | 0.993 | 10 | 4 | 2 |
| **Phenylacetic acids** | | | | | | |
| 4-Hydroxyphenylacetic acid | 30,535 ± 1,017 | 3.33 | 0.998 | 116 | 938 | 2,238 |
| HomoPCA | 2,146 ± 65 | 3.03 | 0.999 | 108 | 117 | 413 |
| Homovanillic acid | 23,907 ± 1,126 | 4.71 | 0.992 | 2,604 | 2,340 | 727 |
| **Hippuric acids** | | | | | | |
| Hippuric acid | 92,688 ± 3,528 | 3.81 | 0.996 | 4 | 0.4 | 70 |
| 3-Methylhippuric acid | 160,138 ± 5,016 | 3.13 | 0.999 | 99 | 43 | 105 |
| 4-Methylhippuric acid | 99,126 ± 4,512 | 4.55 | 0.999 | 77 | 43 | 122 |
| **Internal standards** | | | | | | |
| Phloridzin | 292,333 ± 6,420 | 2.20 | 0.991 | 1 | 0.3 | 1 |
| Scopoletin | 10,817 ± 536 | 4.96 | 0.999 | 23 | 11 | 30 |
| Taxifolin | 124,601 ± 3,176 | 2.55 | 0.995 | 5 | 5 | 6 |
| 7,8-Dihydroxycourmarin | 28,696 ± 1,308 | 4.56 | 0.994 | 19 | 20 | 3 |

[a]Linear regression analysis with a regression equation of $y = ax + b$, where $x$ is the concentration in µM, b is equal to 0 and $y$ is the peak area. LOD, the limit of detection (Signal/Noise = 3); $R^2$, correlation coefficient of regression equations

### 2.3.4. Extraction chromatography

SPE methods were previously optimised for five compounds (cyanidin-3-glucoside, protocatechuic acid, protocatechuic acid-4-glucuronide, phloroglucinaldehyde and taxifolin) at the Institute of Food Research (Norwich, UK). Methods were optimised for sorbent bed material (DSC-18 or Strata-X™), addition of preservative (with or without 10% ascorbate w/v in 10 mM (EDTA), acid modifier (formic acid or HCl), elution volume (1-9 mL) and final concentration [i.e. complete or incomplete (≈ 50 µL remaining) evaporation]. Two sorbents were tested (DSC-18 and Strata-X™). The DSC-18 SPE cartridges were found to be more suitable for use with the urine, whilst within the serum matrix, the Strata-X™ sorbent resulted in higher extraction efficiencies, with improved reproducibility and repeatability compared to samples extracted using the DSC-18 sorbent. The addition of a preservative (10% ascorbate w/v in 0.5 mM EDTA) prior to SPE and the change of acid modifier from formic acid to HCl during SPE had little impact on analyte recovery ($p \geq 0.05$, $n = 3$). Therefore, no preservative was utilised in the present analyses and formic acid was selected as the appropriate acid modifier due to its suitability with ESI-MS methods. An elution volume of 7 mL of 1% formic acid in methanol was selected, as it provided the lowest elution volume with the maximum retention of analytes from serum using both the strata-X (**Figure 2.7**) and DCS-18 (**Figure 2.8**) columns. Complete evaporation of eluent to dryness significantly reduced the recovery of some compounds (including anthocyanins and PGA). Therefore, samples were dried to approximately 50 µL, reconstituted with 200 µL acidified water and a marker (scopoletin) was added to allow calculation of the exact volume:

$$V_1(mL) = \frac{V_2\ (mL)\ x\ C_1\ (\mu M)}{C_2\ (\mu M)}$$

Where $V_1$ is the desired volume, $V_2$ is predicted volume of the sample, $C_1$ is predicted concentration of the sample and $C_2$ is the known concentration of the volume control standard.

The extraction of the analytes of interest from the faecal matrix required a two-stage extraction process due to the complexity of the matrix. The optimised method for faecal extraction involved a combination of methanol extraction, partial evaporation to remove residual methanol followed by SPE of the remaining aqueous phase using Bond Elute C18 (20 mL, 5 g) cartridges with 100% aqueous wash and an elution volume of 20 mL.

**Figure 2.7** Effect of elution volume on the recovery of analytes by solid phase extraction using Strata-X columns with serum.

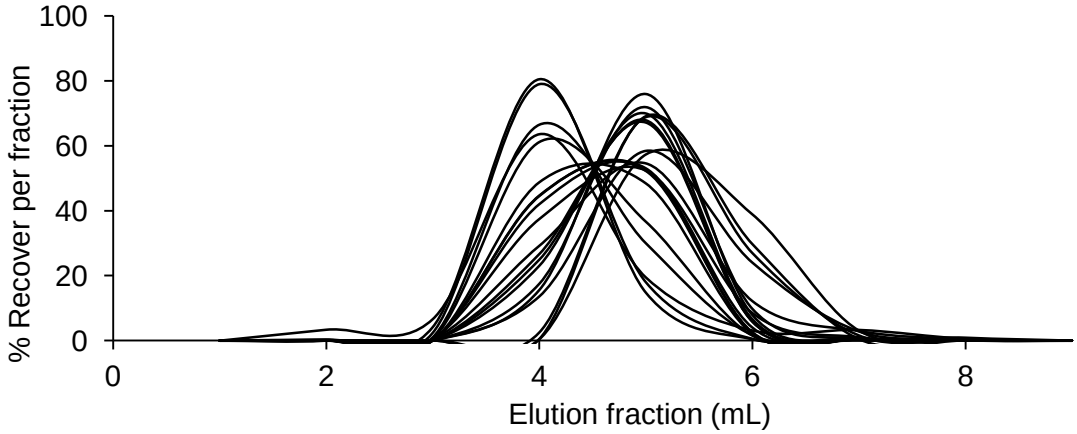


Analytes include cyanidin-3-glucoside, cyanidin-3-rutinoside, pelargonidin-3-glucoside, protocatechuic acid (PCA), vanillic acid (VA), PCA-4-sulfate, VA-4-sulfate, benzoic acid (BA)-4-glucuronide (GlcA), PCA-4-GlcA, VA-4-GlcA, BA-4-sulfate, Methyl-3,4-dihydroxy-benzoate, homoPCA, caffeic acid, hippuric acid, ferulic acid, phloroglucinaldehyde, *p*-courmaric acid, 4-hydroxyBA, 3,4-dihydroxybenzaldehyde, gallic acid and phloridzin.

**Figure 2.8** Effect of elution volume on the recovery of analytes by solid phase extraction using DSC-18 columns with urine.

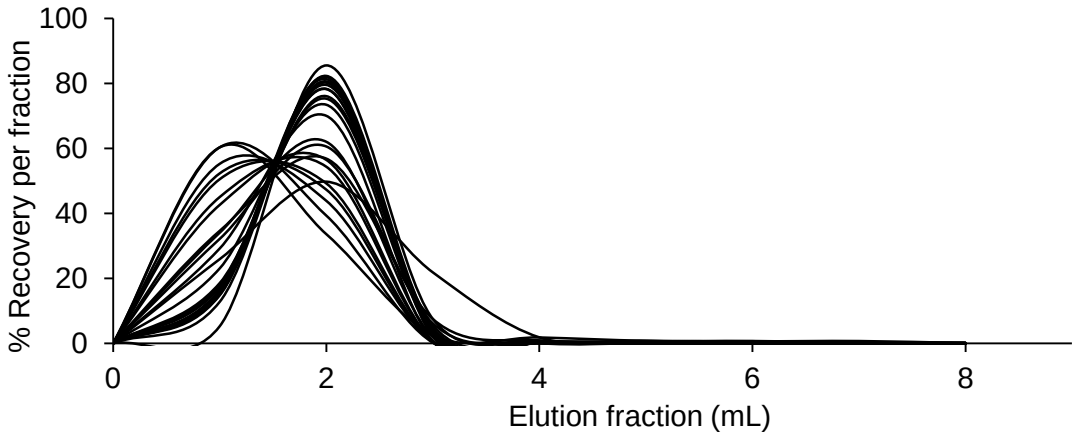


Analytes include cyanidin-3-glucoside, cyanidin-3-rutinoside, pelargonidin-3-glucoside, protocatechuic acid (PCA), vanillic acid (VA), PCA-4-sulfate, VA-4-sulfate, benzoic acid (BA)-4-glucuronide (GlcA), PCA-4-GlcA, VA-4-GlcA, BA-4-sulfate, Methyl-3,4-dihydroxy-benzoate, homoPCA, caffeic acid, hippuric acid, ferulic acid, phloroglucinaldehyde, *p*-courmaric acid, 4-hydroxyBA, 3,4-dihydroxybenzaldehyde, gallic acid and phloridzin.

### 2.3.5. Extraction methods validation

Extraction methods were validated using the 45 phenolic analyte mixture spiked into urine, serum and faecal (as a homogenate) matrices, then extracted using the optimised methods and analysed via HPLC-ESI-MS/MS. The mean recovery of the 45 analytes from urine,

serum and faeces was 88.3 ± 17.8%, 86.5 ± 11.1% and 80.6 ± 20.9% respectively (**Table 2.4**). Of the total 45 analytes, 34, 34, and 26 compounds were extracted with greater than 80% recovery (urine, serum and faeces, respectively). Poor recoveries (<50%) were exhibited for 4-methoxysalicyclic acid, gallic acid and benzoic acid-4-glucuronide in the faeces. The recovery of protocatechuic acid-sulfate, benzoic acid-4-glucuronide and gallic acid from the urine when using DSC-18 SPE cartridges were also poor, but were improved when using Strata X™ columns where the extraction efficiencies of the analytes within serum were all >60% (Table 4). The CV of the extraction efficiency across the 45 analytes averaged 7.9 ± 5.3% for urine, 6.8 ± 5.0% for serum and 14.1 ± 7.9% for faeces.

**Table 2.4** Extraction efficiencies of compounds in urine, serum and faecal matrices.

| Analyte | Extraction Efficiency (% recovery) | | |
|---|---|---|---|
| | **Urine** | **Serum** | **Faeces** |
| | **Anthocyanins** | | |
| Cyanidin-3-glucoside | 97.8 ± 6.2 | 72.1 ± 4.6 | 55.4 ± 9.0 |
| Pelargonidin-3-glucoside | 101.9 ± 6.0 | 74.0 ± 3.4 | 64.5 ± 11.0 |
| | **Benzoic acids** | | |
| 2-Hydroxybenzoic acid | 89.6 ± 1.1 | 81.2 ± 3.0 | 71.2 ± 7.0 |
| 3-Hydroxybenzoic acid | 85.8 ± 10.5 | 92.9 ± 7.6 | 82.9 ± 10.1 |
| 4-Hydroxybenzoic acid | 86.2 ± 2.0 | 86.6 ± 9.8 | 121.1 ± 41.5 |
| 2,3-Dihydroxybenzoic acid | 86.8 ± 3.0 | 73.9 ± 4.4 | 86.6 ± 7.8 |
| 2,4-Dihydroxybenzoic acid | 79.1 ± 10.0 | 97.4 ± 3.0 | 79.9 ± 6.4 |
| Protocatechuic acid (PCA) | 89.7 ± 10.7 | 89.3 ± 6.4 | 80.4 ± 4.3 |
| PCA-3-glucuronide | 94.9 ± 5.0[a] | 92.0 ± 6.3 | 78.4 ± 5.8 |
| PCA-4-glucuronide | 91.8 ± 5.1 | 93.2 ± 1.3 | 84.8 ± 23.4 |
| PCA-3 and 4-sulfate | 92.9 ± 1.9[a] | 67.4 ± 11.5 | 111.0 ± 13.6 |
| 3,5-Dihydroxybenzoic acid | 91.3 ± 16.9 | 80.9 ± 16.7 | 82.0 ± 13.7 |
| Gallic acid | 72.8 ± 3.9[a] | 85.0 ± 7.6 | 10.2 ± 4.6 |
| 2-Methoxybenzoic acid | 90.6 ± 3.5 | 89.6 ± 6.3 | 93.7 ± 10.9 |
| 4-Methoxysalicylic acid | 92.7 ± 2.2 | 85.3 ± 3.6 | 9.3 ± 2.7 |
| 6-Methoxysalicyclic acid | 95.9 ± 1.9 | 85.3 ± 3.1 | 67.7 ± 3.0 |
| Vanillic acid | 91.6 ± 3.9 | 87.3 ± 3.7 | 76.0 ± 8.2 |
| Vanillic acid-4-glucuronide | 74.5 ± 12.8 | 93.6 ± 2.6 | 85.9 ± 12.8 |
| Vanillic acid-4-sulfate | 87.3 ± 7.1 | 92.6 ± 2.6 | 96.2 ± 16.8 |
| Isovanillic acid | 110.7 ± 10.2 | 101.8 ± 5.8 | 79.4 ± 11.6 |
| Isovanillic acid-3-glucuronide | 89.6 ± 5.0 | 86.7 ± 12.0 | 76.6 ± 8.2 |
| Isovanillic acid-3-sulfate | 96.2 ± 6.3 | 92.6 ± 9.3 | 84.2 ± 13.0 |
| Syringic acid | 104.5 ± 8.3 | 87.7 ± 2.6 | 82.7 ± 4.7 |
| 3-Methylgallic acid | 79.6 ± 17.4 | 95.3 ± 3.7 | 75.2 ± 3.8 |
| Benzoic acid-4-glucuronide | 85.8 ± 1.9[a] | 103.5 ± 5.6 | 42.0 ± 11.6 |
| Benzoic acid-4-sulfate | 77.3 ± 7.1 | 94.2 ± 3.3 | 89.6 ± 15.3 |
| | **Benzoates** | | |
| Methyl 3,4-dihydroxybenzoate | 87.2 ± 9.4 | 82.6 ± 17.8 | 79.2 ± 6.1 |
| Methyl 3,4-dimethoxybenzoate | 96.8 ± 3.9 | 73.3 ± 3.2 | 73.0 ± 7.2 |
| Methyl vanillate | 101.5 ± 11.8 | 83.6 ± 2.1 | 80.9 ± 13.6 |
| Methyl gallate | 87.7 ± 13.0 | 64.9 ± 5.3 | 101.4 ± 23.0 |
| | **Hydroxybenzyl alcohol** | | |
| 4-Hydroxybenzyl alcohol | 72.9 ± 8.7 | 80.0 ± 3.9 | 92.7 ± 12.2 |
| | **Phenylpropenoic acids** | | |
| *p*-Coumaric acid | 93.5 ± 10.2 | 88.1 ± 6.0 | 87.6 ± 9.4 |
| Caffeic acid | 78.6 ± 9.1 | 75.7 ± 6.0 | 98.6 ± 12.8 |
| Ferulic acid | 105.3 ± 2.1 | 100.0 ± 4.4 | 74.3 ± 6.8 |

| | | | |
|---|---|---|---|
| Sinapic acid | 110.1 ± 5.6 | 88.7 ± 0.5 | 79.6 ± 9.8 |
| **Benzaldehydes** | | | |
| Phloroglucinaldehyde | 64.5 ± 5.9 | 79.7 ± 8.4 | 66.4 ± 7.0 |
| 4-Hydroxybenzaldehyde | 85.8 ± 8.7 | 73.7 ± 6.1 | 97.0 ± 13.4 |
| 3,4-Dihydroxybenzaldehyde | 77.8 ± 7.9 | 83.8 ± 9.2 | 109.4 ± 26.8 |
| **Phenylacetic acids** | | | |
| 4-Hydroxyphenylacetic acid | 87.2 ± 2.8 | 87.6 ± 7.9 | 82.1 ± 19.9 |
| Homoprotocatechuic acid | 60.0 ± 11.6 | 72.0 ± 3.2 | 88.2 ± 11.8 |
| Homovanillic acid | 81.9 ± 9.7 | 107.3 ± 1.1 | 63.4 ± 7.3 |
| **Hippuric acids** | | | |
| Hippuric acid | NQ[b] | 98.9 ± 2.4 | 87.3 ± 11.5 |
| 3-Methylhippuric acid | 76.6 ± 9.6 | 95.4 ± 0.4 | 85.4 ± 10.5 |
| 4-Methylhippuric acid | 92.5 ± 1.7 | 90.3 ± 6.2 | 77.1 ± 6.2 |
| **Internal standards** | | | |
| Phloridzin | 81.6 ± 6.4 | 77.2 ± 15 | 75.5 ± 7.4 |
| Scopoletin[c] | VC | VC | VC |
| Taxifolin | 96.6 ± 0.9 | 88.6 ± 4.4 | 76.6 ± 11.0 |
| 7,8-Dihydroxycourmarin | 88.8 ± 0.8 | 87.5 ± 5.4 | 98.0 ± 12.5 |

Data expressed as mean ± SD; VC, volume control. [a]Extracted using Strata-X™ as opposed to DSC-18 SPE columns. [b]NQ, Not quantified due to high background concentrations in urine. [c]Scopoletin was used as a volume control standard and was therefore added post extraction only.

### 2.3.6. Validation using clinically derived samples.

Validation of the urine and plasma extraction methods was established using samples collected from a previously undertaken anthocyanin intervention study where participants consumed 500 mg of elderberry derived anthocyanins (**Chapter 4**) (Curtis *et al.*, 2009), whilst the faecal method was validated using samples collected from a previous study where participants consumed 500 mg $^{13}C_5$-cyanidin-3-glucoside (**Chapter 3**) (Czank *et al.*, 2013). The lowest metabolite concentration detected in samples taken at 1, 2 and 3 h post-consumption was investigated, where 36 of the 45 putative compounds were detected in human samples, 26 within urine, 25 within plasma and 24 with faeces. The minimum concentrations identified ranging from 0.4 nM for vanillic acid-sulfate to 0.1 mM for hippuric acid in urine, 2 nM for methyl-3,4-dihydroxybenzoate to 6 µM for hippuric acid in plasma and 0.3 nM for benzoic acid-4-glucuronide to 7 µM for 2,3-dihydroxybenzoic acid in faeces (**Table 2.5**). The maximum concentrations identified within participant samples ranged from 3 m M in urine to 10 µ M in plasma for hippuric acid and 211 µM for ferulic acid in faeces.

**Table 2.5** Minimum and maximum concentrations of analytes detected in spot urine, serum and faecal samples post consumption of 500 mg anthocyanins.

| Analyte | Urine (nM) | | Plasma (nM) | | Faeces (nM) | |
|---|---|---|---|---|---|---|
| | Min[a] | Max[b] | Min[a] | Max[b] | Min[c] | Max[d] |
| **Anthocyanins** | | | | | | |
| Cyanidin-3-glucoside | 2 | 6,348 | 4 | 7 | 2,017 | 2,017 |
| **Benzoic acids** | | | | | | |
| 2-Hydroxybenzoic acid | 37 | 2,919 | 173 | 211 | ND | ND |
| 3-Hydroxybenzoic acid | 60 | 21,024 | 21 | 36 | ND | ND |
| 4-Hydroxybenzoic acid | 656 | 9,892 | 30 | 39 | 34 | 3,026 |
| 2,3-Dihydroxybenzoic acid | 12 | 12,360 | ND | ND | 6,974 | 21,044 |
| Protocatechuic acid (PCA) | 31 | 8,117 | 11 | 24 | 8 | 33,081 |
| PCA-3-glucuronide | 2 | 8,161 | 3 | 15 | 20 | 713 |
| PCA-4-glucuronide | 7 | 2,771 | 4 | 14 | 9 | 1,127 |
| PCA-3 and 4-sulfate | 14 | 29,403 | 734 | 358 | 2 | 872 |
| 3,5-Dihydroxybenzoic acid | 134 | 21,328 | 18 | 50 | ND | ND |
| 4-Methoxysalicylic acid | ND | ND | 0.3 | 2 | 29 | 11,420 |
| Vanillic acid (VA) | 66 | 18,076 | 6 | 62 | 282 | 16,663 |
| VA-4-glucuronide | 74 | 18,929 | 16 | 120 | 29 | 285 |
| VA-4-sulfate | 0.4 | 75,259 | 23 | 161 | 0.3 | 1,968 |
| IsoVA | ND | ND | ND | ND | 177 | 230 |
| IsoVA-3-glucuronide | 4 | 15,680 | 10 | 24 | 18 | 241 |
| IsoVA-3-sulfate | 0.4 | 75,259 | 23 | 161 | 1 | 4,993 |
| Syringic acid | ND | ND | 5 | 22 | ND | ND |
| Benzoic acid-4-glucuronide | 3 | 623 | 7 | 10 | 0.3 | 1,477 |
| Benzoic acid-4-sulfate | ND | ND | 66 | 196 | ND | ND |
| **Benzoates** | | | | | | |
| Methyl-3,4-dihydroxybenzoate | ND | ND | 2 | 6 | 58 | 7,425 |
| Methyl gallate | ND | ND | 3 | 5 | ND | ND |
| Methyl vanillate | ND | ND | ND | ND | 2726 | 2726 |
| **Hydroxybenzyl alcohol** | | | | | | |
| 4-Hydroxybenzyl alcohol | 228 | 17,663 | ND | ND | ND | ND |
| **Phenylpropenoic acids** | | | | | | |
| *p*-Coumaric acid | 13 | 3,040 | ND | ND | ND | ND |
| Caffeic acid | ND | ND | ND | ND | 4,168 | 9,285 |
| Ferulic acid | 15 | 9,908 | 7.7 | 28 | 131 | 211,194 |
| Sinapic acid | 5 | 8,842 | ND | ND | ND | ND |
| **Benzaldehydes** | | | | | | |
| Phloroglucinaldehyde | 7 | 3,477 | 4 | 103 | 10 | 11,216 |
| 4-Hydroxybenzaldehyde | ND | ND | 97 | 182 | 9 | 105 |
| 3,4-Dihydroxybenzaldehyde | ND | ND | 17.3 | 23 | 11 | 724 |
| **Phenylacetic acids** | | | | | | |
| HomoPCA | 309 | 22,045 | ND | ND | 8 | 1,879 |
| HomoVA | 1,493 | 289,697 | ND | ND | ND | ND |
| **Hippuric acids** | | | | | | |
| Hippuric acid | 127,899 | 3,102,601 | 5,771 | 10,106 | 13 | 748 |
| 3-Methylhippuric acid | 29 | 5,831 | ND | ND | ND | ND |
| 4-Methylhippuric acid | 16 | 2,963 | ND | ND | ND | ND |

[a]Minimum and [b]maximum analyte concentration detected within baseline, 1, 2 and 3 h post bolus spot urine and plasma samples of participants (n=15) fed 500 mg elderberry anthocyanins. [c]Minimum and [d]maximum analyte concentration detected within faecal samples, where participants (n=8) were fed 500 mg $^{13}$C-labelled cyanidin-3-glucoside and samples were collected for 48 h post bolus. ND, not detected.

## 2.4. Discussion

The metabolic fate of anthocyanins *in vivo* has remained elusive despite a large number of studies aimed at quantifying them within biological fluids, predominantly due to the low bioavailability of the parent structures and a shortage of quantitative analytical methods optimised for the analysis of anthocyanin metabolites. The objective of the present chapter was to develop methods suitable for establishing the ADME of anthocyanins, including the clearance of their degradation products and metabolites. The present investigation strategy was to first model putative metabolites of anthocyanins to establish a range of targets for method validation, second establish fit for purpose methods for detecting and quantifying the putative metabolites, and third validate the developed methods.

The analytes used in this study were selected based on modelling the products of degradation, phase I, phase II and colonic metabolism of anthocyanins and other similarly structured flavonoids based on previously published studies (Aura *et al.*, 2005; Cheminat *et al.*, 1986; Donovan *et al.*, 1999; Donovan *et al.*, 2002; Fernandes *et al.*, 2008; Forester *et al.*, 2008; Kay *et al.*, 2004; Mazza *et al.*, 1987; Mazza *et al.*, 2002; Moridani *et al.*, 2001; Williamson *et al.*, 2010; Woodward *et al.*, 2009). This approach provided an extensive library of 112 compounds for the optimisation of extraction and detection methodology that can be applied to future studies of ADME. Synthesis of glucuronide and sulfate conjugates of phenolic metabolites was necessary (Zhang *et al.*, 2012) as analytical standards of these phase II metabolites were not commercially available. To the best of the author's knowledge, this comprehensive approach has not been previously published for anthocyanin analysis. The internal standards utilised in this method were selected as they are not endogenously present within humans and have a similar structure to anthocyanins. Phloridzin comprises of two linked phenyl rings, with a glucopyranoside attached and is found in tree bark. Taxifolin is a flavanonol and can be found in conifers such as Chinese yew. It is also found in the açaí palm, in the silymarin extract from the milk thistle seeds.Scopoletin is a coumarin found in the roots of plants in the genus *Scopolia*. It can also be found in vinegar and dandelion coffee.

Initially, chromatographic conditions for the separation and identification of putative anthocyanin metabolites were explored using HPLC-UV/vis, which is routinely used for the detection of intact anthocyanins in biological matrices. Unfortunately, the concentrations of many phenolics found in the biological samples were often below the detection limit of UV/vis detection (data not shown). In addition, numerous phenolic metabolites of anthocyanins absorb at wavelengths common to many compounds naturally present in

baseline biological samples, in contrast to their parent structures which have a relatively unique peak absorbance (525 nM), thus precluding the use of UV/vis detection methods. Therefore, incorporation of MS/MS was necessary for the detection and quantification of the phenolics in the highly complex mixtures of analytes as explored in the present investigation. The HPLC-ESI-MS/MS method was optimised for common parameters, including column, ionic modifier concentration, organic modifier, mobile phase gradient and flow rate. HPLC columns vary according to their sorbent material, pore size and column dimensions whilst analyte retention is influenced by its surface area, polarity and size. Suitable chromatographic separation when using HPLC-MS/MS is difficult when dealing with complex mixtures, and in particular, where compounds of equal mass (isomeric compounds) are present. The majority of studies using RP-HPLC to analyse anthocyanins have utilised C18 packing materials (Felgines *et al.*, 2003; Garcia-Alonso *et al.*, 2009; Kay *et al.*, 2009; Valentova *et al.*, 2007). C18 columns consist of silica particles coated with $C_{18}H_{37}$ alkyl groups, which provide good hydrophobic retention. The Synergi Max RP column is similar to C18, but contains a C12 bonded phase with trimethylsilyl (TMS) end capping, giving it similar hydrophobic selectivity, with less steric hindrance than C18. The Luna C18(2) column contains octadecyl silane ligands bound to the silica surface and the Synergi polar RP column contains ether linked phenyl groups with polar endcaps, giving it high retention of polar and aromatic compounds, especially in the presence of methanol which facilitates π-π bonding. The PFP column is a relatively new stationary phase and incorporates fluorine atoms on the periphery of a phenyl ring, resulting in good peak resolution of aromatic compounds. Of the five columns tested, the present study identified the PFP column as providing the greatest chromatographic separation efficiency under the present conditions. The PFP stationary phase also demonstrated superior resolution of the sulfated conjugates (Figure 2.2), resulting in higher peak intensities (2-10 fold increase) compared to the other stationary phases tested. No column tested was able to effectively separate the isomers of PCA sulfate under the explored conditions.

The pH of the mobile phase can have a large impact on the peak resolution of acids and bases depending on their pKa. Due to the differing behaviours of ions and neutral molecules within a chromatographic column, it is preferred to have a high percentage of the molecule in the same state of ionisation, to prevent the ions gradually separating (Le Chatelier's principle) resulting in the elution of wide peaks. In the present study, the use of 0.1% formic acid within the mobile phase increased peak resolution and resulted in a 389 ± 530% increase in peak height relative to 1% formic acid for the phenolic compounds (Figure 2.4A). The resolution of the analytes was further improved by decreasing the flow rate from 1.5

mL/min to 1 mL/min from 7 to 14 min within the run-time, where the majority of the structurally similar compound were eluting. Moreover, selecting acetonitrile as the organic solvent rather than methanol improved peak resolution, as acetonitrile has a stronger elution strength and lower backpressure than methanol.

The MS source and MRM related parameters were optimised for the analytes of interest in positive and negative mode in order to select the optimum method (i.e. due to their positive change, anthocyanins ionise better in positive mode, whilst phenolic acids tend to provide higher ion intensities in negative mode). Source parameters are responsible for controlling the temperature, voltages and gas flows responsible for nebulising, evaporating, ionising and directing the solvent towards the curtain plate orifice. Therefore, they are important in controlling ion intensity. Source parameters were kept constant throughout an experiment, thus common optimal values for all compounds were used. A high temperature (700 °C) and gas flow (60 psi) appeared particularly important to ensure ionisation of the compounds at this relatively high flow rate. Conversely, MRM related parameters were optimised separately for each compound. They are responsible for fragmenting, selecting and focusing the ions by controlling the potential through the quadruples and therefore control the fragmentation of the compound. However, it should be noted that MS optimisation is instrument specific and the presented values (Table 2.2) should only be used as a guide for method development or validation and most other sources and MS platforms may not be able to deal with flow rates in this range.

LOD represent the lowest concentration at which the test compound that remains detectable, or specifically the concentration at which the analyte yields a peak height signal-to-noise ratio of 3:1. The LODs of the final method ranged from 0.3 nM (for phloridzin in serum) to 2604 nM (for homovanillic acid in urine) (Table 2.5). The LODs of the majority of the compounds were below 100 nM; however, the LODs of 8, 7 and 15 compounds in urine, serum and faeces respectively were above 100 nM, generally a result of poor ionisation and high baseline interference, and should be considered unacceptable. The LOD for homovanillic acid was extremely poor, suggesting the described HPLC-MS/MS method is not optimal for its detection, and alternative techniques such as derivatization followed by GC-MS may be more suitable; yet despite this, it was detected within urine, due to the extremely high concentrations present (1.5 µM). Homoprotocatechuic acid and 2, 3- and 4-hydroxybenzoic acid in urine and 3-hydroxybenzoic acid in serum were also detected in biological samples, despite having a detection limit above 100 nM. However, future clinical studies using these methods should be aware that if undetected, these compounds may still be present at concentrations below 100 nM.

SPE is often the preferred extraction method when using HPLC-MS/MS as it removes salts that may affect ionisation, resulting in a matrix free from interfering elements (Kataoka *et al.*, 2010). It should be noted however that dilution, acidification and syringe filtration (Marks *et al.*, 2009; Mullen *et al.*, 2009; Stalmach *et al.*, 2009a), protein precipitation (Graf *et al.*, 2006; Kay *et al.*, 2004; Marks *et al.*, 2009; Mullen *et al.*, 2009; Stalmach *et al.*, 2009a; Woodward *et al.*, 2009) and liquid-liquid extraction (Graf *et al.*, 2006; Mullen *et al.*, 2002) are also often commonly used techniques in the analysis of polyphenols. These methods were also initially and exhaustively explored, however, due to issues with poor recovery, extremely high variability (inter- and intra-extraction) and insufficient chromatographic resolution of some analytes, they were abandoned in favour of SPE. Thus, SPE was the optimal method for the extraction of anthocyanin metabolites, resulting in mean extraction efficiencies of 88.3 ± 17.8% for urine, 86.5 ± 11.1% for serum and 80.6 ± 20.9% for faeces for the 45 modelled metabolites. In addition, the methods provided acceptable repeatability as the extraction efficiencies averaged from 7.9 ± 5.3% for urine, 6.8 ± 5.0% for serum and 14.1 ± 7.9% for faeces (Table 2.3). For urine extraction, the DSC-18 and Strata-X™ SPE cartridges yielded similar recoveries for cyaniding-3-glucoside, phloroglucinaldehyde and the internal standard (taxifolin), however the binding characteristics of the polymeric divinylbenzene Strata-X™ sorbent allowed large amounts of polar compounds to remain bound to the column after the aqueous wash, resulting in poor resolution of the analytes of interest from co-eluting compounds in the background matrix and thus resulting in higher limits of detection. Therefore, DSC-18 SPE cartridges were selected as they gave superior recoveries for compounds from urine. Within serum, the more selective Strata-X™ cartridges were optimal for the extraction of target analytes, as they afforded significantly higher extraction efficiencies and improved repeatability (77.9 ± 5.2% to 89.2 ± 6.2%) relative to the DSC-18 cartridges (54.1 ± 3.5% to 77.2 ± 14.3%). Within the faecal matrix, the SPE recoveries of the 45 compounds of interest ranged from 9.3 ± 2.7% to 121 ± 41.5% with a high mean recovery of 80.6 ± 20.9%. Recoveries above 100% are commonly observed in SPE methods and can result from the accumulation of error during the extraction process, particularly when the analyte is endogenously present within the sample. The lowest recoveries were observed within the faeces, with 4-methoxysalicylic acid and gallic acid having a recovery of 9% and 10% respectively. The lower recoveries observed within the faecal matrix were likely due to the complexity of the faecal matrix; a proportion of the spiked analyte likely remained bound to the solid matter and the presence of the vast array of microflora may also contribute to the lower recoveries. Together these results demonstrate that despite the complexity of the biological matrices, the presented method is suitable for the recovery of the target analytes.

Validation of the methods for use with clinical samples was carried out on urine and plasma samples derived from 15 participants in a human intervention study feeding 500 mg elderberry anthocyanins (Curtis *et al.*, 2009). The methods described herein were successful in identifying 36 metabolites, comprising of 26 analytes within urine, 25 within serum, and 24 within faeces. The lowest concentrations of the metabolites identified in the urine samples ranged from 0.4 nM for vanillic acid-4-sulfate to 0.1 mM for hippuric acid, while concentrations in the plasma ranged from 2 nM for methyl-3,4-dihydroxybenzoate to 6 µM for hippuric acid and concentrations in the faeces ranged from 0.3 nM for benzoic acid-4-glucuronide to 7 µM for 2,3-dihydroxybenzoic acid (Table 2.5). The identification of these metabolites within clinical samples demonstrates the methods are suitable and have acceptable LODs for the detection of anthocyanin metabolites in clinically relevant samples. Furthermore, quantification was carried out using matrix-matched standard curves rather than standard curves prepared in mobile phase (a common approach), which provides an extra degree of precision as the matrix associated ionisation efficiencies and baseline deviation of the sample and standards are more similar.

## 2.5. Conclusion

The present study describes the development of analytical methods that are suitable for the separation, detection and quantification of a large number of structurally diverse anthocyanin metabolites in clinical samples. The sample extraction and analyte detection methods described are suitable for analysis of the majority of the compounds examined, which included several metabolites that were not available commercially and for which reliable methods had not previously been reported. This work has resulted in the development of methods that are expected to enhance the quality of future studies of anthocyanin ADME, which may in turn identify novel targets for future investigations exploring the biological activity of anthocyanins.

# Chapter 3. The pharmacokinetics of anthocyanins following the ingestion of $^{13}C_5$-cyanidin-3-glucoside in humans

## 3.1. Introduction

In order for anthocyanins to exert protective effects, as reported in many epidemiological studies (Cassidy *et al.*, 2013; Cassidy *et al.*, 2011; Mink *et al.*, 2007), randomised controlled trials (Zhu *et al.*, 2013; Zhu *et al.*, 2011), animal (Wang *et al.*, 2011) and *in vitro* (Edirisinghe *et al.*, 2011; Xu *et al.*, 2004b) studies, they need to be absorbed and reach target tissues in a bioactive form. However, ambiguity has arisen concerning the absorption, distribution, metabolism and elimination (ADME) of anthocyanins, as their recovery from biological samples has been poor, often with nanomolar concentrations observed in plasma. Furthermore, interventions feeding anthocyanin rich foods, including blackberries, strawberries, blackcurrants or cranberries, containing up to 2.4 g anthocyanins, rarely recover more than 1% of the ingested dose (Bub *et al.*, 2001; Cao *et al.*, 2001; Felgines *et al.*, 2005; Kay *et al.*, 2005; Kay *et al.*, 2004; Manach *et al.*, 2005; Matsumoto *et al.*, 2001; Milbury *et al.*, 2002; Milbury *et al.*, 2010; Mullen *et al.*, 2008a; Murkovic *et al.*, 2001). This raises questions regarding the metabolic fate of anthocyanins and similarly the compounds/metabolites responsible for their potential cardio-protective effects.

Due to their unstable nature, it has been proposed that anthocyanins are likely present in the circulation, as degradation products and metabolic intermediates (Kay, 2010). The degradation of anthocyanins to their phenolic acid and aldehyde constituents has been observed *in vitro*, with the degradation products observed within gastric (Woodward *et al.*, 2009) and microbial fermentation studies (Gonzalez-Barrio *et al.*, 2011; Williamson *et al.*, 2010); yet only a few human studies have detected these degradation products within biological samples (Azzini *et al.*, 2010; Czank *et al.*, 2013; Nurmi *et al.*, 2009; Russell *et al.*, 2009; Vitaglione *et al.*, 2007). It is therefore possible that the degradation products are further metabolised *in vivo*, forming a large number of potentially bioactive metabolites.

A study feeding 71 mg anthocyanins within 1 L blood orange juice, implicated the phenolic acid degradation product, protocatechuic acid, as a major anthocyanin metabolite (Vitaglione *et al.*, 2007). In addition, a range of phenolic acids, including vanillic, syringic, caffeic and ferulic acid have been identified within serum, reaching maximum concentrations 4-6 h after the consumption of a bilberry-lingonberry puree (Nurmi *et al.*, 2009). However, the complex

flavonoid and phenolic profile of the intervention food, limited the ability to trace the metabolites back to their source. Further, *in vitro* and human studies indicate that such phenolic acids undergo phase II conjugation (Nardini *et al.*, 2009; Nardini *et al.*, 2006; Woodward *et al.*, 2011), suggesting anthocyanin degradation products can undergo extensive metabolism *in vivo*. Recent evidence also suggests that the major metabolites of anthocyanins are likely to be derived from bacterial fermentation and absorption from the colon (Del Rio *et al.*, 2010; McGhie *et al.*, 2007; Williamson *et al.*, 2010) .

The extensive degradation and metabolism of anthocyanins was recently confirmed in a stable isotope-labelled cyanidin-3-glucoside feeding study in which the relative bioavailability of cyanidin-3-glucoside was established as 12.38 ± 1.38%, based on the recovery of the $^{13}$C-label in the urine and breath (Czank *et al.*, 2013), thus suggesting that the extent of anthocyanin absorption and metabolism had been previously underestimated. Furthermore, given the degradation, short $t_{½}$ and low $C_{max}$ of the parent anthocyanins, the observed cardiovascular benefits of anthocyanin consumption (Cassidy *et al.*, 2013; Cassidy *et al.*, 2011; Erdman *et al.*, 2007; Mink *et al.*, 2007) are likely the consequence of the metabolites, which are present within the circulation for significantly longer and at higher concentrations than the parent anthocyanins. The present study aimed to identify the unique pharmacokinetic profiles of each anthocyanin metabolite, following the consumption of a 500 mg oral bolus dose of $^{13}$C-labelled cyanidin-3-glucoside. The findings from this work will inform the design of future clinical interventions and mechanistic studies exploring the biological activity of anthocyanins.

## 3.2. Materials and methods

### 3.2.1. Chemicals and materials

Unlabelled cyanidin-3-glucoside and peonidin-3-glucoside were obtained from Extrasynthese (Genay, France) as analytical standards. Phase II conjugates of phenolic acids (protocatechuic acid-3-glucuronide, protocatechuic acid-4-glucuronide, vanillic acid-4-glucuronide, isovanillic acid-3-glucuronide, benzoic acid-4-glucuronide, protocatechuic acid-3-sulfate, protocatechuic acid-4-sulfate, vanillic acid-4-sulfate and isovanillic acid-3-sulfate) were synthesised in the School of Chemistry and Centre for Biomolecular Sciences, University of St. Andrews (UK) via recently published methods (Zhang *et al.*, 2012). All other standards (caffeic acid, *p*-courmaric acid, ferulic acid, sinapic acid, 3,4-dihydroxybenzaldehyde, homoprotocatechuic acid and homovanillic acid) were purchased from Sigma-Aldrich (Dorset, UK). Kinetex pentafluorophenol (PFP) HPLC column (2.6 µM,

100 x 4.6 mm) and SecurityGuard® cartridges (PFP, 4.0 x 2.0mm) were purchased from Phenomenex (Macclesfield, UK). HPLC grade methanol and acetonitrile were purchased from Fisher Scientific (Loughborough, UK). Discovery® DSC-18 SPE columns (6 mL, 1 g) and Acrodisc 13 mm, 0.45 µm PTFE syringe filters, ascorbic acid, formic acid and all other chemicals, were purchased from Sigma-Aldrich (Dorset, UK). All water utilised was of Milli-Q grade (18.2 MΩ $cm^{-1}$).

### 3.2.2. Clinical Design

Eight healthy men (n = 8; age, 27.8 ± 8.1 y; BMI, 23.2 ± 1.5 kg/m²) were recruited from the University of East Anglia and local community of Norwich, UK to take part in the study in June-September 2011. In order to maintain a homogenous study population and minimise metabolic variation, male participants were selected, who were non-smokers, moderate drinkers and were not taking any dietary supplements. The protocol was explained to the participants and they provided informed consent. The study was conducted at the Clinical Research and Trials Unit at the University of East Anglia according to the principles expressed in the Declaration of Helsinki and was approved by the local Research Ethics Committee (REC ref: 10/110 H0306/42) and registered at clinicaltrials.gov as NCT01106729.

Cyanidin-3-glucoside was synthesised and isotopically labelled at positions 6, 8, 10, 3' and 5' (**Figure 3.1**) at the University of St. Andrews, Scotland, so that three $^{13}C$ atoms ($^{13}C_3$) were present on the A-ring and two $^{13}C$ atoms ($^{13}C_2$) were present on the B-ring (Zhang *et al.*, 2011). The molecule was established as 99.8% pure, with an enrichment of 99 atom percent at each position and was accurately weighed and encapsulated (250 mg anthocyanin/gelatin capsule) at the Ipswich Hospital Pharmaceutical Manufacturing unit (Czank *et al.*, 2013; Zhang *et al.*, 2011).

**Figure 3.1** Structure and labelling configuration of 6,8,10,3',5'-$^{13}C_5$-cyanidin-3-glucoside.

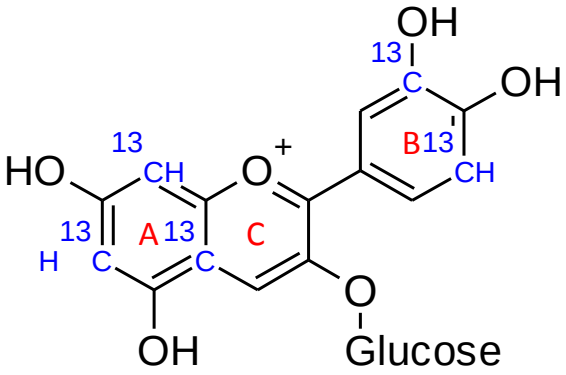

### 3.2.3. Study Protocol

For a seven-day washout period prior to the trial and throughout the three study days, volunteers limited their intake of foods rich in anthocyanins and with a high natural abundance of $^{13}C$ (For exclusion list, refer to Appendix 1). In order to monitor compliance, food diaries were completed during the washout period (three days), the study day and during the 48 h follow-up. Following an overnight fast, baseline faecal (up to 72 h prior to the study day), urine (total morning void of study day), blood and breath samples were collected. Participants were given a single, oral 500 mg bolus of encapsulated $^{13}C_5$-cyanidin-3-glucoside (2 x 250 mg capsules), followed by a standardised anthocyanin free breakfast. Blood and breath samples were collected at 0.5 h, 1 h, 2 h, 4 h, 6 h, 24 h and 48 h following the anthocyanin bolus. Individual urine and faecal total voids were collected throughout the study day (0-6 h) and pooled for 6-24 h and 24-48 h time points (**Figure 3.2**).

**Figure 3.2** Clinical study design summarising the collection of blood and urine samples.

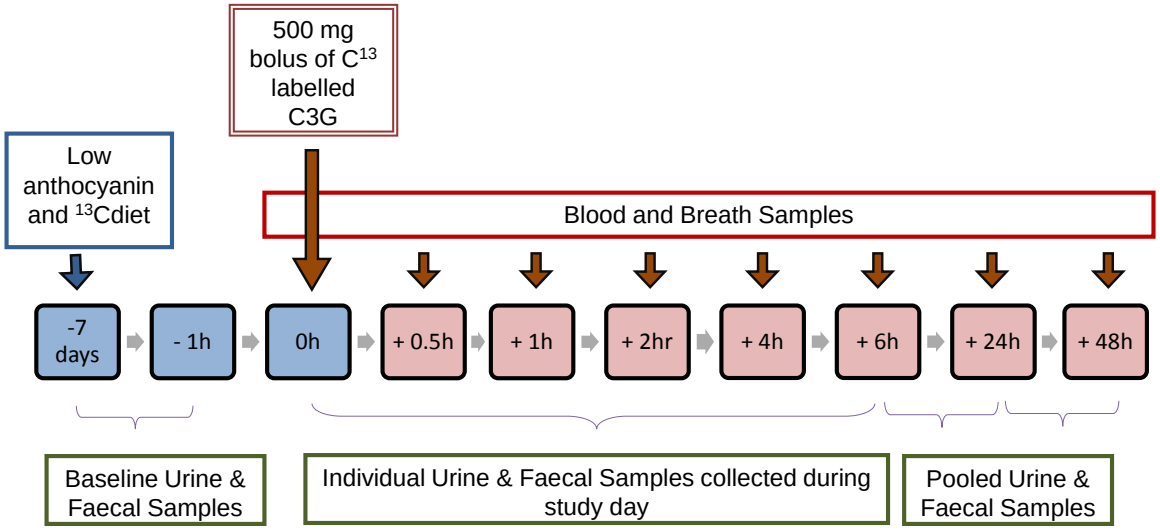


### 3.2.4. Sample collection

Total urine voids were collected into Urisafe® collection containers (VWR, UK) with 100 mg ascorbic acid added to each sample prior to collection and an addition 100 mg was added for every additional 500 mL. In order to prevent degradation of the anthocyanins, the pH of the samples was established using a pH meter (Omega, UK) and manually adjusted to pH 2.4 ± 0.08 with formic acid. Blood samples were collected into sterile, untreated 10 mL vacutainers® (BD, UK). For whole blood isotope ratio mass spectrometry (IRMS) analysis, blood was immediately aliquoted into 1 mL cryogenic vials and flash frozen using liquid nitrogen, whilst for serum collection, blood was inverted and left to clot at room temperature

for 1 h, then centrifuged at 4°C, 1300 g for 10 min. 7.5 mL serum was collected, the pH was measured, 10%vv of 10% acorbate was added to the serum and the pH was manually (dropwise) adjusted to pH 2.4 (final pH, 2.4 ± 0.08) with formic acid. Breath samples were collected using the Alveosampler™ system (QuinTron, Italy) and stored in 10 mL vacutainer® (BD, UK) tubes at room temperature for IRMS. Faecal voids were collected into custom-made stool collection kits, weighed and transferred to cryogenic storage containers (Nalgene, UK) for storage. Following processing, all blood, serum and faeces samples were stored at -80°C until analysis. Note, breath samples were analysed using continuous-flow IRMS (AP 2003; Iso-Prime) and the data are described by Czank *et al.* 2013 (Czank *et al.*, 2013).

### 3.2.5. Sample preparation

Urine and plasma samples were extracted and concentrated at the Institute of Food Research (Norwich, UK) as previously described (**Chapter 2)**. Briefly samples were extracted using DSC-18 (for urine) and Strata-X™ (for plasma) SPE cartridges, evaporated to approximately 50 µL using a Thermo speedvac and diluted with 200 uL of acidified water. 10 µL of 1 mg/mL phloridzin was added as a volume control standard and samples were then syringe filtered prior to analysis.

### 3.2.6. HPLC-MS/MS analysis

HPLC-MS/MS analysis was conducted at the Institute of Food Research (Norwich, UK) using an Agilent 1200 series HPLC system coupled with a ABSciex 4000 MS/MS system, with samples injected onto a Kinetex PFP column as previously described (**Chapter 2**). (Note: the analysis described in the present chapter was conducted by the Institute of Food Research, using the conditions as described in Chapter 2. Retention times were adjusted for the 4000 Q-trap system). Briefly, the mobile phase consisted of 0.1% formic acid (v/v) in water (A) and 0.1% formic acid (v/v) in acetonitrile (B), at a flow rate of 1.5 mL/min at 0 min, 1 mL/min at 7 to 14 min and 1.5 mL/min at 14 to 28 min. The gradient consisted of 1% B at 0 min, 7.5% B at 7 min, 7.6% B at 14 min, 10% B at 17 min, 12% B at 18.5 min, 12.5% B at 20 min, 30% B at 24 min and 90% B at 25 to 28 min. MS/MS source parameters included curtain gas 40 psi, ion spray voltage -4000 V/+5500 V, temperature 700°C and nebulizer and auxiliary gas 60 psi. The system was controlled by Analyst software (v. 1.5, Applied Biosystems/MDS Sciex). Metabolite identification was performed by multiple reaction monitoring (MRM) optimised for the detection of pure standards with *m/z* of the parent and daughter fragments adjusted to +2,+3,+5 Da to allow identification of the $^{13}C$-labelled metabolites derived from the B-ring, A-ring or the parent structure, respectively.

Metabolites were confirmed on the basis of retention time (using authentic and synthesised standards where possible) and three or more parent-daughter ion transitions.

### 3.2.7. Statistics

Pharmacokinetic modelling of metabolites in the serum was performed with the PKSolver 'add-on' for Excel 2010 (Microsoft, California) (Zhang *et al.*, 2010) using non-compartmental analysis with AUC calculated using the trapezoidal rule. Pharmacokinetic parameters were established for each individual analyte and presented as mean ± SD. Urine samples collected during the first 6 h post bolus were grouped together to the nearest hour for graphical interpretation and to calculate total cumulative recovery. The concentration of metabolites was converted to amount recovered from the urine by accounting for the molecular weight of the individual $^{13}$C-labelled metabolites and the volume of the individual participants void and averaged across participants. Recovery of metabolites in the faeces was established from the molecular weight of the $^{13}$C-labelled metabolite and the weight of the individual participants void adjusting for faecal water content as previously described (Czank *et al.*, 2013). Urine and faecal recovery amounts are presented as mean ± SD, n = 8 unless otherwise stated.

## 3.3. Results

### 3.3.1. Metabolite identification

A total of 35 $^{13}$C-labelled analytes (including the parent $^{13}C_5$- cyanidin-3-glucoside) were identified in serum, urine and faecal samples collected over 48 h post-consumption. The metabolites identified included the degradation products of cyanidin-3-glucoside (protocatechuic acid and phloroglucinaldehyde), phase I (dehydroxylation, reduction) and phase II (methyl, sulfate, glycine and glucuronyl) conjugates of cyanidin-3-glucoside, protocatechuic acid and phloroglucinaldehyde and probable bacterial metabolites, including carboxylic, phenylacetic and phenylpropenoic acids. Of the 35 analytes identified, six metabolites (two isomers of cyanidin-glucuronide, methyl-cyanidin-glucuronide and three isomers of methyl-cyanidin-3-glucose-glucuronide; **Table 3.1**) were tentatively identified as having a neutral loss of 176 m/z (glucuronide) whilst sharing common daughter ion transitions with cyanidin-3-glucoside or peonidin-3-glucoside. The remaining 29 metabolites were confirmed by comparison of retention time and MS/MS fragmentation patterns to that of pure standards (Table 3.1).

**Table 3.1** HPLC-MS/MS identification (MRM) of $^{13}$C-labelled cyanidin-3-glucoside (C3G) and its metabolites in the serum, urine and faeces of healthy volunteers (n=8) after the consumption of 500 mg of $^{13}$C-labelled C3G.

| Metabolite | Compound identification | | | | Analytical standards |
|---|---|---|---|---|---|
| | Rt (min) | MRM ion transitions *(m/z)*[a] | Location | # $^{13}$C[b] | $MS^2$ fragments (m/z) |
| Parent anthocyanins | | | | | |
| Cyanidin-3-glucoside (C3G) | 12.6 | 454/292, 246, 218, 133 | Urine, serum, faeces | +5 | 449/287, 241, 213, 128 |
| Cyanidin-glucuronide | 11.7 | 468/292 | Urine | +5 | NA[c] |
| Cyanidin-glucuronide | 16.5 | 468/292 | Urine | +5 | NA[c] |
| Peonidin-3-glucoside | 16.6 | 468/306 | Urine | +5 | 463/301 |
| Methyl-cyanidin-glucuronide | 16.7 | 482/306 | Urine | +5 | NA[c] |
| Methyl-C3G-glucuronide | 5.7 | 644/306 | Urine | +5 | NA[c] |
| Methyl-C3G-glucuronide | 8.0 | 644/306 | Urine | +5 | NA[c] |
| Methyl-C3G-glucuronide | 9.6 | 644/306 | Urine | +5 | NA[c] |
| Degradants | | | | | |
| Protocatechuic acid (PCA) | 4.3 | 155/111, 93, 83 | Urine, serum, faeces | +2 | 153/109, 91, 81 |
| Phloroglucinaldehyde | 7.4 | 156/155, 128, 110, 86 | Urine, serum, faeces | +3 | 153/151, 125, 107, 83 |
| Metabolites | | | | | |
| 3-Hydroxybenzoic acid | 8.1 | 138/95, 67 | Urine, faeces | +2 | 136/93, 65 |
| 4-Hydroxybenzoic acid | 6.5 | 138/95, 67 | Urine, faeces | +2 | 136/93, 65 |
| Benzoic acid-4-glucuronide | 3.0 | 317/175, 155, 113, 95 | Urine, serum, faeces | +2 | 315/175, 153, 113, 93 |
| PCA-3-glucuronide | 4.3 | 331/175, 155, 113, 111 | Urine, serum, faeces | +2 | 329/175, 153, 113, 109 |
| PCA-4-glucuronide | 3.3 | 331/175, 155, 113, 111 | Urine, serum, faeces | +2 | 329/175, 153, 113, 109 |
| PCA-3-sulfate | 6.5 | 235/191, 155, 111 | Urine, serum, faeces | +2 | 233/189, 153, 109, 97 |
| PCA-4-sulfate | 6.2 | 235/191, 155, 111 | Urine, serum, faeces | +2 | 233/189, 153, 109, 97 |
| Vanillic acid (VA) | 9.5 | 169/154, 125, 110 | Urine, serum, faeces | +2 | 167/152, 123,108 |
| IsoVA | 9.9 | 171/153, 127, 95 | Urine, serum, faeces | +2 | 169/151, 125, 93, 65 |
| IsoVA-3-glucuronide | 6.2 | 347/175, 171, 154, 113 | Urine, serum, faeces | +2 | 345/175, 169, 152, 113 |
| VA-4-glucuronide | 4.9 | 347/175, 171, 154, 113 | Urine, serum, faeces | +2 | 345/175, 169, 152, 113 |
| IsoVA-3-sulfate | 8.8 | 247/169, 154, 125, 110 | Urine, serum, faeces | +2 | 245/167, 152, 123, 108 |
| VA-4-sulfate | 8.6 | 247/169, 154, 125, 110 | Urine, serum, faeces | +2 | 245/167, 152, 123, 108 |
| 4-Hydroxyphenylacetic acid | 6.8 | 154/125, 109, 95 | Urine, faeces | +2 | 152/123, 107, 93, 79 |

| | | | | | |
|---|---|---|---|---|---|
| HomoPCA | 4.6 | 171/127, 111, 97 | Urine, faeces | +2 | 169/125, 109, 95 |
| 4-Hydroxybenzaldehyde | 8.5 | 123/110, 94, 67 | Urine, serum, faeces | +2 | 121/108, 92, 65 |
| 3,4-Dihydroxybenzaldehyde | 5.8 | 139/110, 94, 83 | Urine, faeces | +2 | 137/109, 92, 81 |
| Caffeic acid | 10.4 | 183/139, 110, 93 | Faeces | +2 | 181/137, 108, 91 |
| Ferulic acid | 18.8 | 195/180, 150, 136<br>196/181, 151, 137 | Urine, serum, faeces<br>Urine, serum, faeces | +2<br>+3 | 193/178, 148, 134 |
| Hippuric acid | 6.3 | 179/136, 134, 79 | Urine, serum, faeces | +2 | 177/134 ,132, 77 |
| 4-Methoxybenzaldehyde | 19.6 | 169/125, 110, 81 | Faeces | +2 | 167/123, 108, 79 |
| 4-Methoxysalicyclic acid | 20.1 | 155/94, 79, 65<br>156/95, 80, 66 | Faeces<br>Urine | +2<br>+3 | 153/92,77, 63 |
| Methyl vanillate | 21.4 | 185/153, 125, 109 | Faeces | +2 | 183/151, 123, 107, 77 |
| Methyl-3,4-dihydroxybenzoate | 12.9 | 170/111, 93 | Urine, serum, faeces | +2 | 168/109, 91 |

[a]Mass spectra fragments for $^{13}C$ labelled metabolites with +2, +3 and +5 *m/z*. [b] +2, +3 and +5 *m/z* refer to metabolites derived from PCA, PGA and cyanidin respectively. [c]NA, no analytical standard available for confirmation.

### 3.3.2. Serum pharmacokinetics

In serum, a total of 17 $^{13}$C-labelled compounds, comprising cyanidin-3-glucoside, protocatechuic acid, phloroglucinaldehyde, 13 derivatives of protocatechuic acid, and one derivative of phloroglucinaldehyde were detected (**Table 3.2; Figure 3.3; Figure 3.4**). The $C_{max}$ of the analytes ranged from 11 ± 6 nM for protocatechuic acid-3-glucuronide (Figure 2B) to 2.0 ± 3.9 µM for hippuric acid (Figure 3A), with $t_{max}$ between 1.8 ± 0.4 h for cyanidin-3-glucoside and 30.1 ± 22.8 h for vanillic acid-sulfate. Elimination half-lives ($t_{½}$) also ranged from 0.4 h for cyanidin-3-glucoside to 96.5 ± 134.7 h for the A-ring derived ferulic acid (Table 3.2). protocatechuic acid-3-glucuronide was the least abundant metabolite present in serum with an AUC of 60 ± 86 nmol·hL$^{-1}$ while hippuric acid was the most abundant metabolite with an AUC of 46 ± 86 µmol·hL$^{-1}$ (Table 3.2).

**Table 3.2** Serum pharmacokinetic profiles of cyanidin-3-glucoside (C3G), its degradation products and derived metabolites in humans after the consumption of 500 mg $^{13}$C-labelled C3G[a].

| **Metabolite** | **n[b]** | **$C_{max}$ (nM)** | **$t_{max}$ (h)** | **$t_{½}$ (h)** | **$AUC_{0-48}$ (nmol·hL$^{-1}$)** |
|---|---|---|---|---|---|
| *Parent anthocyanins* | | | | | |
| Cyanidin-3-glucoside[e] | 5 | 141 ± 156 | 1.8 ± 0.4 | 0.4 | 278 ± 380 |
| *Degradants* | | | | | |
| Protocatechuic acid (PCA)[g] | 8 | 146 ± 209 | 3.3 ± 2.0 | 9.9 ± 9.0 | 1,377 ± 2,150 |
| Phloroglucinaldehyde[d] | 4 | 582 ± 1072 | 2.8 ± 2.2 | NQ[c] | 7,882 ± 15,535 |
| *Protocatechuic acid derived* | | | | | |
| Benzoic acid-4-glucuronide[f] | 7 | 74 ± 52 | 10.9 ± 9 | 17.1 ± 6.0 | 1,467 ± 1,295 |
| Methyl-3,4-dihydroxybenzoate[g] | 8 | 12 ± 15 | 8.4 ± 16.1 | 21.6 ± 10.3 | 171 ± 197 |
| PCA-3-glucuronide[g] | 5 | 11 ± 6 | 2.7 ± 2.3 | 18.0 ± 22.0 | 60 ± 86 |
| PCA-4-glucuronide[f] | 8 | 68 ± 171 | 3.8 ± 2.1 | 19.4 ± 8.1 | 618 ± 1,384 |
| PCA-sulfates[g] | 8 | 157 ± 329 | 11.4 ± 10.6 | 31.9 ± 38.2 | 1,180 ± 987 |
| Vanillic acid (VA)[c] | 2 | 1,845 ± 1,185 | 12.5 ± 16.3 | 6.4 | 23,319 ± 29,203 |
| IsoVA[b] | 1 | 195 | 2.0 | NQ[c] | 189 |
| VA-4-glucuronide[g] | 8 | 24 ± 11 | 4.8 ± 1.0 | NQ[c] | 74 ± 31 |
| IsoVA-3-glucuronide[g] | 8 | 34 ± 14 | 4.3 ± 1.7 | 1.6 ± 0.2 | 103 ± 37 |
| VA-sulfates[d] | 4 | 430 ± 598 | 30.1 ± 22.8 | NQ[c] | 10,689 ± 15,503 |
| 4-Hydroxybenzaldehyde[f] | 7 | 667 ± 1,727 | 5.6 ± 8.3 | 17.9 ± 17.6 | 663 ± 1,336 |
| Ferulic acid[f] | 7 | 827 ± 982 | 8.2 ± 10.9 | 21.4 ± 15.7 | 17,422 ± 29,246 |
| Hippuric acid [g] | 8 | 1,962 ± 3,928 | 15.7 ± 11.5 | 95.6 ± 134.7 | 46,568 ± 85,731 |
| *Phloroglucinaldehyde derived* | | | | | |
| Ferulic acid[e] | 6 | 87 ± 93 | 13.3 ± 19.2 | 96.5 ± 127.2 | 1,815 ± 2,581 |

[a]Values are expressed as mean ± SD. [b]Metabolite detected in n = number of participants. [c] NQ, not quantifiable as compounds remained sufficiently above baseline at 48h. [d]PCA-sulfate and VA-sulfate isomers could not be separated sufficiently by HPLC to allow individual quantitation and the values presented are cumulative concentration of both isomers. [e]Alternative isomers of ferulic acid include 2-hydroxy-4-methoxycinnamic acid or 4-hydroxy-2-methoxycinnamic acid.

Cyanidin-3-glucoside reached a maximum serum concentration of 141 ± 156 nM (Figure 3.3A), while its degradation products, protocatechuic acid and phloroglucinaldehyde were

present at 146 ± 209 nM (Figure 3.3B) and 0.6 ± 1.1 µM (Figure 3.4C) respectively, with their $t_{max}$ occurring 2-3 h later than that of cyanidin-3-glucoside (3.3 ± 2.0 h and 2.8 ± 2.2 h, respectively; Table 3.2). The metabolites of protocatechuic acid were the dominant species detected in the serum, with hippuric acid, vanillic acid and the B-ring derived ferulic acid representing the most abundant metabolites, having a $C_{max}$ of 2.0 ± 3.9 µM (Figure 3.4A), 1.8 ± 1.2 µM (Figure 3.3C), and 827 ± 982 nM (Figure 3.4B) respectively. Hippuric acid ($t_{½}$, 95.6 ± 134.7 h), protocatechuic acid-sulfate ($t_{½}$, 31.9 ± 38.2 h) and ferulic acid ($t_{½}$ 21. ± 15.7 h) had significantly longer elimination half-lives than protocatechuic acid ($t_{½}$ 9.9 ± 9.0 h; Table 3.2).

Eight sulfated and glucuronidated forms of protocatechuic acid and methylated protocatechuic acid (vanillic acid) were identified within the serum (Figure 2B,C), with the conjugations occurring at both the *meta* and *para* positions. Of these, vanillic acid-sulfate was present in the highest concentration ($C_{max,}$ 430 ± 598 nM; $t_{max,}$ 30.1 ± 22.8 h) followed by protocatechuic acid-4-glucuronide ($C_{max,}$ 68 ± 171 nM; $t_{max,}$ 3.8 ± 2.1 h) and protocatechuic acid-sulfate ($C_{max,}$ 157 ± 329 nM; $t_{max,}$ 11.4 ± 10.6 h) (Table 3.2). In contrast, only one A-ring derived metabolites was identified within the serum, namely ferulic acid ($C_{max,}$ 87 ± 93 nM; $t_{max,}$ 13.3 ± 19.2 h) (Figure 3.4C; Table 3.2).

### 3.3.1. Urinary elimination

In the urine, 31 $^{13}$C-labelled compounds were identified, comprising of cyanidin-3-glucoside, seven methylated and glucuronidated conjugates of cyanidin-3-glucoside and cyanidin, protocatechuic acid, phloroglucinaldehyde, 19 derivatives of protocatechuic acid, and two derivatives of phloroglucinaldehyde (**Table 3.3**). Maximum concentrations of cyanidin-3-glucoside (334 ± 382 nM) and its conjugated derivatives (ranging from 6 ± 5 nM to 206 ± 234 nM) were identified between 1 and 2 h post consumption (**Figure 3.5A**). Protocatechuic acid also reached its maximum concentration (337 ± 332 nM) at 1-2 h (Figure 3.5B), while phloroglucinaldehyde reached its peak concentration (170 ± 118 nM) considerably later (6 to 24 h) (**Figure 3.6C**). The phenolic metabolites were excreted in much higher concentrations than the parent anthocyanins, ranging from 24 ± 17 nM for 3,4-dihydroxybenzaldehyde (Figure 3.6C) to 5.4 ± 13.9 µM for hippuric acid (Figure 3.6A), with peak excretions observed from 0-1 h to 24-48 h post consumption (Table 3.3).

**Figure 3.3** Serum pharmacokinetic profiles of (A) cyanidin-3-glucoside, (B) protocatechuic acid and its metabolites and (C) methylated protocatechuic acid and its metabolites after the consumption of 500 mg $^{13}C_5$- cyanidin-3-glucoside.

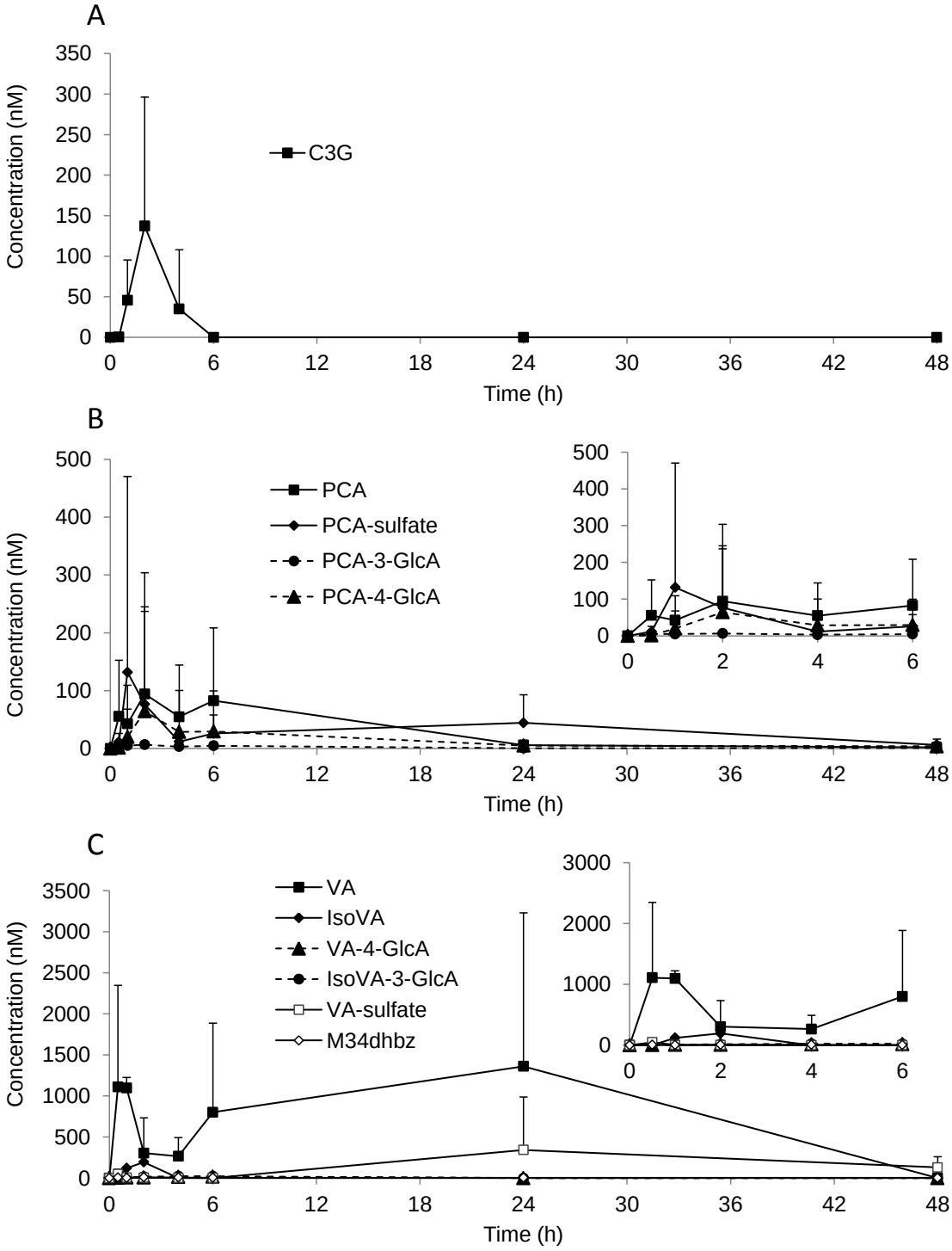


All data is mean ± SD. C3G, cyanidin-3-glucoside; GlcA, glucuronide; M34dhbz, methyl-3,4-dihydroxybenzoate; PCA, protocatechuic acid; VA, vanillic acid.

**Figure 3.4** Serum pharmacokinetic profiles of (A) benzoic acid metabolites, (B) propenoic acid metabolites and (C) A-ring derived and aldehyde metabolites of cyanidin-3-glucoside after the consumption of 500 mg $^{13}C_5$- cyanidin-3-glucoside.

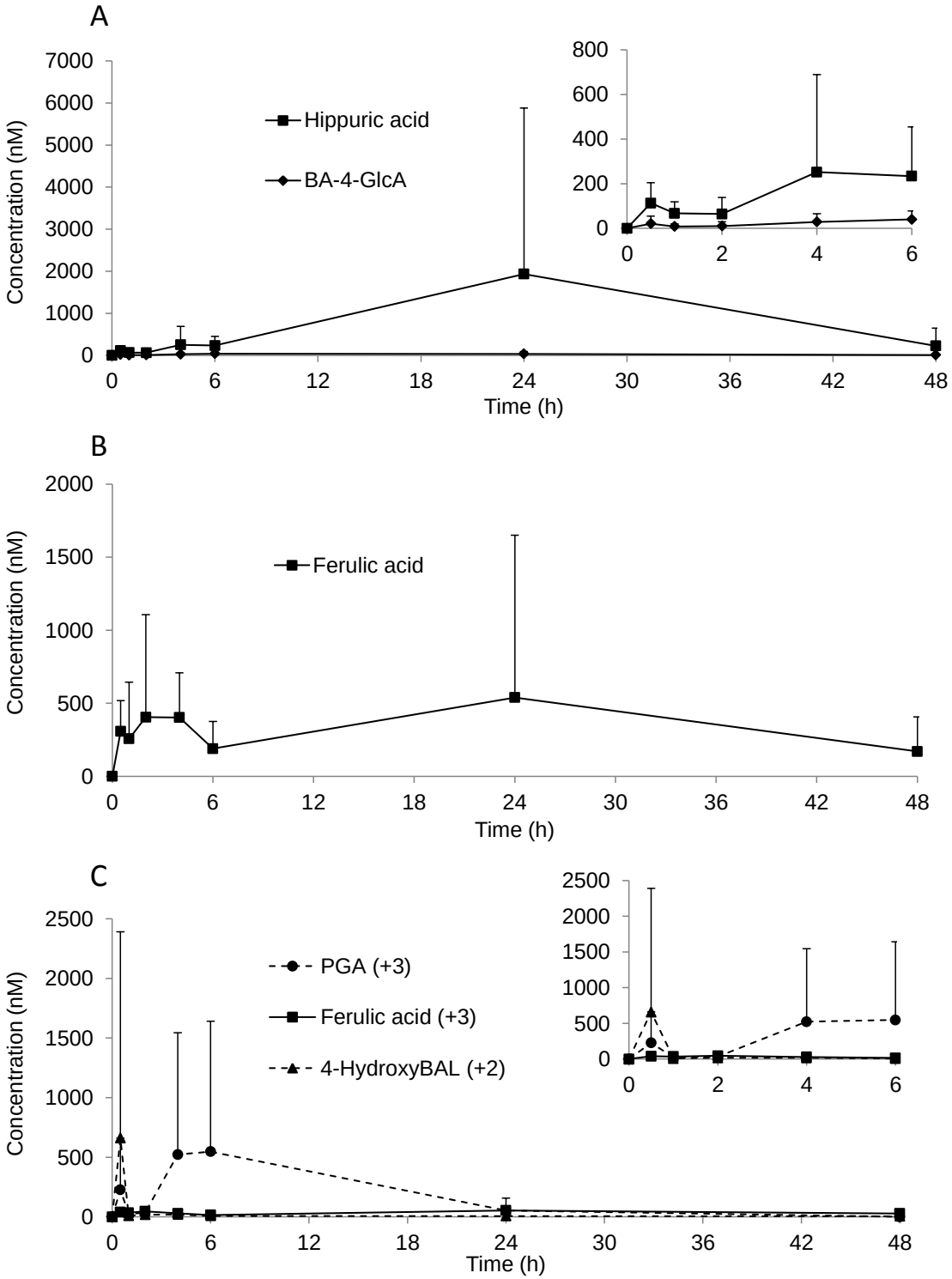


All data is mean ± SD. BA, benzoic acid; BAL, benzaldehyde; GlcA, glucuronide; PGA, phloroglucinaldehyde.

**Table 3.3** Urinary recovery of cyanidin-3-glucoside, its degradation products and derived metabolites in humans after the consumption of 500 mg $^{13}$C-labelled cyanidin-3-glucoside [a].

| Metabolite | n[b] | Maximum concentration (nM) | Time at maximum concentration[c] | Total recovery (μg) |
|---|---|---|---|---|
| *Parent anthocyanin* | | | | |
| Cyanidin-3-glucoside (C3G)[h] | 7 | 334 ± 382 | 1-2 h | 120 ± 159 |
| Cyanidin-glucuronide[d] | 5 | 88 ± 94 | 1-2 h | 24 ± 25 |
| Cyanidin-glucuronide[d] | 3 | 19 ± 12 | 1-2 h | 12 ± 12 |
| Peonidin-3-glucoside | 7 | 76 ± 113 | 1-2 h | 23 ± 28 |
| Methyl cyanidin-glucuronide[e] | 5 | 206 ± 234 | 1-2 h | 75 ± 80 |
| Methyl C3G-glucuronide[e] | 4 | 6 ± 5 | 1-2 h | 2 ± 2 |
| Methyl C3G-glucuronide[e] | 4 | 14 ± 13 | 1-2 h | 7 ± 7 |
| Methyl C3G-glucuronide[e] | 5 | 20 ± 19 | 1-2 h | 10 ± 12 |
| *Degradants* | | | | |
| Protocatechuic acid (PCA) | 8 | 337 ± 332 | 1-2 h | 72 ± 59 |
| Phloroglucinaldehyde | 8 | 170 ± 118 | 6-24 h | 67 ± 60 |
| *Protocatechuic acid derived* | | | | |
| Hydroxybenzoic acid[f] | 5 | 49 ± 24 | 1-2 h | 13 ± 8 |
| Vanillic acid (VA) | 4 | 3412 ± 624 | 1-2 h | 960 ± 700 |
| IsoVA | 4 | 212 ± 290 | 1-2 h | 80 ± 108 |
| Methyl-3,4-dihydroxybenzoate | 8 | 108 ± 111 | 3-4 h | 21 ± 23 |
| Benzoic acid-4-glucuronide | 7 | 129 ± 124 | 4-5 h | 53 ± 48 |
| PCA-3-glucuronide | 8 | 301 ± 204 | 1-2 h | 198 ± 117 |
| PCA-4-glucuronide | 8 | 233 ± 184 | 1-2 h | 100 ± 86 |
| PCA-3-sulfate | 8 | 1,112 ± 900 | 1-2 h | 322 ± 247 |
| PCA-4-sulfate | 8 | 1,244 ± 941 | 1-2 h | 492 ± 546 |
| VA-4-glucuronide | 8 | 762 ± 351 | 4-5 h | 618 ± 310 |
| IsoVA-3-glucuronide | 8 | 699 ± 254 | 5-6 h | 527 ± 261 |
| VA-4-sulfate | 7 | 1,682 ± 2,379 | 3-4 h | 449 ± 297 |
| IsoVA-3-sulfate | 5 | 822 ± 1,246 | 3-4 h | 183 ± 208 |
| Hippuric acid | 8 | 5,417 ± 13,876 | 6-24 h | 2,416 ± 6,288 |
| Ferulic acid | 8 | 1,840 ± 1,858 | 24-48 h | 798 ± 836 |
| 4-Hydroxyphenylacetic acid | 3 | 391 ± 197 | 4-5 h | 50 ± 3 |
| HomoPCA | 1 | 82 | 24-48 h | 28 |
| 4-Hydroxybenzaldehyde | 2 | 97 ± 133 | 5-6 h | 10 ± 13 |
| 3,4-Dihydroxybenzaldehyde | 6 | 24 ± 17 | 0-1 h | 6 ± 7 |
| *Phloroglucinaldehyde derived* | | | | |
| Ferulic acid[g] | 8 | 474 ± 770 | 0-1 h | 225 ± 496 |
| 4-Methoxysalicyclic acid | 1 | 172 | 3-4 h | 65 |

[a]Values are expressed as mean ± SD. [b]Metabolites detected in n= number of participants. [c]Samples were pooled within participants urine voids, for t=0-1 h (n=3), t=1-2 h (n=5), t=2-3 h (n=6), t=3-4 h (n=6), t=4-5 h (n=4), t=5-6 h (n=8), t=6-24 h (n=8) and t=24-48 h (n=8). [d]Quantified relative to C3G. [e]Quantified relative to peonidin-3-glucoside. [f]Includes both isomers (3-hydroxybenzoic acid and 4-hydroxybenzoic acid). [h]Alternative isomers of ferulic acid include 2-hydroxy-4-methoxycinnamic acid or 4-hydroxy-2-methoxycinnamic acid.

**Figure 3.5** Urinary elimination profiles of (A) cyanidin-3-glucoside and its metabolites, (B) protocatechuic acid and its metabolites and (C) methylated protocatechuic acid and its metabolites after the consumption of 500 mg $^{13}C_5$- cyanidin-3-glucoside.

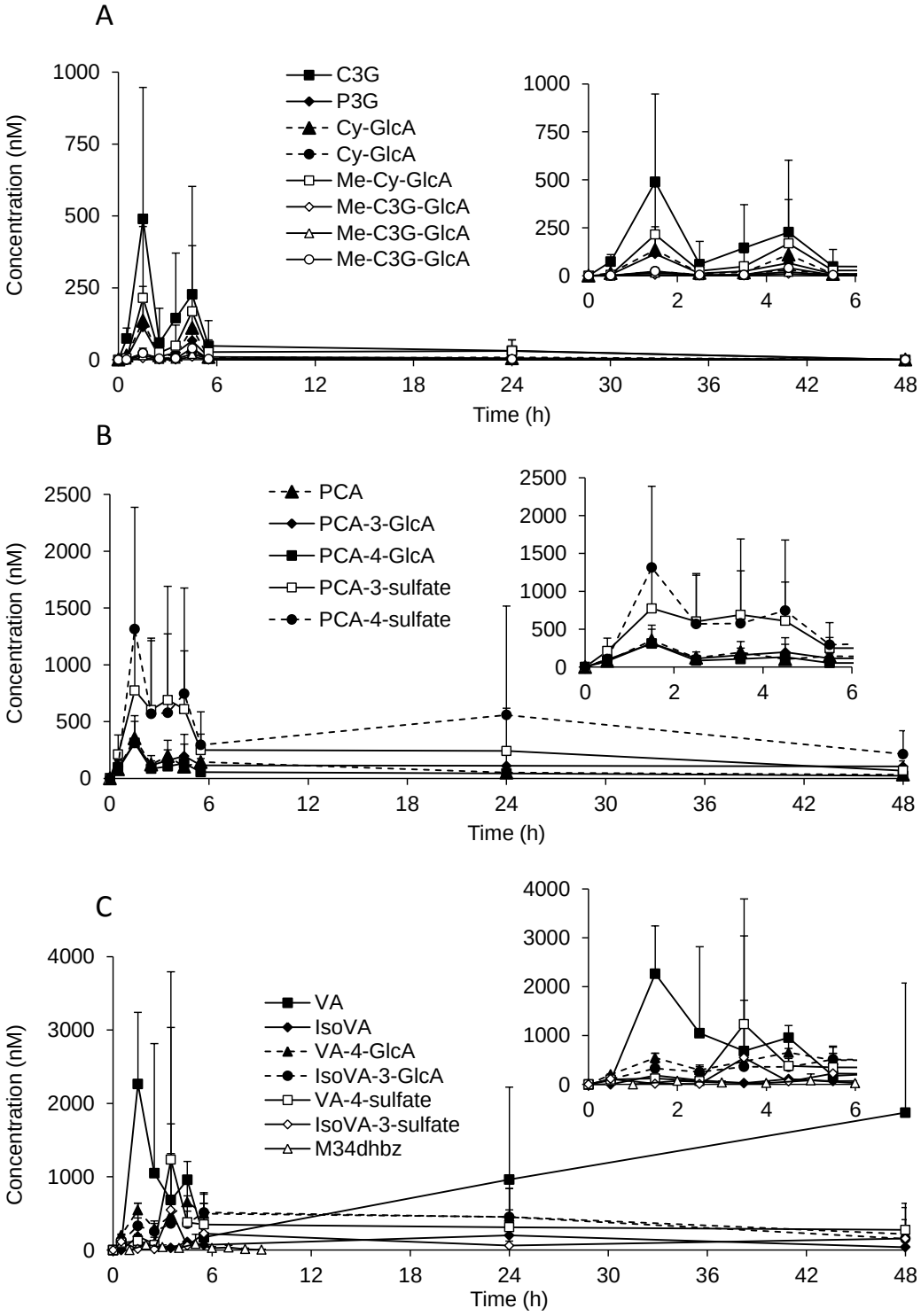


All data is mean ± SD. C3G, cyanidin-3-glucoside; Cy, cyanidin; GlcA, glucuronide; M34dhbz, methyl-3,4-dihydroxybenzoate; Me, methylated; P3G, peonidin-3-glucoside; PCA, protocatechuic acid; VA, vanillic acid.

**Figure 3.6** Urinary elimination profiles of (A) benzoic acid metabolites, (B) propenoic acid metabolites and (C) A-ring derived and aldehyde metabolites of cyanidin-3-glucoside after the consumption of 500 mg $^{13}C_5$- cyanidin-3-glucoside.

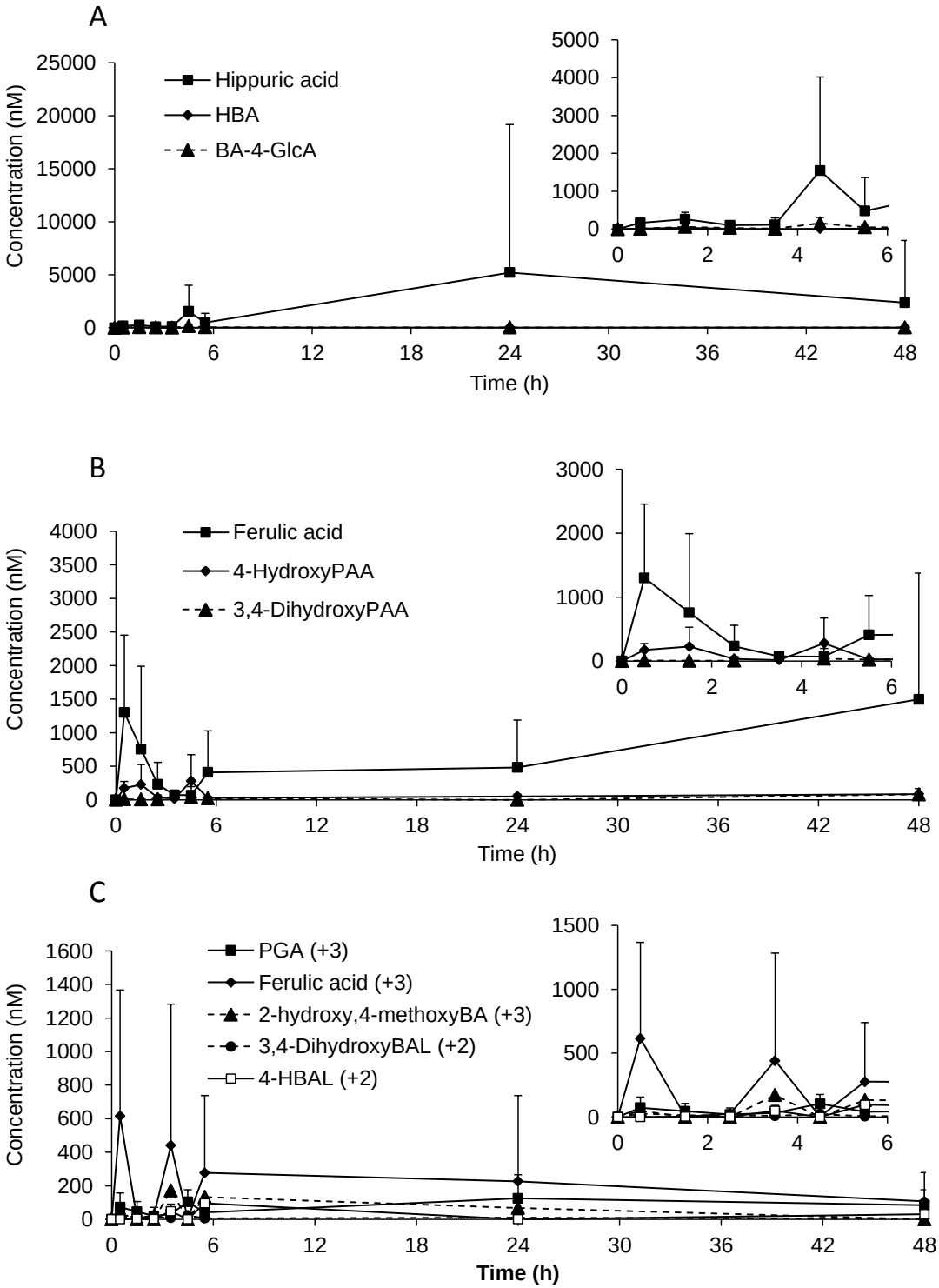


All data is mean ± SD. 4-HBAL, 4-hydroxybenzaldehyde; BA, benzoic acid; BAL, benzaldehyde; GlcA, glucuronide; PAA, phenylacetic acid; PGA, phloroglucinaldehyde.

### 3.3.2. Recovery of faecal metabolites

A total of 28 $^{13}$C-labelled compounds were detected in the faeces, including cyanidin-3-glucoside, protocatechuic acid, phloroglucinaldehyde, 24 B-ring derived metabolites and one A-ring derived metabolite (**Table 3.4**). B-ring derived ferulic acid was present at the highest concentrations within the faeces, with a maximum recovery of 2.4 ± 5.8 mg at 6-24 h post bolus, followed by the A-ring derived ferulic acid (470 ± 972 µg) and protocatechuic acid (361 ± 622 µg; Table 3.4).

**Table 3.4** Total faecal recovery of cyanidin-3-glucoside its degradation products and derived metabolites at 0-6 h, 6-24 h and 24-48 h after the consumption of 500 mg $^{13}$C-labelled C3G[a].

| Metabolite | Recovery (µg) | | |
|---|---|---|---|
| | 0-6 h | 6-24 h | 24-48 h |
| *Parent anthocyanin* | | | |
| Cyanidin-3-glucoside | ND | 70 [b] | 20 [b] |
| *Degradants* | | | |
| Protocatechuic acid | ND | 361 ± 622 [f] | 222 ± 357 [h] |
| Phloroglucinaldehyde | ND | 2 ± 3 [e] | 111 ± 193 [g] |
| *Protocatechuic acid derived* | | | |
| Hydroxybenzoic acid | ND | ND | 22 ± 20 [d] |
| 2,3-Dihydroxybenzoic acid | ND | ND | 440 ± 540 [c] |
| 4-Methoxysalicyclic acid | ND | 1 [b] | 273 ± 386 [c] |
| Vanillic acid | ND | 55 ± 2 [c] | 49 ± 37 [d] |
| Isovanillic acid | ND | 11 [b] | 9 [b] |
| Methyl-3,4-dihydroxybenzoate | ND | 167 ± 174 [d] | 92 ± 121 [g] |
| Methyl vanillate | ND | 35 [b] | ND |
| Benzoic acid-4-glucuronide | 2[b] | 7 ± 7 [f] | 15 ± 23 [i] |
| Protocatechuic acid-3-glucuronide | ND | 23 ± 38 [d] | 49 [b] |
| Protocatechuic acid-4-glucuronide | ND | 16 ± 43 [g] | 20 ± 46 [i] |
| Protocatechuic acid-3-sulfate | 0.1[b] | 30 ± 39 [c] | 12 ± 21 [e] |
| Protocatechuic acid-4-sulfate | ND | 23 ± 3 [d] | 12 ± 18 [d] |
| Vanillic acid-4-glucuronide | 4[b] | 3 [b] | 10 ± 14 [d] |
| Isovanillic acid-3-glucuronide | 2[b] | 1 [b] | 13 ± 15 [c] |
| Vanillic acid-4-sulfate | 1[b] | ND | 69 ± 68 [d] |
| Isovanillic acid-3-sulfate | ND | 1 ± 0.4[c] | 176 ± 247 [c] |
| Hippuric acid | ND | 12 ± 20 [d] | 28 ± 39 [c] |
| Caffeic acid | ND | 25 [b] | 355 ± 177 [c] |
| Ferulic acid | ND | 2,373 ± 5,811 [e] | 1,455 ± 3,336 [g] |
| 4-Hydroxyphenylacetic acid | ND | 7 [b] | 55 [b] |
| Homoprotocatechuic acid | 2[b] | 10 ± 8 [e] | 13 ± 17[f] |
| 4-Hydroxybenzaldehyde | ND | 1 ± 1 [c] | 0.1[b] |
| 4-Methoxybenzaldehyde | ND | 21 [b] | ND |
| 3,4-Dihydroxybenzaldehyde | ND | 3 ± 5 [c] | 5 ± 5 [i] |
| *Phloroglucinaldehyde derived* | | | |
| Ferulic acid[j] | ND | 470 ± 972 [c] | 241 ± 345 [f] |

[a]For 0-6 h, n=2; 6-24 h, n=8 and 24-48 h, n=8 participants provided samples; Values are expressed as mean ± SD, where metabolites were detected in [b]n=1, [c]n=2, [d]n=3, [e]n=4, [f]n=5, [g]n=6, [h]n=7, [i]n=8 participants; ND, not detected; [j]could alternatively represent 2-hydroxy-4-methoxycinnamic acid or 4-hydroxy-2-methoxycinnamic acid.

## 3.4. Discussion

Interest in anthocyanins continues to grow as a result of their reported cardiovascular activity (Cassidy *et al.*, 2013; Cassidy *et al.*, 2011; Mink *et al.*, 2007). The present chapter describes the first anthocyanin intervention trial to use an isotopically labelled marker to establish the pharmacokinetics of anthocyanins and anthocyanin metabolites in humans (Czank *et al.*, 2013). In previous labelled flavonoid studies, 4-$^{14}$C-quercetin has been fed to human volunteers (Walle *et al.*, 2001), and was recovered predominantly in the form of $CO_2$. This was likely primarily due to the position of the $^{14}$C label on the C=O bond of the C-ring. In contrast, a 2-$^{14}$C-quercetin-4'-glucoside study conducted in rats detected minimal radioactivity outside of the gastrointestinal tract, with the majority of the label observed within the colon and rapidly removed from circulation by the kidneys or excreted within faeces (Mullen *et al.*, 2008b). An anthocyanin labelled study which fed $^{14}$C-cyanidin-3-glucoside with the labelling on the six carbons within the B-ring, by direct stomach intubation to mice (Felgines *et al.*, 2010) obtained 92% recovery of the label in mice which were sacrificed after 3 h, most of which was within the gastrointestinal tract. This is the first study to feed an isotopically labelled anthocyanin to humans, and improves on previous tracer studies by increasing the number of positions containing a labelled carbon to enable the degradation of anthocyanins A- and B-ring to be traced. Furthermore, as the A ring contains three $^{13}$C labelled carbons, whilst the B-ring has two, the origin of the labelled metabolites in the present study could be defined.

Metabolite identification in previous human studies feeding anthocyanins has generally been limited to phase II conjugates of cyanidin-3-glucoside or cyanidin (Felgines *et al.*, 2003; Felgines *et al.*, 2005; Kay *et al.*, 2005; Kay *et al.*, 2004; Manach *et al.*, 2005), with only a limited number of human and animal studies identifying phenolic acid degradation products and/or colonic metabolites (Kim *et al.*, 1998; McGhie *et al.*, 2007; Nurmi *et al.*, 2009; Vitaglione *et al.*, 2007). By utilising the targeted labelling of the A- and B-rings of cyanidin-3-glucoside (Figure 1), the present study was able to confirm the pharmacokinetics of the phenolic conjugates of anthocyanins, through the identification of $^{13}C_5$, $^{13}C_3$ and $^{13}C_2$ derived metabolites of the parent structure. This strategy allowed for the establishment of pharmacokinetic profiles of 17 metabolites in the circulation as well as the elimination of 31 and 28 metabolites in the urine and faeces respectively. In addition, we have tentatively identified sulfate and glucuronide conjugates of phenylacetic and phenylpropenoic acids using $MS^3$, however standards were not available to confirm their identity with certainty, so

they have not been included in the present pharmacokinetic analysis. To our knowledge, this diversity of anthocyanin metabolites has not been demonstrated previously in humans.

In the present study, cyanidin-3-glucoside reached a maximum serum concentration of 141 ± 70 nM at 1.8 ± 0.2 h (Figure 3.3A). In addition, seven methylated and glucuronidated conjugates of cyanidin-3-glucoside and cyanidin were identified within the urine, reaching cumulative concentrations of 425 ± 72 nM at 1-2 h post bolus (Figure 3.5A), which is in accordance with previous studies (Kay *et al.*, 2004; Manach *et al.*, 2005; McGhie *et al.*, 2007). However, the parent anthocyanin only represented 2% of the total metabolites found in the circulation, and was only present for a relatively short period of time (t½, 0.4 h; Table 3.2), thus suggesting anthocyanin bioactivity is likely to be mediated by high concentrations of its phenolic intermediates as opposed to the parent structure.

It is well established that cyanidin-3-glucoside degrades to protocatechuic acid and phloroglucinaldehyde when incubated at neutral pH (Kay *et al.*, 2009; Woodward *et al.*, 2009) and this is corroborated by the present data, as protocatechuic acid ($t_{max,}$ 3.3 ± 0.7 h; Figure 3.3B) and phloroglucinaldehyde ($t_{max,}$ 2.8 ± 1.1 h; Figure 3.4C) were some of the earliest phenolic metabolites identified in the circulation (Table 3.2). In a previous study in which blood orange juice was fed, protocatechuic acid was identified as the major metabolite of cyanidin-3-glucoside, with concentrations reaching 492 ± 62 nM; around 250 fold higher than the cyanidin-3-glucoside reported in the serum (Vitaglione *et al.*, 2007). In the present study protocatechuic acid was observed at maximum concentrations of 147 ± 74 nM, thus suggesting it is not the major metabolite of anthocyanins. Interestingly, the A-ring derived degradation product, phloroglucinaldehyde, was present at concentrations greater than either cyanidin-3-glucoside or protocatechuic acid in the serum, exhibiting a $C_{max}$ of 582 ± 536 nM (Table 3.2 & Figure 3.4C). However, it was not detected in urine at any appreciable concentration ($C_{max,}$ 170 ± 42 nM; Table 3.3 & Figure 3.6C), suggesting it was further metabolised prior to elimination.

Multiple phase II metabolites of protocatechuic acid were detected in early (0.5 h to 1 h) serum samples, suggesting that the degradation of anthocyanins *in vivo* is swiftly followed by further biotransformation, and this is likely to be an important pathway for the clearance of anthocyanins from the body.

Hippuric acid was identified as the major metabolite of anthocyanins in the present study, reaching maximum concentration of 1962 ± 1389 nM in serum (Table 3.2) and 5,417 ± 4,507

nM in urine (Table 3.3). Hippuric acid has been speculated to be a common metabolite for many flavonoids (Pero, 2010) but it is a challenging metabolite to identify without the use of a carbon-label, due to its high background levels derived from other dietary and endogenous (i.e., protein metabolism and amino acid catabolism) sources, where it is reported to reach 1-2 mM concentrations in human urine (Pero, 2010; Toromanović *et al.*, 2008). The detection of $^{13}C_2$-labelled hippuric acid in the present study indicates hippuric acid is likely formed by the dehydroxylation of protocatechuic acid to benzoic acid, and its subsequent conjugation with glycine, or alternatively from the alpha-oxidation and dehydroxylation of hydroxyphenylacetic acids (Mullen *et al.*, 2008b). This suggests that glycine conjugation is a key conjugation process responsible for the clearance of phenolic metabolites of cyanidin-3-glucoside from the body.

Vanillic acid, the methylated metabolite of protocatechuic acid, was also present in the serum in high concentrations ($C_{max}$, 1.8 ± 0.8 µM; Table 3.2 & Figure 3.3C); however, it was only identified in the serum of two participants. In the majority of participants, sulfation appeared to be the preferential metabolic process for the clearance of protocatechuic acid, as protocatechuic acid-sulfate ($C_{max,}$ 157 ± 116 nM; Figure 3.3B) and vanillic acid-sulfate ($C_{max,}$ 430 ± 299 nM; Figure 2C) were detected in much higher concentrations than their unconjugated or glucuronide counterparts. Protocatechuic acid-4-glucuronide ($C_{max,}$ 68 ± 61 nM), vanillic acid-4-glucuronide ($C_{max,}$ 24 ± 4 nM) and isovanillic acid-3-glucuronide ($C_{max,}$ 35 ± 5 nM) were also present, albeit at much lower concentrations (Table 3.2 & Figure 3.3B,C). This pattern of elimination of protocatechuic acid metabolites in the serum was mirrored in the urine, with vanillic acid detected at the highest concentrations ($C_{max,}$ 3.4 ± 0.3 µM), followed by *meta* and *para* sulfated and glucuronidated conjugates of protocatechuic acid and vanillic acid (detected at concentrations ranging from 234 ± 65 nM to 1.7 ± 0.9 µM; Table 3.3). Di-methylation of protocatechuic acid was also observed by the presence of methyl-3,4-dihydroxybenzoate and methyl vanillate, however, methyl vanillate was only detected in the faeces (Table 3.4), suggesting that di-methylation of protocatechuic acid results in biliary elimination or is an exclusive product of microbial metabolism. Therefore, a primary route of metabolism and subsequent elimination of cyanidin-3-glucoside appears to be through degradation to protocatechuic acid, followed by rapid methylation of the catechol group to form vanillic acid, and subsequent sulfate and glucuronide conjugation, thus increasing its polarity and elimination from the body. This finding is supported by previous studies feeding catechin to rats and guinea pigs, where unconjugated metabolites represented only 3.5-4.4% of the recovered phenolic metabolites (DasandGriffiths, 1969). Minimal amounts of Phase I metabolites of protocatechuic acid were also detected in this study,

including 3,4-dihydroxybenzaldehyde ($C_{max,}$ 24 ± 7 nM; Figure 3.6C) and hydroxybenzoic acid ($C_{max,}$ 49 ± 11 nM; Figure 3.6A) within urine and 4-hydroxybenzaldehyde within serum ($C_{max,}$ 667 ± 653 nM; Figure 3.4C ) and urine ($C_{max,}$ 97 ± 94 nM; Figure 3.6C), suggesting that phase I metabolism may not be a highly utilised pathway for anthocyanin metabolism.

Many metabolites of cyanidin-3-glucoside in the present study appeared to follow biphasic serum kinetics, displaying an initial serum peak between 0-5 h followed by a second peak after 6-48 h (Figure 3.3 & Figure 3.4). Biphasic absorption of delphinidin-3-glucoside has previously been reported in rats, with maximum plasma concentrations reported at 15 and 60 min (Ichiyanagi *et al.*, 2004) and also within human studies feeding flavonoids, where metabolites including caffeic acid, ferulic acid and ferulic acid-sulfate were reported to follow biphasic plasma kinetic patterns (Azzini *et al.*, 2007; Rodriguez-Mateos *et al.*, 2013; Stalmach *et al.*, 2009a; Wittemer *et al.*, 2005). The biphasic profiles most likely results from metabolism occurring in different tissues, including the liver and at different sites within the intestine. For example, the initial peak in protocatechuic acid concentrations may result from the rapid degradation and absorption of cyanidin-3-glucoside following exposure to the higher pH found within the small intestine. In contrast, the second peak at 6-24 h post bolus may result from the catabolic cleavage of the C-ring of anthocyanins by microflora within the large intestine or alternatively from enterohepatic recirculation.

A total of three A-ring derived metabolites were identified in serum, urine and faeces (phloroglucinaldehyde, ferulic acid and 4-methoxysalicyclic acid) in the present study. However, the route of elimination of the A-ring derived metabolites is less clear than for protocatechuic acid. Interestingly, the A-ring derived metabolite, tentatively identified as ferulic acid within the serum, urine and faeces, matched the molecular weight (+3), fragmentation pattern, and had a similar retention time to the ferulic acid standard (Table 3.1). However, the exact structural conformation of $^{13}C_3$-ferulic acid cannot be established with certainty, as other probable isomers could result from the methylation of the A-ring hydroxyl to form either 2-hydroxy-4-methoxyphenyl prop-2-enoic acid or 4-hydroxy-2-methoxy phenyl prop-2-enoic acid (also known as 2-hydroxy-4-methoxycinnamic acid and 4-hydroxy-2-methoxycinnamic acid, respectively). These compounds have the same molecular formula as ferulic acid and could be formed without structural rearrangements of methoxy or hydroxyl moieties, as required to form ferulic acid from phloroglucinaldehyde. We are not aware of previous studies reporting 2-hydroxy-4-methoxycinnamic acid or 4-hydroxy-2-methoxy cinnamic acid metabolites of flavonoids and more work is required to confirm the exact structural identity of the metabolite, as presently there are no available

commercial standards for these phenylpropenoic isomers. In addition, A-ring derived 3,4-dihydroxybenzaldehyde and methyl 3,4-dihydroxybenzoate were tentatively identified within post bolus samples; however due to the low concentrations observed, they were not included in the present analyses. The absence of phloroglucinaldehyde derived metabolites of anthocyanins is not surprising considering the high reactivity of aldehydes (Keppler *et al.*, 2005). An *in vitro* faecal fermentation study which incubated phenolic acids and phloroglucinaldehyde in sterilised caecum inoculum filtrate from pigs at the physiological conditions found in the intestine (pH 6.4, 37 ºC), found phenolic acids were stable within the sterilised samples. However phloroglucinaldehyde was degraded extensively, with only small amounts remaining detectable after 24 h. Possible pathways for aldehyde instability include condensation with free amine groups of amino acids or proteins and formation of imine (Keppler *et al.*, 2005). However, at present little is known about the metabolism of phloroglucinaldehyde and further studies are required to delineate the mechanisms involved in its metabolism and clearance.

Colonic metabolism has long been speculated to be a major contributor to the overall metabolism of anthocyanins (Cardona *et al.*, 2013; Williamson *et al.*, 2010) and our $^{13}$C-labelled cyanidin-3-glucoside study reported 32 ± 6% of the recovered $^{13}$C-label in faeces (Czank *et al.*, 2013). It has been proposed that phenylpropenoic acids arise from cyanidin-3-glucoside as a result of bacterial cleavage of the C-ring in the colon (Forester *et al.*, 2008; González-Barrio *et al.*, 2010), which is supported by the detection of caffeic acid and its methyl metabolite, ferulic acid, within the faeces in the present investigation. The absence of caffeic acid from the serum and urine despite its abundance within the faeces (Table 3.4) suggests the catechol group of caffeic acid is rapidly methylated to yield ferulic acid, either during intestinal absorption, prior to entry into the systemic circulation or by the liver. The rapid metabolism of caffeic acid has been observed in previous phenolic acid intervention studies, where caffeic acid is reported at significantly lower concentrations than its methyl, glucuronyl and sulfate conjugates (Nardini *et al.*, 2006). In addition, ferulic acid was detected within serum and urine within 4 h of consumption, indicating that ferulic acid may in part be formed proximal to the colon (i.e., the mid and lower small intestine).

Based on the findings of this study, the metabolism of anthocyanins can be summarised as undergoing a combination of multiple biotransformations . The parent compound appears to undergo methylation and glucuronidation to some extent, however it primarily undergoes degradation, followed by significant phase II conjugation, particularly methylation and

**Figure 3.7** Proposed pathway for the metabolism of cyanidin-3-glucoside in humans.

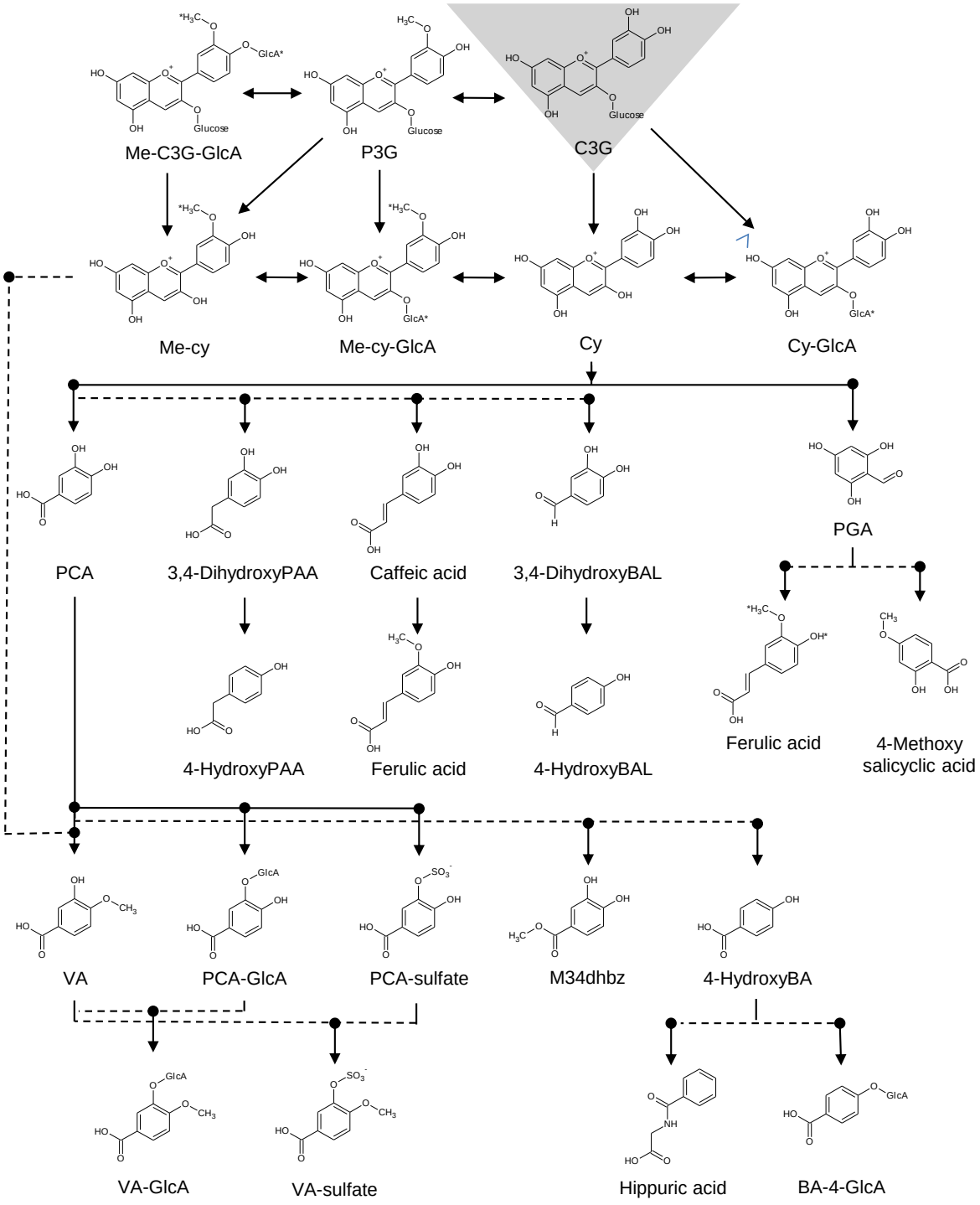


*Conjugates represent unknown structural position. BA, benzoic acid; BAL, benzaldehyde; C3G, cyanidin-3-glucoside; Cy, cyanidin; GlcA, glucuronide; Me, methoxy; M34dhbz, methyl-3,4-dihydroxybenzoate; P3G, peonidin-3-glucoside; PAA, phenylacetic acid; PGA, phloroglucinaldehyde.

sulfation. Given the early timing and high concentrations of protocatechuic acid and phloroglucinaldehyde observed in this study, it is clear that cyanidin-3-glucoside spontaneously degrades to protocatechuic acid and phloroglucinaldehyde in the small intestine; however, colonic metabolism is also likely to play a significant role. Dehydroxylation by colonic bacteria, to form hydroxybenzoic acid, followed by conjugation with glycine to form hippuric acid, appears to be the definitive elimination pathway. Finally, the metabolism of phloroglucinaldehyde to phenylpropenoic acids, which are similar to, or include ferulic acid, may be responsible for the detoxification and elimination of phloroglucinaldehyde.

The major limitation of the present method is its targeted approach, which relies on pure standards and MRM for identification. This approach is highly sensitive, however, it does not allow for the identification of unknown/untargeted metabolites. Additionally, synthesis of the speculated metabolites is necessary to confirm their identities. Alternative spectroscopy techniques, such as GC-MS/MS and high resolution time of flight (TOF) MS would aid in identifying further metabolites not captured by the present method. As many of the metabolites did not completely returned to baseline by 48 h, a longer blood, urine and faecal sampling time may have increased the recovery of metabolites. Despite these limitations, this human study has demonstrated for the first time that a wide array of metabolites are recovered by the described extraction and detection methods and these data represent a considerable advancement in our understanding of anthocyanin ADME.

## 3.5. Conclusion

In conclusion, the present chapter describes the identification of an extensive number of anthocyanin metabolites. The appearance of multiple peaks across the 48 h time period, and their wide range of elimination half-lives, suggest that the clearance of anthocyanins involves multiple processes, including enterohepatic recirculation, hepatic recycling, and microbial metabolism, with an extended period of intestinal absorption from both the small and large intestine. This study provides new insights into the metabolism of anthocyanins, which should inform the design of future clinical studies exploring the bioactivity of these potentially important dietary compounds.

# Chapter 4. Identification of anthocyanin metabolites following the ingestion of an extract derived from elderberries in humans

## 4.1. Introduction

As discussed in the foregoing chapter, despite the body of evidence for the cardioprotective effects of dietary anthocyanins (Cassidy *et al.*, 2013; Cassidy *et al.*, 2011; Erdman *et al.*, 2007; Mink *et al.*, 2007), the mechanisms involved remain poorly understood due to an incomplete understanding of their bioavailability and metabolism. Anthocyanins are reported to have a low bioavailability, with the majority of studies reporting a recovery of <1% of the ingested anthocyanin dose (Kay *et al.*, 2005; Manach *et al.*, 2005; McGhie *et al.*, 2007). Numerous human feeding studies have explored the absorption, distribution, metabolism and elimination (ADME) of anthocyanins, however most studies reported conjugated derivatives (methyl, glucuronide, sulfate) of parent anthocyanins to be the major metabolites in the circulation post consumption, with maximum serum concentrations ranging from 1.4 nM to 547 nM, between 0.5 h and 1.5 h ($t_{max}$) post consumption (Kay *et al.*, 2004; Manach *et al.*, 2005; McGhie *et al.*, 2007). At neutral pH, anthocyanins are susceptible to degradation (González-Barrio *et al.*, 2010; Woodward *et al.*, 2009), especially if their sugar moiety is hydrolysed, which may occur due to the action of lactase phlorizin hydrolase or cytosolic β-glucosidase within the intestinal epithelial cells (Crozier *et al.*, 2009; Day *et al.*, 2000; Del Rio *et al.*, 2010). Therefore, it has been proposed that anthocyanins are likely present in the circulation, as degradation products and metabolic intermediates (Kay, 2010).

Previously, human interventions feeding dried cranberry juice, strawberry or bilberry-loganberry extracts to humans identified potential metabolites of anthocyanins in plasma and urine including hippuric acid, benzoic acid, 4-hydroxybenzoic acid, protocatechuic acid, dihydroxybenzoic acids, caffeic acid, *p*-courmaric acid, ferulic acid, sinapic acid, 2-hydroxyphenylacetic acid, homovanillic acid, vanillic acid and 4-hydroxyphenlyacetic acid (Nurmi *et al.*, 2009; Russell *et al.*, 2009; Valentova *et al.*, 2007; Zhang *et al.*, 2004). However, a limitation of these data is that the origin of the phenolics could not be traced with certainty to the anthocyanins fed. Until recently, this was predominantly due to a lack of human anthocyanin studies feeding a labelled bolus. In addition, the varied and complex boluses of polyphenol rich food as utilised in previous interventions, further complicates the elucidation of the metabolic pathway of anthocyanins. However, as described previously

(Chapter **3**), we recently conducted an isotopic labelled anthocyanin intervention study, which fed 500 mg $^{13}$C-labelled cyanidin-3-glucoside to eight men and reported >40% recovery of the 500 mg anthocyanin bolus in serum, urine breath and faeces. The dose was recovered as 25 phenolic metabolites, attaining total peak concentrations of 5.97 ± 2.14 μM in the serum and 10.77 ± 4.52 μM in the urine (Czank *et al.*, 2013). The present study aimed to progress this work by confirming the metabolism of anthocyanins derived from an anthocyanin rich dietary source (elderberries; *Sambucus nigra*), as opposed to a pure synthetic anthocyanin, in order to explore the metabolism of anthocyanin derived phenolics from a food source. Elderberries provide a suitable source of anthocyanins as unlike fruits such as blueberries, which contain many different forms of anthocyanins, elderberries are specifically rich in in one form, namely cyanidin glycosides, and predominantly cyanidin-3-glucoside and cyanidin-3-sambubioside (Neveu *et al.*, 2010). Cyanidin-3-sambubioside-5-glucoside, cyanidin-3,5-diglucoside, cyanidin-3-rutinoside, pelargonidin-3-glucoside and pelargonidin-3-sambubioside are also found in low concentrations making up generally less than 7% of the total anthocyanins (Neveu *et al.*, 2010; Wu *et al.*, 2004).

Here we used stored samples from a previously completed 12 week anthocyanin intervention, where healthy post-menopausal women were fed 500 mg/day of anthocyanins derived from 2 g of elderberry extract (Curtis *et al.*, 2009). The present study investigated the impacts of a single bolus (500 mg anthocyanins; acute postprandial effect) and repeated daily doses (postprandial effect after 12 weeks chronic supplementation) on metabolite excretion, to establish if chronic exposure altered metabolism or elimination. To the best of our knowledge this is the first study to describe the impact of acute versus chronic anthocyanin exposure on anthocyanin derived phenolic metabolites within postprandial samples.

## 4.2. Materials and methods

### 4.2.1. Chemicals

Cyanidin-3-glucoside, peonidin-3-glucoside, pelargonidin-3-glucoside, cyanidin-3-sambubioside cyanidin-3-rutinoside and cyanidin-3,5-diglucoside were obtained from Extrasynthese (Genay, France). Phase II conjugates of phenolic acids (protocatechuic acid-3-glucuronide, protocatechuic acid-4-glucuronide, vanillic acid-4-glucuronide, benzoic acid-4-glucuronide, isovanillic acid-3-glucuronide, isovanillic acid-3-sulfate, protocatechuic acid-4-sulfate, vanillic acid-4-sulfate, protocatechuic acid-3-sulfate and benzoic acid-4-sulfate) were synthesised in the School of Chemistry and Centre for Biomolecular Sciences, University of

St. Andrews (UK) via recently published methods (Zhang *et al.*, 2012). All other compounds (2-hydroxybenzoic acid, 3-hydroxybenzoic acid, 4-hydroxybenzoic acid, 3,5-dihydroxy-benzoic acid, protocatechuic acid, 2,3-dihydroxybenzoic acid, 2,4-dihydroxybenzoic acid, gallic acid, 2-methoxybenzoic acid, 3-methoxybenzoic acid, 4-methoxybenzoic acid, 6-methoxysalicyclic acid, vanillic acid, isovanillic acid, methyl-3,4-dihydroxybenzoate, methyl-3,4-dimethoxy-benzoate,4-methoxysalicyclic acid methyl vanillate, methyl gallate, 3-methylgallic acid, syringic acid, caffeic acid, sinapic acid, *p*-coumaric acid, ferulic acid, phloroglucinaldehyde, 4-hydroxybenzaldehyde, 2,4-dihydroxybenzaldehyde, 3,4-dihydroxy-benzaldehyde, 2-hydroxy-4-methoxybenzaldehyde, 4-methoxybenzaldehyde, homo-vanillic acid, 4-hydroxyphenylacetic acid, homoprotocatechuic acid, 4-hydroxybenzyl alcohol, hippuric acid, 3-methylhippuric acid, 4-methylhippuric acid, phloridzin and scopoletin) were purchase from Sigma-Aldrich (Dorset, UK). HPLC grade methanol, acetonitrile and hydrochloric acid (HCl) were purchased from Fisher Scientific (Loughborough, UK) and all other chemicals, were purchased from Sigma-Aldrich (Dorset, UK). All water utilised was of Milli-Q grade (18.2 MΩ cm-1).

### 4.2.2. Materials

Strata-X™ solid phase extraction (SPE) columns (6 mL, 500 mg), Kinetex pentafluorophenol (PFP) HPLC column (2.6 µm, 100 x 4.6 mm, 100 Å) and SecurityGuard® cartridges (PFP, 4.0 x 2.0 mm) were purchased from Phenomenex (Cheshire, UK). Discovery® DSC-18 SPE columns (6 mL, 1 g) and Acrodisc 13mm, 0.45 µm PTFE syringe filters were purchased from Sigma-Aldrich (Dorset, UK).

### 4.2.3. Analysis of elderberry extract

The anthocyanin content of the elderberry (*Sambucus nigra*) extract (standardised to 25% anthocyanins) obtained from Artemis International (Fort Wayne, Indianapolis) was previously established as 500 mg anthocyanins (cyanidin-3-glucoside and cyanidin-3-sambubioside, quantified as cyanidin-3-glucoside equivalents) per 2 g extract (Curtis *et al.*, 2009). The phenolic profile was presently established through HPLC-ESI-MS/MS analysis, where prior to analysis, 500 mg of elderberry extract was dissolved in 2 mL of 0.1% HCl and 5 mL acidified methanol (0.1% vv. HCl) and sonicated for 30 min in a chilled waterbath following syringe filtration. The polyphenol content of the breakfast foods was estimated using phenol explorer (Neveu *et al.*, 2010).

### 4.2.4. Study design

Samples were analysed from a parallel-designed, randomised, placebo-controlled study previously conducted in 2005-2007, which explored the effect of anthocyanins on cardiovascular bioactivity and liver function (Curtis *et al.,* 2009). The study fed elderberry extract or placebo to 52 (26 in treatment and 26 in placebo group) healthy (age, 58.2 ± 5.6 y; BMI, 24.7 ± 0.6 kg/m²) postmenopausal women (Curtis *et al.*, 2009). Participants underwent a seven day washout-period (avoiding anthocyanin rich foods and limiting tea and chocolate intake) and were then assigned to consume either two elderberry capsules (125 mg anthocyanins/tablet) or identically coloured opaque placebo capsules (0 mg anthocyanins/tablet) in the morning and evening each day for 12 weeks. Dietary restrictions were continued throughout the duration of the 12wk intervention. The elderberry capsules provided a daily total of 2 g elderberry extract, containing 500 mg total anthocyanins whilst the placebo capsules contained 500 mg of cellulose. Participants were assessed following a single bolus dose (week 0, acute) and following 12 weeks of continuous supplementation (week 12, chronic), where blood and urine samples were collected in the fasting period (baseline) and over 3 h following the consumption of a 500 mg oral bolus dose of anthocyanins (equivalent to the daily dose administered throughout the study). An anthocyanin and caffeine free breakfast of cereal [Weetabix™ (Weetabix Ltd, UK) or Cornflakes (Kelloggs™, UK)], white toast with margarine/butter, milk and water was provided *ad labitum* on the intervention days. Postprandial blood and urine samples (50 mL sample) were collected for 3 h (t=1, 2, 3 h) following ingestion (**Figure 4.1**). Blood was collected in EDTA tubes and plasma obtained by centrifugation at 1500 x 3 g for 15 min, where urine and plasma samples were acidified with HCl (to a final concentration of 1% vv) prior to storage at -80 °C until analysis. The study protocol was approved by the Norfolk Research Ethics Committee, conducted at the University Clinical Research and Trials Unit and all participants provided written informed consent. In the present analytical investigation, a random subset of the banked samples from 15 of the 26 participants on the anthocyanin treatment were analysed to explore the effect of 12wks repeated dosing on anthocyanin metabolism (the placebo group was not explored).

### 4.2.5. Creatinine analysis

Urine creatinine concentrations were established on an iLab 650 Chemistry Analyzer using the IL Test Creatinine-0018257240 kit (Instrumentation Laboratory, Italy). The kit measures creatinine based on the colorimetric reaction of creatinine with picric acid under alkali conditions (ClarkandThompson, 1949). Quality control samples indicated a CV=4.26%.

Urine samples were adjusted for creatinine concentration, and are therefore expressed as ratios per mM creatinine.

**Figure 4.1** Clinical study design summarising the collection of blood and urine samples.

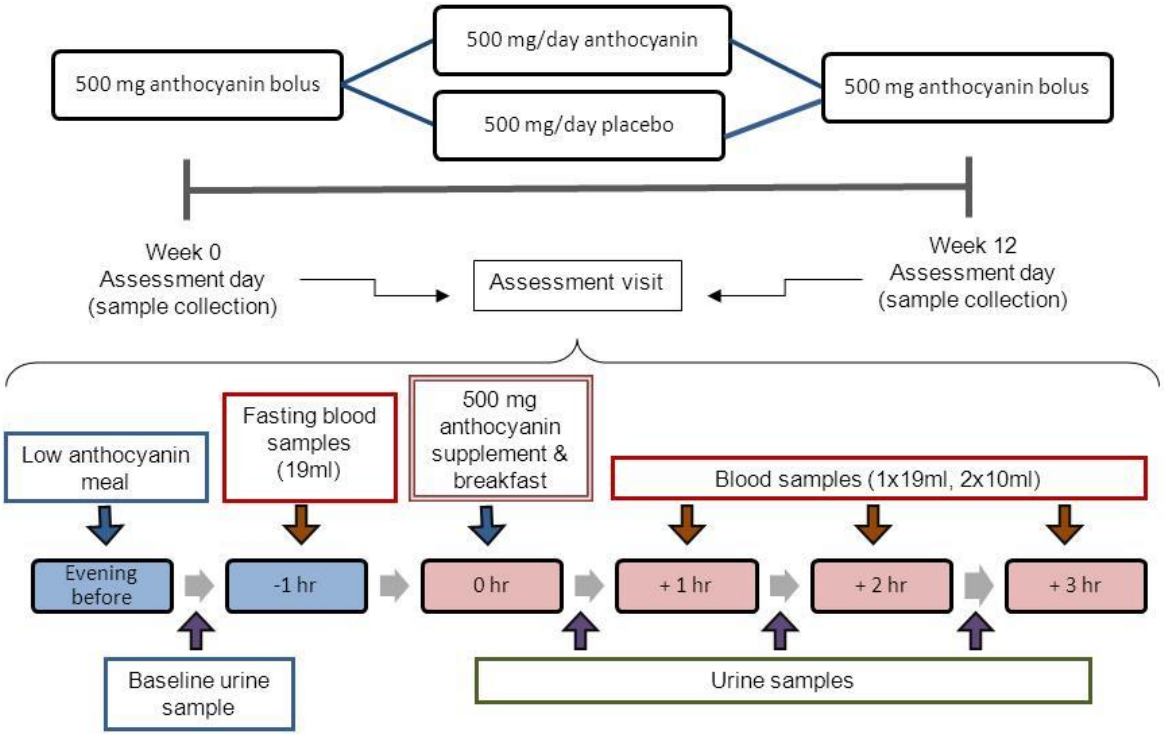


### 4.2.6. Sample preparation

The extraction methods used for the purification and concentration of metabolites from biological samples were as previously optimised in Chapter 2. Briefly, samples were extracted using DSC-18 (for urine) and Strata-X™ (for plasma) SPE cartridges which were preconditioned with one column volume (6 mL) of acidified methanol (10% formic acid (v/v) in methanol) followed by one column volume of acidified water [10% formic acid (v/v) in water (pH 2.4)]. Samples were loaded onto the cartridge with 2 mL water (pH 2.4), washed, evaporated to dryness under vacuum, eluted with 7 mL acidified methanol and evaporated to approximately 50 µL using a Thermo speedvac. The concentrated extract was re-suspended in 200 µL water (pH 2.4), 10 µL of 1 mg/ml scopoletin was added as a volume control standard post extraction and samples were then syringe filtered through 0.45 µm PTFE syringe filters and stored at -80 ºC until analysis. Individual analysis of the urine samples was carried out to establish metabolite variation between participants, whilst plasma samples were pooled prior to extraction, by taking 66.7 µL of plasma from each participant (n = 15; for a total volume of 1 mL) at each time point, thus providing a ‘snapshot’ of the

plasma metabolic profile. The extraction efficiency of the solid phase extraction methods for cyanidin-3-glucoside and the 17 phenolic metabolites identified in urine and plasma was previously established (**Chapter 2**) as 88.0 ± 5.4% (CV, 8.6 ± 5.4%) for urine and 86.9 ± 9.1% (CV, 8.2 ± 5.9%) for plasma, for n = 3 replicates of each analyte.

### 4.2.7. HPLC-ESI-MS/MS analysis

The HPLC-ESI-MS/MS conditions used for the identification of metabolites in biological samples were as previously optimised in Chapter 2. Briefly, HPLC-ESI-MS/MS analysis was carried out on an Agilent 1200 series HPLC system coupled with an AB Sciex 3200 Q-trap MS/MS system equipped with an electrospray ionisation (ESI) Turbo V source and samples were injected onto a Kinetex PFP column. The mobile phase consisted of 0.1% formic acid (v/v) in water (A) and 0.1% formic acid (v/v) in acetonitrile (B), at a flow rate of 1.5 mL/min-1 at 0 min, 1 mL/min at 7 to 14 min and 1.5 mL/min at 14 to 28 min. The gradient consisted of 1% B at 0 min, 7.5% B at 7 min, 7.6% B at 14 min, 10% B at 17 min, 12% B at 18.5 min, 12.5% B at 20 min, 30% B at 24 min, 90% B at 25 to 28 min. MS/MS source parameters included curtain gas 40, ionspray voltage -4000V / +5500V, temperature 700 °C, nebulizer gas 60 psi and auxiliary gas 60 psi. The system was controlled by Analyst software (v. 1.5, Applied Biosystems/MDS Sciex).

Multiple reaction monitoring (MRM) scans were performed using conditions optimised for the detection of pure standards (**Chapter 2, Table 2.2**). Metabolites were confirmed on the basis of retention time and the presence of two or more ion transitions. The peak area of the most intense ion transition was determined from the chromatograph and used for quantification. Seven-point calibration curves ranging from 0 to 10 µM for the analysis of the anthocyanin conjugates and from 0 to 50 µM for the analysis of phenolic metabolites were utilised for quantification. The calibration curves were prepared by spiking a standard mixture of the compounds into a matched-matrix (pooled blank/baseline urine or plasma from all participants) and were baseline adjusted to account for any interference from analytes present in baseline samples, such as phenolic compounds. For anthocyanin conjugates, where the corresponding standards were not available, compounds were putatively identified based on the parent-daughter fragmentation pattern (cyanidin-glucuronide, 463/287; cyanidin-3-glucoside-disulfate, 609/287; cyanidin-diglucuronide, 639/287; cyanidin-glucuronide-sulfate, 541/285 (negative mode); peonidin-glucuronide, 477/301; peonidin-3-glucoside-glucuronide, 639/301; cyanidin-3-sambubioside,5-glucoside, 743/287; pelargonidin-3-sambubioside, 565/271) and quantified relative to cyanidin-3-glucoside or peonidin-3-glucoside (where appropriate).

The HPLC-MS/MS methods were previously validated for linearity and precision across all metabolites (**Chapter 2**). Six point standard curves ranging from 1.25 to 20 µM were constructed from analytical standards and injected six times. The precision was established as 1.4% to 8.2% and linearity of the standard curves was established as $r^2$= 0.991 to 1.000 (CV, 0.2%) across the identified metabolites. In addition, there was a between run variation of 9.17% CV for quality control standards, injected between every eight samples run.

### 4.2.8. Statistics

All statistical analyses were performed using SPSS for Windows statistical software package (version 18.0). Within-subject comparisons were analysed using an ANOVA with repeated-measures general linear model, with Greenhouse-Geisser correction for non-spherical data and Bonferroni adjustment (within-subjects, baseline, 0-1 h, 1-2 h, 2-3 h) for pairwise comparisons. Between-group comparisons were analysed using ANOVA with repeated-measures general linear model, with Bonferroni adjustment (within-subjects, week 0 and week 12 at baseline, 0-1 h, 1-2 h, 2-3 h). Unless otherwise stated, results are expressed as mean ± SD and $p<0.05$ was considered significant. Baseline refers to the fasting samples collected prior to the consumption of the anthocyanin bolus. No statistical analyses were possible for the pooled plasma samples (n=1; 15 participants plasma pooled at each individual time point).

## 4.3. Results

### 4.3.1. Elderberry extract composition

Independent analysis of the commercially available elderberry-derived anthocyanin extract identified 15 phenolic acids, aldehydes or benzoates (hereafter referred to as phenolics) present, accounting for 203 mg total phenolics per gram of elderberry extract (**Table 4.1**). Protocatechuic acid was identified in the highest concentrations, constituting 68.3% of the total phenolics identified, followed by phloroglucinaldehyde (7.7%) and caffeic acid (7.3%). The anthocyanin content of the elderberry bolus was previously established as 250 mg anthocyanin/g extract (Curtis *et al.*, 2009), predominantly consisting of cyanidin-3-glucoside (53.5%) and cyanidin-3-sambubioside (39.5%) (Neveu *et al.*, 2010). Elderberries are also reported to contain low amounts of cyanidin-3-sambubioside-5-glucoside (6%) and cyanidin-3,5-diglucoside (1%) (Neveu *et al.*, 2010). A total proximate analysis of the extract was not conducted to establish the composition of the remaining 55% by weight; however elderberries have a reported relative composition of 18.4% carbohydrate, 0.7% protein, 0.5%

fat, 0.5% organic acids and 6.2% quercetin (Neveu *et al.*, 2010; Saxholt *et al.*, 2008; Veberic *et al.*, 2009).

**Table 4.1** Phenolics identified via HPLC-ESI-MS/MS within elderberry extract standardised to 25% anthocyanins obtained from Artemis International.

| Compound | Concentration (mg/g extract) | % of total |
|---|---|---|
| Protocatechuic acid | 138.59 ± 4.48 | 68.31 |
| Phloroglucinaldehyde | 15.65 ± 1.18 | 7.71 |
| Caffeic acid | 14.74 ± 1.10 | 7.27 |
| 4-Hydroxybenzoic acid | 11.28 ± 0.28 | 5.56 |
| p-Courmaric acid | 9.43 ± 0.32 | 4.65 |
| Vanillic acid | 2.70 ± 0.13 | 1.33 |
| 4-Hydroxybenzaldehyde | 2.51 ± 0.01 | 1.24 |
| Methyl-3,4-dihydroxybenzoate | 1.85 ± 0.14 | 0.91 |
| Gallic acid | 1.54 ± 1.18 | 0.76 |
| Ferulic acid | 1.39 ± 0.08 | 0.69 |
| 3,4-Dihydroxybenzaldehyde | 1.37 ± 0.02 | 0.68 |
| Sinapic acid | 1.10 ± 0.22 | 0.54 |
| Homoprotocatechuic acid | 0.38 ± 0.03 | 0.19 |
| Isovanillic acid | 0.30 ± 0.01 | 0.15 |
| Methyl gallate | 0.04 ± 0.00 | 0.02 |

Values represent mean ± SD, n=3.

### 4.3.2. Identification of anthocyanin metabolites in urine and plasma

Twenty-eight metabolites were identified in the urine following acute and chronic anthocyanin consumption. 17 were phenolics and 11 were anthocyanin conjugates (**Table 4.2**). Levels of the phenolic metabolites ranged from 145 ± 86 to 7382 ± 5927 nM/mM creatinine, whilst the parent anthocyanins were identified at levels of 0.1 ± 0.3 to 309 ± 673 nM/mM creatinine at 3 h following acute anthocyanin consumption. In plasma, 21 metabolites were identified, of which 17 were phenolics and four were anthocyanin conjugates (**Table 4.3**), and the cumulative phenolic metabolites were present at 45 fold higher concentrations (at a range of 2 to 358 nM at 3 h following acute anthocyanin consumption) relative to their parent anthocyanins (at a range of 2 to 11 nM at 3 h following acute anthocyanin consumption). Due to a similarity of data following acute and chronic anthocyanin consumption, specific figures in the text will now refer solely to data following the acute dose unless stated otherwise.

The metabolites identified within the urine (Table 4.2) and plasma (Table 4.3) differed substantially. The plasma contained aldehydes (4-hydroxybenzaldehyde and 3,4-

dihydroxybenzaldehyde), benzoic acids (4-methoxysalicyclic acid, benzoic acid-4-sufate) and methyl derivatives of protocatechuic acid (methyl-3,4-dihydroxybenzoate and syringic acid), which were absent from the urine. By comparison, the urine contained more anthocyanin conjugates, cinnamic acids (*p*-courmaric and sinapic acid), phenylacetic acids [homovanillic acid and homoprotocatechuic acid (also known as 3,4-dihydroxyphenylacetic acid)], 3,5-dihydroxybenzoic acid and 4-hydroxybenzyl alcohol, which were absent from the plasma.

### 4.3.3. Anthocyanins within urine and plasma

Anthocyanins reached maximal urinary levels of 548 ± 219 nM/mM creatinine 3 h following intake of the elderberry extract (Table 4.3). In 3 h post intake urine samples, cyanidin-3-glucoside was present at levels of 309 ± 673 nM/mM creatinine and cyanidin-3-sambubioside was identified at levels reaching 99 ± 116 nM/mM creatinine. In addition, nine conjugates of cyanidin were putatively identified in urine samples: two cyanidin glucuronides, cyanidin-diglucuronide, cyanidin-3-glucoside-disulfate, peonidin-3-glucoside, peonidin-glucuronide and three peonidin-3-glucoside-glucuronides, reaching cumulative levels of 140 ± 33 nM/mM creatinine 3 h post bolus (Table 4.3 & **Figure 4.2**).

Within pooled plasma samples, anthocyanins reached a maximum concentration of 34 nM, 2 h post bolus, where cyanidin-3-glucoside and cyandin-3-sambubioside were present in concentrations of 7 nM and 16 nM respectively (Table 4.3). Only two anthocyanin conjugates, namely cyanidin-glucuronide and peonidin-glucuronide were identified within the plasma and were found at maximum concentrations of 2 nM and 9 nM at 2 h and 3 h post bolus respectively (Table 3.4). Furthermore, no anthocyanins were present within week 0 baseline samples, however, low concentrations (22 ± 5 nM in urine, Table 4.2 and 1 nM in plasma, Table 4.3) were identified within week 12 baseline samples, approximately 12 h following the previous anthocyanin dose. A high inter-individual variation in anthocyanin concentration was observed between participants, with the urinary concentration of cyanidin-3-glucoside ranging from 21 to 2666 nM/mM creatinine, 3 h following anthocyanin supplementation (Figure 4.3).

**Table 4.2** Ratio of anthocyanins, anthocyanin conjugates and phenolics in urine samples following acute and chronic intake of anthocyanins from an elderberry extract, expressed per mM creatinine.

| Compound | Ratio, nM/mM creatinine (% of total metabolites)[a] | | | | | Previously identified in urine |
|---|---|---|---|---|---|---|
| | Baseline | t(0-1 h) | t(1-2 h) | t(2-3 h) | Total | |
| C3G[b] | ND | 5 ± 7 (0.05) | 168 ± 317 (0.76) | 309 ± 673 (0.93) | 481 ± 385 | (Bitsch *et al.*, 2004b; |
| C3G[c] | 6 ± 11 (0.05) | 11 ± 15 (0.05) | 151 ± 241 (1.17) | 232 ± 303 (1.81) | 400 ± 212 | Cao *et al.*, 2001; Czank *et al.*, 2013; Milbury *et al.*, 2002; Mülleder *et al.*, 2002; Murkovic *et al.*, 2001; Wu *et al.*, 2002) |
| Cyanidin-3-sambubioside[b] | ND | 2 ± 4 (0.02) | 42 ± 55 (0.19) | 99 ± 116 (0.30) | 142 ± 75 | (Bitsch *et al.*, 2004b; |
| Cyanidin-3-sambubioside[c] | 6 ± 5 (0.05) | 9 ± 9 (0.05) | 36 ± 28 (0.29) | 100 ± 69 (0.79) | 152 ± 53 | Cao *et al.*, 2001; Milbury *et al.*, 2002; Mülleder *et al.*, 2002; Murkovic *et al.*, 2001; Wu *et al.*, 2002) |
| Cyanidin-glucuronide[b,d] | ND | 2 ± 5 (0.02) | 25 ± 44 (0.12) | 41 ± 39 (0.12) | 68 ± 33 | (Czank *et al.*, 2013) |
| Cyanidin-glucuronide[c,d] | 2 ± 2 (0.01) | 5 ± 5 (0.02) | 20 ± 14 (0.16) | 67 ± 53 (0.53) | 94 ± 38 | |
| Cyanidin-glucuronide[b,d] | ND | 0.1 ± 0.2 (0) | 1 ± 2 (0.01) | 4 ± 4 (0.01) | 5 ± 3 | (Czank *et al.*, 2013) |
| Cyanidin-glucuronide[c,d] | 1 ± 2 (0.01) | 1 ± 2 (0.01) | 2 ± 2 (0.02) | 7 ± 7 (0.06) | 11 ± 5 | |
| Cyanidin-diglucuronide[b,d] | ND | 0 ± 0 (0) | 0.1 ± 0.3 (0) | 0.1 ± 0.3 (0) | 0.3 ± 0.2 | NA |
| Cyanidin-diglucuronide[c,d] | 0 ± 0 (0) | 0 ± 0 (0) | 0.1 ± 0.1 (0) | 0.3 ± 0.4 (0) | 0.4 ± 0.3 | |
| C3G-disulfate[b,d] | ND | ND | 1 ± 1 (0) | 1 ± 2 (0) | 2 ± 1 | NA |
| C3G-disulfate[c,d] | 0.03 ± 0.07 (0) | 0.02 ± 0.06 (0) | 0.5 ± 1.0 (0) | 1 ± 2 (0.01) | 1.9 ± 0.3 | |
| P3G[b] | ND | 1 ± 1 (0) | 9 ± 10 (0.04) | 18 ± 21 (0.05) | 27 ± 13 | (Czank *et al.*, 2013; |
| P3G[c] | 1 ± 1 (0.05) | 1 ± 1 (0) | 6 ± 5 (0.05) | 18 ± 10 (0.14) | 25 ± 9 | Wu *et al.*, 2002) |
| Peonidin-glucuronide[b,e] | ND | 2 ± 5 (0.02) | 35 ± 57 (0.16) | 69 ± 61 (0.21) | 105 ± 50 | (Czank *et al.*, 2013; |
| Peonidin-glucuronide[c,e] | 6 ± 8 (0) | 8 ± 7 (0.04) | 31 ± 22 (0.24) | 120 ± 83 (0.94) | 164 ± 63 | Wu *et al.*, 2002) |
| P3G-glucuronide[b,e] | ND | 0 ± 0.1 (0) | 1 ± 2 (0.01) | 3 ± 3 (0.01) | 4 ± 2 | (Czank *et al.*, 2013) |
| P3G-glucuronide[c,e] | 0.2 ± 0.3 (0) | 0.3 ± 0.3 (0) | 1 ± 1 (0.01) | 4 ± 2 (0.03) | 5 ± 2 | |

| | | | | | | |
|---|---|---|---|---|---|---|
| P3G-glucuronide[b,e] | ND | 0 ± 0.1 (0) | 1 ± 1 (0) | 1 ± 1 (0) | 2 ± 1 | (Czank *et al.*, 2013) |
| P3G-glucuronide[c,e] | 0.1 ± 0.2 (0) | 0.1 ± 0.2 (0) | 0.4 ± 0.4 (0) | 1 ± 1 (0.01) | 2 ± 1 | |
| P3G-glucuronide[b,e] | ND | 0.1 ± 0.3 (0) | 2 ± 2 (0.01) | 4 ± 4 (0.01) | 6 ± 3 | (Czank *et al.*, 2013) |
| P3G-glucuronide[c,e] | 0.4 ± 0.5 (0) | 0.4 ± 0.4 (0) | 2 ± 1 (0.01) | 5 ± 3 (0.04) | 7 ± 2 | |
| 4-Hydroxybenzoic acid[b] | 904 ± 694 (9.28) | 1386 ± 941 (13.44) | 1897 ± 1026 (8.54)[f] | 1985 ± 985 (5.89)[f] | 6172 ± 998 | (Czank *et al.*, 2013; |
| 4-Hydroxybenzoic acid[c] | 781 ± 466 (6.16) | 1251 ± 692 (6.19) | 1275 ± 571 (10.06) | 1451 ± 910 (11.45) | 4758 ± 829 | Nurmi *et al.*, 2009; Russell *et al.*, 2009) |
| PCA[b] | 70 ± 52 (0.72) | 155 ± 209 (1.50) | 802 ± 768 (3.61) | 1534 ± 1232 (4.55)[f] | 2560 ± 929 | (Czank *et al.*, 2013; |
| PCA[c] | 90 ± 49 (0.71) | 194 ± 147 (0.96) | 760 ± 514 (6.00) | 1520 ± 940 (12.00) | 2564 ± 949 | Koli *et al.*, 2010; Nurmi *et al.*, 2009; Russell *et al.*, 2009; Vitaglione *et al.*, 2007) |
| 3,5-Dihydroxybenzoic acid[b] | 258 ± 261 (2.65) | 327 ± 220 (3.17) | 1015 ± 556 (4.57) | 1862 ± 1016 (5.52)[f] | 3462 ± 878 | NA |
| 3,5-Dihydroxybenzoic acid[c] | 333 ± 285 (2.63) | 421 ± 279 (2.09) | 1119 ± 1108 (8.83) | 1975 ± 1546 (15.58) | 3848 ± 1180 | |
| VA[b] | 215 ± 145 (2.21) | 321 ± 275 (3.11) | 2110 ± 2031 (9.51) | 4345 ± 3205 (12.88)[f] | 6991 ± 2511 | (Czank *et al.*, 2013; |
| VA[c] | 185 ± 116 (1.46) | 367 ± 204 (1.82) | 1762 ± 1257 (13.9) | 3522 ± 2843 (27.79) | 5835 ± 2566 | Koli *et al.*, 2010; Nurmi *et al.*, 2009; Russell *et al.*, 2009) |
| Phloroglucinaldehyde[b] | 3 ± 3 (0.03) | 37 ± 81 (0.35) | 309 ± 368 (1.39)[f] | 602 ± 632 (1.79)[f] | 951 ± 433 | (Czank *et al.*, 2013) |
| Phloroglucinaldehyde[c] | 41 ± 44 (0.32) | 120 ± 181 (0.59) | 320 ± 245 (2.53) | 703 ± 510 (5.55) | 1184 ± 459 | |
| HomoVA[b] | 3695 ± 2647(37.95) | 3508 ± 2390 (34.03) | 5403 ± 3880 (24.34) | 7382 ± 5927 (21.88)[g] | 19989 ± 4172 | (Koli *et al.*, 2010; |
| HomoVA[c] | 5833 ± 5379 (46.03) | 9402 ± 9721 (46.56) | 7386 ± 4468 (58.29) | 8812 ± 4576 (69.54) | 31433 ± 6270 | Nurmi *et al.*, 2009) |
| HomoPCA[b] | 870 ± 521 (8.93) | 1095 ± 902 (10.62) | 1453 ± 1023 (6.55) | 1945 ± 1302 (5.77)[f] | 5363 ± 1037 | (Koli *et al.*, 2010; |
| HomoPCA[c] | 1289 ± 1205 (10.17) | 2054 ± 1847 (10.17) | 1755 ± 1154 (13.85) | 2213 ± 2094 (17.46) | 7312 ± 1557 | Nurmi *et al.*, 2009) |
| 4-Hydroxybenzyl alcohol[b] | 716 ± 321 (7.35) | 790 ± 420 (7.67) | 1074 ± 564 (4.84) | 1397 ± 700 (4.14)[f] | 3977 ± 575 | NA |
| 4-Hydroxybenzyl alcohol[c] | 882 ± 387 (6.96) | 1634 ± 1058 (8.09) | 1460 ± 924 (11.52) | 1971 ± 2013 (15.56) | 5947 ± 1178 | |
| *p*-Courmaric acid[b] | 77 ± 82 (0.79) | 76 ± 70 (0.74) | 132 ± 94 (0.59) | 203 ± 144 (0.6)[f] | 488 ± 112 | (Koli *et al.*, 2010; |
| *p*-Courmaric acid[c] | 61 ± 33 (0.48) | 106 ± 117 (0.52) | 125 ± 67 (0.98) | 191 ± 114 (1.51) | 483 ± 114 | Nurmi *et al.*, 2009; Russell *et al.*, 2009) |
| Ferulic acid[b] | 141 ± 131 (1.44) | 408 ± 754 (3.95) | 1338 ± 1171 (6.03)[f] | 1517 ± 1344 (4.50)[f] | 3404 ± 1116 | (Czank *et al.*, 2013; |
| Ferulic acid[c] | 115 ± 128 (0.90) | 273 ± 251 (1.35) | 1010 ± 933 (7.97) | 1039 ± 537 (8.20) | 2436 ± 923 | Koli *et al.*, 2010; |

| | | | | | | |
|---|---|---|---|---|---|---|
| | | | | | | Nurmi *et al.*, 2009; Russell *et al.*, 2009) |
| Sinapic acid[b] | 110 ± 176 (1.13) | 210 ± 232 (2.03) | 1120 ± 903 (5.05)[f] | 1205 ± 943 (3.57)[f] | 2645 ± 826 | (Russell *et al.*, 2009) |
| Sinapic acid[c] | 105 ± 205 (0.83) | 342 ± 501 (1.7) | 920 ± 644 (7.26) | 1102 ± 925 (8.7) | 2470 ± 809 | |
| PCA-3-glucuronide[b] | 32 ± 32 (0.33) | 30 ± 32 (0.29) | 163 ± 157 (0.73) | 350 ± 190 (1.04)[f] | 576 ± 179 | (Czank *et al.*, 2013) |
| PCA-3-glucuronide[c] | 38 ± 18 (0.3) | 58 ± 84 (0.29) | 179 ± 147 (1.41) | 460 ± 276 (3.63) | 735 ± 233 | |
| PCA-4-glucuronide[b] | 44 ± 33 (0.45) | 36 ± 37 (0.34) | 91 ± 71 (0.41)[f] | 145 ± 86 (0.43)[f] | 315 ± 74 | (Czank *et al.*, 2013) |
| PCA-4-glucuronide[c] | 46 ± 23 (0.36) | 57 ± 68 (0.28) | 87 ± 42 (0.68) | 177 ± 89 (1.40) | 366 ± 83 | |
| IsoVA-3-glucuronide[b] | 271 ± 479 (2.79) | 230 ± 352 (2.23) | 660 ± 615 (2.97)[f] | 1226 ± 774 (3.64)[f] | 2387 ± 692 | (Czank *et al.*, 2013) |
| IsoVA-3-glucuronide[c] | 241 ± 196 (1.90) | 350 ± 515 (1.73) | 696 ± 442 (5.49) | 1286 ± 788 (10.15) | 2573 ± 717 | |
| VA-4-glucuronide[b] | 427 ± 307 (4.38) | 306 ± 157 (2.97) | 1154 ± 750 (5.2) | 2296 ± 946 (6.81)[f] | 4183 ± 1005 | (Czank *et al.*, 2013) |
| VA-4-glucuronide[c] | 468 ± 219 (3.69) | 585 ± 613 (2.90) | 1001 ± 539 (7.90) | 2432 ± 1289 (19.19) | 4485 ± 1157 | |
| PCA-sulfate[b,h] | 183 ± 291 (1.88) | 153 ± 182 (1.48) | 885 ± 1215 (3.99) | 2014 ± 1765 (5.97)[f] | 3235 ± 1303 | (Czank *et al.*, 2013) |
| PCA-sulfate[c,h] | 240 ± 370 (1.90) | 313 ± 574 (1.55) | 1289 ± 1856 (10.17) | 2436 ± 1972 (19.22) | 4278 ± 1689 | |
| VA-sulfate[b,i] | 1723 ± 1418 (17.69) | 1231 ± 980 (11.94) | 2314 ± 2114 (10.42) | 3176 ± 2478 (9.41)[g] | 8444 ± 1938 | (Czank *et al.*, 2013) |
| VA-sulfate[c,i] | 1902 ± 1185 (15.01) | 2632 ± 3661 (13.03) | 2830 ± 1622 (22.34) | 3638 ± 2090 (28.71) | 11003 ± 2372 | |

C3G, cyanidin-3-glucoside; ND, not detected; NA, not previously identified following anthocyanin consumption. P3G, peonidin-3-glucoside; PCA, protocatechuic acid; VA, vanillic acid [a]Values represent mean ratios ± SD with % of total metabolites represented in brackets, n=15; all samples have been adjusted for creatinine concentration. [b]Metabolite level following acute (500 mg) anthocyanin consumption (week 0). [c]Metabolite level following chronic (500 mg/day for 12 weeks) anthocyanin consumption (week 12). [e]No standard available, quantified relative to cyanidin-3-glucoside.[c]No standard available, quantified relative to peonidin-3-glucoside. [f]Significantly increased compared to baseline values (repeated measures, $p < 0.05$). [g]Significance indicated by ANOVA with Greenhouse-Geisser adjustment but post hoc tests did not reach significance ($p > 0.05$). [h]PCA-3-sulfate co-elutes with PCA-4-sulfate. [i]Vanillic acid-4-sulfate co-elutes with isovanillic acid-3-sulfate.

**Table 4.3** Concentration of anthocyanins, anthocyanin conjugates and phenolics in plasma samples following acute and chronic intake of anthocyanins from an elderberry extract.

| Compound | Concentration, nM (% of total metabolites)[a] | | | | | Previously identified in plasma |
|---|---|---|---|---|---|---|
| | Baseline | 1 h | 2 h | 3 h | Total | |
| Cyanidin-3-glucoside[a,f] | ND | 4 (0.63) | 7 (0.82) | 5 (0.38) | 16 | (Czank *et al.*, 2013; Milbury *et al.*, 2002) |
| Cyanidin-3-glucoside[b] | 1 (0.15) | 1 (0.21) | 7 (1.08) | 6 (0.86) | 15 | |
| Cyanidin-3-sambubioside [a,f] | ND | 10 (1.44) | 16 (1.85) | 11 (0.91) | 38 | (Czank *et al.*, 2013; Milbury *et al.*, 2002) |
| Cyanidin-3-sambubioside[b] | ND | 8 (1.28) | 18 (2.74) | 15 (2.27) | 41 | |
| Cyanidin-glucuronide[a,d,f] | ND | ND | 2 (0.27) | 2 (0.18) | 5 | NA |
| Cyanidin-glucuronide[b] | ND | ND | 3 (0.39) | 5 (0.75) | 7 | |
| Peonidin-glucuronide[a,e,f] | ND | 2 (0.24) | 8 (0.96) | 9 (0.71) | 19 | NA |
| Peonidin-glucuronide | 1 (0.13) | 3 (0.41) | 15 (2.20) | 21 (3.22) | 39 | |
| Protocatechuic acid (PCA)[a,f] | 11 (2.71) | 12 (1.72) | 14 (1.65) | 24 (1.93) | 61 | (Azzini *et al.*, 2010; Czank *et al.*, 2013; Koli *et al.*, 2010; Russell *et al.*, 2009) |
| PCA[b] | 17 (3.84) | 24 (3.94) | 10 (1.54) | 20 (3.03) | 71 | |
| 3,5-Dihydroxybenzoic acid[a,f] | 20 (5.05) | 18 (2.67) | 8 (4.39) | 50 (3.92) | 126 | NA |
| 3,5-Dihydroxybenzoic acid[b] | 26 (5.86) | 23 (3.78) | 25 (3.69) | 31 (4.82) | 105 | |
| Vanillic acid (VA)[a,f] | 6 (1.64) | 35 (5.13) | 62 (7.03) | 58 (4.60) | 161 | (Czank *et al.*, 2013; Koli *et al.*, 2010; Russell *et al.*, 2009) |
| VA[b] | 12 (2.70) | 41 (6.58) | 54 (8.05) | 40 (6.24) | 147 | |
| Syringic acid[a,f] | 5 (1.16) | 17 (2.44) | 22 (2.56) | 15 (1.20) | 59 | NA |
| Syringic acid[b] | 11 (2.41) | 24 (3.95) | 30 (4.43) | 13 (2.01) | 78 | |
| 4-Methoxysalicyclic acid[a,f] | 1 (0.23) | 0.3 (0.05) | 1 (0.07) | 2 (0.13) | 3 | NA |
| 4-Methoxysalicyclic acid[b] | 1 (0.19) | 1 (0.17) | 1 (0.12) | 1 (0.15) | 4 | |
| Methyl-3,4-dihydroxybenzoate[a,f] | 3 (0.71) | 2 (0.33) | 6 (0.68) | 6 (0.48) | 17 | (Czank *et al.*, 2013) |
| Methyl-3,4-dihydroxybenzoate[b] | 7 (1.48) | 3 (0.43) | 3 (0.38) | 5 (0.72) | 16 | |
| Phloroglucinaldehyde[a,f] | 4 (1.05) | 21 (3.02) | 102 (11.69) | 72 (5.66) | 199 | (Czank *et al.*, 2013) |
| Phloroglucinaldehyde[b] | 35 (7.77) | 34 (5.48) | 62 (9.2) | 73 (11.29) | 203 | |
| 3,4-Dihydroxybenzaldehyde[a,f] | 17 (4.43) | 18 (2.65) | 23 (2.62) | 21 (1.68) | 80 | NA |
| 3,4-Dihydroxybenzaldehyde[b] | 26 (5.92) | 19 (3.09) | 12 (1.80) | 11 (1.73) | 69 | |

| | | | | | | |
|---|---|---|---|---|---|---|
| 4-Hydroxybenzaldehyde[a,f] | 97 (24.74) | 146 (21.29) | 182 (20.80) | 150 (11.85) | 575 | NA |
| 4-Hydroxybenzaldehyde[b] | 120 (26.97) | 109 (17.65) | 120 (17.90) | 95 (14.67) | 444 | |
| Ferulic acid[a,f] | 8 (1.97) | 27 (3.92) | 28 (3.23) | 22 (1.70) | 84 | (Czank *et al.*, 2013; Zhang *et* |
| Ferulic acid[b] | 3 (0.71) | 23 (3.66) | 21 (3.12) | 134 (2.13) | 60 | *al.*, 2004) |
| PCA-3-glucuronide[a,f] | 3 (0.79) | 8 (1.10) | 15 (1.75) | 15 (1.22) | 41 | (Czank *et al.*, 2013) |
| PCA-3-glucuronide[b] | 6 (1.24) | 11 (1.78) | 13 (1.97) | 16 (2.43) | 45 | |
| PCA-4-glucuronide[a,f] | 6 (1.43) | 4 (0.52) | 10 (1.14) | 14 (1.11) | 33 | (Czank *et al.*, 2013) |
| PCA-4-glucuronide[b] | 4 (0.96) | 8 (1.33) | 11 (1.63) | 8 (1.24) | 31 | |
| IsoVA-3-glucuronide[a,f] | 10 (2.65) | 13 (1.97) | 24 (2.71) | 22 (1.71) | 69 | NA |
| IsoVA-3-glucuronide[b] | 15 (3.42) | 13 (2.15) | 20 (3.03) | 37 (5.68) | 85 | |
| VA-4-glucuronide[a,f] | 16 (4.21) | 33 (4.85) | 78 (8.91) | 120 (9.49) | 248 | NA |
| VA-4-glucuronide[b] | 22 (4.90) | 30 (4.78) | 90 (13.41) | 115 (17.87) | 256 | |
| PCA-sulfate [a,f,g] | 92 (23.55) | 74 (10.78) | 115 (13.17) | 358 (28.31) | 640 | (Czank *et al.*, 2013) |
| PCA-sulfate[b] | 25 (5.53) | 49 (7.91) | 26 (3.81) | 34 (5.30) | 133 | |
| VA-sulfate[a,f,g] | 27 (6.79) | 161 (23.43) | 23 (2.67) | 93 (7.36) | 304 | (Czank *et al.*, 2013) |
| VA-sulfate[b] | 41 (9.29) | 92 (14.96) | 40 (5.99) | 19 (3.01) | 193 | |
| Benzoic acid-4-sulfate[a,f] | 66 (16.89) | 81 (11.82) | 97 (11.02) | 196 (15.48) | 439 | NA |
| Benzoic acid-4-sulfate[b] | 74 (16.56) | 102 (16.45) | 91 (13.53) | 68 (10.59) | 334 | |
| Total anthocyanins[a] | 0 | 16 | 34 | 28 | 78 | |
| Total anthocyanins[b] | 1 | 12 | 43 | 46 | 102 | |
| Total phenolic metabolites[a] | 391 | 670 | 842 | 1238 | 3140 | |
| Total phenolic metabolites[b] | 445 | 606 | 627 | 599 | 2277 | |

ND, not detected. NA, not previously identified following anthocyanin consumption. [a]Metabolite concentration following acute (500 mg) anthocyanin consumption (week 0); [b]Metabolite concentration following chronic (500 mg/day for 12 wks) anthocyanin consumption (wk 12). [c]Values represent concentrations of a pooled sample (n=1) from 15 participants samples, with % of total metabolites represented in brackets. [d]No standard available, quantified relative to cyanidin-3-glucoside. [e]No standard available, quantified relative to peonidin-3-glucoside. [f]Visual increase in concentration compared to baseline values (no statistical analysis possible as a result of using a pooled sample). [g]PCA-3-sulfate co-elutes with PCA-4-sulfate. [h]Vanillic acid-4-sulfate co-elutes with isovanillic acid-3-sulfate.

**Figure 4.2** Structures and HPLC-ESI-MRM traces of anthocyanins identified within 3 h post bolus urine samples.

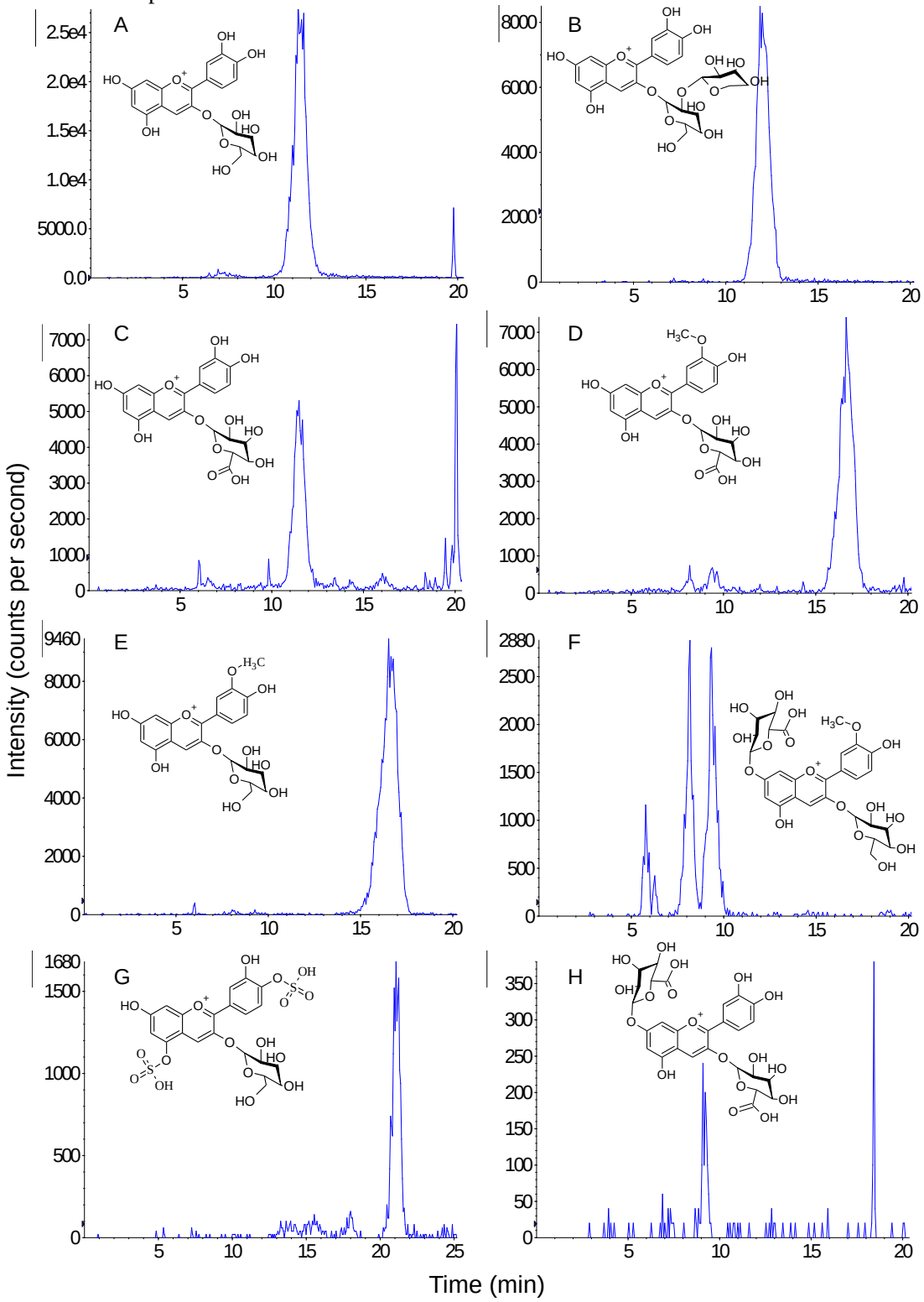


Multiple reaction monitoring (MRM) chromatograms. Structures illustrate possible conjugation positions, actual positions are unknown. (A) cyanidin-3-glucoside, *m/z* 449/287; (B) cyanidin-3-sambubioside, *m/z* 581/287; (C) cyanidin-glucuronide, *m/z* 463/287; (D) peonidin-glucuronide, *m/z* 477/301; (E) peonidin-3-glucoside, *m/z* 463/301; (F) peonidin-3-glucoside-glucuronide, *m/z* 639/301; (G) cyanidin-3-glucoside-disulfate, *m/z* 609/287; (H) cyanidin-diglucuronide, *m/z* 639/287.

**Figure 4.3** Anthocyanins identified in individual participants urine samples following acute (500 mg) anthocyanin consumption.

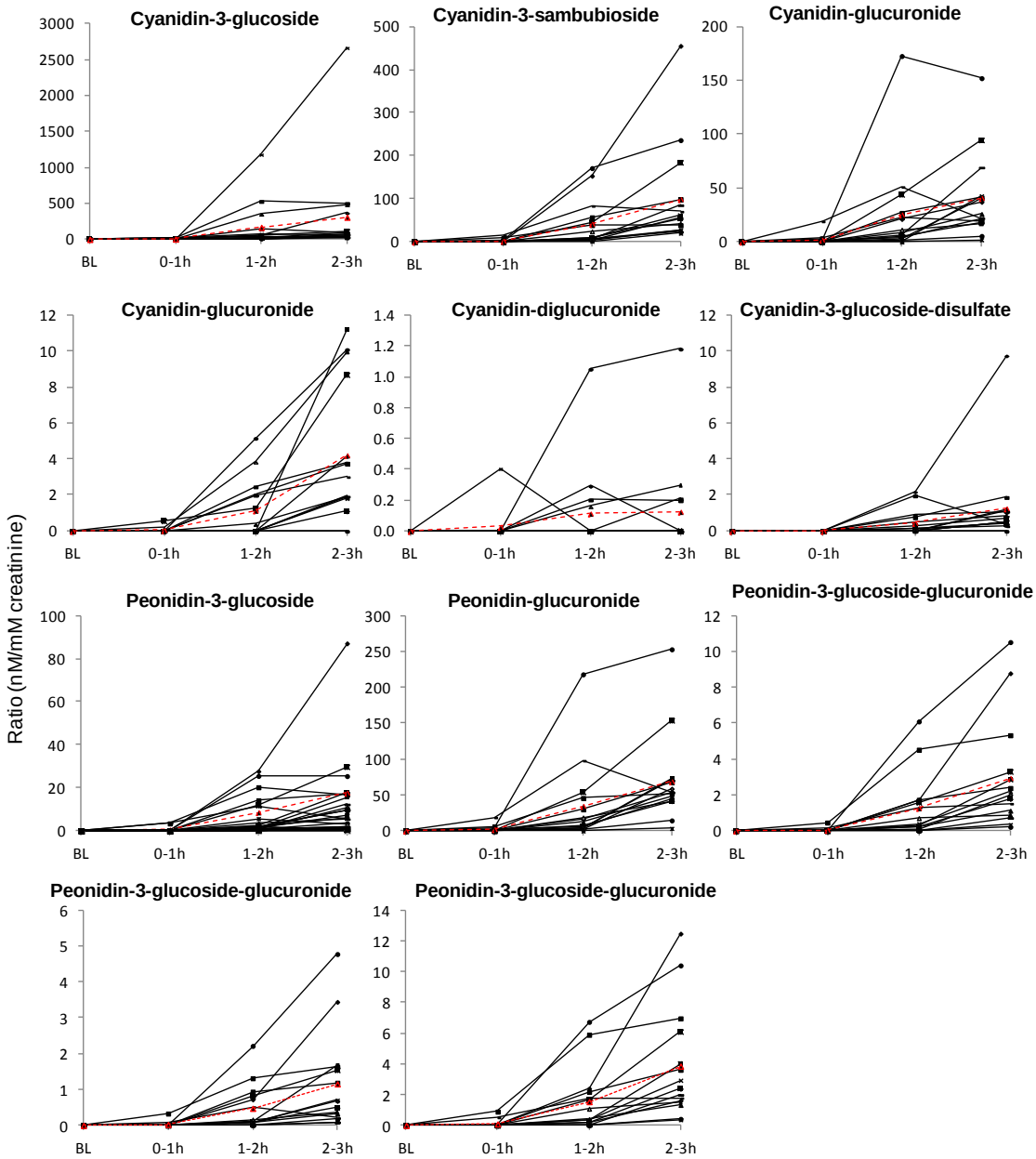


Solid black lines indicate individual participant excretion (n=15), dashed line illustrates mean. Values are adjusted for creatinine concentrations (nM/mM creatinine).

### 4.3.4. Phenolic metabolites within urine and plasma

There was high variability observed in the levels of individual phenolic metabolites, where protocatechuic-4-glucuronide (**Figure 4.4**) and *p*-courmaric acid (**Figure 4.5**) were present in the lowest ratios, reaching 145 ± 86 and 203 ± 144 nM/mM creatinine respectively (Table 4.2), whilst homovanillic acid and vanillic acid reached the highest ratios at 3 h, representing levels of 7.4 ± 5.9 and 4.3 ± 3.2 µM/mM creatinine respectively (Figure 4.5).

Within plasma, total concentrations of metabolites cumulatively reached 1.2 µM, 3 h post bolus, representing an 0.8 µM increase from baseline values (Table 4.3); where protocatechuic acid-sulfate reached the highest concentration (358 nM) while 4-methoxysalicyclic acid was identified at the lowest concentration (2 nM) within plasma. The maximum concentration for the majority of the compounds was at 2 h, however, protocatechuic acid, 3,5-dihydroxybenzoic acid, 4-methoxysalicyclic acid, protocatechuic acid-4-glucuronide, vanillic acid-4-glucuronide, protocatechuic acid-3 & 4-sulfate and benzoic acid-4-sulfate had not reached maximum concentration by 3 h.

**Figure 4.4** Ratios of glucuronide and sulfate phenolic conjugates identified in individual participant urine samples following acute (500 mg) anthocyanin consumption, expressed per mM creatinine.

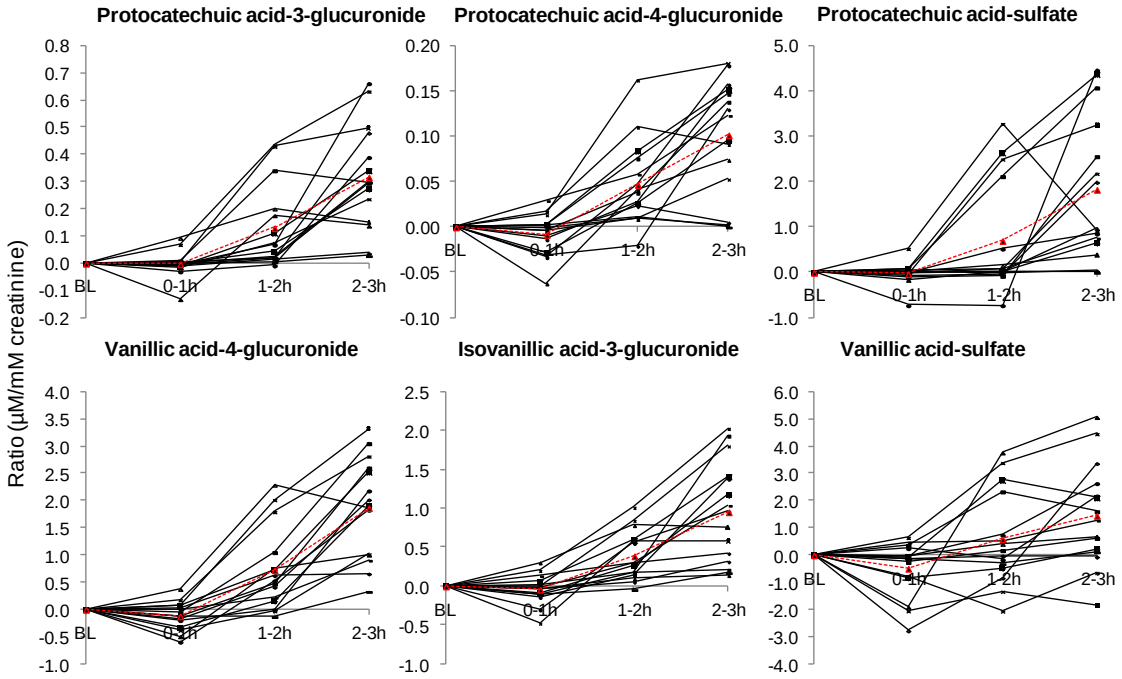


Solid lines indicate individual participant excretion (n=15), dashed line illustrates mean. Values are adjusted for creatinine concentrations (µM/mM creatinine).

**Figure 4.5** Ratios of phenolic metabolites identified in individual participants urine samples following acute (500 mg) anthocyanin consumption.

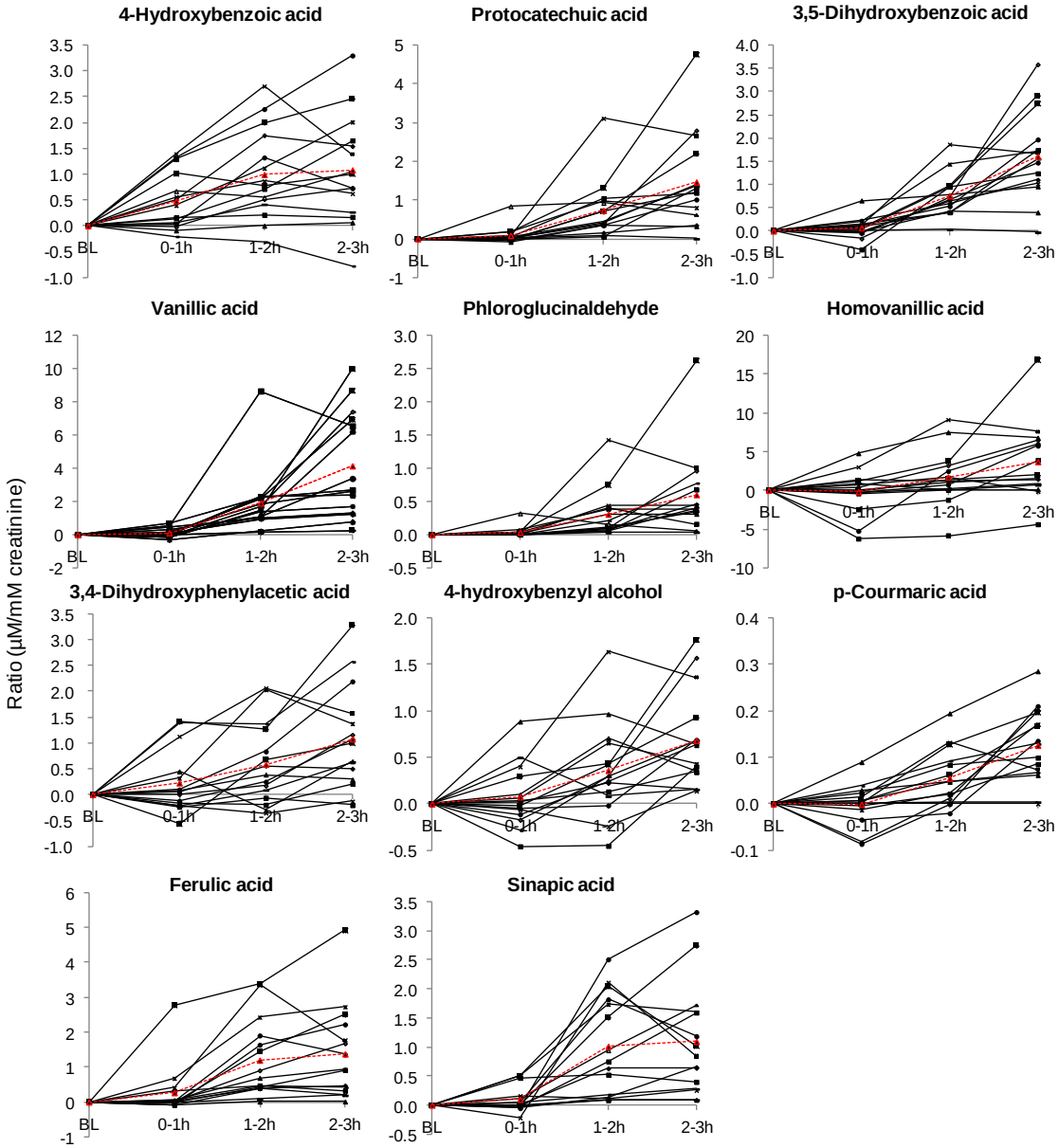


Solid lines indicate individual participant excretion (n=15), dashed line illustrates mean. Values are adjusted for creatinine concentrations (µM/mM creatinine).

### 4.3.5. Effect of sustained dosing on metabolite excretion

There was no significant difference (repeated measures ANOVA with Bonferroni correction; $p>0.05$) in the level of metabolites in postprandial urine collected following a single acute anthocyanin dose (week 0) and following 12 weeks chronic anthocyanin consumption (week 12), when comparing individual metabolite levels or when grouping compounds by structure (anthocyanins, hydroxybenzoic, hydroxybenzoate, aldehyde, phenylacetic, phenylalcohol or phenylpropanoic) and conjugation reaction type (methylation, glucuronidation or sulfation).

Due to the use of pooled plasma samples (n=1), no statistical comparisons were possible with plasma. However there was a visible increase in anthocyanins (78 nM at week 0 versus 100 nM at week 12) and decrease in hydroxybenzoic acids (3 nM at week 0 versus 2 nM at week 12) following sustained dosing (**Figure 4.6**); however this was not mirrored in the urine analysis.

### 4.3.6. Phenolic compounds not increased from baseline values

The levels of seven compounds identified in urine and six compounds identified in plasma (**Table 4.4**) did not increase from baseline following the consumption of 500 mg elderberry anthocyanins. The compounds included 2-, 3-, and 4-hydroxybenzoic acid, benzoic acid-4-glucuronide, 2,3-dihydroxybenzoic acid, methylgallate, hippuric acid and 3- and 4-methylhippuric acid.

**Figure 4.6** Baseline (BL) and post bolus (0-3 h) anthocyanins and metabolite concentrations in plasma.

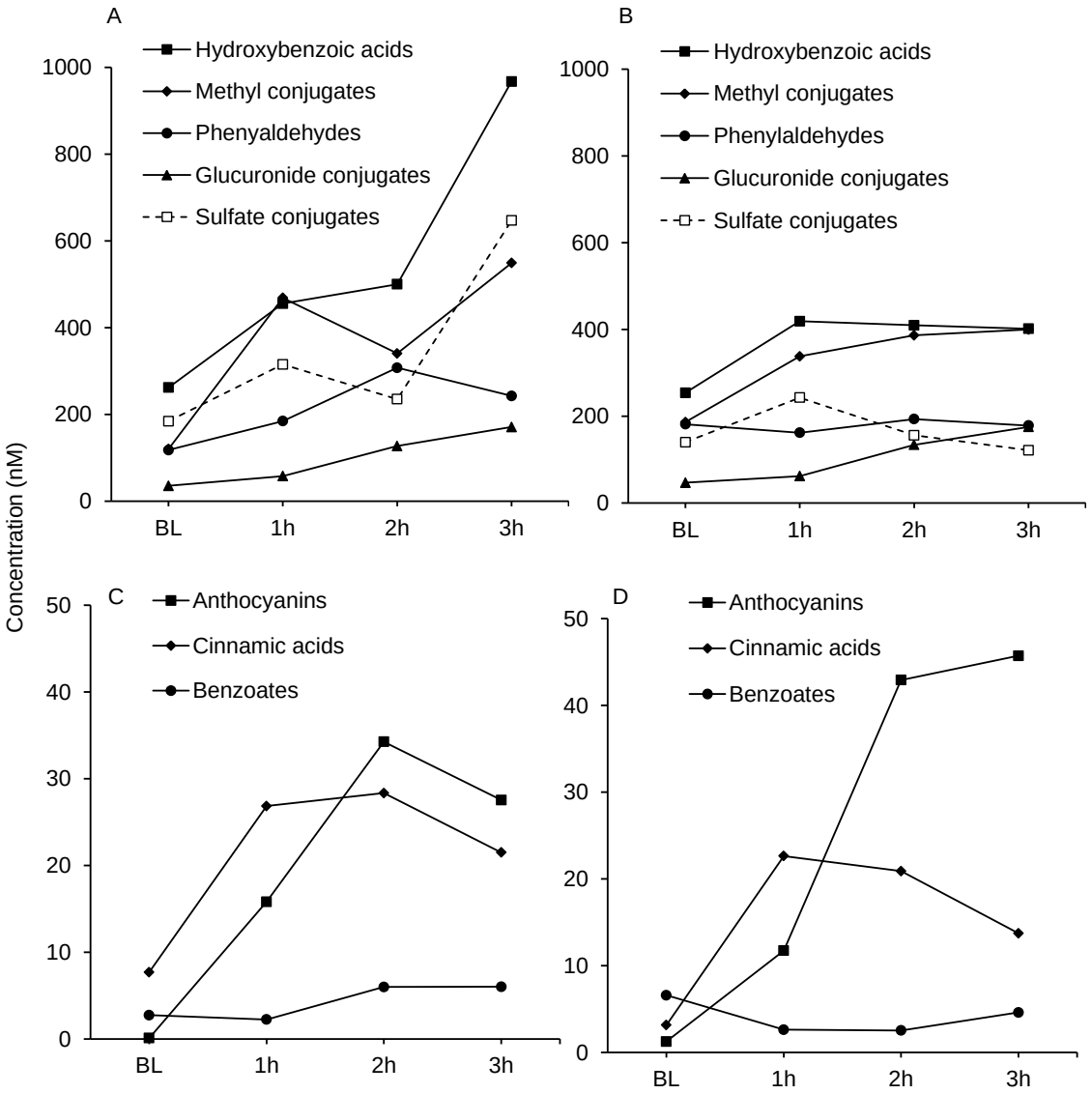


(A) Concentration of major anthocyanin metabolites (>150 nM) identified in a pooled sample from n=15 participants, following a single bolus and (B) following 12-wk supplementation; (C) concentration of minor anthocyanin metabolites (<150 nM) identified following a single bolus and (D) following 12-wk supplementation. Metabolites are classified by conjugation/ structure where hydroxybenzoic acids include protocatechuic acid (PCA), 3,5-dihydroxybenzoic acid, vanillic acid (VA), syringic acid, 4-methoxysalicyclic acid, PCA-3-glucuronide, PCA-4-glucuronide, VA-4-glucuronide, isoVA-3-glucuronide, PCA-sulfate and VA-sulfate; methyl conjugates include VA, syringic acid, 4-methoxysalicyclic acid,methyl-3,4-dihydroxybenzoate, ferulic acid, VA-4-glucuronide, isoVA-3-glucuronide and VA-sulfate; phenylaldehydes include phloroglucinaldehyde, 4-hydroxybenzaldehyde and 3,4-dihydroxybenzaldehyde; glucuronide conjugates include PCA-3-glucuronide, PCA-4-glucuronide VA-3-glucuronide and isoVA-3-glucuronide; sulfate conjugates include PCA-sulfate, VA-sulfate and benzoic acid-4-sulfate; anthocyanins include cyanidin-3-glucoside, cyanidin-3-sambubioside, cyanidin-glucuronide and peonidin-glucuronide; cinnamic acids include ferulic acid; and benzoates include methyl-3,4-dihydroxybenzoate.

**Table 4.4** Phenolic compounds in (A) urine and (B) plasma following acute and chronic intake of anthocyanins from an elderberry extract, which demonstrated no increase from baseline ratios.

A. **Urine**

| Compound | Ratio, per mM creatinine ± SD | | | | Previously identified in urine |
|---|---|---|---|---|---|
| | Baseline | t(0-1 h) | t(1-2 h) | t(2-3 h) | |
| 2-Hydroxybenzoic acid[a] (nM) | 56 ± 50 | 54 ± 41 | 45 ± 35 | 77 ± 49 | (Russell *et al.*, 2009) |
| 2-Hydroxybenzoic acid[b] (nM) | 52 ± 33 | 63 ± 55 | 38 ± 28 | 59 ± 48 | |
| 3-Hydroxybenzoic acid[a] (µM) | 273 ± 316 | 259 ± 284 | 365 ± 305 | 319 ± 307 | (Czank *et al.*, 2013) |
| 3-Hydroxybenzoic acid[b] (µM) | 734 ± 1007 | 1215 ± 1384 | 1147 ± 1362 | 1014 ± 1189 | |
| 2,3-Dihydroxybenzoic acid[a] (nM) | 110 ± 210 | 55 ± 31 | 75 ± 42 | 123 ± 80 | |
| 2,3-Dihydroxybenzoic acid[b] (nM) | 70 ± 46 | 108 ± 115 | 81 ± 46 | 108 ± 95 | |
| Benzoic acid-4-glucuronide[a] (nM) | 17 ± 22 | 21 ± 34 | 19 ± 26 | 19 ± 26 | (Czank *et al.*, 2013) |
| Benzoic acid-4-glucuronide[b] (nM) | 10 ± 8 | 41 ± 115 | 14 ± 16 | 20 ± 21 | |
| Hippuric acid[a] (µM) | 246 ± 154 | 267 ± 177 | 257 ± 160 | 227 ± 929 | (Czank *et al.*, 2013) |
| Hippuric acid[b] (µM) | 204 ± 107 | 300 ± 237 | 220 ± 106 | 216 ± 124 | |
| 3-Methylhippuric acid[a] (nM) | 96 ± 148 | 125 ± 183 | 117 ± 162 | 114 ± 156 | |
| 3-Methylhippuric acid[b] (nM) | 44 ± 29 | 57 ± 37 | 47 ± 22 | 49 ± 32 | |
| 4-Methylhippuric acid[a] (nM) | 44 ± 76 | 54 ± 81 | 48 ± 54 | 46 ± 51 | |
| 4-Methylhippuric acid[b] (nM) | 23 ± 18 | 20 ± 21 | 20 ± 13 | 26 ± 21 | |

B. Plasma

| Compound | Concentration (nM) | | | | | Previously identified in plasma |
|---|---|---|---|---|---|---|
| | Baseline | 1 h | 2 h | 3 h | Total | |
| Hippuric acid[a] (µM) | 10 | 7 | 6 | 6 | 30 | (Czank *et al.*, 2013) |
| Hippuric acid[b] (µM) | 8 | 6 | 6 | 6 | 26 | |
| Methylgallate[a] (nM) | 5 | 5 | 4 | 3 | 17 | |
| Methylgallate[b] (nM) | 3 | 3 | 4 | 3 | 13 | |
| Benzoic acid-4-glucuronide[a] (nM) | 10 | 10 | 8 | 7 | 34 | (Czank *et al.*, 2013) |

| | | | | | | |
|---|---|---|---|---|---|---|
| Benzoic acid-4-glucuronide[b] (nM) | 5 | 5 | 3 | 2 | 15 | |
| 4-Hydroxybenzoic acid[a] (nM) | 39 | 36 | 32 | 30 | 137 | (Azzini *et al.*, 2010; Russell *et al.*, 2009; Zhang *et al.*, 2004) |
| 4-Hydroxybenzoic acid[b] (nM) | 37 | 25 | 28 | 25 | 115 | |
| 3-Hydroxybenzoic acid[a] (nM) | 21 | 35 | 26 | 29 | 111 | (Zhang *et al.*, 2004) |
| 3-Hydroxybenzoic acid[b] (nM) | 51 | 46 | 35 | 18 | 150 | |
| 2-Hydroxybenzoic acid[a] (nM) | 173 | 211 | 191 | 172 | 747 | |
| 2-Hydroxybenzoic acid[b] (nM) | 186 | 149 | 80 | 102.33 | 517 | |

[a]Metabolite concentration following acute (500 mg) anthocyanin consumption (week 0); [b]Metabolite concentration following chronic (500 mg/day for 12 wks) anthocyanin consumption (wk 12).

## 4.4. Discussion

The elderberry extract fed during the present study contained 500 mg anthocyanins, which is equivalent to consuming approximately 38 g of elderberries, 84 g blackcurrants or 290 g blackberries (Curtis *et al.*, 2009; Neveu *et al.*, 2010). In order to establish the phenolic profile of the elderberry extract, the present study carried out a secondary analysis of a recent batch of 25% anthocyanin elderberry extract from Artemis, as this was not established in the original investigation. Fifteen phenolics (Table 4.1) were identified within the extract, including protocatechuic acid (139 ± 4 mg/g extract), phloroglucinaldehyde (16 ± 1 mg/g extract), caffeic acid (15 ± 1 mg/g extract) and 4-hydroxybenzoic acid (11 ± 0.3 mg/g extract). Therefore, the present study provided a bolus which closely mimicked a dietary source of anthocyanins, albeit it was derived from dried and ground berries.

In the present investigation, 28 metabolites were identified in urine (11 anthocyanin conjugates and 17 phenolic metabolites, Table 4.2) and 21 metabolites were identified in plasma (four anthocyanin conjugates and 17 phenolic metabolites, Table 4.3). In addition, seven compounds identified in urine and six compounds identified in plasma demonstrated no postprandial increase in concentration, suggesting there presence was derived from the 'background' diet or endogenous protein turnover.

Anthocyanins were present at nanomolar levels in urine, with cyanidin-3-glucoside reaching 309 ± 673 nM/mM creatinine and cyanidin-3-sambubioside reaching 99 ± 116 nM/mM creatinine after 3 h; which is in accordance with data derived from previous studies (Bitsch *et al.*, 2004b; Cao *et al.*, 2001; Felgines *et al.*, 2005; Garcia-Alonso *et al.*, 2009; Kay *et al.*, 2005; Kay *et al.*, 2004; Wu *et al.*, 2002). The conjugated anthocyanins reached cumulative levels of 140 ± 33 nM/mM creatinine after 3 h. The conjugated metabolites include methylated, glucuronidated and disulfated cyanidin-3-glucoside and methylated, glucuronidated and diglucuronidated conjugates of the aglycone, cyanidin (Table 4.2). The most predominate conjugation reaction for anthocyanins was glucuronidation (seven glucuronide conjugates identified), followed by methylation (five methyl conjugates identified), with many anthocyanins undergoing multiple conjugation reactions. It should be noted that peonidin was not present in the elderberry extract and therefore the identification of peonidin conjugates in the plasma and urine is indicative of the methylation of cyanidin. However, in the absence of standards for many of the anthocyanin conjugates, the identity and conjugation positions cannot be confirmed. Several peaks in the chromatograms with the same mass and fragmentation pattern (two transitions) as cyanidin-glucuronide and peonidin-glucoside-glucuronide (Figure 4.2) do however provide evidence to suggest

conjugations occurred at several positions on the anthocyanin structure. Previous elderberry interventions have predominantly identified cyanidin-3-glucoside and cyanidin-3-sambubioside in post bolus urine samples (Milbury *et al.*, 2002; Mülleder *et al.*, 2002; Murkovic *et al.*, 2001). Wu *et al*. identified four anthocyanin conjugates, including peonidin-3-sambubioside and cyanidin-3-glucoside-monoglucuronide, which were not identified in the present study (Wu *et al.*, 2002). However, to the best of our knowledge the anthocyanin conjugates identified here represent the largest number of metabolic conjugates of elderberry anthocyanins identified to date. In addition, despite creatinine adjustment, the ratios of total anthocyanins quantified within urine after 2-3 h following intake are amongst the highest reported to date.

In plasma, lower concentrations of a smaller range of metabolites were identified compared to urine. The four most abundant anthocyanin metabolites identified in urine were detected in plasma; cyanidin-3-glucoside was present at 7 nM, cyanidin-3-sambubioside at 16 nM, cyanidin-glucuronide at 2 nM and peonidin-glucuronide at 8 nM, at the 2 h time point following acute anthocyanin consumption (Table 4.3).

The majority of previous investigations into anthocyanin metabolism have predominantly focused on identifying intact anthocyanins, however anthocyanins are inherently unstable and degrade at neutral pH into their phenolic acid and aldehyde constituents (Kay *et al.*, 2009; Woodward *et al.*, 2009). The present study focused on the identification of phenolic metabolites. Protocatechuic acid and phloroglucinaldehyde, the degradation products of cyanidin-3-glucoside, were detected in both urine and plasma. Protocatechuic acid reached levels of 1.5 ± 1.2 µM/mM creatinine and 24 nM after 3 h in urine (Table 4.2) and plasma (Table 4.3) respectively. Limited previous data has quantified protocatechuic acid following anthocyanin consumption. Russell *et al*. (Russell *et al.*, 2009) and Nurmi *et al*. (Nurmi *et al.*, 2009) identified protocatechuic acid in urine samples following strawberry and bilberry-loganberry consumption, and reported 2.3 µM at 3 h post bolus; which is similar to the ratios observed in the present study. Vitaglione *et al*. (Vitaglione *et al.*, 2007) also previously reported protocatechuic acid to be the major metabolite of cyanidin-glucosides in humans, identifying plasma concentrations of 492 nM following consumption of blood orange juice, yet failed to identify it within the urine. Protocatechuic acid is naturally present in many fruits, including elderberries, where the present study identified it as the most abundant phenolic, present at concentrations of 139 mg/g extract (**Table 4.1**). The presence of protocatechuic acid in the background diet may have led to an overestimation of anthocyanin derived protocatechuic acid in this and previous interventions.

Phloroglucinaldehyde was identified at maximum ratios of 602 ± 632 nM/mM creatinine at 3 h and 103 nM at 2 h in urine (Table 4.2) and plasma (Table 4.3) respectively. Protocatechuic acid and phloroglucinaldehyde were identified in our study feeding $^{13}$C-labelled cyanidin-3-glucoside, where together they reached maximum concentrations of 507 nM/mM creatinine in urine and 728 nM in plasma (**Chapter 3**) (Czank *et al.*, 2013). As would be expected, the urinary levels of protocatechuic acid were higher in the present study, likely due to their presence within the elderberry extract and the absence of the use of a labelled marker. However, the plasma concentrations of the degradation products were lower, possibly due to the degradation products reaching maximum concentration at 6 h post bolus within the labelled study. To our knowledge, this is the first study where phloroglucinaldehyde has been identified in human blood or urine following a fruit derived anthocyanin intervention.

Our data suggest that the degradation products of anthocyanins undergo phase I and II metabolism to produce conjugated phenolic acids, where methylated (vanillic acid), glucuronidated (protocatechuic acid-3-glucuronide, protocatechuic acid-4-glucuronide, vanillic acid-4-glucuronide and isovanillic acid-3-glucuronide), sulfated (protocatechuic acid-sulfate and vanillic acid-sulfate) and de/hydroxylated (4-hydroxybenzoic acid and 3,5-dihydroxybenzoic acid) metabolites of protocatechuic acid were identified. Vanillic acid-4-glucuronide demonstrated the largest increase from baseline values in urine, reaching levels of 2.3 ± 0.9 μM/mM creatinine 3 h post bolus (Table 4.2) and protocatechuic acid-sulfate demonstrated the largest increase in concentration from baseline plasma, reaching concentrations of 358 nM 3 h following intake (Table 4.3). 4-Hydroxybenzoic acid and vanillic acid have previously been identified within biological samples following bilberry-lingonberry (Nurmi *et al.*, 2009), cranberry juice (Zhang *et al.*, 2004) and strawberry consumption (Azzini *et al.*, 2010). Whilst the glucuronidated and sulfated metabolites have been identified at concentrations up to 1.9 ± 0.7 μM (for protocatechuic acid-3-glucuronide) in our study feeding $^{13}$C-labelled cyanidin-3-glucoside (Czank *et al.*, 2013); the present study is the first to identify them following a fruit derived anthocyanin intervention.

Anthocyanins may alternatively form phenylpropenoic, phenylacetic and phenylalcohol structures. Homovanillic acid, homoprotocatechuic acid, 4-hydroxybenzyl alcohol, *p*-courmaric acid, ferulic acid and sinapic acid were detected at increased concentrations within postprandial urine samples (Table 4.2) and syringic acid, 4-methoxysalicyclic acid, methyl-3,4-dihydroxybenzoate, 3,4-dihydroxybenzaldehyde, 4-hydroxybenz-aldehyde and ferulic acid were detected at increased concentrations within postprandial plasma samples (Table 4.3). Of these, homovanillic acid, homoprotocatechuic acid, *p*-courmaric acid, ferulic acid

and sinapic acid have been previously detected within urine (Nurmi *et al.*, 2009; Russell *et al.*, 2009) and ferulic acid has previously been identified within plasma (Zhang *et al.*, 2004) following phenolic rich anthocyanin interventions. The origin of the phenolic metabolites identified in the present study cannot be confirmed with certainty without the use of a labelled anthocyanin. However, many have recently been confirmed as anthocyanin metabolites through the use of a $^{13}$C-labelled anthocyanin bolus (Czank *et al.*, 2013), where metabolites including ferulic acid, 3- and 4-hydroxybenzoic acid, 3,4-dihydroxybenzaldehyde, 4-hydroxyphenylacetic acid and methyl-3,4-dihydroxybenzoate were identified (Table 4.2 & Table 4.3).

A high inter-individual variation in metabolite excretion was observed between participants; for example, levels of protocatechuic acid ranged from 0.03 to 4.9 μM/mM creatinine within 3 h post bolus urine samples of the n=15 participants. This likely results from individual biological variations, including variations in gut microflora, enzyme and receptor levels.

Phenolic metabolites were identified reaching ratios of 24 μM/mM creatinine above baseline values, whilst concentrations of 5.97 ± 2.14 μM were obtained from feeding the same dose of pure $^{13}$C-labelled cyanidin-3-glucoside (Czank *et al.*, 2013). Therefore, as would be expected with the inclusion of additional phenolics within a natural food bolus, the present study shows phenolics to accumulate at higher concentrations following the consumption of anthocyanins within a food matrix as opposed to a pure bolus. The phenylacetic structures, homovanillic acid and homoprotocatechuic acid, which together provided a 4762 nM/mM creatinine increase from baseline urinary levels appeared to be major anthocyanin metabolites in urine, but were absent from plasma. Similarly, *p*-courmaric acid, sinapic acid, 3,5-dihydroxybenzoic acid and 4-hydroxybenzyl alcohol were also identified within urine, but were absent from the plasma. The presence of some metabolites in the urine but not the plasma suggests some compounds in the plasma were below the detection limit of the methodology but became detectable as they were concentrated by the kidneys and excreted into the urine. Alternatively, conjugation could occur in the kidney prior to excretion.

The plasma contained 4-hydroxybenzaldehyde, 3,4-dihydroxybenzaldehyde, 4-methoxy salicyclic acid, benzoic acid-4-sulfate, methyl-3,4-dihydroxybenzoate and syringic acid which were absent from urine samples. The appearance of metabolites in the plasma but not in the urine suggests some metabolites may have been metabolised further within the plasma, or were eliminated by the biliary route, and either metabolised further by colonic bacteria and reabsorbed or excreted. This is supported by the identification of methyl-3,4-dihydroxybenzoate and 4-methoxysalicyclic acid within faecal samples following our recent

human study feeding $^{13}$C-labelled cyanidin-3-glucoside (Czank *et al.*, 2013). Conjugates of phenolic degradation products of anthocyanins appear in the circulation as early as 1 h post consumption (Table 4.3) (Czank *et al.*, 2013), suggesting they do not follow the commonly reported elimination profiles of other flavonoids, such as quercetin and epicatechin, which require bacterial catabolism to liberate free phenolic intermediates, and therefore appear much later in the circulation (Aura *et al.*, 2002; GriffithsandBarrow, 1972; Manach *et al.*, 2005; Mullen *et al.*, 2008b; Selma *et al.*, 2009; Winter *et al.*, 1989). The early appearance of phenolic metabolites in the present study likely results from the instability of anthocyanins at physiological pH (pH 5-7) (González-Barrio *et al.*, 2010; Mullen *et al.*, 2008b; Williamson *et al.*, 2010), resulting in their rapid degradation and metabolism within the proximal and distal small intestine, where bacteria are still present at varying densities (Berg, 1996).

In the present study a number of unconjugated metabolites, including protocatechuic acid, *p*-courmaric acid and homoprotocatechuic acid were identified. Although flavonoids are generally reported in the circulation as conjugated metabolites (Hollman, 2004), unconjugated phenolic acids have been reported at levels similar to those detected within the present intervention study (Czank *et al.*, 2013; Nurmi *et al.*, 2009; Russell *et al.*, 2009) and their presence in the current study, likely reflects the instability and rapid degradation of anthocyanins.

Several of the putative phenolic metabolites explored (hippuric acid, 2-, 3- and 4-hydroxybenzoic acid and benzoic acid-4-glucuronide) were not found to significantly increase from baseline concentrations (Table 4.4). These compounds were initially explored as putative metabolites as they have been previously reported as possible anthocyanin or flavonoid metabolites. Hippuric acid, 3-hydroxybenzoic acid, and benzoic acid-4-glucuronide have been identified as anthocyanin metabolites in our study feeding $^{13}$C-labelled cyanidin-3-glucoside (Czank *et al.*, 2013). Hippuric acid, which was present at the highest concentration, reaching millimolar levels within urine in the present study, is formed from the reaction of benzoic acid with glycine, and is a common product of protein (Pero, 2010) or dietary polyphenol metabolism (Del Bo' *et al.*, 2012; Mulder *et al.*, 2005). Similarly, 2-, 3- and 4-hydroxybenzoic acids have been reported in multiple anthocyanin intervention studies (Azzini *et al.*, 2010; Nurmi *et al.*, 2009; Russell *et al.*, 2009; Zhang *et al.*, 2004). Whilst these phenolics did not increase in concentration from baseline levels, and are therefore predominantly derived from other source in the 'background' diet or endogenous protein turnover (Toromanović *et al.*, 2008), anthocyanin metabolism likely contributes to their concentrations in biofluids to some extent (as indicated by their presence following consumption of a labelled anthocyanin).

The present study is the first study to look at postprandial phenolic metabolite excretion following chronic anthocyanin intake for 12 weeks. A previous flavonoid intervention found two weeks daily quercetin supplementation resulted in increased plasma quercetin concentrations (Egert *et al.*, 2008) suggesting reduced clearance of quercetin following repeated dosing. However, there was no significant impact of 12wks continuous dosing on urinary metabolite excretion in the present study. This is in accordance with a previous 8wk berry intervention which found no effect of chronic intake on fasting polyphenol concentrations (Koli *et al.*, 2010), and suggests there is little risk of bioaccumulation or toxicity associated with the consumption of anthocyanins. There was an increase in plasma anthocyanins (78 nM at wk0 versus 100 nM at wk12) and decrease in hydroxybenzoic acids (3 nM at wk0 versus 2 nM at wk12) following sustained dosing (Figure 4.6); however, no statistical comparisons were possible due to the use of pooled plasma samples (n=1). This observation was not apparent in the urine analysis. In addition, based on the large inter-individual variation in metabolite excretion reported herein, (Figure 4.3, Figure 4.4 & Figure 4.5) differences in plasma levels of the anthocyanins or hydroxybenzoic acids are not likely to have reached statistical significance.

In contrast to our recent intervention study where we fed pure, $^{13}$C-labelled synthetic cyanidin-3-glucoside (Czank *et al.*, 2013), here we administered a matrix which more closely mimics a dietary source of anthocyanins, such as that found in a single serving of some berries (Curtis *et al.*, 2009; Neveu *et al.*, 2010). Whilst the present study therefore provides a comprehensive account of the metabolism of anthocyanins following acute and chronic consumption of elderberries, there are certain limitations with this work. Although the use of a food source of anthocyanins, as opposed to a pure chemical better represents habitual dietary intake, it complicates the elucidation of anthocyanin derived metabolites. Phenolic compounds are ubiquitous within plants (DykesandRooney, 2007; Schmitzer *et al.*, 2010) and were present at quantities of 0.04 to 139 mg/g within the elderberry extract (Table 4.1) and breakfast consisting of Weetabix, Cornflakes or toast. As the intervention meal was fed *ad labitum*, and intakes were not reported, the phenolic intake could not be quantitatively established with accuracy. However, database analysis of the main ingredients present within the breakfast (unprocessed wheat, barley and maize) indicated that the foods likely contained six of the metabolites identified in the present study, at concentrations ranging from 0.01 to 0.15 mg/100 g FW (Neveu *et al.*, 2010), presuming the phenolics are not degraded during processing. In addition, some of the metabolites identified in the present study are typically associated with the colonic metabolites of other phenolic compounds (WilliamsonandClifford, 2010) and could therefore be derived from the prior consumption of

a range of polyphenolic compounds other than anthocyanins. For example, propenoic acids and phenylacetic acids are reported metabolites of flavonols and procyanidins (Del Rio *et al.*, 2013; Selma *et al.*, 2009). However, only metabolites which increased from fasted/baseline levels were reported presently and in addition, 19 and 11 of the metabolites identified in urine and serum respectively, including ferulic acid and phase II conjugates of protocatechuic acid and vanillic acid, were recently reported in a $^{13}$C-labelled anthocyanin feeding study (Czank *et al.*, 2013). Together this suggests that the metabolites identified within the present study were derived, at least in part, from the consumed anthocyanins. Nevertheless, without the use of a labelled anthocyanin, it is not possible to categorically define the origin of all phenolics within the diet, and therefore the contribution of phenolic acids from other sources consumed prior to the fast or in the breakfast cannot be definitively excluded.

The samples collected in the present study were limited to 3 h post bolus sampling, and longer duration sampling following acute exposure would have allowed us to conduct a more comprehensive pharmacokinetic analysis. In addition, there are a number of substances known to interfere with the creatinine assay (WeberandVan Zanten, 1991), however we found no reports in the literature of anthocyanins interfering with creatinine measurements. Anthocyanins do absorb at the same wavelength as the assay substrate (510/570 nm), however they would have minimal absorbance intensity under the alkaline conditions of the assay (Fossen *et al.*, 1998) and are therefore likely to have minor impact on assay sensitivity. The collection and measurement of complete urine voids would have allowed total recoveries to be calculated as opposed to reporting creatinine adjusted ratios. Finally, as polyphenol metabolites are generally more concentrated in the urine, and urinary clearance generally reflects the circulating plasma pool of polar metabolites, plasma samples were pooled to reduce analytical costs. This may be seen as a further limitation of the present analysis as it reduces the intrinsic variability in clearance kinetics between participants. In order to determine whether there was an increase in anthocyanin recovery and decrease in hydroxybenzoic acid recovery following sustained dosing (Figure 4.6), the present study would need to have analysed participant plasma samples individually.

## 4.5. Conclusion

The present study identifies a greater number of anthocyanin metabolites and higher metabolite concentrations than previously reported, with phenolic metabolites identified at 60 and 45 fold higher concentrations than their parent compounds in urine and plasma respectively. No significant difference in metabolism or clearance was identified following

chronic anthocyanin consumption, suggesting there is no alteration in metabolic processing following 12wks repeated dosing. These results therefore indicate that anthocyanins degrade and are extensively metabolised *in vivo*, and adds further weight to the suggestion that it is the accumulation of multiple low molecular weight phenolic metabolites within plasma, which may be responsible for the reported bioactivity of anthocyanins.

# Chapter 5. Structural elucidation of novel conjugated metabolites of anthocyanins using enhanced mass spectrometry scanning ($MS^3$)

## 5.1. Introduction

High dietary intakes of anthocyanins have been linked to decreased risk of cardiovascular disease (Cassidy *et al.*, 2013; Cassidy *et al.*, 2011; Mink *et al.*, 2007; Rissanen *et al.*, 2003). However, owing to their apparent low bioavailability, phenolic degradation products of anthocyanins may be responsible for their bioactivity. The identification of 29 anthocyanin metabolites in urine was previously described based on their retention time and fragmentation pattern in relation to analytical standards (de Ferrars *et al.*, 2013) (**Chapter 4**). This was confirmed via a tracer study, where 500 mg isotopically labelled $^{13}C_5$-cyanidin-3-glucoside was fed to eight male participants (Czank *et al.*, 2013) (**Chapter 3**). Biological samples were collected for 48 h post-bolus and were analysed using isotope-ratio mass spectrometry (IRMS) and HPLC-MS/MS. The study identified 35 metabolites of $^{13}C_5$-cyanidin-3-glucoside, which accounted for 37 ± 14% of the total $^{13}C$ recovered in the urine (Czank *et al.*, 2013), however, a significant portion of the label (63%) remained unaccounted for.

A limitation of previous analyses was that the methods focused on identifying and quantifying metabolites for which standards were commercially available or had been synthesised, and methods were not developed to detect or quantify other conjugates. Phenolic acids commonly undergo phase II conjugation (methyl, sulfate, *O*-glucuronide, glycine or glutathione) *in vivo*, to increase their polarity and elimination from the body (Hollman, 2004). Therefore, it is likely that the presence of further conjugated metabolites accounts for a large proportion of the unidentified label. Sulfation and glucuronidation, two prevalent phase II metabolic processes, are mediated by sulfotransferases (SULTs) and uridine-5'-diphosphoglucuronosyl-transferases (UDPDG) respectively (Wu *et al.*, 2011). Previously, ten sulfated and glucuronidated conjugates of 4-hydroxybenzoic acid, protocatechuic acid and vanillic acid were synthesised at the University of St. Andrews (UK), which enabled their identification within post bolus urine and serum samples (Czank *et al.*, 2013; de Ferrars *et al.*, 2013). The aim of the present study was to use enhanced $MS^3$ scans to detect and elucidate the structure of additional sulfated and glucuronidated conjugates of anthocyanin metabolites for which standards are not currently available. Urine samples derived from an intervention trial feeding 500 mg elderberry anthocyanins, (de

Ferrars *et al.*, 2013) (**Chapter 4)** and an intervention feeding 500 mg $^{13}C_5$-labelled cyanidin-3-glucoside (Czank *et al.*, 2013; de Ferrars *et al.*, 2014) (**Chapter 3**) were utilised in the present analysis.

## 5.2. Materials and methods

### 5.2.1. Chemicals and materials

All standards used for quantification were purchase from Sigma-Aldrich (Dorset, UK). Kinetex pentafluorophenol (PFP) HPLC column (2.6 µM, 100 x 4.6 mm) and SecurityGuard® cartridges (PFP, 4.0 x 2.0 mm) were purchased from Phenomenex (Macclesfield, UK). HPLC grade methanol, acetonitrile and formic acid were purchased from Fisher Scientific (Loughborough, UK). Discovery® DSC-18 SPE columns (6 mL, 1 g) and Acrodisc 13 mm, 0.45 µm PTFE syringe filters, ascorbic acid, formic acid and all other chemicals, were purchased from Sigma-Aldrich (Dorset, UK). All water utilised was of Milli-Q grade (18.2 MΩ $cm^{-1}$).

### 5.2.1. Elderberry derived anthocyanin intervention

Urine samples from a 12 week elderberry extract supplementation trial were collected as described previously (de Ferrars *et al.*, 2013) (**Chapter 4**). Briefly, biological samples were derived from a 12 week anthocyanin intervention trial, where following an overnight fast healthy post-menopausal women (n=15; age, 58.2 ± 5.6 y; BMI, 24.7 ± 0.6 kg/m²) consumed 500 mg/day elderberry anthocyanins (Curtis *et al.*, 2009) and blood and urine samples were collected at baseline and at 1 h, 2 h and 3 h post bolus.

### 5.2.1. Isotopically labelled cyanidin-3-glucoside intervention

Urine samples from a $^{13}$C-labelled cyanidin-3-glucoside intervention study were collected as described previously (**Chapter 3**) (Czank *et al.*, 2013). Briefly, following an overnight fast, a baseline urine (total morning void of study day) sample was collected. Male participants (n=8; age, 27.8 ± 8.1 y; BMI, 23.2 ± 1.5 kg/m²) were given a single, oral 500 mg bolus of encapsulated $^{13}C_5$-cyanidin-3-glucoside (2 x 250 mg capsules) followed by a standardised anthocyanin free breakfast. Cyanidin-3-glucoside was isotopically labelled at positions 6, 8, 10, 3' and 5' (**Figure 5.1**) at the University of St. Andrews, Scotland, so that three $^{13}$C atoms ($^{13}C_3$) were present on the A-ring and two $^{13}$C atoms ($^{13}C_2$) were present on the B-ring (Zhang *et al.*, 2011). Individual urine voids were collected throughout the study day (0-6 h) and pooled for 6-24 h and 24-48 h time points.

**Figure 5.1** Structure and labelling configuration of 6,8,10,3',5'-$^{13}C_5$-cyanidin-3-glucoside.

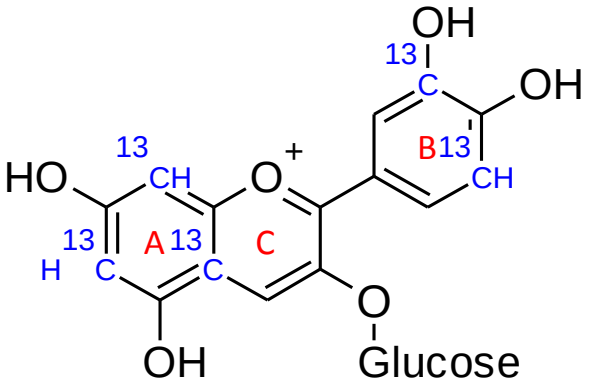


### 5.2.2. Sample preparation

Urine samples were extracted and concentrated as previously published (de Ferrars *et al.*, 2013) **Chapter 2.** Briefly urine samples were extracted using DSC-18 (6 mL, 1 g) SPE cartridges, evaporated to approximately 50 µL using a Thermo speedvac and diluted with 200 µL of 1% formic acid in milliQ water (pH 2.4). 10 µL of 1 mg/mL scopoletin was added as a volume control standard and samples were then filtered using Acrodisc PTFE syringe filters (13 mm, 0.45 µm).

### 5.2.3. Metabolite modelling/study design

In order to identify conjugated metabolites of anthocyanins, an approach was used whereby the fragmentation patterns of the possible sulfated and glucuronidated conjugates of previously identified metabolites [**Chapter 3 & 4** (Czank *et al.*, 2013; de Ferrars *et al.*, 2013; de Ferrars *et al.*, 2014)] were modelled based on the known fragmentation patterns of commercially available phenolic compounds (non-conjugated standards) (**Chapter 2**) and their commonly reported transitions (**Table 5.1**) (Boss *et al.*, 1999; Farrell *et al.*, 2011; Huang *et al.*, 2010; Keski-Hynnilä *et al.*, 2002; Levsen *et al.*, 2005; Liu *et al.*, 2007; Qu *et al.*, 2001; Stalmach *et al.*, 2009a; Wong *et al.*, 2010; Woodward *et al.*, 2011; Wu *et al.*, 2011). Briefly, in negative mode glucuronides produce ions that are 176 Da higher than those of the non-conjugated metabolite. Following collision induced fragmentation, an abundant fragment [*M*-H-176]$^-$, which correspond to the fragments resulted from the neutral loss of a glucuronic acid from the deprotonated molecule, and a less abundant ion at *m/z* 175 is typically observed (Farrell *et al.*, 2011; Keski-Hynnilä *et al.*, 2002; Qu *et al.*, 2001; Stalmach *et al.*, 2009a; Woodward *et al.*, 2011). In addition, secondary fragment ions at *m/z* 113 (resulting from the loss of $CO_2$ and water from the glucuronide ion, *m/z* 175) and a less intense ion at *m/z* 85 (from the extrusion of CO from *m/z* 113) may appear (Farrell *et al.*,

2011; Levsen *et al.*, 2005; Stalmach *et al.*, 2009a). Therefore, in order to model the MRM fragmentation patterns of possible *O*-glucuronide metabolites used to trigger an information dependant acquisition (IDA) $MS^3$ scan, the $[M\text{-H+176}]^-$ parent ion and the $[M\text{-H-176}]^-$ and *m/z* 175 daughter ions were used (Table 5.1).

**Table 5.1** Modelled fragmentation patterns of possible *O*-glucuronide and *O*-sulfate conjugates of anthocyanin metabolites.

| Conjugate | Parent mass | Parent ion $[M\text{-H}]^-$ | Daughter ion | Putative fragments |
|---|---|---|---|---|
| Dihydroxybenzoic acid-GlcA | 330.24 | 329 | 153 | 285,175,113,109 |
| Dihydroxybenzoic acid-sulfate | 234.18 | 233 | 153 | 189,109,97,80 |
| Methoxybenzoic acid-GlcA | 328.27 | 327 | 151 | 283,175,113,107 |
| Methoxybenzoic acid-sulfate | 232.21 | 231 | 151 | 187,107,97,80 |
| Hydroxymethoxybenzoic acid-GlcA | 344.27 | 343 | 167 | 299,175,123,113 |
| Hydroxymethoxybenzoic acid-sulfate | 248.21 | 247 | 167 | 203,123,97,80 |
| Hydroxybenzaldehyde-GlcA | 298.25 | 297 | 121 | 253,175,113 |
| Hydroxybenzaldehyde-sulfate | 202.18 | 201 | 121 | 157,97,80 |
| Dihydroxybenzaldehyde-GlcA | 314.24 | 313 | 137 | 269,175,113,93 |
| Dihydroxybenzaldehyde-sulfate | 218.18 | 217 | 137 | 173,137,97,93,80 |
| Hydroxymethoxybenzaldehyde-GlcA | 328.27 | 327 | 151 | 283,175,113,107 |
| Hydroxymethoxybenzaldehyde-sulfate | 232.21 | 231 | 151 | 187,107,97,80 |
| Hydroxyphenylacetic acid-GlcA | 328.27 | 327 | 151 | 283,175,113,107 |
| Hydroxyphenylacetic acid-sulfate | 232.21 | 231 | 151 | 203,123,97,80 |
| Dihydroxyphenylacetic acid-GlcA | 344.37 | 343 | 167 | 299,175,123,113 |
| Dihydroxyphenylacetic acid-sulfate | 248.21 | 247 | 167 | 203,123,97,80 |
| Hydroxymethoxyphenylacetic acid-GlcA | 358.30 | 357 | 181 | 313,175,137,113 |
| Hydroxymethoxyphenylacetic acid-sulfate | 262.24 | 261 | 181 | 217,137,97,80 |
| Hydroxycinnamic acid-GlcA | 340.28 | 339 | 163 | 295,175,119,113 |
| Hydroxycinnamic acid-sulfate | 244.22 | 233 | 163 | 189,119,97,80 |
| Dihydroxycinnamic acid-GlcA | 356.28 | 355 | 179 | 311,175,135,113 |
| Dihydroxycinnamic acid-sulfate | 260.22 | 259 | 179 | 215,135,97,80 |
| Hydroxymethoxycinnamic acid-GlcA | 370.31 | 369 | 193 | 325,175,149,113 |
| Hydroxymethoxycinnamic acid-sulfate | 274.25 | 273 | 193 | 229,149,97,80 |
| Dimethoxyhydroxycinnamic acid-GlcA | 400.33 | 399 | 223 | 355,179,175,113 |
| Dimethoxyhydroxycinnamic acid-sulfate | 304.27 | 303 | 223 | 259,179,97,80 |

GlcA, glucuronide

Ionisation of intact sulfated conjugates results in the formation of a molecular ion, $[M\text{-H+80}]^-$. Collision-induced fragmentation of the molecular ions of sulfate esters results in a loss of 80 Da, producing an abundant $[M\text{-H-}SO_3]^-$ fragment. Alternatively, a loss of 98 Da may occur from $[M\text{-H-}H_2SO_4]^-$ which is represented by a *m/z* 97 Da (Levsen *et al.*, 2005). If the charge resides with the sulfate group, radical ions at *m/z* -80 from $SO_3^{-\bullet}$ and at *m/z* -97 from $HSO_4^-$ may form. Sulfates other than esters only demonstrate the formation the $[M\text{-H-}SO_3]^-$ and *m/z* -80 ions, which enables both types of conjugate to be distinguished (Boss *et al.*, 1999; Lin *et al.*, 2007). Therefore, in order to model the MRM fragmentation patterns of

possible sulfate metabolites used to trigger the dependant $MS^3$ scan, the $[M\text{-H+80}]^-$ parent ion and the $[M\text{-H-80}]^-$ and *m/z* 80 daughter ions were used (Table 5.1).

### 5.2.4. HPLC-MS/MS analysis

HPLC-MS/MS analysis was performed on an Agilent 1200 series HPLC system coupled with a ABSciex 3200 Q-trap MS/MS system, with samples injected onto a Kinetex PFP column as previously published (de Ferrars *et al.*, 2013) (**Chapter 2**). Briefly, the mobile phase consisted of 0.1% formic acid (v/v) in water (A) and 0.1% formic acid (v/v) in acetonitrile (B), at a flow rate of 1.5 mL/min at 0 min, 1 mL/min at 7 to 14 min and 1.5 mL/min at 14 to 28 min. The gradient consisted of 1% B at 0 min, 7.5% B at 7 min, 7.6% B at 14 min, 10% B at 17 min, 12% B at 18.5 min, 12.5% B at 20 min, 30% B at 24 min and 90% B at 25 to 28 min. MS/MS source parameters included curtain gas 40 psi, ion spray voltage -4000 V/+5500 V, temperature 700 °C and nebulizer and auxiliary gas 60 psi. The system was controlled by Analyst software (v. 1.5, Applied Biosystems/MDS Sciex). For IDA analysis, multiple reaction monitoring (MRM) or neutral loss (NL) survey scans were used, with transitions above 2000 cps triggering enhanced resolution (ER) and data dependent enhanced product ion (EPI) scans (total cycle time, 1.2 s). Quantification was carried using MRM, where the peak area of the most intense ion transition was determined from the chromatograph and used for quantification. Seven-point calibration curves were prepared by spiking the analytes of interest into a matched-matrix, with the coefficient of determination ($r^2$) established as linear. Unless otherwise stated, all conjugated metabolites were quantified relative to their deconjugated, commercially available standard. For samples derived from the $^{13}C$ intervention, the concentration of metabolites was converted to amount recovered from the urine by accounting for the molecular weight of the individual $^{13}C$-labelled metabolites and the volume of the individual participants void and averaged across participants.

## 5.3. Results

Putative identification of the conjugates was achieved using HPLC-$MS^3$ in consecutive reaction monitoring mode. MRM of the conjugated parent ion $[M\text{-H}]^-$ and unconjugated daughter fragment (*O*-glucuronide conjugate $[M\text{-H-175}]^-$ or *O*-sulfate conjugate $[M\text{-H-80}]^-$) was used to select the compounds of interest for further fragmentation via information dependent EPI scans. The resulting $MS^3$ daughter ions were compared to the fragmentation patterns modelled previously based on the known fragmentation pattern of commercially available standards and commonly established metabolite fragmentation patterns (Table 5.1). A total of 17 novel phase II metabolites of anthocyanins (**Table 5.2**) were putatively detected

within urine samples derived from intervention trials feeding either 500 mg $^{13}$C-labelled cyanidin-3-glucoside or 500 mg elderberry derived anthocyanins. Unless stated otherwise, the fragments described below represent the unlabelled mass.

Three peaks were identified as having a parent ion [*M*-H]$^-$ at *m/z* 247 and a daughter ion at *m/z* 167, which represents the parent-daughter transitions common between sulfated conjugates of hydroxymethoxybenzoic acid, dihydroxyphenylacetic acid or methyl-dihydroxybenzoate. Peak 1 (*m/z* 247/167; $R_t$, 4.12 min; **Figure 5.2**) and peak 2 (*m/z* 247/167; $R_t$, 12.27 min; **Figure 5.3**) were identified within urine derived from both the elderberry and $^{13}$C-labelled anthocyanin trials. Peak 3 (*m/z* 247/167; $R_t$, 13.08 min; **Figure 5.4**) was identified within urine from the $^{13}$C-labelled intervention trial only, with a mass of +2 Da, indicating the metabolite was derived from the anthocyanin B-ring (Table 5.2). Further fragmentation of peak 1 using $MS^3$ produced ions at *m/z* 123 (elderberry trial) and *m/z* 125 ($^{13}$C-labelled intervention trial) representing the loss of the sulfate and carboxylic groups [*M*-H-80-44]$^-$. In addition, ions were produced at *m/z* 203 representing the loss of a carboxylic group [*M*-H-44]$^-$. Peak 2 yielded fragments at *m/z* 137 (elderberry trial) and *m/z* 139 ($^{13}$C-labelled intervention trial) representing the loss of sulfate and methoxy groups [*M*-H-80-30]$^-$. Additionally, peak 2 produced a large daughter fragment at *m/z* 152 which may correspond to the fragment observed following the loss of a methyl $CH_3$ group producing a [*M*-H-15]$^-$ anion radical, thus suggesting that peak 2 likely corresponds to a methoxyhydroxybenzoic acid or methyl-dihydroxybenzoates, whilst peaks 1 and 3 likely correspond to a sulfate of dihydroxyphenylacetic acid. However, due to the lack of commercially available or synthetic standards, the exact identity of these structures cannot be established with certainty.

Peaks 1, 2 and 3 were quantified relative to homoprotocatechuic acid (3,4-dihydroxyphenylacetic acid), an unconjugated, commercially available standard. Following $^{13}$C-cyanidin-3-glucoside consumption, maximum concentrations ranging from 394 ± 268 nM (peak 3) to 1307 ± 826 nM (peak 2) were identified in urine samples 6-24 h post anthocyanin consumption (**Table 5.3** & **Figure 5.5**). In addition, maximum concentrations of 211 ± 167 nM/mM creatinine (peak 2) to 705 ± 694 nM/mM creatinine (peak 1) were observed at 3 h following elderberry anthocyanin consumption (**Table 5.4**).

**Table 5.2** HPLC-$MS^3$ identification of *O*-glucuronide and sulfate metabolites in urine of human volunteers from intervention study feeding 500 mg elderberry anthocyanins or 500 mg $^{13}C_5$-cyanidin-3-glucoside.

| Peak # | Compound | Elderberry intervention | | | $^{13}C_5$-cyanidin-3-glucoside intervention | | |
|---|---|---|---|---|---|---|---|
| | | $R_t$ (min) | $[M-H]^-$ (*m/z*)[a] | $MS^3$ (*m/z*)[b] | $R_t$ (min) | $[M-H]^-$ (*m/z*)[a] | $MS^3$ (*m/z*)[b] |
| **1** | Dihydroxyphenylacetic acid-sulfate | 4.07 | 247 | 203,167[c],123 | 4.12 | 249[c] | 203,169[c],154,125 |
| **2** | Methyl-dihydroxybenzoate-sulfate | 12.28 | 247[c] | 201,167[c],137 | 12.27 | 249[c] | 203,169[c],154,139,80 |
| **3** | Dihydroxyphenylacetic acid-sulfate | ND | ND | ND | 13.08 | 249[c] | 203,169[c],137 |
| **4** | Dihydroxybenzoic acid-GlcA | 7.75 | 329[c] | 175,153,113,109,85 | ND | ND | ND |
| **5** | Dihydroxybenzoic acid-GlcA | 9.53 | 329[c] | 175,153,113 | ND | ND | ND |
| **6** | Dihydroxyphenylacetic acid-GlcA | 16.00 | 343[c] | 175,167[c],123,113 | ND | ND | ND |
| **7** | Dihydroxycinnamic acid-sulfate | 11.30 | 259[c] | 215,179[c],147,135 | ND | ND | ND |
| **8** | Dihydroxycinnamic acid-sulfate | 13.50 | 259[c] | 215,179[c],135,97 | ND | ND | ND |
| **9** | Dihydroxycinnamic acid-sulfate | 14.10 | 259[c] | 215,179[c],135 | ND | ND | ND |
| **10** | Dihydroxycinnamic acid-GlcA | 9.59 | 355[c] | 311,193,179[c],175,135,113,85 | 9.14 | 357[c] | 313,181[c],175,137,113,109,95,85 |
| **11** | Hydroxymethoxycinnamic acid-GlcA | 9.90 | 369[c] | 193[c],178,175,149,137,134,113,85 | 9.34 | 371[c] | 195[c],175,113,95,85 |
| **12** | Hydroxymethoxycinnamic acid-GlcA | 12.37 | 369[c] | 193[c],178,175,149,137,134,113,85 | ND | ND | ND |
| **13** | Hydroxymethoxycinnamic acid-sulfate | 17.95 | 273[c] | 229,193[c],178,149,134,97 | ND | ND | ND |
| **14** | Dimethoxyhydroxycinnamic acid-sulfate | 15.91 | 303[c] | 259,223[c],208,193,179,164,149,135,97 | ND | ND | ND |
| **15** | Dimethoxyhydroxycinnamic acid-GlcA | ND | ND | ND | 7.81 | 401[c] | 357,225[c],210,195,180,175,113 |
| **16** | Dimethoxyhydroxycinnamic acid-GlcA | 10.62 | 399[c] | 223[c],179,175,151,113,85 | ND | ND | ND |
| **17** | Dimethoxyhydroxycinnamic acid-GlcA | 11.95 | 399[c] | 223[c],208,179,175,164,113 | 12.65 | 401[c] | 225[c],175,85 |

GlcA, glucuronide; ND, not detected; $R_t$, retention time. [a]Parent ion. [b]Daughter fragments, identified via multiple reaction monitoring triggered enhanced product ion (MRM-IDA-EPI) scan. [c]Indicates fragment transitions used for quantification.

**Figure 5.2** Enhanced product ion (MS3) scan of peak 1, putatively identified as dihydroxyphenylacetic acid-sulfate (Rt, 4.12 min).

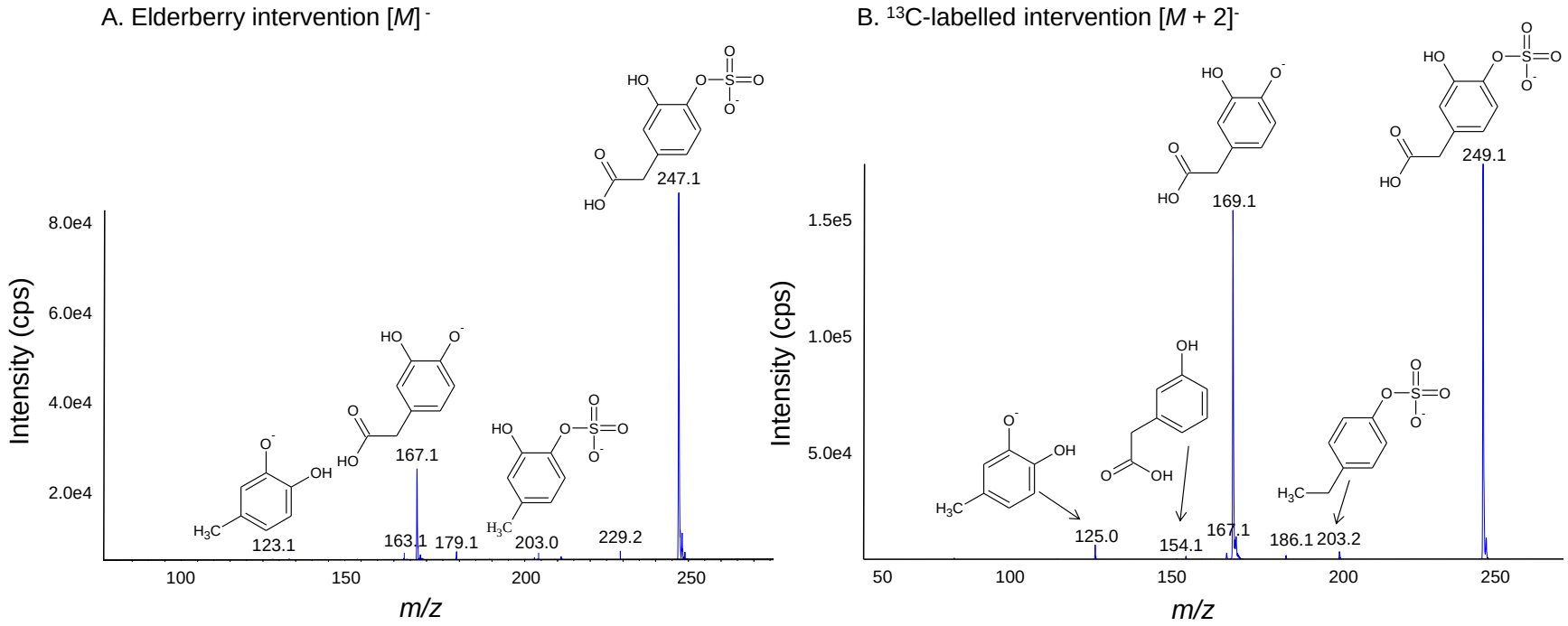


Data derived from pooled post bolus urine samples, where participants were fed (A) 500 mg elderberry anthocyanins or (B) 500 mg $^{13}C_5$-cyanidin-3-glucoside.

**Figure 5.3** Enhanced product ion ($MS^3$) scan of peak 2 putatively identified as dihydroxybenzoic acid-sulfate ($R_t$, 12.27 min).

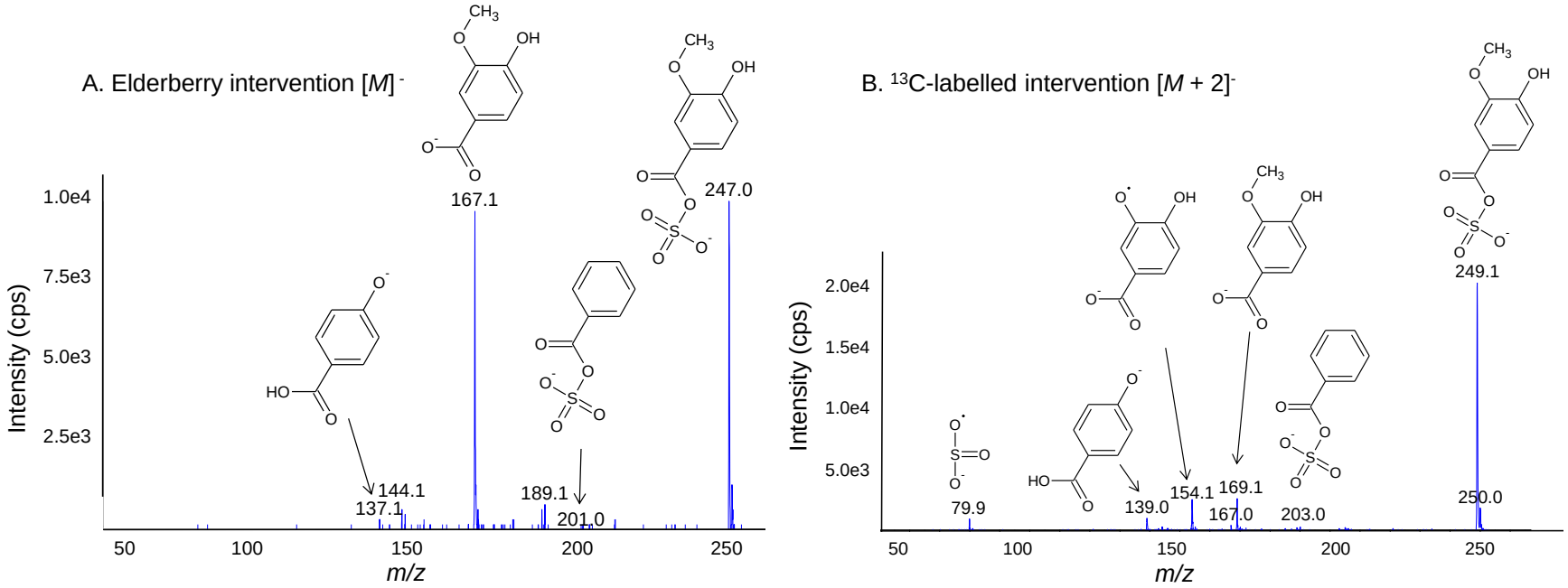


Data derived from pooled post bolus urine samples, where participants were fed (A) 500 mg elderberry anthocyanins or (B) 500 mg $^{13}C_5$-cyanidin-3-glucoside.

**Figure 5.4** Enhanced product ion ($MS^3$) scan of peak 3 putatively identified as dihydroxyphenylacetic acid-sulfate **(**$R_t$, 13.08 min).

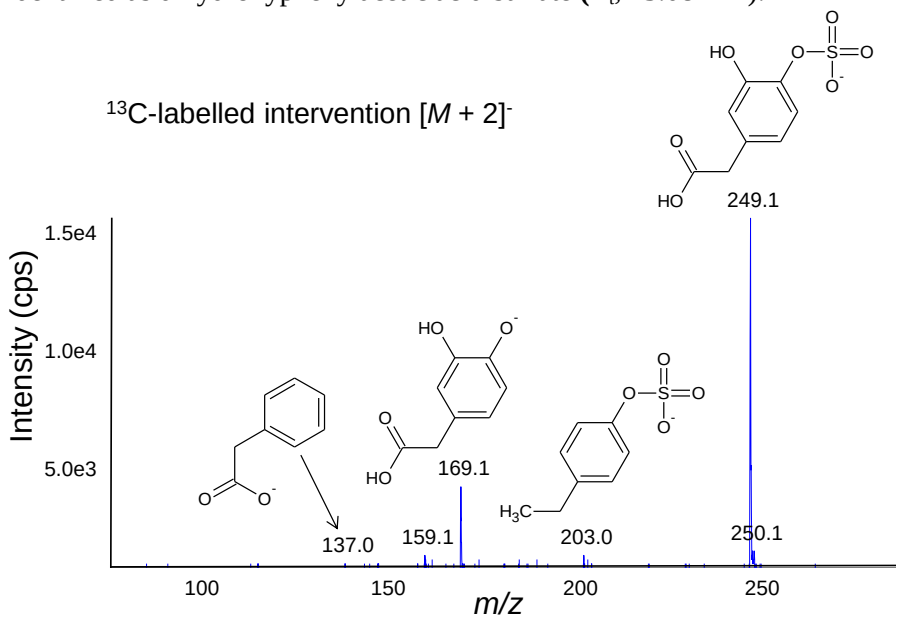


Data derived from pooled post bolus urine samples, where participants were fed 500 mg $^{13}C_5$-cyanidin-3-glucoside.

**Table 5.3** Concentration of putative metabolites in urine samples following acute intake of 500 mg bolus $^{13}C_5$-cyanidin-3-glucoside[a].

| Peak # | Metabolite | $R_t$ (min) | $C_{max}$ (nM) | $T_{max}$ | Total recovery (µg) |
|---|---|---|---|---|---|
| **1** | Dihydroxyphenylacetic acid-sulfate | 4.12 | 1,148 ± 1,193 | 6-24 h | 351 ± 363 |
| **2** | Methyl-dihydroxybenzoate-sulfate | 12.27 | 1,307 ± 826 | 6-24 h | 691 ± 507 |
| **3** | Dihydroxyphenylacetic acid-sulfate | 13.08 | 394 ± 268 | 6-24 h | 128 ± 121 |
| **4** | Dihydroxybenzoic acid-GlcA | ND | ND | ND | ND |
| **5** | Dihydroxybenzoic acid-GlcA | ND | ND | ND | ND |
| **6** | Dihydroxyphenylacetic acid-GlcA | ND | ND | ND | ND |
| **7** | Dihydroxycinnamic acid-sulfate | ND | ND | ND | ND |
| **8** | Dihydroxycinnamic acid-sulfate | ND | ND | ND | ND |
| **9** | Dihydroxycinnamic acid-sulfate | ND | ND | ND | ND |
| **10** | Dihydroxycinnamic acid-GlcA[b] | 9.14 | 738 ± 774 | 24-48 h | 398 ± 394 |
| **11** | Hydroxymethoxycinnamic acid-GlcA | 9.34 | 364 ± 160 | 6-24 h | 332 ± 189 |
| **12** | Hydroxymethoxycinnamic acid-GlcA | ND | ND | ND | ND |
| **13** | Hydroxymethoxycinnamic acid-sulfate | ND | ND | ND | ND |
| **14** | Dimethoxyhydroxycinnamic acid-sulfate | ND | ND | ND | ND |
| **15** | Dimethoxyhydroxycinnamic acid-GlcA | 7.81 | 430 ± 610 | 5-6 h | 151 ± 172 |
| **16** | Dimethoxyhydroxycinnamic acid-GlcA | ND | ND | ND | ND |
| **17** | Dimethoxyhydroxycinnamic acid-GlcA | 12.65 | 304 ± 429 | 24 h | 187 ± 271 |

GlcA, glucuronide. [a]Values are expressed as mean ± SD, metabolites were detected in n=8 participants unless otherwise stated; [b]detected in n=3. For $T_{max}$, samples were pooled across participants for 1 h time periods, for t=0-1 h (n=3), t=1-2 h (n=5), t=2-3 h (n=6), t=3-4 h (n=6), t=4-5 h (n=4), t=5-6 h (n=8), t=6-24 h (n=8) and t=24-48 h (n=8). Unless stated otherwise, metabolites were quantified relative to the commercially available unconjugated analytical standard using their respective quantification transitions.

**Figure 5.5** Urinary elimination profiles of putative conjugated metabolites of cyanidin-3-glucoside in eight healthy male participants after the consumption of 500 mg $^{13}C_5$-cyanidin-3-glucoside.

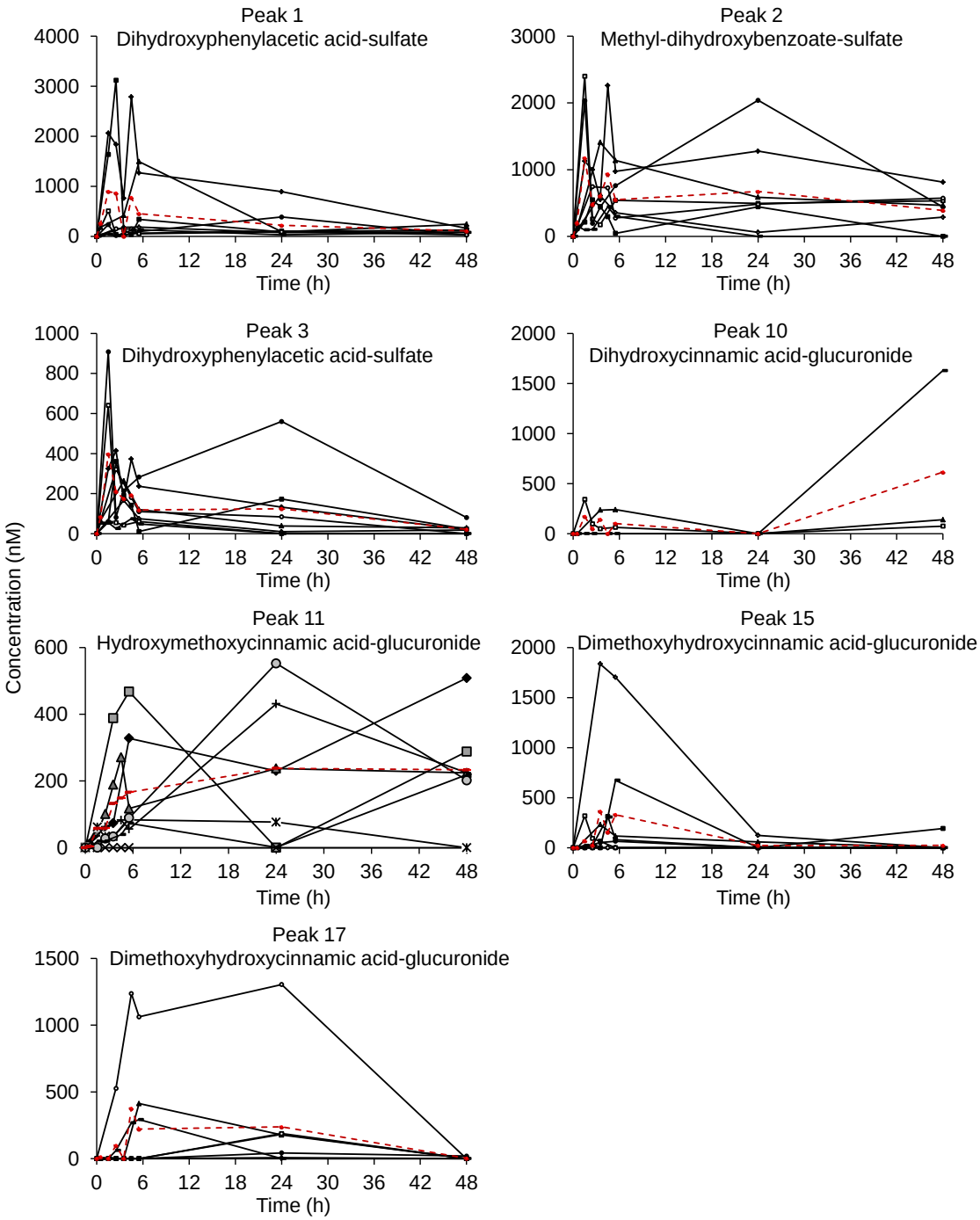


Broken line indicates mean. Peak numbers refer to metabolites listed in Table 5.2.

**Table 5.4** Ratio of putative metabolites in urine samples following acute (500 mg) and chronic (500 mg/day for 12 week) intake of anthocyanins from an elderberry extract, expressed per mM creatinine.

| Peak # | Compound | $R_t$ (min) | Ratio nM/mM creatinine (% of total metabolites)[c] | | | | |
|---|---|---|---|---|---|---|---|
| | | | Baseline | t(0-1 h) | t(1-2 h) | t(2-3 h) | Total |
| **1** | Dihydroxyphenylacetic acid-sulfate[a] | 4.07 | 274 ± 254 | 334 ± 470 | 517 ± 784 | 705 ± 694 | 1,831 ± 1,937 |
| | Dihydroxyphenylacetic acid-sulfate[b] | | 314 ± 272 | 649 ± 776 | 552 ± 443 | 661 ± 553 | 2,176 ± 1,620 |
| **2** | Methyl-dihydroxybenzoate-sulfate[a] | 12.28 | 106 ± 140 | 76 ± 86 | 162 ± 139 | 211 ± 167 | 555 ± 462 |
| | Methyl-dihydroxybenzoate-sulfate[b] | | 101 ± 123 | 59 ± 68 | 147 ± 126 | 174 ± 165 | 482 ± 350 |
| **3** | Dihydroxyphenylacetic acid-sulfate | ND | ND | ND | ND | ND | ND |
| **4** | Dihydroxybenzoic acid-GlcA[a] | 7.75 | 78 ± 73 | 201 ± 338 | 986 ± 981 | 1,370 ± 868 | 2,635 ± 1,515 |
| | Dihydroxybenzoic acid-GlcA[b] | | 147 ± 111 | 318 ± 308 | 1,043 ± 657 | 1,527 ± 1,126 | 3,035 ± 1,678 |
| **5** | Dihydroxybenzoic acid-GlcA[a] | 9.53 | 30 ± 60 | 103 ± 216 | 661 ± 679 | 1,051 ± 802 | 1,845 ± 1,129 |
| | Dihydroxybenzoic acid-GlcA[b] | | 103 ± 59 | 208 ± 220 | 642 ± 396 | 1,011 ± 611 | 1,964 ± 916 |
| **6** | Dihydroxyphenylacetic acid-GlcA[a] | 16.00 | 171 ± 204 | 268 ± 440 | 1,664 ± 2,150 | 2,809 ± 1,913 | 4,913 ± 3,999 |
| | Dihydroxyphenylacetic acid-GlcA[b] | | 786 ± 1,507 | 477 ± 349 | 1,877 ± 1,351 | 3,775 ± 2,549 | 6,915 ± 3,269 |
| **7** | Dihydroxycinnamic acid-sulfate[a] | 11.30 | 106 ± 87 | 78 ± 60 | 95 ± 79 | 171 ± 151 | 449 ± 333 |
| | Dihydroxycinnamic acid-sulfate[b] | | 100 ± 73 | 112 ± 100 | 93 ± 53 | 124 ± 106 | 429 ± 216 |
| **8** | Dihydroxycinnamic acid-sulfate[a] | 13.50 | 186 ± 273 | 99 ± 131 | 138 ± 96 | 311 ± 297 | 735 ± 721 |
| | Dihydroxycinnamic acid-sulfate[b] | | 46 ± 47 | 80 ± 90 | 167 ± 164 | 278 ± 260 | 572 ± 432 |
| **9** | Dihydroxycinnamic acid-sulfate[a] | 14.10 | 63 ± 75 | 42 ± 42 | 92 ± 78 | 170 ± 129 | 367 ± 243 |
| | Dihydroxycinnamic acid-sulfate[b] | | 25 ± 24 | 40 ± 37 | 87 ± 49 | 154 ± 118 | 306 ± 157 |
| **10** | Dihydroxycinnamic acid-GlcA[a] | 9.59 | 52 ± 76 | 34 ± 37 | 51 ± 91 | 38 ± 27 | 175 ± 183 |
| | Dihydroxycinnamic acid-GlcA[b] | | 37 ± 63 | 34 ± 34 | 32 ± 26 | 39 ± 27 | 141 ± 138 |
| **11** | Hydroxymethoxycinnamic acid-GlcA[a] | 9.90 | 316 ± 334 | 653 ± 853 | 2,018 ± 1,773 | 2,339 ± 1,472 | 5,326 ± 3,959 |
| | Hydroxymethoxycinnamic acid-GlcA[b] | | 267 ± 335 | 482 ± 540 | 1,423 ± 1,089 | 1,827 ± 1,470 | 3,999 ± 2,649 |
| **12** | Hydroxymethoxycinnamic acid-GlcA[a] | 12.37 | 1,078 ± 1,965 | 882 ± 1,353 | 1,424 ± 1,485 | 1,730 ± 1,170 | 5,115 ± 5,594 |
| | Hydroxymethoxycinnamic acid-GlcA[b] | | 379 ± 353 | 534 ± 461 | 855 ± 437 | 1,333 ± 934 | 3,100 ± 1,694 |
| **13** | Hydroxymethoxycinnamic acid-sulfate[a] | 17.95 | 9,560 ± 11,132 | 10,006 ± 11,184 | 18,954 ± 18,097 | 20,877 ± 15,015 | 59,397 ± 45,900 |
| | Hydroxymethoxycinnamic acid-sulfate[b] | | 3,070 ± 2,974 | 5,181 ± 5,497 | 15,328 ± 13,486 | 16,242 ± 11501 | 39,821 ± 19,425 |
| **14** | Dimethoxyhydroxycinnamic acid-sulfate[a] | 15.91 | 668 ± 1,104 | 510 ± 678 | 1,023 ± 1,035 | 1,086 ± 772 | 3,288 ± 2,802 |
| | Dimethoxyhydroxycinnamic acid-sulfate[b] | | 556 ± 1,804 | 362 ± 550 | 864 ± 769 | 1,036 ± 1,119 | 2,819 ± 2,252 |

| | | | | | | | |
|---|---|---|---|---|---|---|---|
| **15** | Dimethoxyhydroxycinnamic acid-GlcA | ND | ND | ND | ND | ND | ND |
| **16** | Dimethoxyhydroxycinnamic acid-GlcA[a] | 10.62 | 70 ± 188 | 114 ± 277 | 297 ± 977 | 61 ± 58 | 543 ± 1,042 |
| | Dimethoxyhydroxycinnamic acid-GlcA[b] | | 1,052 ± 2,857 | 864 ± 2,425 | 402 ± 1,088 | 363 ± 740 | 2,681 ± 7,067 |
| **17** | Dimethoxyhydroxycinnamic acid-GlcA | 11.95 | 52 ± 78 | 248 ± 451 | 899 ± 1,052 | 1,036 ± 892 | 2,235 ± 2,112 |
| | Dimethoxyhydroxycinnamic acid-GlcA[b] | | 97 ± 221 | 331 ± 655 | 808 ± 825 | 917 ± 812 | 2,153 ± 1,798 |

ND, not detected; GlcA, glucuronide; t, time. Metabolite concentration following [a]acute (500 mg) anthocyanin consumption (week 0) and [b]chronic (500 mg/day for 12 weeks) anthocyanin consumption (week 12); [c]Values represent mean concentrations ± SD, n=15; all samples have been adjusted for creatinine concentration; Unless stated otherwise, metabolites were quantified relative to the commercially available unconjugated analytical standard using their respective quantification transitions.

In addition to the identification of protocatechuic acid-3-glucuronide and protocatechuic acid-4-glucuronide, which were previously described (de Ferrars *et al.*, 2013) (**Chapters 3 & 4**), a further two peaks were identified as having a parent ion at *m/z* 329 and a daughter ion at *m/z* 153 and were tentatively identified as dihydroxybenzoic acid-glucuronide (**Figure 5.6**). Peak 4 (*m/z* 329/153; $R_t$, 7.75 min) and peak 5 (*m/z* 329/153; $R_t$, 9.53 min) were identified within urine derived from the elderberry anthocyanin trial. Fragmentation of the compounds using $MS^3$ produced ions at *m/z* 175 (glucuronide ion), 113 (the loss of $CO_2$ and $H_2O$ from the glucuronide ion), 109 representing the loss of the glucuronide and carboxylic groups [*M*-H-176-44]$^-$ and 85 (the loss of $CO_2$, $H_2O$ and CO from the glucuronide ion) (Table 5.2). Peaks 4 and 5 were quantified relative to protocatechuic acid and were identified at maximum concentrations of 1427 ± 1126 nM/mM creatinine and 1.1 ± 0.8 µM/mM creatinine respectively, 3 h following the consumption of 500 mg elderberry anthocyanins (Table 5.4).

Peak 6 (*m/z* 343/167; $R_t$, 16.00 min; **Figure 5.7**) was identified within urine samples from the elderberry intervention trial, based on a [*M*-H]$^-$ at *m/z* 343, which produced a $MS^2$ ion at *m/z* 167, representing the loss of the glucuronide group [*M*-H-176]$^-$. These transitions correspond to the parent-daughter transitions common between glucuronide conjugates of hydroxy-methoxybenzoic acid, dihydroxyphenylacetic acid and methyl-dihydroxybenzoate. $MS^3$ fragmentation of the molecule produced ions at *m/z* 175 representing a glucuronide anion, 123 [*M*-H-176-44]$^-$ and 113 representing the loss of $CO_2$ and $H_2O$ from the glucuronide anion (Table 5.2). Due to the lack of ion at *m/z* 152 [*M*-H-15]$^-$, indicating the absence of a methyl $CH_3$ group, peak 6 was putatively identified as a glucuronide of dihydroxyphenylacetic acid and quantified relative to homoprotocatechuic acid. It was identified at maximum concentrations of 3.8 ± 2.5 µM/mM creatinine, 3 h following 500 mg elderberry consumption (Table 5.4).

**Figure 5.6** Enhanced product ion ($MS^3$) scan of peak 4 ($R_t$, 7.75 min) and peak 5 ($R_t$, 9.53 min) putatively identified as dihydroxybenzoic acid-glucuronides.

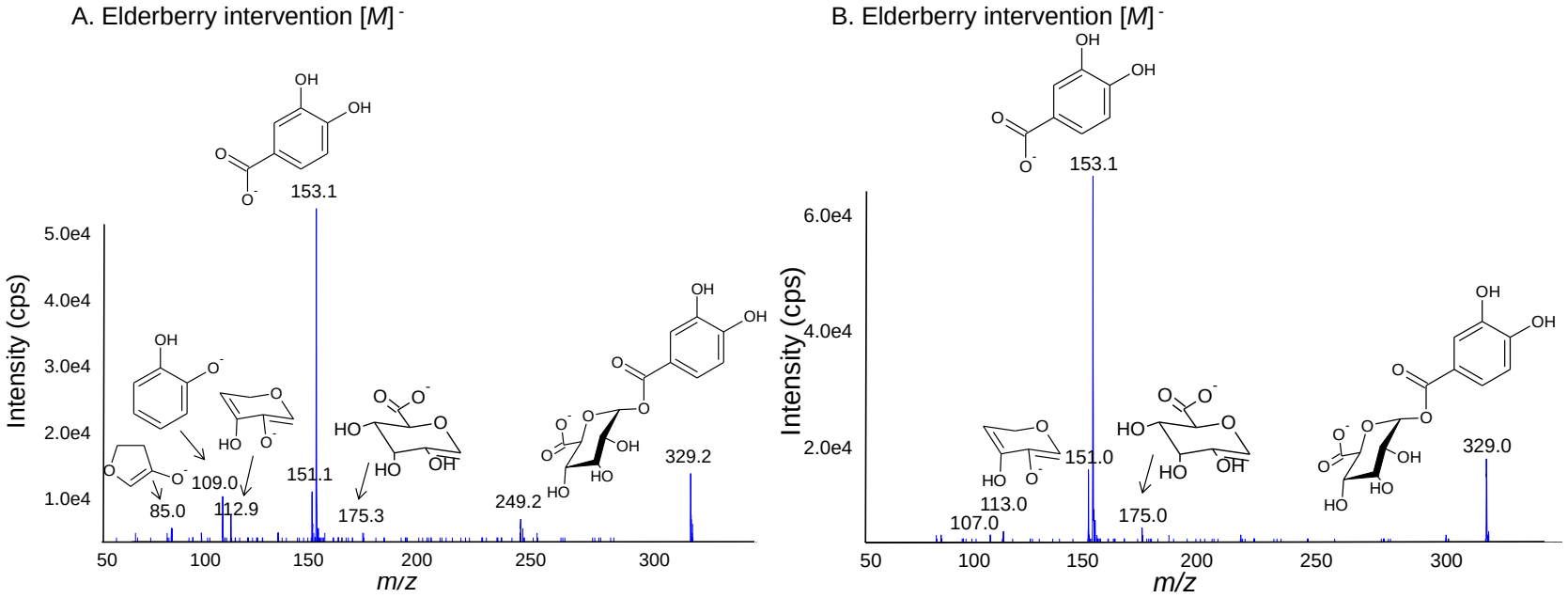


Data derived from pooled post bolus urine samples, where participants were fed 500 mg elderberry anthocyanins.

**Figure 5.7** Enhanced product ion ($MS^3$) scan of peak 6 putatively identified as dihydroxyphenylacetic acid-glucuronide **(**$R_t$, 16.00 min).

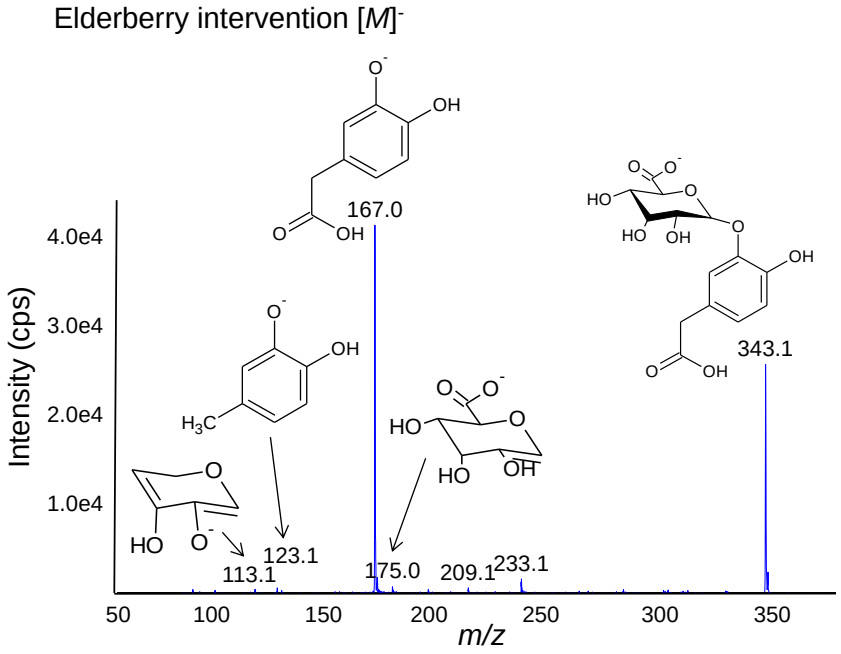


Data derived from pooled post bolus urine samples, where participants were fed 500 mg elderberry anthocyanins.

Peak 7 (*m/z* 259/179; $R_t$, 11.30 min), Peak 8 (*m/z* 259/179; $R_t$, 13.50 min) and Peak 9 (*m/z* 259/179; $R_t$, 14.10 min) were putatively identified as a dihydroxycinnamic acid-sulfates, most likely derived from caffeic acid (**Figure 5.8**). The peaks were identified based on a [*M*-H]$^-$ at *m/z* 259, which produced an $MS^2$ ion at *m/z* 179, representing the loss of the sulfate group [*M*-H-80]$^-$. The $MS^3$ fragmentation patterns produced ions at *m/z* 215 representing the loss of a carboxylic group [*M*-H-44]$^-$, 135 representing the loss of a sulfate and carboxylic group [*M*-H-80-44]$^-$ and 95 indicting the presence of a sulfate anion) (Table 5.2). The dihydroxycinnamic acid-sulfates were quantified relative to caffeic acid and found at maximum concentrations ranging from 170 ± 129 nM/mM creatinine to 311 ± 297 nM/mM creatinine, 3 h post elderberry anthocyanin consumption (Table 5.4).

**Figure 5.8** Enhanced product ion ($MS^3$) scan of (A) peak 7 ($R_t$, 11.30 min), (B) peak 8 ($R_t$, 13.50 min) and (C) peak 9 ($R_t$, 14.10 min) putatively identified as dihydroxycinnamic acid-sulfate**.**

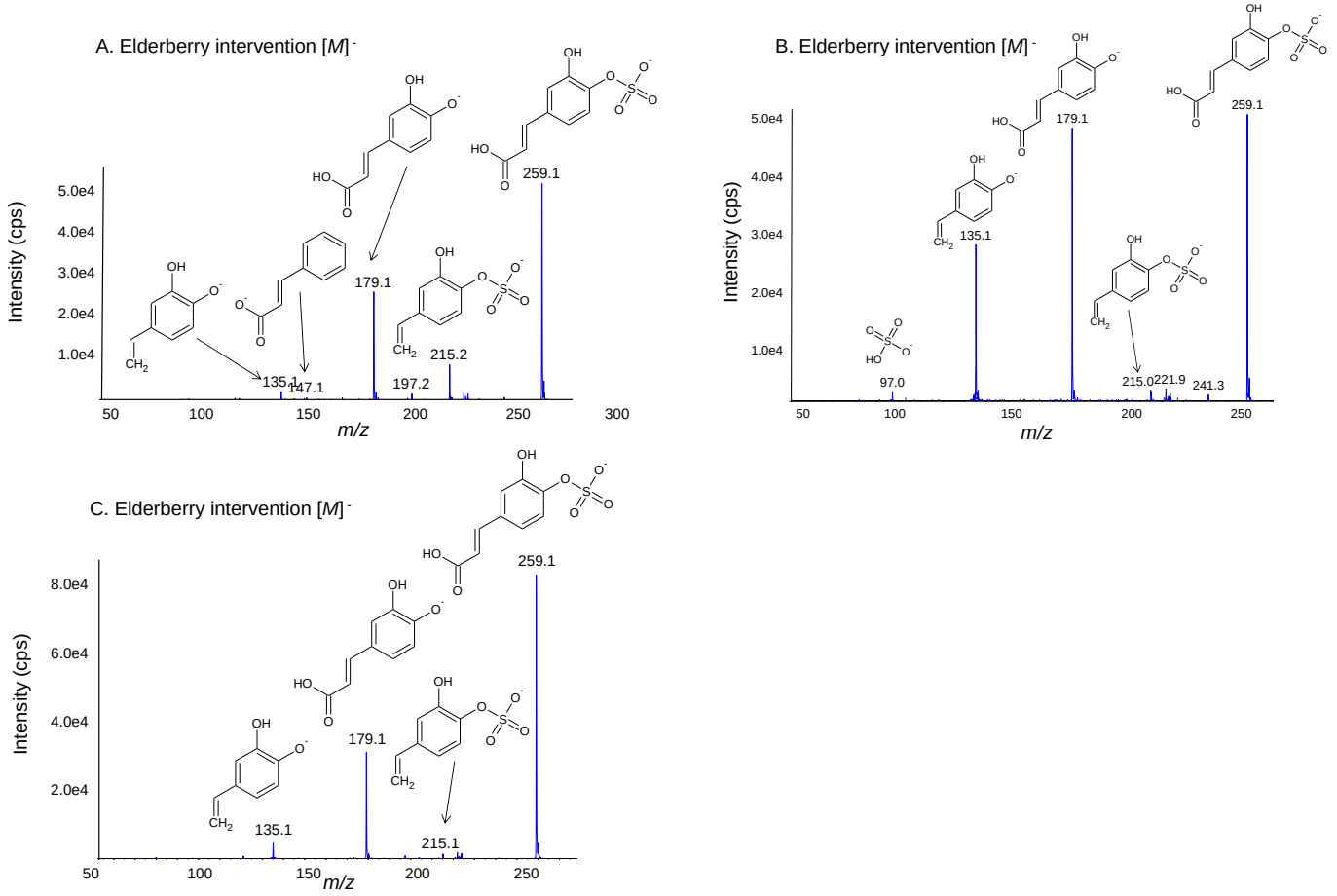


Data derived from pooled post bolus urine samples, where participants were fed 500 mg elderberry anthocyanins.

Peak 10 (*m/z* 355/179; $R_t$, 9.14 min; **Figure 5.9**) was detected within urine samples from the $^{13}$C-labelled and elderberry anthocyanin intervention trials and was putatively identified as dihydroxycinnamic acid-glucuronide. As it was derived from the B-ring of cyanidin-3-glucoside (+2 Da), it was most likely a glucuronide conjugate of caffeic acid. The conjugate was identified based on a $[M\text{-H}]^-$ at *m/z* 355, which produced an $MS^2$ ion at *m/z* 179, representing the loss of the glucuronide group $[M\text{-H-176}]^-$. The $MS^3$ fragmentation patterns produced ions at *m/z* 311 representing the loss of a carboxylic group $[M\text{-H-44}]^-$, 175 (glucuronide ion), 135, representing the loss of a glucuronide ion and carboxylic group $[M\text{-H-176-44}]^-$, 113 (glucuronide ion) and 85 (glucuronide ion) (Table 5.3). Peak 10 was quantified relative to caffeic acid and found at maximum concentrations of 51 ± 91 nM/mM creatinine, 2 h following the consumption of 500 mg elderberry anthocyanins (Table 5.4) and 783 ± 774 nM, 48 h post consumption of 500 mg $^{13}$C-labelled cyanidin-3-glucoside (Figure 5.5).

Peak 11 (*m/z* 369/193; $R_t$, 9.34 min; **Figure 5.10**), detected within urine samples from the $^{13}$C-labelled and elderberry anthocyanin intervention trials and peak 12 (*m/z* 369/193; $R_t$, 12.37 min; Figure 5.10), detected within the elderberry urine samples only were putatively identified as hydroxymethoxycinnamic acid-glucuronides (Table 5.2), mostly likely derived from ferulic acid. The conjugates were detected based on a $[M\text{-H}]^-$ at *m/z* 369, which produced an $MS^2$ ion at *m/z* 193, representing the loss of the glucuronide group $[M\text{-H-176}]^-$. The $MS^3$ fragmentation pattern produced ions at *m/z* 178 $[M\text{-H-176-15}]^-$, 175 (glucuronide ion), 149 representing the loss of a glucuronide ion and carboxylic group $[M\text{-H-176-44}]^-$, 137 representing the loss of the glucuronide ion and cinnamic acid $[M\text{-H-176-44-12}]^-$, 134 representing the loss of a glucuronide ion, carboxylic group and methyl $CH_3$ group $[M\text{-H-176-44-15}]^-$, 113 (glucuronide ion) and 85 (glucuronide ion). The hydroxymethoxycinnamic acid-glucuronides were quantified relative to ferulic acid; peak 11 was identified at maximum concentrations of 2.3 ± 1.5 µM/mM creatinine, 3 h following the consumption of 500 mg elderberry anthocyanins (Table 5.4) and 364 ± 160 nM, 24 h post consumption of 500 mg $^{13}$C-labelled cyanidin-3-glucoside (Figure 5.5). Peak 12 was identified at maximum concentrations of 1.7 ± 1.2 µM/mM creatinine, 3 h following the consumption of 500 mg elderberry anthocyanins (Table 5.4).

**Figure 5.9** Enhanced product ion ($MS^3$) scan of peak 10 putatively identified as dihydroxycinnamic acid-glucuronide **(**$R_t$, 9.14 min)

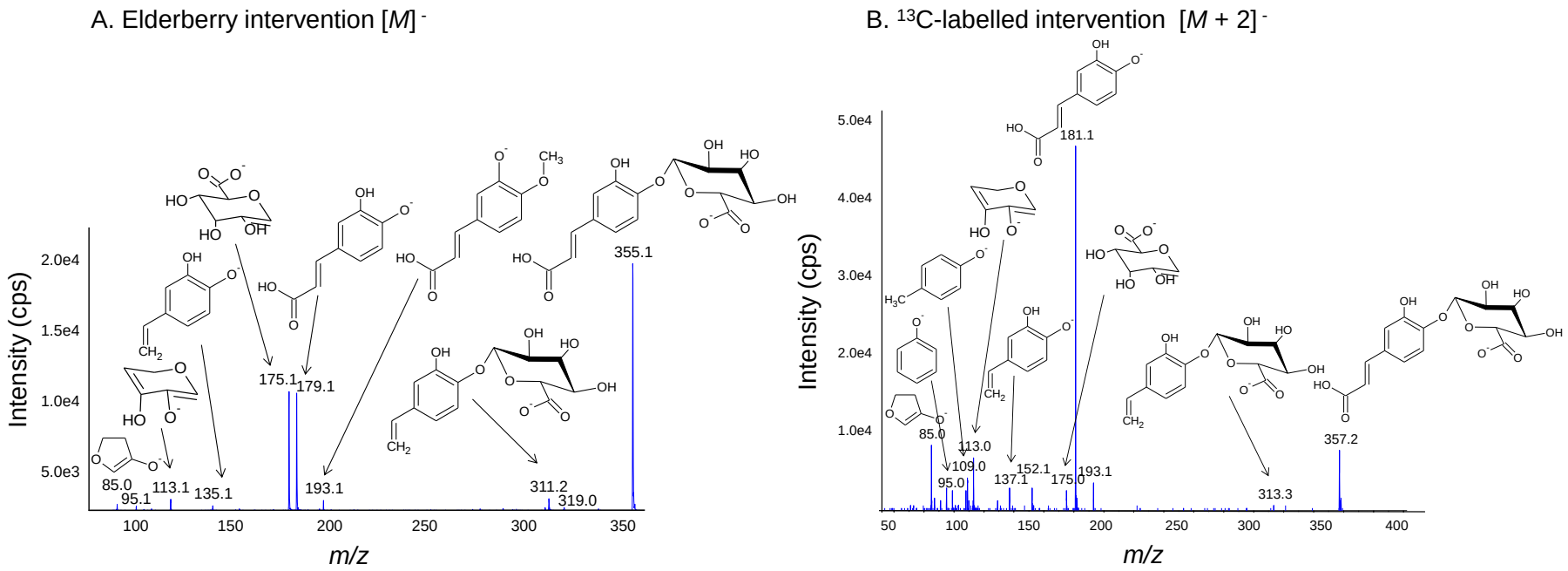


Data derived from pooled post bolus urine samples, where participants were fed (A) 500 mg elderberry anthocyanins and (B) 500 mg $^{13}C_5$-cyanidin-3-glucoside.

**Figure 5.10** Enhanced product ion ($MS^3$) scan of (A & B) peak 11 ($R_t$, 9.90 min) and (C) peak 12 ($R_t$, 12.37 min) putatively identified as hydroxymethoxycinnamic acid-glucuronides.

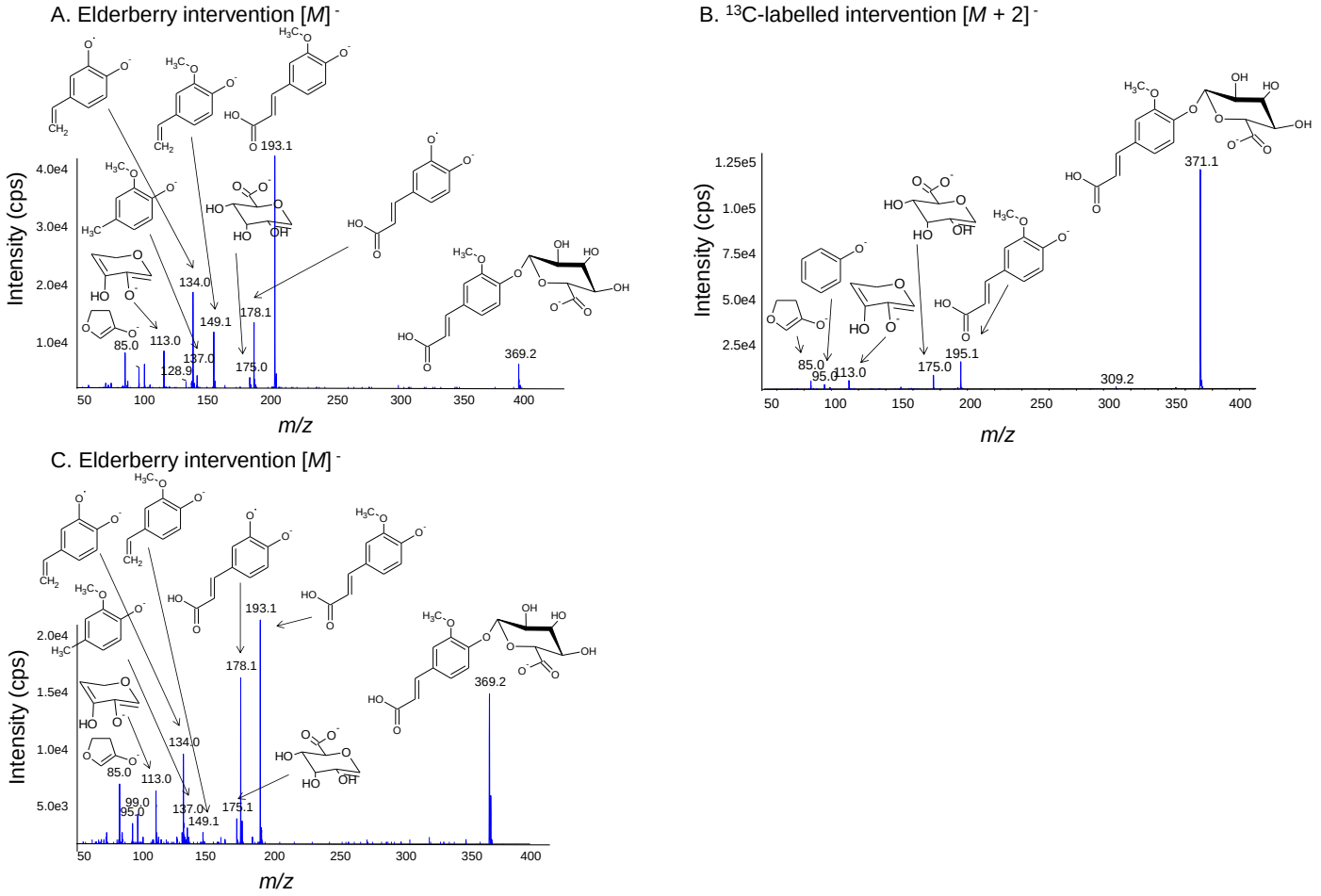


Data derived from pooled post bolus urine samples, where participants were fed (A & C) 500 mg elderberry anthocyanins or (B) 500 mg $^{13}C_5$-cyanidin-3-glucoside.

Peak 13 (*m/z* 273/193; $R_t$, 17.95 min; **Figure 5.11**) was putatively identified within urine samples post elderberry anthocyanin consumption, as a hydroxymethoxycinnamic acid-sulfate, most likely derived from ferulic acid. It was identified based on a $[M\text{-H}]^-$ at *m/z* 273 which produced an $MS^2$ ion at *m/z* 193, representing the loss of the sulfate group $[M\text{-H-80}]^-$. The $MS^3$ fragmentation patterns produced ions at *m/z* 229 represent the loss of a carboxylic group $[M\text{-H-44}]^-$, 178 representing the loss of a sulfate and methyl $CH_3$ group $[M\text{-H-80-15}]^-$, 149 representing the loss of a sulfate and carboxylic group $[M\text{-H-80-44}]^-$, and 134 representing the loss of a sulfate, carboxylic and methyl $CH_3$ group $[M\text{-H-80-44-15}]^-$. Peak 13 reached maximum levels of 20.9 ± 15.0 µM/mM creatinine 3 h post bolus when quantified relative to ferulic acid, representing a 11.3 µM/mM creatinine increase from baseline concentrations (Table 5.4).

**Figure 5.11** Enhanced product ion ($MS^3$) scan of peak 13 putatively identified as hydroxymethoxycinnamic acid-sulfate ($R_t$, 17.95 min).

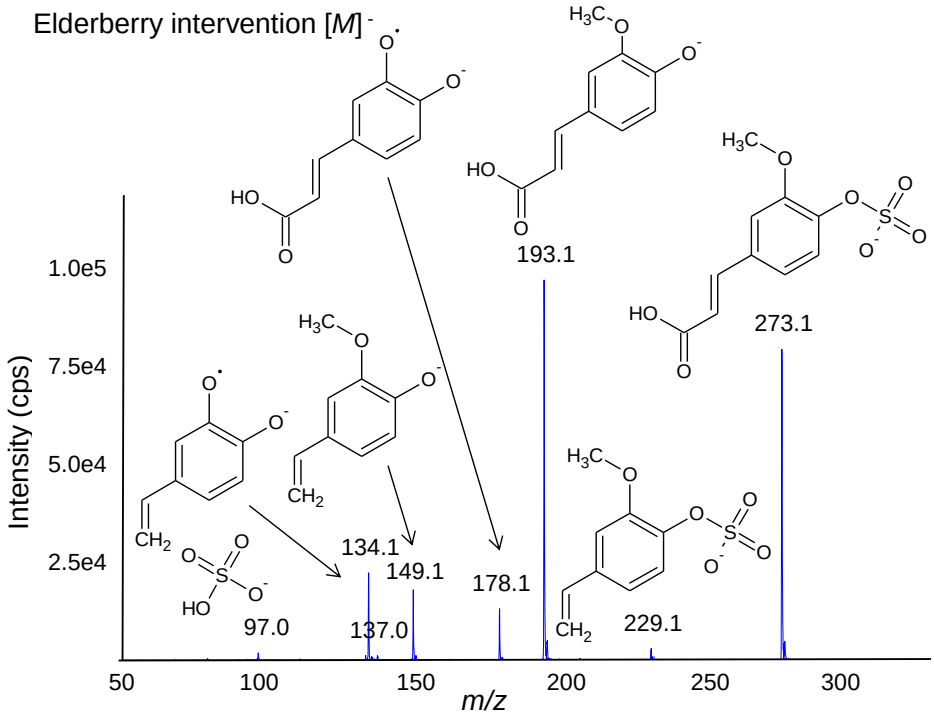


Data derived from pooled post bolus urine samples, where participants were fed 500 mg elderberry anthocyanins.

Peak 14 (*m/z* 303/223; Rt, 15.91 min; **Figure 5.12**) was putatively identified as a dimethoxyhydroxycinnamic acid-sulfate (Table 5.2). It was identified within elderberry derived urine samples based on a $[M\text{-H}]^-$ at *m/z* 303, which produced an $MS^2$ ion at *m/z* 223, representing the loss of the sulfate group $[M\text{-H-80}]^-$. The $MS^3$ fragmentation patterns produced ions at *m/z* 259 representing the loss of a carboxylic group $[M\text{-H-44}]^-$, 208

representing the loss of a carboxylic and methyl group [*M*-H-44-15]$^-$, 193 representing the loss of a sulfate and methoxy group [*M*-H-80-30]$^-$, 179 [*M*-H-80-30-16]$^-$, 164 representing the loss of a sulfate, carboxylic and methyl group [*M*-H-80-44-15]$^-$, 149 representing the loss of a sulfate, carboxylic and methoxy group [*M*-H-80-44-30]$^-$ and 135 representing the loss of a sulfate, carboxylic, methoxy and methyl group [*M*-H-80-44-30-15]$^-$. Peak 14 reached maximum concentrations of 1.1 ± 0.8 µM/mM creatinine 3 h post bolus when quantified relative to sinapic acid, representing an increase of 418 nM/mM creatinine from baseline concentrations (Table 5.4).

**Figure 5.12** Enhanced product ion ($MS^3$) scan of peak 14 putatively identified as dimethoxyhydroxycinnamic acid-sulfate ($R_t$, 15.91 min).

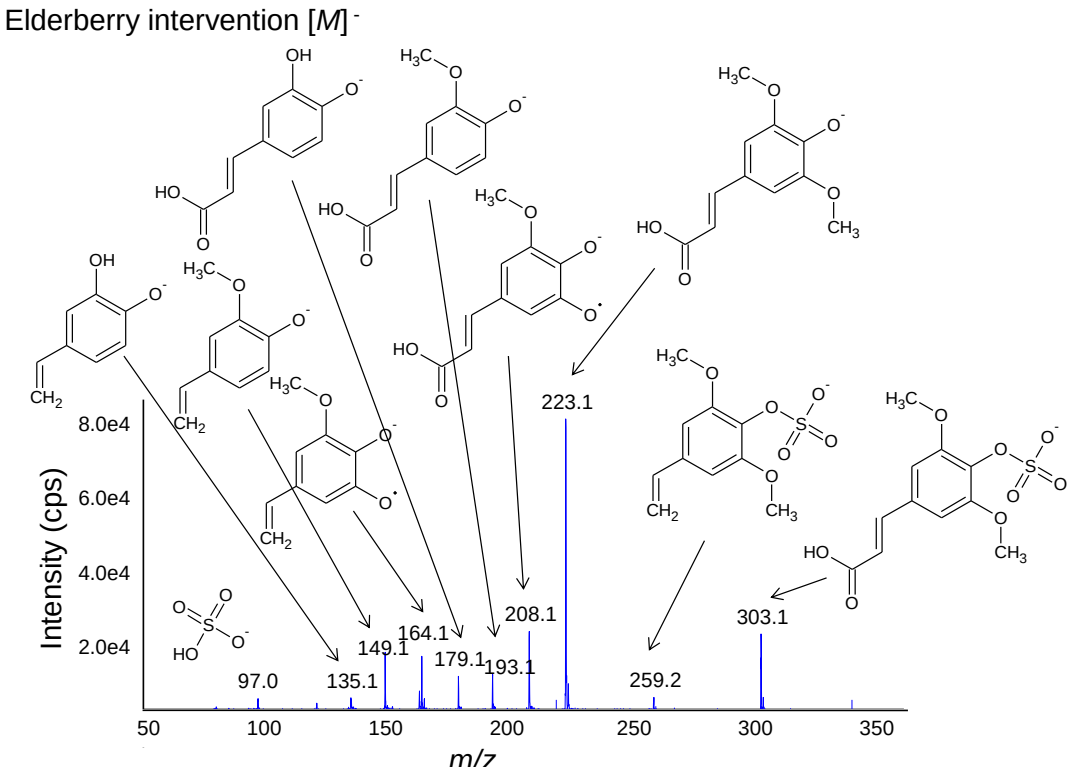


Data derived from pooled post bolus urine samples, where participants were fed 500 mg elderberry anthocyanins.

Peak 15 (*m/z* 399/223; $R_t$, 7.81 min) detected within urine samples following $^{13}$C-cyanidin-3-glucoside consumption, peak 16 (*m/z* 399/223; $R_t$, 10.62 min) detected within elderberry derived samples and peak 17 (*m/z* 399/223; $R_t$, 12.65 min) detected in urine samples from both clinical trials (Table 5.2), were putatively identified as dimethoxyhydroxycinnamic acid-glucuronides (**Figure 5.13**). The conjugates were detected based on a [*M*-H]$^-$ at *m/z* 399, which produced an $MS^2$ ion at *m/z* 223, representing the loss of the glucuronide group [*M*-H-176]$^{-.}$ The $MS^3$ fragmentation patterns produced multiple ions, including at *m/z* 355

representing the loss of a carboxylic group [*M*-H-44]$^-$, 208 representing the loss of a glucuronide ion and methyl group [*M*-H-176-15]$^-$, 175 (glucuronide ion), 164 representing the loss of a glucuronide ion, carboxylic and methyl group [*M*-H-176-44-15]$^-$, 113 (glucuronide ion) and 85 (glucuronide ion). This fragmentation pattern, +2 Da, was matched within the $^{13}$C-samples, indicating the metabolite was derived from the anthocyanin B-ring. The conjugates were quantified relative to sinapic acid; peak 15 was identified in the highest concentrations within the urine samples from the $^{13}$C-cyanidin-3-glucoside intervention, reaching maximum concentrations of 430 ± 610 nM, 5-6 h post bolus, whilst peak 17 was identified at highest concentrations within the elderberry intervention urine samples, reaching 1.0 ± 0.9 μM/mM creatinine, 3 h post bolus.

**Figure 5.13** Enhanced product ion ($MS^3$) scan of (A) peak 16 ($R_t$, 7.81 min), (B) peak 15 ($R_t$, 10.62 min) and (C & D) peak 17 ($R_t$, 12.65 min) putatively identified as dimethoxyhydroxycinnamic acid-glucuronides.

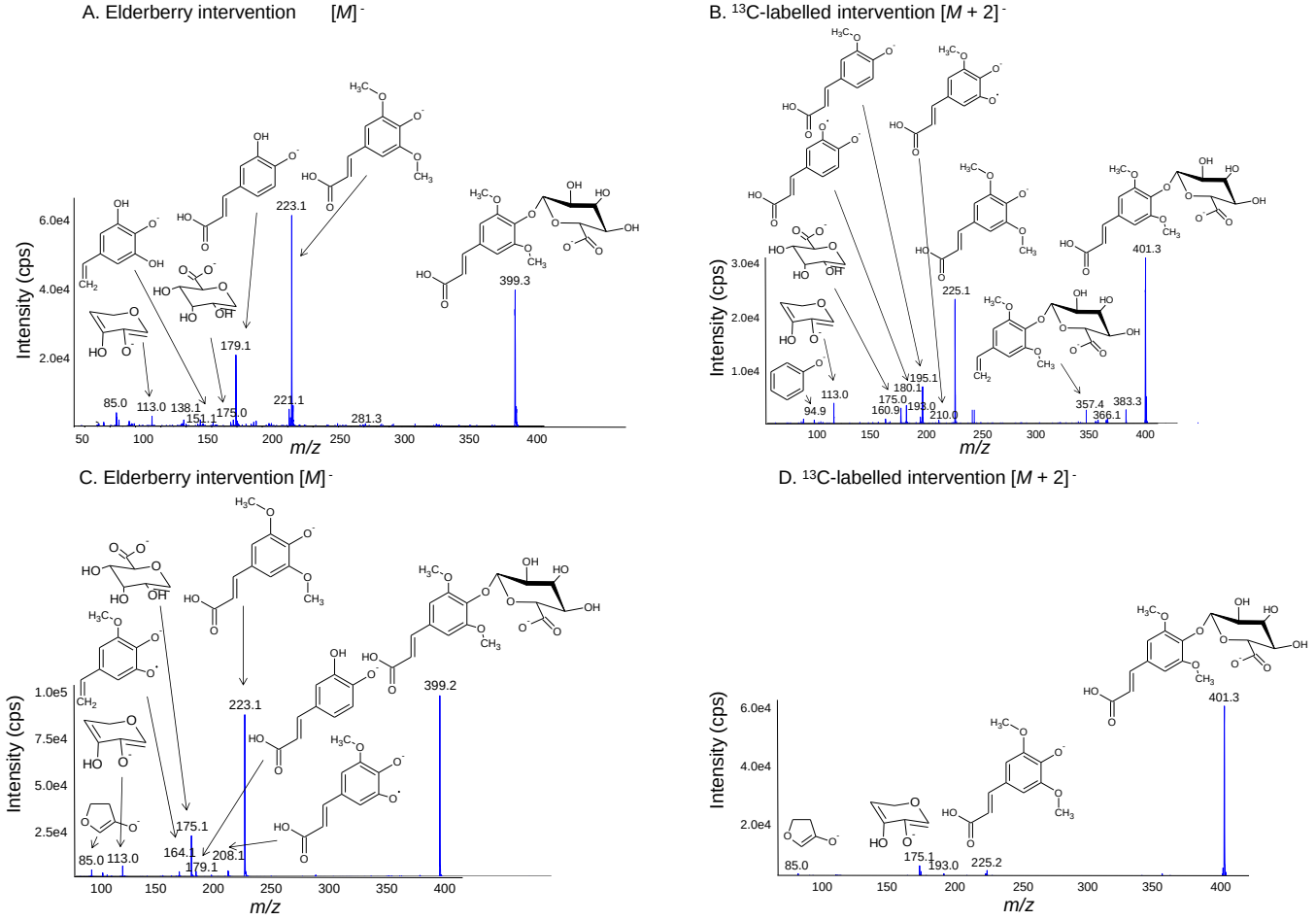


Data derived from pooled post bolus urine samples, where participants were fed (A & C) 500 mg elderberry anthocyanins or (B & D) 500 mg $^{13}C_5$-cyanidin-3-glucoside.

## 5.4. Discussion

Our recently conducted $^{13}C_5$-cyanidin-3-glucoside intervention identified 35 metabolites of cyanidin-3-glucoside, accounting for 37 ± 14% of the total $^{13}C$ recovered in the urine (Czank *et al.*, 2013). The present chapter aimed to further determine the metabolite fate of the remainder of the anthocyanin bolus, as the unidentified metabolites likely play a role in the perceived bioactivity of anthocyanins against cardiovascular disease. Until the major metabolites present following the consumption of anthocyanin-rich foods are realised, the mechanisms associated with their health effects will remain undefined.

In the present study, a total of 17 previously unidentified phase II (nine glucuronidated and eight sulfated) metabolites of anthocyanins (Table 5.2) were putatively identified within urine samples derived from intervention trials feeding either 500 mg $^{13}C$-labelled cyanidin-3-glucoside or 500 mg elderberry derived anthocyanins. *O*-Glucuronide conjugates are reportedly best observed under ESI conditions (Keski-Hynnilä *et al.*, 2002), and in negative ionisation mode produce ions that are 176 Da higher than those of non-conjugated metabolite. Therefore, the search for the presence of unknown *O*-glucuronide anthocyanin metabolites was initially conducted using non targeted scans including a neutral loss scan (Qu *et al.*, 2001) for the *m/z* loss of 176, scanned over ranges covering 200 to 400 Da and 400 to 1200 Da. Enhanced MS scans (EMS) over ranges of 100 Da from 100 to 1200 Da were also conducted. However, the scans were too general, and signal noise was too high to provide good MS spectral scans for the identification of the majority of the low concentrations of anthocyanin derived metabolites. Thus a more specific method was employed, where targeted MRM methods were developed for the detection of modelled conjugates (Table 5.2) and used to trigger an EPI scan using the IDA function, with enhanced resolution (ER) scans built into the method to improve peak sensitivity. In contrast to the non-targeted survey scans such as a neutral loss scan, a major limitation of MRM-IDA methods is their inability to detect unexpected metabolites, which are not included in the MRM transitions of predicted metabolites. Thus, the effectiveness of metabolite screening by MRM is dependent on a suitable selection of theoretical metabolite ions and their product ions (Huang *et al.*, 2010). The present study incorporated both methods in the analysis of urine samples, and putatively identified nine glucuronide conjugates.

Following fragmentation, glucuronide conjugates reportedly produce an abundant fragment $[M\text{-H-}176]^-$, corresponding to the neutral loss of glucuronic acid from the deprotonated molecule, a less abundant ion at *m/z* 175, and secondary fragment ions at *m/z* 113 (resulting

from the loss of $CO_2$ and water from the glucuronide ion) and *m/z* 85 (from the extrusion of CO from *m/z* 113) (**Figure 5.14**) (Farrell *et al.*, 2011; Keski-Hynnilä *et al.*, 2002; Levsen *et al.*, 2005; Qu *et al.*, 2001; Stalmach *et al.*, 2009a; Woodward *et al.*, 2011). The loss of 176 Da and the formation of *m/z* 175 and 113 fragments was observed for all nine glucuronides putatively identified in the present study and the formation of the less abundant *m/z* 85 fragment was observed for six of the glucuronide conjugates (Table 5.2).

**Figure 5.14** Example fragmentation of a glucuronyl moiety conjugated to protocatechuic acid in negative-ion MS/MS mode.

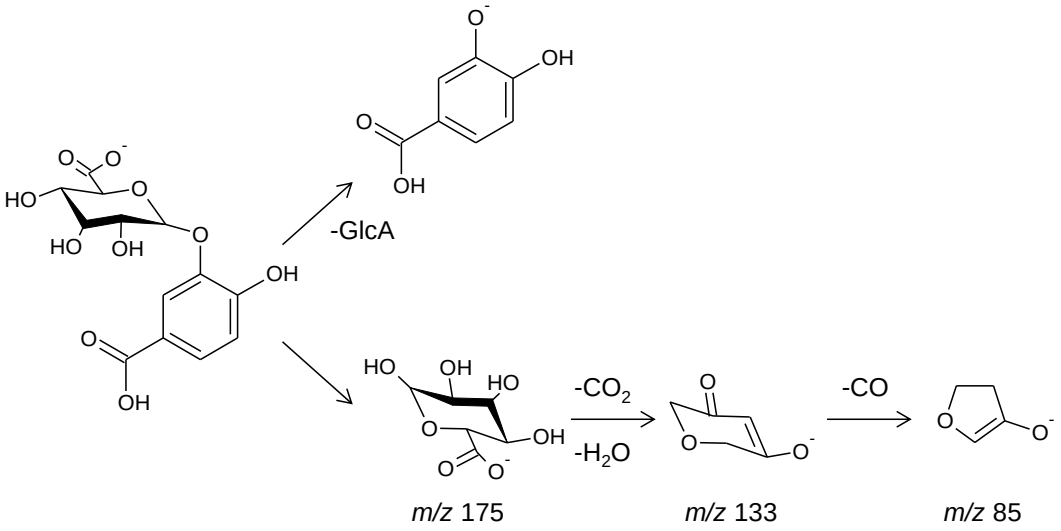


Adapted from (Levsen *et al.*, 2005).

Conjugations with sulfuric acid consist of the transfer of a sulfate group from 3'-phosphoadenosine-5'-phosphosulfate (PAPS) in the presence of SULTs forming a molecular ion $[M\text{-H+80}]^-$ (Wu *et al.*, 2011). Collision-induced fragmentation of the molecular of sulfate ester results in a loss of 80 Da, producing an abundant $[M\text{-H-SO}_3]^-$ fragment (Keski-Hynnilä *et al.*, 2002). Alternatively, the loss of 98 Da from $[M\text{-H-H}_2\text{SO}_4]^-$ has been reported to occur, which is represented by a *m/z* 97 Da (Levsen *et al.*, 2005). If the charge resides with the sulfate group, radical ions at *m/z* -80 from $SO_3^{-\bullet}$ and at *m/z* -97 from $HSO_4^-$ may form (**Figure 5.15**) (Boss *et al.*, 1999; Lin *et al.*, 2007). In the present study, all sulfated conjugates were identified by the presence of the $[M\text{-H+80}]^-$ parent ion and the $[M\text{-H-80}]^-$ daughter ion. Peaks 8, 13 and 14 also showed the presence of *m/z* 97, whilst peak 2 formed *m/z* 80.

**Figure 5.15** Possible fragmentation of sulfuric acid conjugated to protocatechuic acid in negative-ion MS/MS mode.

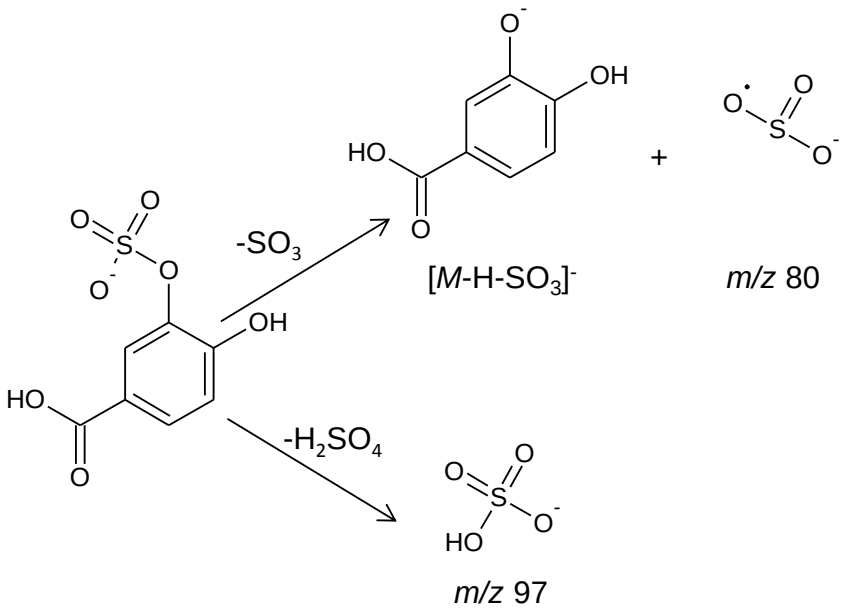


Adapted from (Boss *et al.*, 1999; Lin *et al.*, 2007).

In negative ion mode phenolic compounds containing a carboxylic group, such as carboxylic acids and cinnamic acids are known to produce a deprotonated $[M\text{-H}]^-$ molecule and a $[M\text{-H-}44]^-$ fragment ion via the loss of a $CO_2$ group from the carboxylic acid moiety (**Figure 5.16**) (Sun *et al.*, 2007). This is consistent with the $MS^3$ fragmentation of the 11 cinnamic acid conjugates identified in the present study, where the conjugates were identified via the loss of the conjugated sulfate $[\text{M-H-80}]^-$, glucuronide $[\text{M-H-176}]^-$, and carboxylic $[M\text{-H-44}]^-$ group. Where present, hydroxyl (OH) groups were cleaved, producing characteristic $[M\text{-H-}17]^-$ fragment ions (Figure 5.16) (Liu *et al.*, 2007; Sun *et al.*, 1997). In addition, methoxy groups typically show the loss of the methyl $CH_3$ group, providing a $[M\text{-H-}15]^-$ anion radical (Figure 5.16), which was observed for seven of the conjugates identified.

The position of the conjugation groups could not be ascertained in the present study. However, recent work into the regioselective sulfation and glucuronidation of phenolics indicates that for hydroxycinnamic acids which contain a catechol group, such as caffeic acid, the sulfate conjugation preferentially occurs at the 3-OH group, whilst glucuronidation occurs at both the 3-OH and 4-OH positions, depending on the UDPDG subgroup (Wong *et al.*, 2010; Wu *et al.*, 2011).

**Figure 5.16** Proposed MS fragmentation pathway for [*M*-H]$^-$ ions of 1) vanillic acid; 2) 3,4-dihydroxybenzaldehyde; 3) ferulic acid

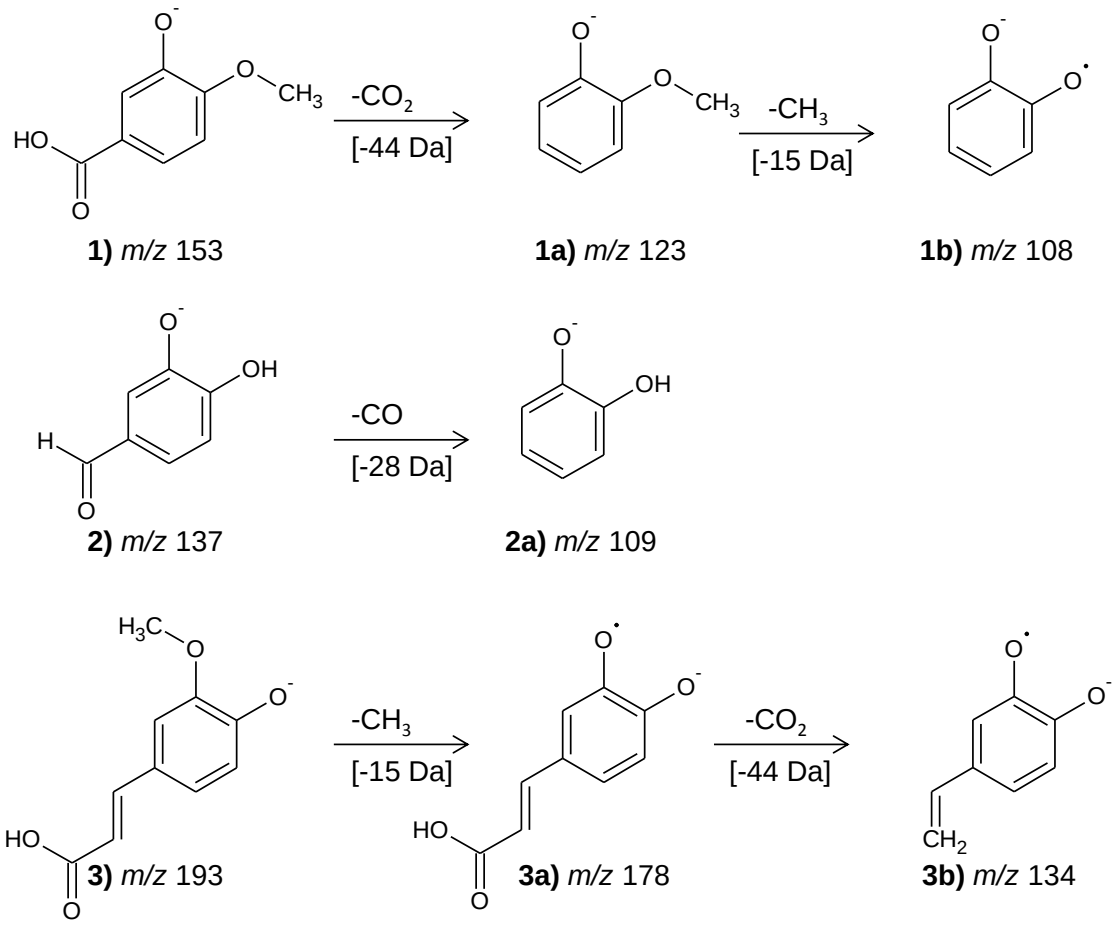


Due to the absence of commercially available standards, identified metabolites were quantified relative to their unconjugated standards, in order to get an approximation of the concentrations present. Seven previously unidentified metabolites were identified within urine samples derived from the study feeding 500 mg $^{13}C_5$-cyanidin-3-glucoside. A high inter-individual variation in metabolite concentration was observed between participants (Figure 5.5), with dihydroxycinnamic acid-glucuronide (peak 10) only detected in urine derived from three participants. The post ingestion $C_{max}$ values ranged from 304 ± 429 nM (116 ± 140 µg) for dimethoxyhydroxycinnamic acid-glucuronide (peak 17) to 1307 ± 826 nM (291 ± 245 µg) for methyl-dihydroxybenzoate-sulfate (peak 2; Table 5.3). These concentrations are similar to the maximum concentrations observed for the unconjugated phenolic metabolites identified previously (**Chapter 3**), which ranged from 24 ± 17 nM (6.3 ± 6.5 µg) for 3,4-dihydroxybenzaldehyde to 5.4 ± 13.9 µM (2416 ± 6288 µg) for hippuric acid (de Ferrars *et al.*, 2014). However, the time at peak excretion was generally later than observed for the unconjugated metabolites, with values ranging from 5-6 h to 24-48 h post bolus in the present study, compared to the values of 0-1 h to 24-48 h observed previously

(**Chapter 3**). This is likely due to colonic metabolism playing a significant role in their formation.

The recovery of the conjugated metabolites identified within urine from the $^{13}$C-labelled anthocyanin study ranged from 0.03 ± 0.02% for dihydroxyphenylacetic acid-sulfate (peak 3) to 0.14 ± 0.10% for methyl-dihydroxybenzoate-sulfate (peak 2). Together, the seven conjugated metabolites identified accounted for 0.45 ± 0.14% of the given bolus. However, this is an estimation due to the lack of commercially available standards which would enable accurate quantification.

Fifteen previously unidentified conjugated metabolites were detected within the urine samples derived from the intervention feeding 500 mg elderberry derived anthocyanins to postmenopausal females. Post ingestion $C_{max}$ values ranging from 38 ± 27 nM/mM creatinine for dihydroxycinnamic acid-glucuronide (peak 10) to 20.9 ± 15.0 µM/mM creatinine for hydroxymethoxycinnamic acid-sulfate (peak 13) were observed within the 2-3h postprandial samples following acute (week 0) anthocyanin consumption (Table 5.4). These concentrations are generally similar to the concentrations of un-conjugated metabolites identified previously following elderberry consumption, which ranged from 145 ± 86 to 7382 ± 5927 nM/mM creatinine in urine. Likewise, there was also no significant impact of 12wks continuous dosing on urinary metabolite excretion of the conjugated metabolites (Table 5.4).

A number of the metabolites identified within urine samples from the elderberry intervention trial were absent from the urine samples of the participant who consumed the isotopically labelled anthocyanins. There are several possibilities for this; firstly, the metabolites identified may not originate from anthocyanins, but from other phenolic compounds within the elderberry extract or the breakfast given. This is plausible, as phenolic compounds are ubiquitous within our diets (Dykes *et al.*, 2007; Schmitzer *et al.*, 2010). For example, green tea can provide over 100 mg phenolics /100mL (Kodama *et al.*, 2010) and onions can contain 69 mg phenolics/100 g of onion (Yang *et al.*, 2004). Secondly, the absence of the metabolites may results from inter-individual variation between participants, particularly because the studies were conducted using two very different population groups (postmenopausal women versus men aged 27.8 ± 8.1 y). Thirdly, the elderberry bolus contained a range of anthocyanin glycosides in addition to cyanidin-3-glucoside (including cyanidin-3-sambubioside, cyanidin-3-sambubioside-5-glucoside and cyanidin-3,5-diglucoside, **Chapter 4**), which were not present within the $^{13}$C-labelled bolus. The presence

of more complex sugars may result in the employment of differing metabolic pathways. For example, a study feeding blueberries to volunteers with an end ileostomy achieved higher recoveries for anthocyanins conjugated to arabinosides than to glucosides (Kahle *et al.*, 2006). Finally, the conjugated metabolites may be present but at concentrations below the detection limit within the $^{13}$C-labelled urine samples. Further work using synthesised standards would be required to confirm these metabolites.

There are certain limitations with this work. Although the metabolites in the present study were identified based on the presence of at least three, and in some cases up to eight transitions, due to the absence of commercially available standards the identity of the metabolites and the position of the conjugation could not be established with certainty. In addition, the quantification of metabolites was conducted relative to the closest commercially available unconjugated analytical standard. In order to increase the accuracy of this data, conjugated standards would need to be synthesised. An alternative approach often used within metabolomic studies is to use enzyme hydrolysis to confirm the identity of the conjugated compounds. This was attempted in the present study, where following, urine samples were evaporated with 10 x 1 mL 50 mM sodium phosphate buffer to remove the methanol/acid. Samples were subsequently hydrolysed overnight with 80 μL sulfatase (from *Aerobacter aerogenes,* Type VI, 2-5units/mg protein, 10-20units/ml) or 29.9 μL glucuronidase (from *Escherichia coli*, 20,000,000-60,000,000 units/g protein) and were re-extracted to remove the buffer from the sample matrix. However, analysis of the samples illustrated that the enzymes did not efficiently hydrolyse the conjugated forms of protocatechuic acid and vanillic acid. Future work should focus on the hydrolysis of non-acidified samples prior to SPE.

The present study analysed samples derived from two anthocyanin intervention studies. The elderberry intervention study fed 500 mg elderberry derived anthocyanins within 1 g elderberry extract. As discussed previously (**Chapter 4**), the use of an unlabelled anthocyanin bolus complicates the elucidation of the anthocyanin derived metabolites as phenolic compounds are ubiquitous within plants (Dykes *et al.*, 2007; Schmitzer *et al.*, 2010) and were present in the elderberry extract and breakfast (**Chapter 4**). Whilst only metabolites which increased from baseline values were described in the present chapter, it is not possible to categorically define the origin of phenolics which were identified within the elderberry intervention trial. A further limitation of the present study was that it focused on the analysis of urine samples. Whilst plasma provides a better representation for bioavailability, urine was selected for analysis because metabolites are generally more

concentrated within the urine, which enabled the collection of superior $MS^3$ data. In addition, the urine analysis should ultimately reflect plasma clearance for the majority of the metabolites. Future work should focus on quantifying the levels on conjugated metabolites in plasma.

## 5.5. Conclusion

Overall, the presence of glucuronide and sulfate conjugates of previously identified metabolites indicates a much higher relative anthocyanin bioavailability than previously reported. The mechanisms of action and relative importance of these metabolites on risk factors associated with cardiovascular disease should be the focus of future anthocyanin research.

# Chapter 6. The effects of select anthocyanin metabolites on sVCAM-1 and IL-6 expression in HUVECs

## 6.1. Introduction

A high consumption of anthocyanins has been associated with a reduced risk of cardiovascular disease (CVD) (Cassidy *et al.*, 2011; Mink *et al.*, 2007). Mechanistic studies exploring this bioactivity have suggested that this may in part be due to their anti-inflammatory activity. Inflammation is a complex and necessary defence mechanism whereby leukocytes migrate into damaged tissues, to destroy agents which may potentially cause further damage (García-Lafuente *et al.*, 2009), however chronic inflammation is detrimental to health and has been found to be involved in the development of many diseases, including atherosclerosis, diabetes and cancer (Dandona *et al.*, 2004; Epstein *et al.*, 1999; Libby *et al.*, 2002).

Inflammation drives the formation and progression of atherosclerotic plaques through initiating the expression of cell adhesion molecules and cytokines, which leads to the recruitment and aggregation of leukocytes (Libby *et al.*, 2002). Vascular cell adhesion molecule (VCAM-1) is transcriptionally induced in endothelial cells and plays a key role in leukocyte attachment and transmigration. Following pro-atherogenic stimulation and the recruitment of leukocytes by selectins (Blankenberg *et al.*, 2003), VCAM-1 participates in the firm adhesion of leukocytes to the endothelium, resulting in their immobilisation and enabling transmigration of the leukocytes towards the site of tissue damage or infection. VCAM-1 also interacts with integrin α4β1, which induces signals within endothelial cells, including the activation of NADPH oxidase to catalyse the production of reactive oxygen species (ROS), thus triggering change in endothelial cell morphology, and allowing leukocyte emigration (Matheny *et al.*, 2000). The adhesion of leukocytes triggers the secretion of inflammatory molecules, including cytokines such as interleukin-6 (IL-6), which futher perpetuates inflammation.

IL-6 is a pleiotropic cytokine, which is produced at sites of inflammation in order to stimulate an immune response to fight infection. IL-6 stimulates the production of inflammatory proteins by a diverse range of cells, including T-cells and smooth muscle cells (Schuett *et al.*, 2009). IL-6 activates specific intracellular signal transduction pathways,

through binding to its receptor (IL-6R), which leads to the recruitment and complexation of two gp130 molecules, and perpetuates downstream signalling pathways such as janus kinase (JAK) and signal transducer and activator of transcription (STAT), which ultimately lead to the transcription of inflammatory genes (Schuett *et al.*, 2009).

Tumor necrosis factor alpha (TNF-α) and CD40L are potent inducers of both VCAM-1 and IL-6. TNF-α is a member of a group of cytokines involved in regulating immune cells during systemic inflammation. It is predominately produced by activated macrophages and in target cells can stimulate the activation of the mitogen activated protein kinases (MAPK) and nuclear factor-κB (NF-κB) pathways (Baud *et al.*, 2001). CD40 is a member of the TNF receptor family, and is constitutively expressed on many cell types, including endothelial cells (Miller *et al.*, 1998) and interacts with CD40L, an activation induced transmembrane protein which is expressed on activated T-cells. The ligation between CD40L and CD40 initiates intracellular signalling, which eventually leads to the transcription of pro-inflammatory and pro-atherogenic genes, including IL-6 and VCAM-1 (Pamukcu *et al.*, 2011).

Anthocyanins have been reported to modulate the expression of VCAM-1 and IL-6 in humans, mice and endothelial cells (Chao *et al.*, 2013; Kim *et al.*, 2006; Miyazaki *et al.*, 2008; Nizamutdinova *et al.*, 2009; Speciale *et al.*, 2010; Xia *et al.*, 2009). Humans fed 320 mg/day anthocyanins for 24 weeks (Zhu *et al.*, 2013) and mice fed purple sweet potato for four weeks (Miyazaki *et al.*, 2008) had significantly lower plasma levels of soluble VCAM-1 (sVCAM-1). Similarly *in vitro,* pre-treatment of TNF-α challenged endothelial cells with black soybean anthocyanins (Chao *et al.*, 2013; Kim *et al.*, 2006; Nizamutdinova *et al.*, 2009) and grape seed extract (Sen *et al.*, 2001) has been shown to reduce VCAM-1 expression. Furthermore, 1, 10 and 100 μM concentrations of cyanidin-3-glucoside and peonidin-3-glucoside resulted in a dose-dependent decrease in IL-6 secretion in endothelial cells following CD40L stimulation (Xia *et al.*, 2009).

Due to the low bioavailability of parent anthocyanins (Czank *et al.*, 2013; de Ferrars *et al.*, 2013; Milbury *et al.*, 2002), their protective effects may be due to anti-inflammatory activities of their degradation products and metabolites, rather than the direct effect of the parent anthocyanins. However, until recently, little was known concerning the bioavailability of anthocyanin metabolites, therefore their bioactivity remained relativity unexplored. The B-ring degradation product of cyanidin-3-glucoside, protocatechuic acid has previously been demonstrated to reduce VCAM-1 protein and mRNA production in TNF-α-induced mouse

aortic endothelial cells at concentrations of 20 µM and 40 µM (Wang *et al.*, 2010). In addition, mice fed protocatechuic acid for 20 weeks had significantly reduced plasma levels of sVCAM-1 (Wang *et al.*, 2010) and vanillic acid has been shown to reduce plasma IL-6 levels in mice (Kim *et al.*, 2010). Less is known concerning the inflammatory bioactivity of the phenylacetic metabolites in human endothelial cells, although they were present at high concentrations within urine following anthocyanin consumption (de Ferrars *et al.*, 2013).

The present chapter investigates the anti-inflammatory activity of six previously established anthocyanin metabolites (Czank *et al.*, 2013; de Ferrars *et al.*, 2013), namely protocatechuic acid, homoprotocatechuic acid and 3,4-dihydroxybenzalehyde and their respective methylated counterparts, vanillic acid, homovanillic acid, and vanillin (The aim of the present chapter was to investigate the anti-inflammatory activity of protocatechuic acid, vanillic acid, homoprotocatechuic acid, homovanillic acid, 3,4-dihydroxybenzaldehyde and vanillin at a range of physiologically relevant concentrations (0.01µM to 10 µM) on the production of VCAM-1 and IL-6 in human umbilical vein endothelial cells (HUVECs) following stimulation with either CD40L or TNF-α.

**Figure 6.1**). Following 500 mg anthocyanin consumption, these compounds have been identified in serum at maximum concentrations of 146 ± 74 nM for protocatechuic acid and 1,845 ± 838 nM for vanillic acid, and in urine at maximum concentrations of 1,945 ± 1,302 nM for homoprotocatechuic acid, 7,382 ± 5,927 nM for homovanillic acid and 24 ± 7 nM for 3,4-dihydroxybenzaldehyde (de Ferrars *et al.*, 2013; de Ferrars *et al.*, 2014). These six metabolites were selected as the bioactivity of the more prevalent glucuronide and sulfate metabolites is currently been undertaken within the Department of Nutrition (unpublished data). In addition, these six metabolites were selected to provide an insight into structural activity relationships, as the effect of a catechol group versus methylated catechol group and of a carboxylic versus phenylacetic versus phenylaldehyde functional group on metabolite bioactivity could be explored.

The aim of the present chapter was to investigate the anti-inflammatory activity of protocatechuic acid, vanillic acid, homoprotocatechuic acid, homovanillic acid, 3,4-dihydroxybenzaldehyde and vanillin at a range of physiologically relevant concentrations (0.01μM to 10 μM) on the production of VCAM-1 and IL-6 in human umbilical vein endothelial cells (HUVECs) following stimulation with either CD40L or TNF-α.

**Figure 6.1** Structures of anthocyanin metabolites screened for their effect on CD40L and TNF-α stimulated VCAM-1 and IL-6 expression in HUVECs.

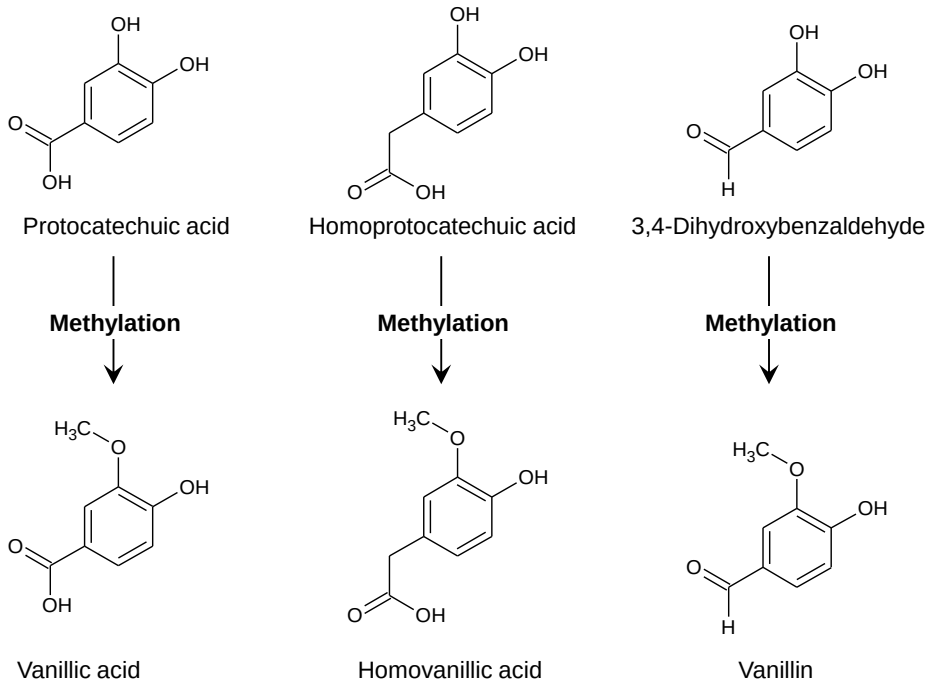


## 6.2. Materials and methods

### 6.2.1. Materials and Reagents

Protocatechuic acid, homoprotocatechuic acid, vanillic acid, homovanillic acid, 3,4-dihydroxybenzaldehyde and vanillin were purchased from Sigma-Aldrich (Dorset, UK). Standards were prepared at concentrations of 200 mM in 100% dimethylsulphoxide (DMSO, molecular biology grade) from Sigma-Aldrich (Dorset, UK). Cell proliferation reagent WST-1 [(4-[3-(4-Iodophenyl)-2-(4-nitrophenyl)-2H-5-tetrazolio]-1,3-benzene disulphonate)] was obtained from Roche Applied Science (Burgess Hill, UK). DuoSet® human VCAM-1 ELISA kit and DuoSet® human IL-6 ELISA kit were purchased from R&D systems (Abingdon, UK). Lyphilized recombinant human TNF-α (10 μg) was purchased from Invitrogen (Paisley, UK). Fibronectin was purchased from Sigma-Aldrich (Dorset, UK), foetal calf serum (FCS; heat-inactivated) from was purchased from Biosera (Ringmer, UK), RPMI1640 media, penicillin/streptomycin, L-Glutamine and fetal bovine serum were purchased from PAA (Pasching, Austria), penicillin/streptomycin was purchased from Promocell (Heidelberg, Germany) and 1 mg/mL human monoclonal antibody blocking CD40 was purchased from Enzo Life Sciences (Exeter, UK). Cryo-preserved, early passage, human umbilical vein endothelial cells (HUVECs) from pooled donors, large vessel endothelial cell growth medium, trypsin, EDTA and gentamicin and amphotericin B supplements were

purchased from Caltag Medsystems (Buckingham, UK). Cryo-preserved D1.1 Jurkat cells were generously provided by Dr. Maria O'Connell, Senior Lecturer, Department of Pharmacy, University of East Anglia (Norwich, UK). TRIzol® reagent was purchased from Invitrogen (Paisley, UK), chloroform and propan-2-ol were purchased from Fisher Scientific (Loughborough, UK) and 200 proof ethanol was purchased from Sigma-Aldrich (Dorset, UK). Nunclon™ Δ 75cm$^2$ flasks and Nunclon$^{TM}$ Δ 24 well plates were purchased from PAA (Somerset, UK)], 96-well microplates were purchased from BD Falcon® (Oxford, UK).

### 6.2.2. HUVEC cell culture.

Cryo-preserved HUVECs from pooled donors were cultured in Nunclon™ Δ 75cm$^2$ flasks coated with fibronectin (0.26 μg/cm$^2$), and grown in large vessel endothelial cell growth medium (proprietary basal medium formulation supplemented with growth factor and antibiotic (gentamicin & amphotericin B) supplements, to a final concentration of 2% v/v foetal bovine serum) at 37 °C with 5% $CO_2$. HUVECs were sub-cultured to 90-95% confluence before they were split using 0.025% trypsin and 0.01% EDTA. All experiments were conducted between passages two to four.

### 6.2.3. D1.1 Jurkat cell culture

D1.1 cells were cultured in Nunclon™ Δ 75 cm$^2$ flasks in RPMI1640 media supplemented with 10% foetal bovine serum, 2 mM L-Glutamine (200 mM) and 1% penicillin/streptomycin (100 x concentrate). Cell density was calculated using trypan blue (a diazo dye which colours dead cells) and the cell density was maintained between 6 x 10$^5$ and 1 x 10$^6$ cells/mL.

### 6.2.4. Cytotoxicity assay

Cell viability was assessed using cell proliferation reagent WST-1; the assay was conducted using 96-well microplates coated with fibronectin (0.41 μg/cm$^2$), seeded with HUVECs at a density of ~20,000 cells/well. Cells were subsequently grown to confluence (~24-48 h at 37°C and 5% $CO_2$). The culture medium was then aspirated and 100 μL of the treatment compounds prepared in supplemented large vessel endothelial cell growth medium at concentrations of 0.1, 1, 10, and 100 μM. Controls consisted of wells containing media and 0.05% DMSO, with no cells (blank), media and cells (control), 0.05% DMSO in media and cells (vehicle control) and PBS and cells (negative control). Three replicates were carried out for each control and treatment solution. The microplates were incubated for 24 h at 37 °C and 5% $CO_2$, after which 10 μL WST-1 reagent was added to each well and the plates were

incubated for a further 2 h. Absorbance was then measured at 440 nm with a reference wavelength measured at 650 nm using a microplate reader [Fluostar Omega, BMG Labtech (Aylesbury, UK)].

### 6.2.5. CD40L induced IL-6 and sVCAM1 expression in HUVECS

HUVECs were cultured as described above and split into 24 well plates coated with fibronectin (0.25 μg/cm$^2$) at a seeding density of ~60,000 cells/well. The cells were grown to 90-95% confluence (~24-48 h at 37°C and 5% $CO_2$), the culture medium was aspirated and the HUVECs were co-incubated with CD40L expressing Jurkat D1.1 cells (1 x $10^6$ cells/well) and the treatments (600 μL/well) for 24 h. All treatment compounds were prepared in large vessel endothelial cells growth media at final concentrations of 0.01, 0.1, 1 and 10 μM. Each experiment contained controls, which consisted of un-stimulated cells (media only), D1.1 cells but no treatment compound (positive control) and D1.1 cells preincubated for 1 h with 15 μg/mL anti-CD40L antibody (negative control). The plates were incubated for 24 h at 37 °C and 5% $CO_2$, after which the media was collected and stored in eppendorf tubes and the plates were washed with warm PBS. The media and plates were then stored at -80 °C until analysis.

### 6.2.6. TNF-α induced IL-6 and sVCAM-1 expression in HUVECS

HUVECs were cultured as described above and split into 24 well plates coated with fibronectin (0.25 μg/cm$^2$) at a seeding density of ~60,000 cells/well. The cells were grown to 90-95% (~24-48 h at 37 °C and 5% $CO_2$), the culture medium was aspirated and the HUVECs were co-incubated for 24 h in 600 μL/well of large vessel endothelial cell growth media supplemented with TNF-α (10 ng/mL) and the treatment compounds at concentrations of 0.01, 0.1, 1 and 10 μM. Controls consisted of un-stimulated cells (media only) and 10 ng/mL TNF-α without treatment compounds (positive control). The plates were incubated for 24 h at 37 °C and 5% $CO_2$, after which the media was collected and stored in eppendorf tubes. The media and plates were then stored at -80 °C until analysis.

### 6.2.7. sVCAM1 ELISA

ELISA for human sVCAM-1 was performed using a DuoSet® kit purchased from R&D systems (Abingdon, UK) according to the manufacturer's instructions. The sensitivity of the ELISA was 16.63 pg/mL. Prior to ELISA, samples were centrifuged for 10 min at 4 °C and 13,000 rpm to pellet the D1.1 cells or any cell debris, and the media from the TNF-α stimulated cells was diluted (2/1) in reagent diluent. The kit used a mouse anti-human VCAM-1 capture antibody (2 μg/mL in 1% PBS) and biotinylated sheep anti-human

VCAM-1 detection antibody (200 ng/mL in reagent diluent). sVCAM-1 was quantified via colorimetric assay, measuring at 450 nm and 570 nm (as reference wavelength) using a BMG microplate reader [Fluostar Omega, BMG Labtech (Aylesbury, UK)]

### 6.2.8. IL-6 ELISA

ELISA for human IL-6 was performed using a DuoSet® kit purchased from R&D systems (Abingdon, UK) according to the manufacturer's instructions. The sensitivity of the ELISA was 9.38 pg/mL. Prior to ELISA, samples were centrifuged for 10 min at 4 °C and 13,000 rpm to pellet the D1.1 cells or any cell debris, and the media from the TNF-α stimulated cells was diluted (2/1) in reagent diluent. The kit used a mouse anti-human IL-6 capture antibody (2 µg/mL in reagent diluent) and biotinylated goat anti-human IL-6 detection antibody (50 ng/mL in reagent diluent). IL-6 was quantified via colorimetric assay, measuring at 450 nm and 570 nm (as reference wavelength) using a BMG microplate reader [Fluostar Omega, BMG Labtech (Aylesbury, UK)]

### 6.2.9. RNA extraction

HUVECs within the stored 24 well plates were homogenised with 500 µL/well TRIzol® and the RNA was extracted using 100 µL/sample chloroform. The samples were vortexed and centrifuged (12,000 × *g* for 10 min at 4°C) and 100 µL of the clear aqueous layer was collected and vortexed with 250 µL propan-2-ol. The samples were centrifuged again (12,000 × *g* for 10 min at 4°C) and the supernatant was discarded leaving the RNA pellet. The pellets were washed with 500 µL of 75% ethanol, vortexed and centrifuged (7,500 × *g* for 5 min at 4°C). The supernatant was discarded and the pellets were air-dried before being re-suspended in 20 µL DEPC-treated nuclease-free water, vortexed and heated it at 57.5°C for 10 min to aid solubility. The quantification of RNA was performed using a NanoDrop®2000 spectrophotometer.

### 6.2.10. Reverse transcription

Reverse transcription was carried out using 1 µg of RNA. Initially, any genomic DNA contamination was eliminated by incubating the RNA solution with 1 µL/reaction DNase reaction buffer, 1 µL/reaction DNase-1 and 0.25 µL/reaction RiboLock RNase inhibitor at 37°C for 30 min. DNase-1 was then inactivated through the addition of 1 µL/reaction of 50 mM EDTA along with 1µL/reaction oligo (dT) primers and 1 µL/reaction dNTP PCR mix, followed by incubation at 65°C for 10 min. The oligo (dT) primers were subsequently annealed through the addition of 4 µL/reaction first strand buffer, 1 µL/reaction RiboLock RNase inhibitor, 1 µL/reaction of 100 mM dithiothreitol (DTT) and incubated for 2 min at

42°C. Finally, the reverse transcription of mRNA was conducted by incubating the reaction mix with 1 µL/reaction SuperScript® II at 42°C for 50 min, followed by 70°C for 15 min to inactivate the SuperScript® II. The resulting complementary DNA (cDNA) was then diluted to a concentration of 5 ng/µL in DEPC-treated nuclease-free water and stored at 4°C until required for RT-qPCR

### 6.2.11. VCAM-1 and IL-6 RT-qPCR

The RT-qPCR was conducted using 5 µL/reaction (25 ng) of cDNA mixed with 1 µL/reaction VCAM-1 primer, 8.33 µL/reaction real time PCR master mix with SYBR® green and made up to 20 µL/reaction with 5.67 µL DEPC-treated nuclease-free water. The RT-qPCR was performed using Applied Biosystems 7500 Real-Time PCR System (Life Technologies, Paisley, UK) where the enzymes were activated for 10 min at 95°C followed by 50 cycles of denaturation at 95°C for 15 seconds and the data collection took place at 60 °C for 1 min. The target genes (VCAM-1 or IL-6) were normalised against two geNorm housekeeping reference genes, PRDM4 and UBE2D2. The expression of target gene was quantified by ΔCt, where $\Delta Ct = Ct_{\text{target gene}} / Ct_{\text{geomean of references gene}}$. The forward and reverse primer sequences for VCAM-1 were CAG GCT AAG TTA CAT ATT GAT GAC AT and GAG GAA GGG CTG ACC AAG AC respectively and the forward and reverse primer sequences for IL-6 were GCA GAA AAC AAC CTG AAC CTT and ACC TCA AAC TCC AAA AGA CCA respectively. A melt curve was performed following RT-qPCR to confirm that the pure product was amplified.

### 6.2.12. Statistical analysis.

For WST-1 cytotoxicity and ELISA data, analysis of variance (ANOVA) with Tukey post-hoc test was performed on three biological replicates (with each biological replicate representing the mean of two technical replicates) using SPSS for Windows statistical software package (version 18.0; IBM, New York, USA) and significance was determined at the 5% level. The statistical analysis was conducted on raw data and mean values were graphed as percentage of the positive control with error bars representing % coefficient of variation (%CV).

For RT-qPCR data, analysis of variance (ANOVA) with Tukey post-hoc test was performed on three biological replicates using SPSS and significance was determined at the 5% level. Statistical analyses was conducted using normalised (for PRDM4 and UBE2D2 housekeeping genes) mRNA levels, represented as fold change relative to un-stimulated (basal) mRNA levels, with error bars representing SD.

## 6.3. Results

### 6.3.1. Cytotoxicity assay

Six treatment compounds (protocatechuic acid, homoprotocatechuic acid, vanillic acid, homovanillic acid, 3,4-dihydroxybenzaldehyde and vanillin) were screened for cytotoxicity at four concentrations (0.1, 1, 10, and 100 μM) (**Figure 6.2**). No significant effects ($p > 0.01$) on endothelial cell viability were observed following 24 h incubation of HUVECs with the vehicle control (0.05% DMSO) or any of the treatment compounds.

**Figure 6.2** Assessment of cytotoxicity of six treatment compounds using WST-1 following 24 h incubation with cultured HUVECs.

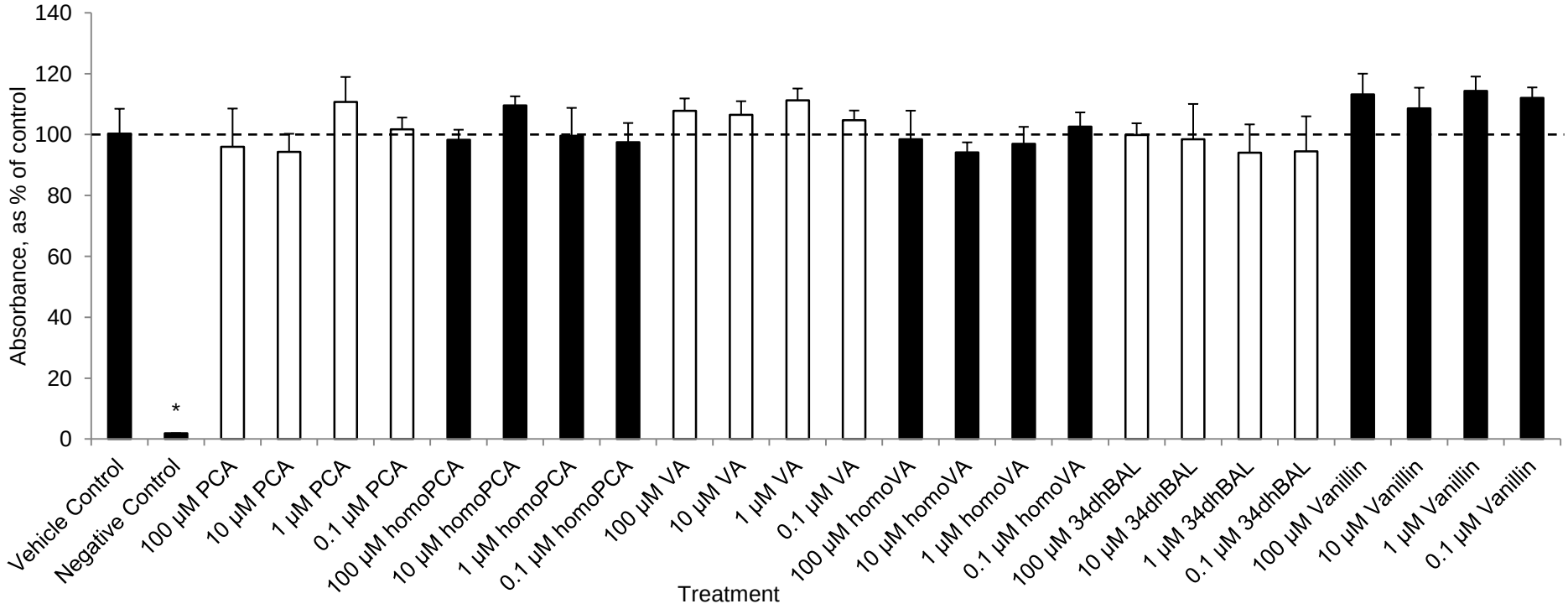


Cell viability (mean absorbance as percentage of mean control absorbance) for control (supplemented culture medium), vehicle control (culture medium with 0.05% DMSO), negative control (PBS) and 100, 10, 1 and 0.1 µM of treatment compounds. Data shown as mean ± CV, n=3. *Significance $p \leq 0.01$ (ANOVA with Tukey post-hoc) relative to control incubations. PCA, protocatechuic acid; VA, vanillic acid; 34dhBAL, 3,4-dihydroxybenzaldehyde.

### 6.3.2. CD40L induced sVCAM-1 protein production

Incubation of HUVECs with CD40L resulted in a 14.7 fold increase in the production of sVCAM-1 compared to un-stimulated HUVECs ($p<0.01$). This was attenuated to basal levels when HUVECs were treated with D1.1 cells, which had been pre-incubated with 15 µg/mL anti-CD40L antibody (**Figure 6.3**).

**Figure 6.3** sVCAM-1 protein production in CD40L stimulated cells.

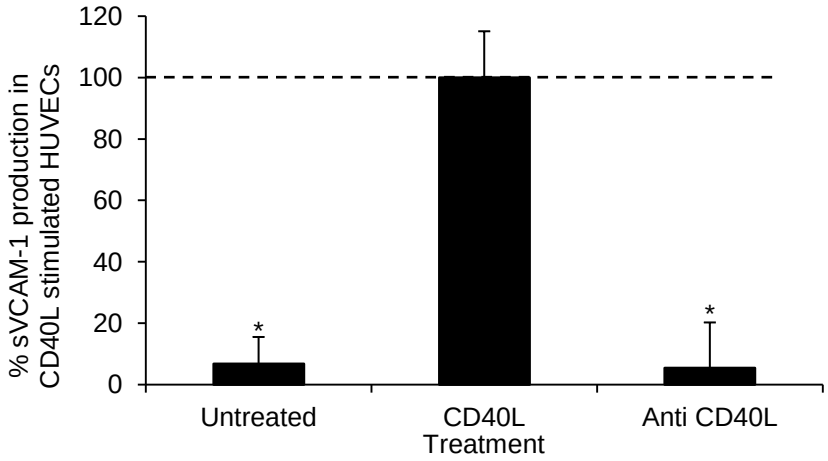


HUVECs were co-incubated with CD40L expressing Jurkat D1.1 cells (1 x $10^6$ cells/well) for 24 h and supernatants were used to quantify sVCAM-1 protein production via ELISA. All data is expressed as % mean ± %CV (n=3) relative to CD40L control. *Significance $p \leq 0.01$ (ANOVA with Tukey post-hoc) relative to CD40L control.

The effect of six anthocyanin metabolites on sVCAM-1 production in CD40L stimulated HUVECs was examined by incubating CD40L with and without treatment compounds at 0.01, 0.1, 1 and 10 µM for 24 h. Following the co-incubation of HUVECs with CD40L expressing Jurkat D1.1 cells and the treatment compounds, all six compounds tested demonstrated a significant ($p \leq 0.01$) reduction in sVCAM-1 production (**Figure 6.4**). The largest reduction in sVCAM-1 production was observed for protocatechuic acid at 0.01 µM (86.9 ± 20.8%; Figure 6.4A) followed by vanillin (82.5 ± 34.8%; Figure 6.4F) and homoprotocatechuic acid (81.8 ± 31.6%; Figure 6.4B) at 10 µM. Vanillic acid (Figure 6.4D) and homovanillic acid (Figure 6.4E) only showed a significant reduction in sVCAM-1 production at the highest concentration tested (10 µM), whilst protocatechuic acid displayed a negative dose response and homoprotocatechuic acid, 3,4-dihydroxybenzaldehyde (Figure 6.4C) and vanillin also showed a significant reduction at the lower concentrations tested.

**Figure 6.4** sVCAM-1 protein production following treatment with anthocyanin metabolites in CD40L stimulated cells.

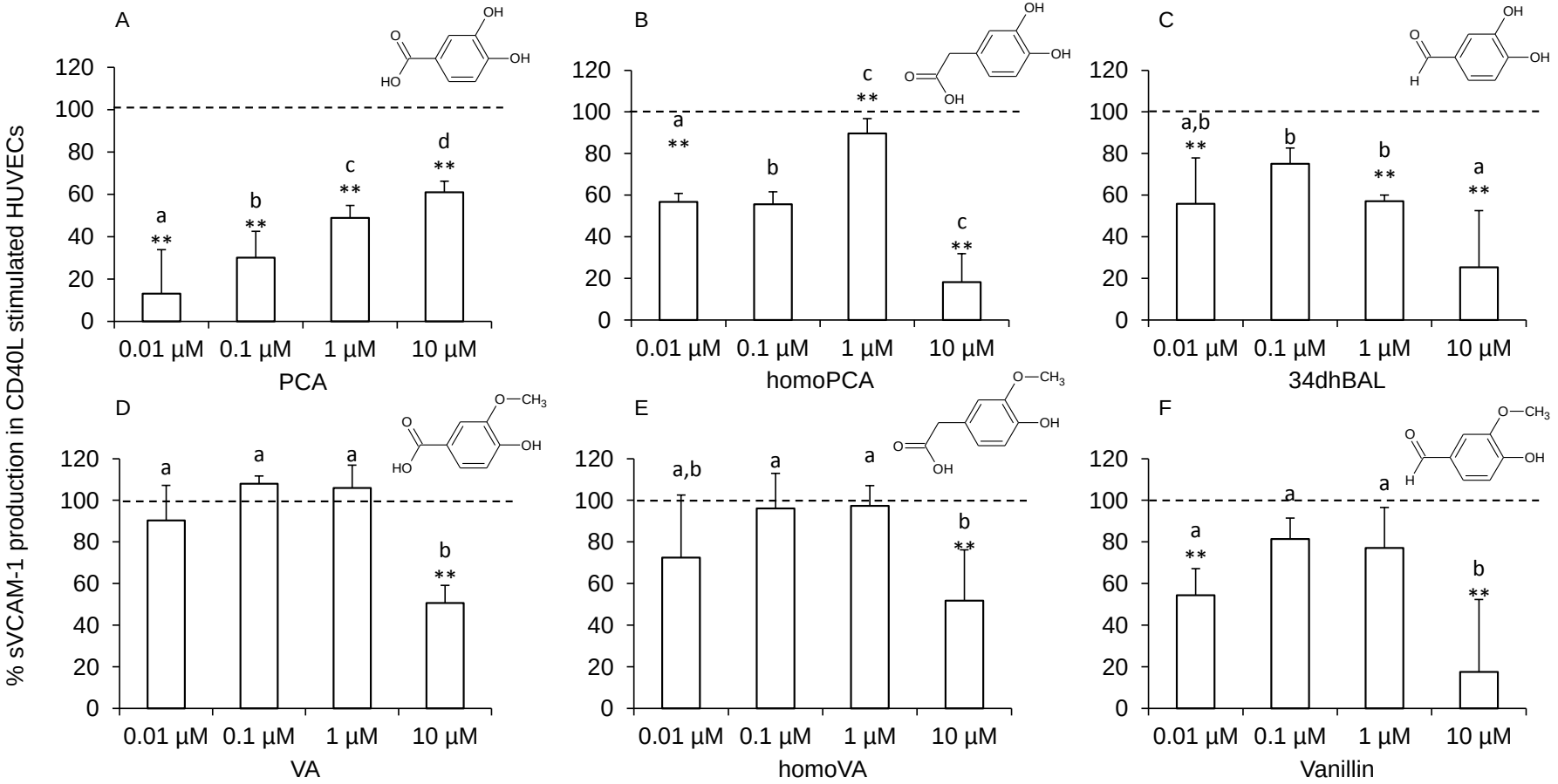


HUVECs were co-incubated with CD40L expressing Jurkat D1.1 cells (1 x $10^6$ cells/well) and the treatment compounds for 24 h and supernatants were used to quantify sVCAM-1 protein production via ELISA. All data is expressed as % mean ± %CV (n=3) relative to CD40L control. Significance: **p≤0.01 (ANOVA with Tukey post-hoc) relative to CD40L control. [a,b,c,d]Bars for treatments with different superscript letters are significantly different ($p < 0.05$). 34dhBAL, 3,4-dihydroxybenzaldehyde; PCA, protocatechuic acid; VA, vanillic acid.

### 6.3.3. CD40L induced IL-6 protein production

Incubation of HUVECs with CD40L resulted in a 1.9 fold increase in the production of IL-6 compared to un-stimulated HUVECs ($p<0.01$). This increase was attenuated to basal levels when HUVECs were treated with D1.1 cells, which had been pre-incubated with 15 µg/mL anti-CD40L antibody (**Figure 6.5**).

**Figure 6.5** IL-6 protein production in CD40L stimulated cells.

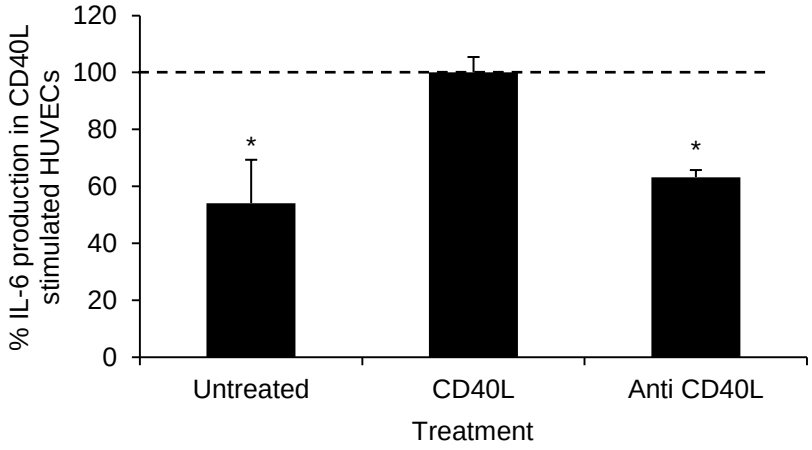


HUVECs were co-incubated with CD40L expressing Jurkat D1.1 cells ($1 \times 10^6$ cells/well) for 24 h and supernatants were used to quantify IL-6 protein production via ELISA. All data is expressed as % mean ± %CV (n = 3) relative to CD40L control. *Significance $p \leq 0.01$ (ANOVA with Tukey post-hoc) relative to CD40L control.

The effect of six anthocyanin metabolites on IL-6 production in CD40L stimulated HUVECs was examined by incubating CD40L with and without treatment compounds at 0.01, 0.1, 1 and 10 µM for 24 h. Following the treatment of CD40L challenged HUVECs with the anthocyanin metabolites, all six compounds tested demonstrated a significant ($p \leq 0.01$) reduction in IL-6 production (**Figure 6.6**). Vanillin (Figure 6.6F) and 3,4-dihydroxybenzaldehyde (Figure 6.6C) demonstrated the largest reduction in IL-6 production at 10 µM (86.4 ± 36.7% and 86.2 ± 9.6% reduction respectively) followed by protocatechuic acid at 0.01 µM (79.3 ± 22.0%) (Figure 6.6A). Vanillic acid (Figure 6.6D) and homovanillic acid (Figure 6.6E) only showed a reduction in sVCAM-1 production at the highest dose (10 µM), whilst homoprotocatechuic acid (Figure 6.6B) was bioactive over all four concentrations tested. 3,4-Dihydroxybenzaldehyde and vanillin were bioactive at the highest (10 µM) and lowest (0.01 µM) concentrations tested, whilst decreasing concentrations of protocatechuic acid resulted in significantly ($p<0.01$) lower levels of IL-6.

**Figure 6.6** IL-6 protein production following treatment with anthocyanin metabolites in CD40L stimulated cells.

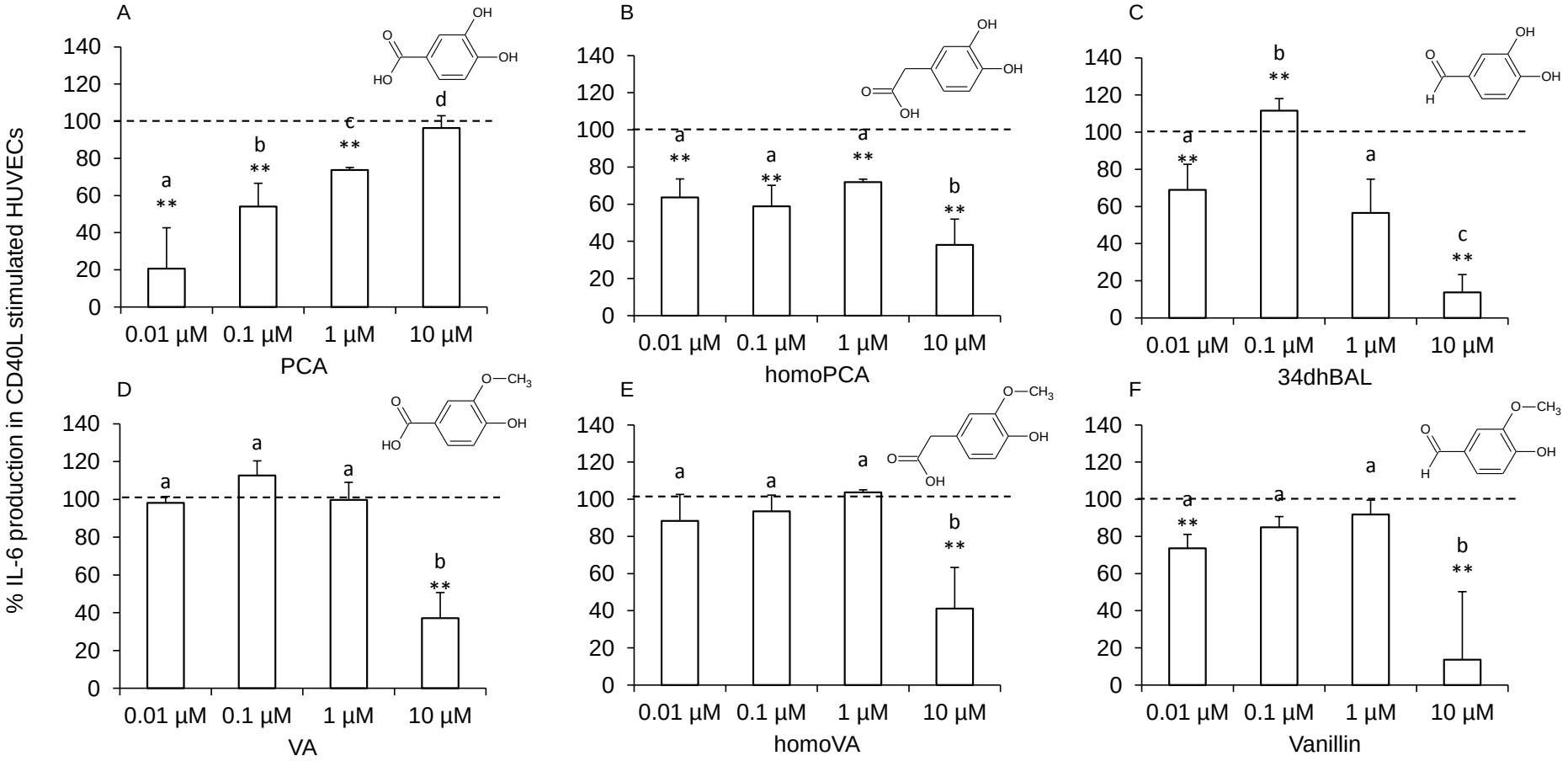


HUVECs were co-incubated with CD40L expressing Jurkat D1.1 cells (1 x $10^6$ cells/well) and the treatment compounds for 24 h and the supernatants were used to quantify IL-6 protein production via ELISA. All data is expressed as % mean ± %CV (n=3) relative to CD40L control. Significance: **p≤0.01 (ANOVA with Tukey post-hoc) relative to CD40L control. [a,b,c,d]Bars for treatments with different superscript letters are significantly different ($p < 0.05$). 34dhBAL, 3,4-dihydroxybenzaldehyde; PCA, protocatechuic acid; VA, vanillic acid.

### 6.3.1. TNF-α induced sVCAM-1 protein production

Incubation of HUVECs with TNF-α resulted in a 25 fold increase in the production of sVCAM-1 compared to un-stimulated HUVECs ($p<0.01$) (**Figure 6.7**).

**Figure 6.7** sVCAM-1 protein production in TNF-α stimulated cells.

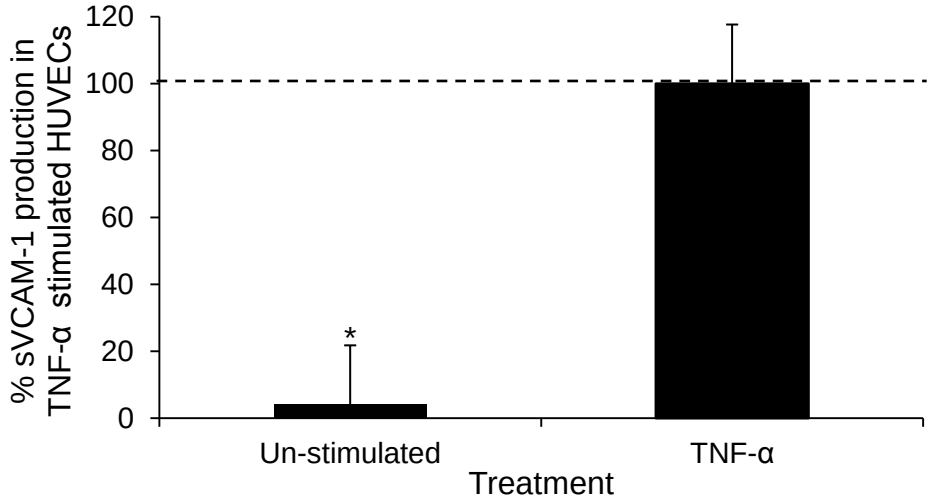


HUVECs were co-incubated with TNF-α (10 ng/mL) for 24 h and supernatants were used to quantify sVCAM-1 protein production via ELISA. All data is expressed as % mean ± %CV (n = 3) relative to CD40L control. *Significance $p\leq0.01$ (ANOVA with Tukey post-hoc) relative to TNF-α control.

The effect of six anthocyanin metabolites on sVCAM-1 production in TNF-α stimulated HUVECs was examined by incubating TNF-α stimulated HUVECs with and without treatment compounds at 0.01, 0.1, 1 and 10μM for 24 h (**Figure 6.8**). Following the treatment of TNF-α challenged HUVECs with the anthocyanin metabolites, three compounds, namely homoprotocatechuic acid (Figure 6.8B), 3,4-dihydroxybenzaldehyde (Figure 6.8C), and vanillin (Figure 6.8F) significantly ($p\leq0.01$) reduced sVCAM-1 production. Two compounds, vanillic acid (Figure 6.8D) and homovanillic acid (Figure 6.8E) demonstrated a trend ($p\leq0.2$) towards reduced sVCAM-1 production, whilst protocatechuic acid (Figure 6.8A) had no significant effect on sVCAM-1 production at any concentration. 3,4-Dihydroxybenzaldehyde (83.1 ± 39.2%) demonstrated the largest reduction in IL-6 production at 0.01 μM, followed by homoprotocatechuic acid at 10 μM (72.8 ± 20.9%) and homovanillic acid at 1 μM (61.8 ± 51.5%).

**Figure 6.8** sVCAM-1 protein production following treatment with anthocyanin metabolites in TNF-α stimulated cells.

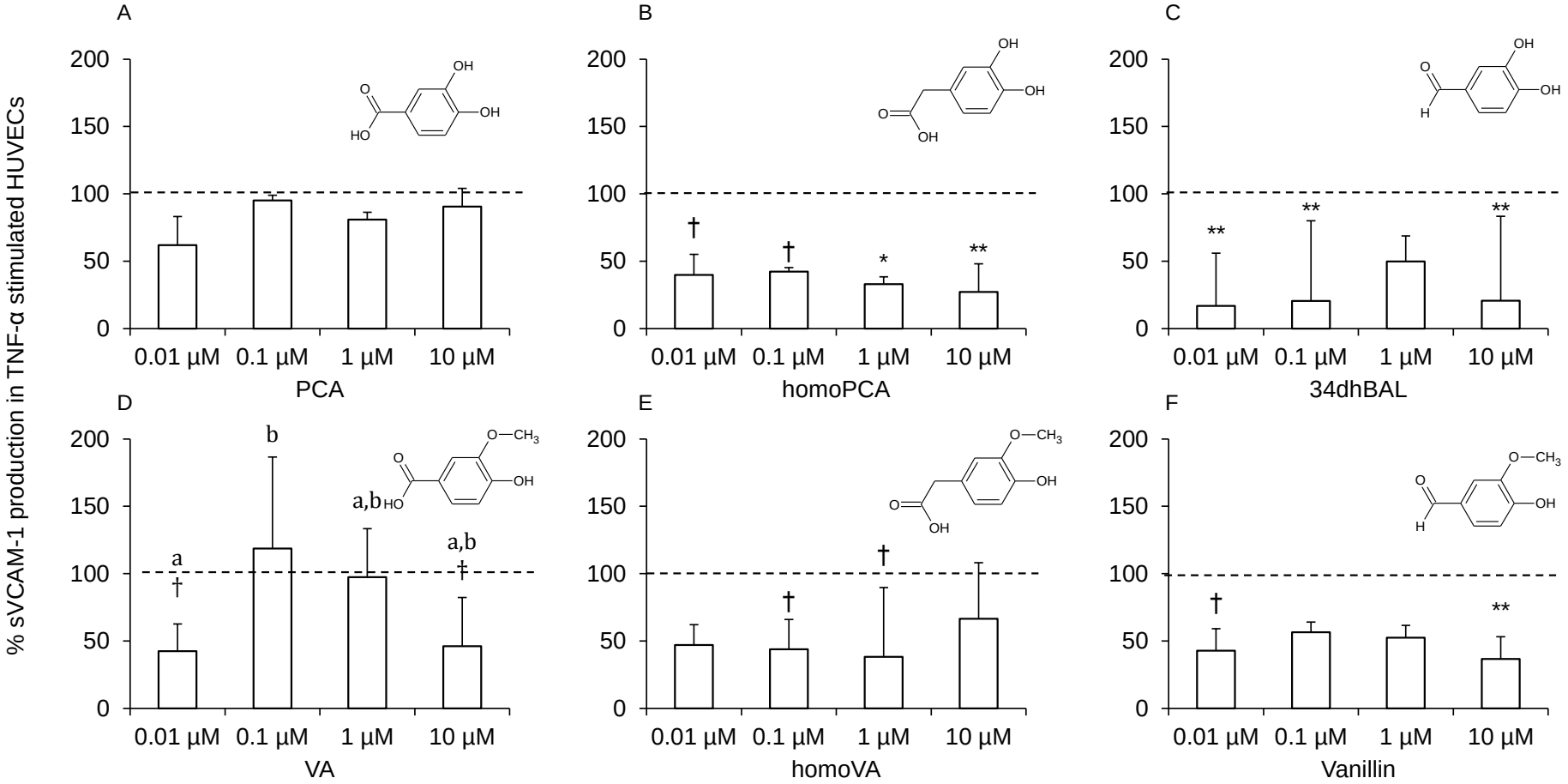


HUVECs were co-incubated with TNF-α (10 ng/mL) and the treatment compounds for 24 h and supernatants were used to quantify sVCAM-1 protein production via ELISA. All data is expressed as % mean ± %CV (n=3) relative to TNF-α control. Significance: †trend, p≤0.2; *p≤0.05; **p≤0.01 (ANOVA with Tukey post-hoc) relative to TNF-α control. [a,b]Bars for treatments with different superscript letters are significantly different ($p < 0.05$). 34dhBAL, 3,4-dihydroxybenzaldehyde; PCA, protocatechuic acid; VA, vanillic acid.

### 6.3.2. TNF-α induced IL-6 protein production

Incubation of HUVECs with TNF-α resulted in an eight fold increase in the production of IL-6 compared to un-stimulated HUVECs ($p<0.01$) (**Figure 6.9**).

**Figure 6.9** IL-6 protein production in TNF-α stimulated cells.

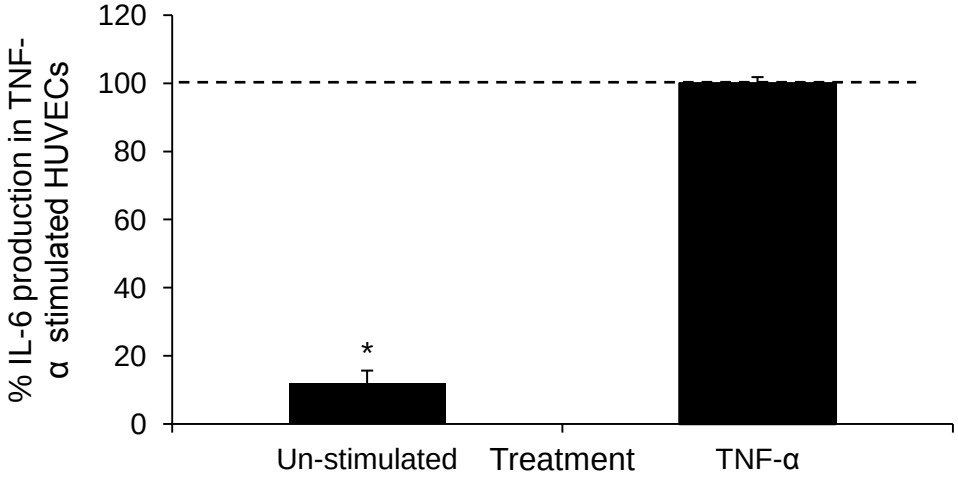


HUVECs were co-incubated with TNF-α (10 ng/mL) for 24 h and supernatants were used to quantify IL-6 protein production via ELISA. All data is expressed as % mean ± %CV (n = 3) relative to CD40L control. *Significance $p \leq 0.01$ (ANOVA with Tukey post-hoc) relative to TNF-α control.

The effect of six anthocyanin metabolites on IL-6 production in TNF-α stimulated HUVECs was examined by incubating TNF-α and HUVECs with and without treatment compounds at 0.01, 0.1, 1 and 10 μM for 24 h. Following the treatment of TNF-α stimulated HUVECs with the anthocyanin metabolites, all six compounds tested demonstrated a significant ($p \leq 0.01$) reduction in IL-6 production (**Figure 6.10**). Homoprotocatechuic acid (Figure 6.10B) and 3,4-dihydroxybenzaldehyde (Figure 6.10C) demonstrated the largest reduction in IL-6 production, of 88.4 ± 42.6% and 85.3 ± 24.4% respectively, followed by homovanillic acid (67.2 ± 9.1%) (Figure 6.10E). Vanillin resulted in the smallest reduction in IL-6 (44.8 ± 21.8) (Figure 6.10F) over the concentrations tested.

**Figure 6.10** IL-6 protein production following treatment with anthocyanin metabolites in TNF-α stimulated cells.

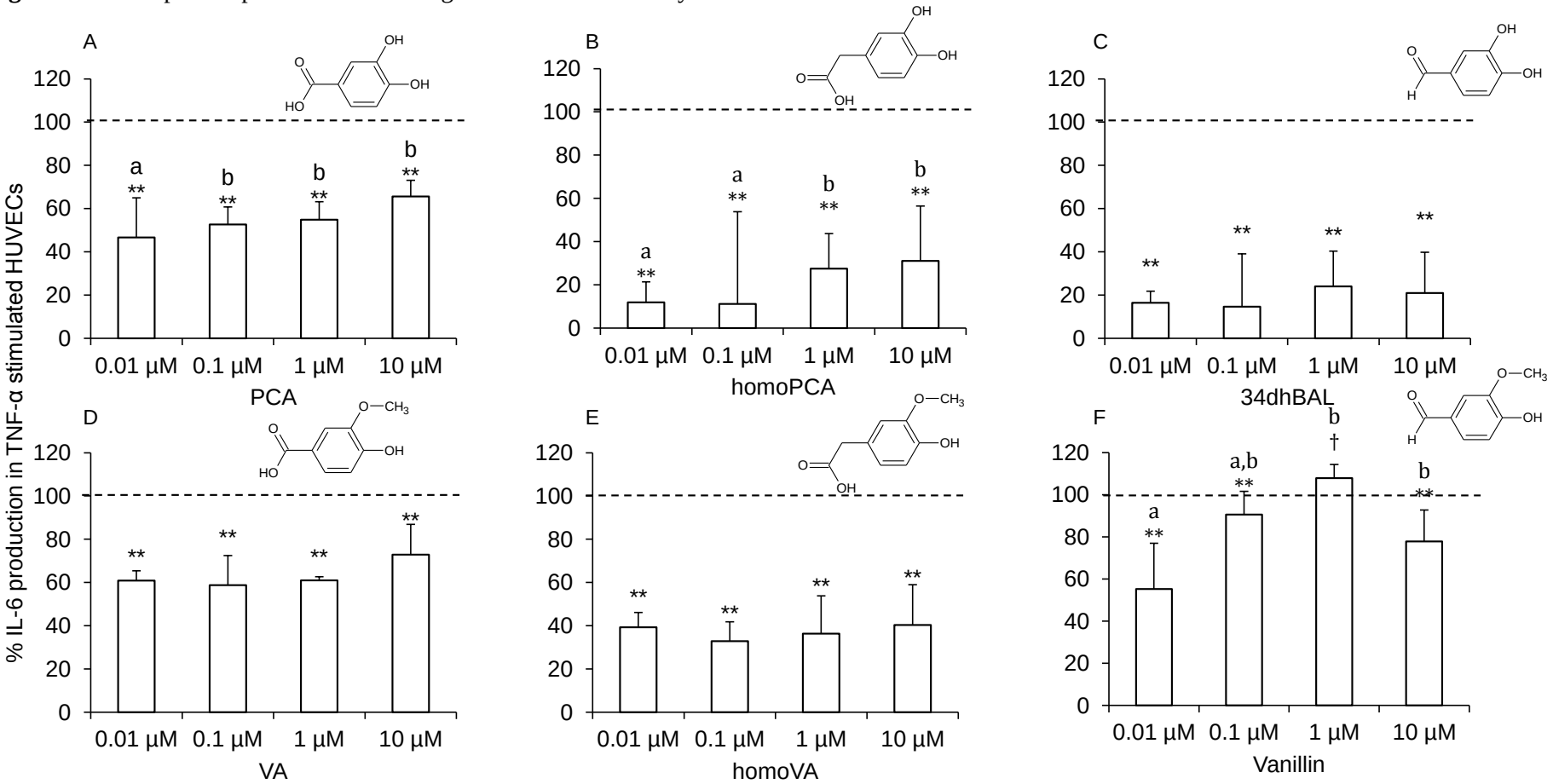


HUVECs were co-incubated with TNF-α (10 ng/mL) and the treatment compounds for 24 h and the supernatants were used to quantify IL-6 protein production via ELISA. All data is expressed as % mean ± %CV (n=3) relative to TNF-α control. Significance: †trend, p≤0.2; **p≤0.01 (ANOVA with Tukey post-hoc) relative to TNF-α control. [a,b]Bars for treatments with different superscript letters are significantly different ($p < 0.05$). 34dhBAL, 3,4-dihydroxybenzaldehyde; PCA, protocatechuic acid; VA, vanillic acid.

### 6.3.3. CD40L induced IL-6 and VCAM-1 mRNA.

A 50.1 ± 3.1 fold increase in sVCAM-1 mRNA levels was observed when HUVECs were incubated with CD40L compared to unstimulated cells. This was attenuated to a 5.3 ± 1.7 fold increase through the addition of 15 µg/mL anti-CD40L antibody (**Figure 6.11A**). Three of the treatment compounds significantly ($p \leq 0.01$) reduced the levels of VCAM-1 mRNA at 10 µM. Homoprotocatechuic acid resulted in the smallest increase in mRNA post CD40L stimulation (2.9 ± 0.8 fold increase) followed by 3,4-dihydroxybenzaldehyde (15.3 ± 2.5 fold increase) and vanillin (16.7 ± 7.1 fold increase). However, protocatechuic acid, vanillic acid and homovanillic acid had no significant effect.

The incubation of HUVECs with CD40L for 24 h had no significant impact on IL-6 mRNA levels compared to untreated or anti-CD40L antibody treated cells (Figure 6.11B). However, all compounds, except homoprotocatechuic acid, resulted in a significant ($p \leq 0.05$) decrease in IL-6 mRNA levels compared to CD40 positive control.

### 6.3.4. TNF-α induced IL-6 and VCAM-1 mRNA.

An 824.9 ± 173.5 fold increase in VCAM-1 mRNA levels ($p \leq 0.01$) was observed when HUVECs were incubated with TNF-α (10 ng/mL) compared to unstimulated cells (**Figure 6.12A**). Co-incubation of TNF-α stimulated HUVECs with 10 µM vanillic acid significantly ($p \leq 0.01$) attenuated the increase in VCAM-1 mRNA production to 144.3 ± 55.1 fold increase from baseline. Co-incubation with 10 µM 3,4-dihydroxybenzaldehyde (426.5 ± 121.5 fold increase from baseline) and vanillin (456.5 ± 280.1 fold increase from baseline) indicated a trend ($p \leq 0.2$) towards attenuating the increase in TNF-α stimulated VCAM-1 mRNA production. The remaining compounds (protocatechuic acid, homoprotocatechuic acid and homovanillic acid) had no significant impact on VCAM-1 mRNA levels ($p > 0.2$) (Figure 6.12A).

A 3.8 ± 0.1 fold increase in IL-6 mRNA levels was observed when HUVECs were incubated with TNF-α (10 ng/mL). Co-incubation of TNF-α stimulated HUVECs with 10 µM vanillic acid indicated a trend ($p \leq 0.2$) towards attenuating the TNF-α stimulated increase in IL-6 mRNA levels to a 1.8 ± 0.6 fold increase from baseline. However, the remaining compounds had no significant impact on IL-6 mRNA levels ($p > 0.2$) (Figure 6.12B)

**Figure 6.11** CD40L induced (A) VCAM-1 and (B) IL-6 mRNA levels following treatment with 10 μM anthocyanin metabolites.

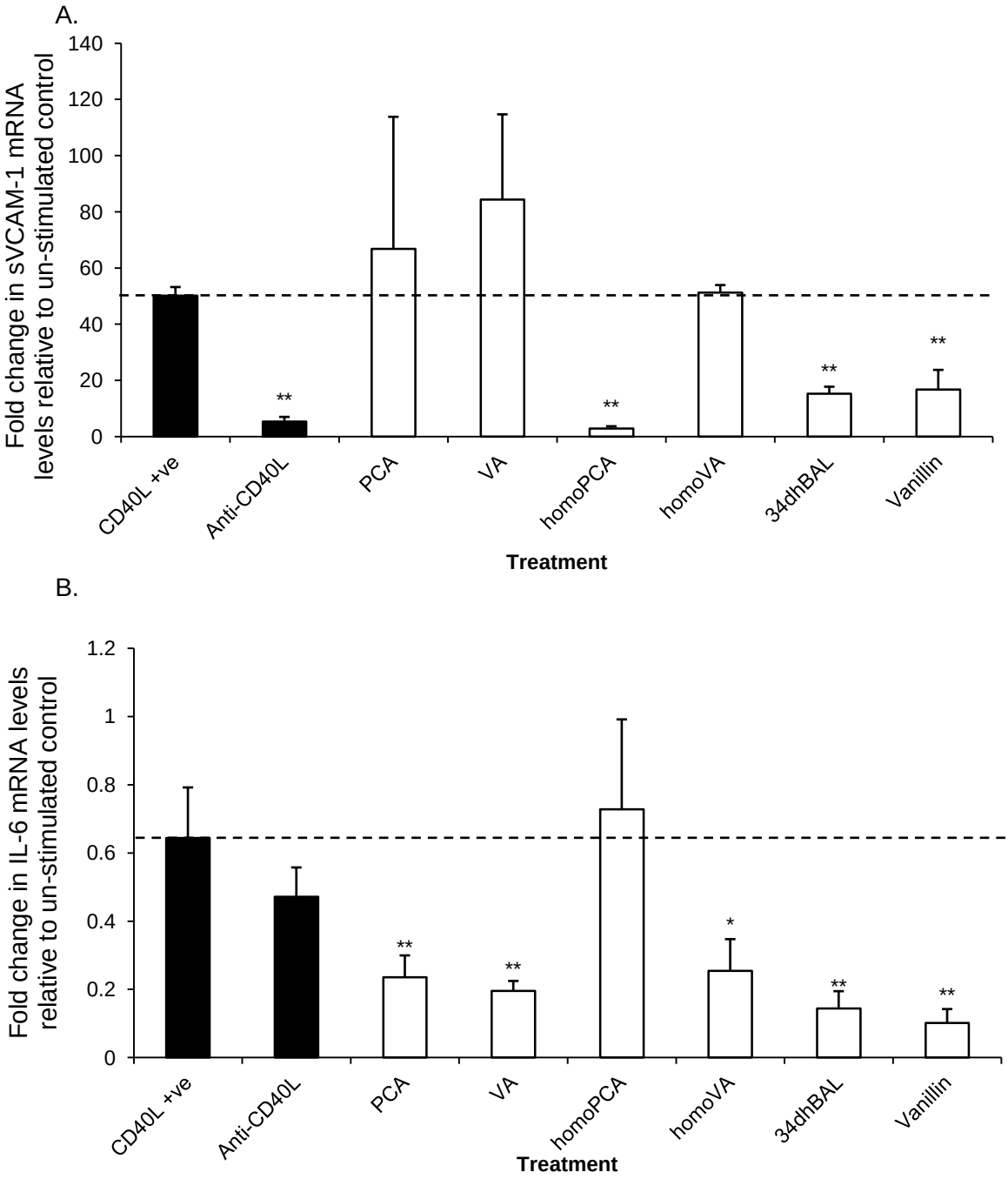


HUVECs were co-incubated with CD40L expressing Jurkat D1.1 cells (1 x $10^6$ cells/well) for 24h. Cell lysates were then used to quantify mRNA levels via RT-qPCR. All data was expressed relative to un-stimulated (basal) mRNA levels as mean fold ± SD (n=3) Significance: *p≤0.05; **p≤0.01 (ANOVA with Tukey post-hoc) relative to CD40L control. 34dhBAL, 3,4-dihydroxybenzaldehyde; PCA, protocatechuic acid; VA, vanillic acid.

**Figure 6.12** TNF-α induced (A) VCAM-1 and (B) IL-6 mRNA levels following treatment with 10 μM anthocyanin metabolites.

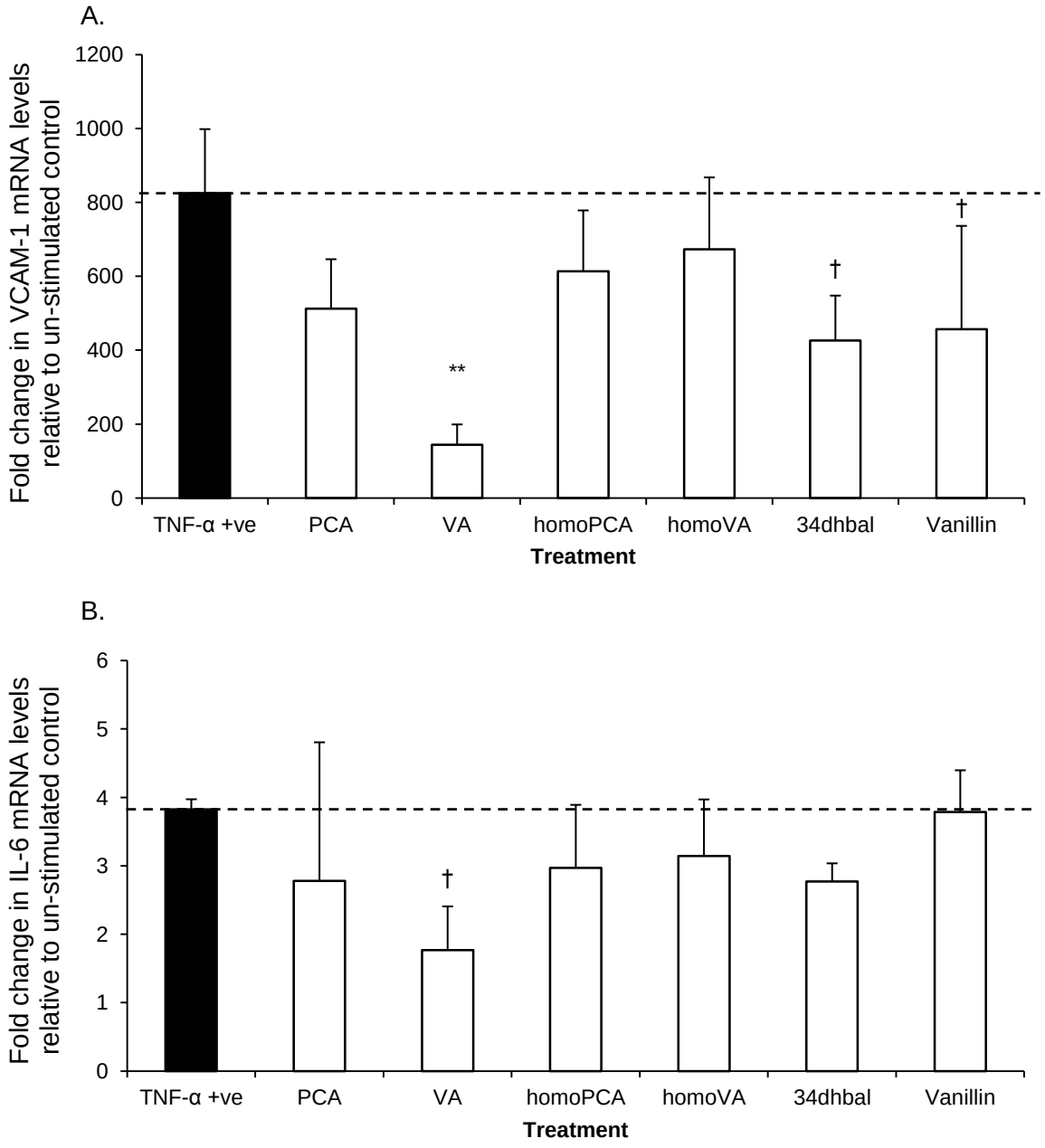


TNF-α (10 ng/mL) was co-incubated with or without treatment compounds at 10 μM for 24 h. Cell lysates were then used to quantify mRNA levels via RT-qPCR. All data is expressed relative to un-stimulated (basal) mRNA levels as mean fold ± SD (n=3). Significance: †trend, $p \leq 0.2$; **$p \leq 0.01$ (ANOVA with Tukey post-hoc) (ANOVA with Tukey post-hoc) relative to TNF-α control. 34dhBAL, 3,4-dihydroxybenzaldehyde; PCA, protocatechuic acid; VA, vanillic acid.

## 6.4. Discussion

Previously *in vitro* experiments into anthocyanin bioactivity have commonly used treatment doses, up to 2.2 mM (1 mg/mL) of anthocyanins (Youdim *et al.*, 2000). The treatment compounds used in the present study have been identified at maximum concentrations of up to 2 µM in serum and urine following the consumption of 500 mg $^{13}$C-labelled cyanidin-3-glucoside (de Ferrars *et al.*, 2014). Therefore, the treatment concentrations of 0.01 µM to 1 µM were chosen based on their physiological relevance, and 10 µM was selected as representing a potential maximal obtainable concentration, albeit outside normal dietary levels.

There were no significant effects ($p > 0.01$) of any treatment compound on endothelial cell viability following a 24 h incubation of HUVECs with WST-1 reagent (Figure 6.2). This confirms that ≤100 µM concentrations of the compounds are not cytotoxic to human vascular endothelial cells over a 24 h period, and that the doses used in the present study are suitable for the assessment of their vascular biological activity.

Anthocyanins have been shown to reduce the development of inflammation in human (Cassidy *et al.*, 2013; Zhu *et al.*, 2013), animal (Miyazaki *et al.*, 2008) and cell models (Chao *et al.*, 2013; Kim *et al.*, 2006; Miyazaki *et al.*, 2008; Nizamutdinova *et al.*, 2009; Xia *et al.*, 2009). However, bioavailability studies have shown that metabolites of anthocyanins are present at much higher concentrations than the anthocyanins themselves (Czank *et al.*, 2013; de Ferrars *et al.*, 2013). This has led to the hypothesis that anthocyanins may exert their bioactive effects through the effects of their metabolites (Kay, 2010). The adhesion of circulating leukocytes to the intimal endothelial monolayer is one of the earliest events in the development of atherosclerosis, and the process depends upon the complex interactions of multiple adhesion molecules and their receptors including VCAM-1, ICAM-1, selectins and integrins. IL-6 is a pleiotropic cytokine, whose expression is rapidly induced in response cytokines and is associated with a wide range of inflammatory functions, from B-lymphocyte differentiation to adhesion molecule recruitment (Schuett *et al.*, 2009). The current study focused on the effect of anthocyanin metabolites on sVCAM-1 and IL-6, as their inhibition may prevent or attenuate the progression of atherosclerosis through a decrease in the recruitment, differentiation and activation of a wide range of inflammatory mediators.

A key finding of the present study was that all compounds tested significantly reduced the production of sVCAM-1 (Figure 6.4) and IL-6 (Figure 6.6) following stimulation of HUVECs with CD40L, thus demonstrating that the degradation products and metabolites of anthocyanins have anti-inflammatory properties. Protocatechuic acid demonstrated an inverse dose dependent response following stimulation of HUVECs with CD40L, resulting in decreasing sVCAM-1 and IL-6 production at the lower concentrations. This effect was not observed with its methyl or phenylacetic acid derivatives. All other compounds tested were most active at the highest concentrations (10 μM) following stimulation with CD40L. Furthermore, vanillin and 3,4-dihydroxybenzaldehyde may reflect an inverse U-shaped response, decreasing sVCAM-1 and IL-6 levels at the highest (10 μM) and lowest (0.01 μM) concentrations tested, thus suggesting these metabolites do not follow a classical linear dose response. Previous studies have also suggested precedence *in vivo* for a non-linear dose response for flavonoid activity (Kay *et al.*, 2012; Rodriguez-Mateos *et al.*, 2013).

Little difference in sVCAM-1 and IL-6 production was observed between structures containing carboxylic, phenylacetic and benzaldehyde functional groups following CD40L stimulation. In contrast, the effect of methylation of the catechol group generally resulted in a decreased bioactivity following CD40L stimulation as protocatechuic acid (87 ± 21%) and homoprotocatechuic acid (82 ± 21%) demonstrated a higher maximum reduction in sVCAM-1 than vanillic acid (49 ± 9%) and homovanillic acid (48 ± 24%). Furthermore, protocatechuic acid, homoprotocatechuic acid and 3,4-dihydroxybenzaldehyde demonstrated a significant decrease in sVCAM-1 and IL-6 protein production over a larger range of concentrations than their methylated derivatives, thus suggesting the catechol group plays an important role in the bioactivity of the metabolite in CD40L stimulated cells. The presence of two hydroxyl groups in an *ortho* position have previously been shown to be important in the radical scavenging activity of flavonoids (Pereira *et al.*, 2009; Yokozawa *et al.*, 1998), with *O*-methylation of the catechol group resulting in a significant decrease in anti-oxidant activity (Amaral *et al.*, 2009; Cao *et al.*, 1997; Mladěnka *et al.*, 2010). However, to the best of the authors knowledge, the effect of a catechol or methylated catechol group on VCAM-1 or IL-6 production has not previously been investigated in CD40L stimulated cells.

Following TNF-α stimulation, all compounds tested significantly reduced the protein production of IL-6 (Figure 6.10). However, only homoprotocatechuic acid, 3,4-dihydroxybenzaldehyde and vanillin significantly reduced sVCAM-1 levels. Vanillic acid and homovanillic acid suggested a trend ($p \leq 0.2$) towards reducing sVCAM-1 levels and

protocatechuic had no significant effect (Figure 6.8). The effect of methylation of the catechol group on the treatment compounds also generally resulted in a decreased bioactivity in TNF-α stimulated HUVECs. This effect was most evident for the benzaldehydes, with 3,4-dihydroxybenzaldehyde demonstrating a higher reduction in sVCAM-1 (83 ± 39%) and IL-6 (85 ± 24%) production compared to vanillin (63 ± 16% and 44 ± 22% reduction for sVCAM-1 and IL-6 respectively). The enhanced bioactivity of compounds containing a catechol group over a methylated-catechol group has been previously observed for flavonoids (Spencer *et al.*, 2003; Williams *et al.*, 2004). The functional group also appeared to affect the bioactivity of the metabolites, with phenylacetic acids and benzaldehydes appearing more bioactive than carboxylic acids following TNF-α stimulation, with 3,4-dihydroxybenzaldehyde demonstrating the largest reduction in sVCAM-1(83 ± 39%), closely followed by homoprotocatechuic acid (73 ± 20%) and protocatechuic acid (38 ± 21%; Figure 6.8). A similar effect was observed for IL-6 production (Figure 6.8).

Following CD40L stimulation, VCAM-1 mRNA levels in HUVECs were increased 50-fold over baseline values (Figure 6.3). Incubation with the three compounds (homoprotocatechuic acid, 3,4-dihydroxybenzaldehyde and vanillin) which resulted in the largest reduction in sVCAM-1 protein levels at 10 μM following CD40L stimulation, also resulted in a significant decrease in VCAM-1 mRNA levels. Similarly, VCAM-1 mRNA levels demonstrated an 825-fold increase over baseline values following TNF-α stimulation, and co-incubation with vanillic acid significantly ($p \leq 0.01$) reduced the levels of VCAM-1 mRNA, whilst co-incubation with 3,4-dihydroxybenzaldehyde and vanillin indicated a trend ($p \leq 0.2$) towards the reduction of VCAM-1 mRNA. Together, these results suggest that some metabolites reduce VCAM-1 by down regulating the transcription of VCAM-1 mRNA. However, little is known concerning the mechanisms by which these treatment compounds regulate the expression of sVCAM-1 and IL-6. The down regulation of VCAM-1 mRNA production may be mediated by the inhibition of nuclear factor- κB (NF-κB) (Karlsen *et al.*, 2007; Wang *et al.*, 2010). NF-κB, one of the key transcription factors in mammals, is activated by numerous pro-inflammatory stimuli and controls the expression of multiple genes involved in inflammatory response and secretion of cytokines and chemokines (Bremner *et al.*, 2002). Protocatechuic acid at concentrations of 20 μM and 40 μM has previously been reported to suppress TNF-α stimulated VCAM-1 production in mouse aortic endothelial cells through the inhibition of TNF-α induced NF-κB activation (Wang *et al.*, 2010). A decrease in IL-6 expression and inhibition of NF-κB p65 following supplementation with vanillic acid was also observed in mice with ulcerative colitis (Figure 6.13) (Kim *et al.*, 2010). Furthermore, anthocyanins and protocatechuic acid have been

shown to suppress lipopolysaccharide (LPS) and CD40L stimulated NF-κB activation through inhibiting IκBα phosphorylation and the translocation of NF-κB (p65) into the nucleus (Figure 6.13) (Min *et al.*, 2010; Speciale *et al.*, 2010; Xia *et al.*, 2009), although this was not observed within HUVECs treated with 100 µM protocatechuic acid (Zhou-Stache *et al.*, 2002). Protocatechuic acid has also been shown to reduce the LPS stimulated production of inflammatory cytokines through inhibiting the activation of c-Jun N-terminal kinases (JNK), extracellular-signal-regulated kinases (ERK) and p38, within the MAPK pathway in macrophages (Figure 6.13) (Min *et al.*, 2010). Additionally, anthocyanins have also been shown to supress phosphorylation of STAT-3 (Signal Transducer and Activator of Transcription-3) but not STAT-1 within the JAK (janus kinase)/STAT activation pathway (Nizamutdinova *et al.*, 2009). However, a mechanistic study would be required to elucidate the mechanisms by which the metabolites reduced sVCAM-1 and IL-6 levels, which is beyond the scope of the present study and should be the focus of future research.

No significant change in VCAM-1 mRNA levels was observed for protocatechuic acid, vanillic acid and homovanillic acid following CD40L stimulation (Figure 6.11A) or in homoprotocatechuic acid following TNF-α stimulation (Figure 6.12A), despite a significant reduction in sVCAM-1 protein production at 10 µM. There are many possibilities to explain this. As the current investigation looked at levels of sVCAM-1 rather than membrane bound VCAM-1 (Fotis *et al.*, 2012), it is possible that the treatment compounds interfered with the proteolytic cleavage of VCAM-1, thus reducing the abundance within the media, but not at the mRNA level (CarterandWicks, 2001). Alternatively, the phenolic compounds may act to stabilise the mRNA transcripts or may reduce the levels of sVCAM-1 through post-translational modifications (Carter *et al.*, 2001).

Treatment of HUVECs with CD40L alone (positive control) did not result in up-regulation of IL-6 mRNA levels compared to unstimulated cells (Figure 6.11B). Despite this, a significant decrease in IL-6 mRNA levels from the CD40L positive control was observed for all compounds except homoprotocatechuic acid. The lack of an up-regulation in IL-6 mRNA levels, despite up-regulation of IL-6 protein levels following CD40L stimulation may be the result of mRNA transcription, translation and degradation prior to 24 h. The peak in protein levels observed at 24 h could therefore have been detected following the peak in mRNA levels. A time course experiment would be necessary to confirm this hypothesis, which is beyond the scope of the present study and is the focus of future work within our laboratory.

In contrast a four-fold increase in IL-6 mRNA levels, compared to unstimulated cells, was observed following TNF-α stimulation (Figure 6.12B). Co-incubation with vanillic acid suggested a trend ($p \leq 0.2$) towards attenuating the levels of IL-6 mRNA compared to unstimulated cells, however, no other compound significantly affected IL-6 mRNA production. As discussed above, this may be due to the phenolic compounds acting through stabilisation or other post-translational modifications, such as interfering with the glycosylation of IL-6 (Santhanam *et al.*, 1989).

**Figure 6.13** Activation of NF-κB and MAPK signalling pathways by CD40-CD40L and TNF-α.

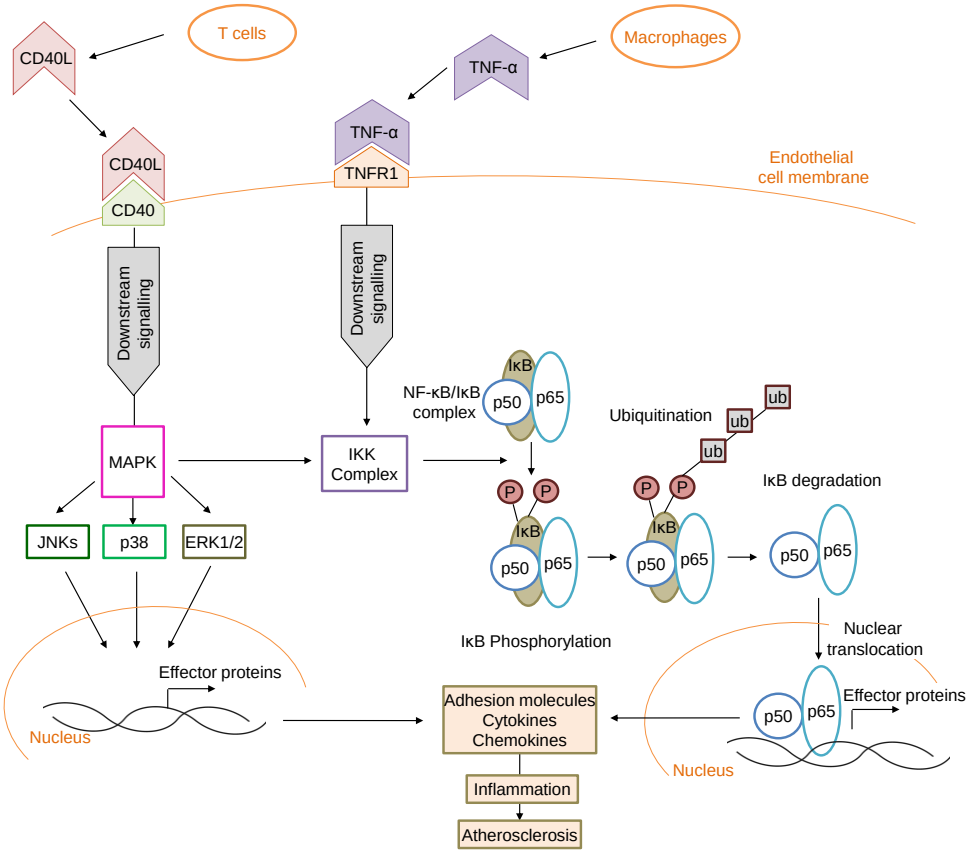


Adapted from (Bremner *et al.*, 2002; Pamukcu *et al.*, 2011). CD40L, Cluster of differentiation 40 ligand; ERK, extracellular-signal-regulated kinases; IKK, inhibitory-κB kinase; JNK, c-Jun N-terminal kinases; MAPK, mitogen-activated protein kinase complex; NF-κB, nuclear factor-κB; P, phosphate; p38, mitogen-activated protein kinase; p50, NF-κB p50 subunit; p65, NF-κB p65 subunit; TNF-α, tumour necrosis factor-α; TNFR1, TNF receptor-1; ub, ubiquitination.

Whilst the present screening data provides a novel insight into the effect of anthocyanin metabolites on the production of sVCAM-1 and IL-6 in vascular endothelial cells, there are certain limitations involved with the study. HUVECs are widely used for general research into vasculature activity, however an arterial cell type, such as human coronary artery

endothelial cells (HCAECs) or human aortic endothelial cells (HAECs) may be more relevant for assessing the potential modulatory effects of anthocyanin metabolites on sVCAM-1 and IL-6 production (Bouïs *et al.*, 2001). Moreover, experimental results obtained from different HUVEC isolates cannot be easily compared to each other because of different donor origins (Bouïs *et al.*, 2001). However, HUVECs from a single batch of pooled donors were utilised in the present study to minimise this limitation.

There are a number of research areas that should be addressed to progress the present work further. Firstly, the anthocyanin metabolites in the present study were co-incubated with the stimulus (CD40L or TNF-α). However, in previous anthocyanin bioactivity studies HUVECs were pre-incubated with the treatment compounds for 24 h, then washed with PBS prior to stimulation (Speciale *et al.*, 2010). The study found that pre-treatment with cyanidin-3-glucoside significantly suppressed TNF-α induced endothelial activation (Speciale *et al.*, 2010). Future research is needed to establish whether pre-incubation of HUVECs with anthocyanin metabolites also results in a protective effect against the production of inflammatory biomarkers. Secondly, future research should investigate the bioactivity of individual metabolites versus combinations of metabolites in order to establish whether anthocyanin metabolites have additive or synergistic bioactive effects. Thirdly, future research is required to determine whether the bioactivity of metabolites observed in the present study would also be observed following stimulation with other stimuli involved in atherosclerosis and CVD, such as oxidised low density lipoprotein (oxLDL) or peroxynitrite ($ONOO^-$). Similarly, soluble CD40L, which is secreted by activated platelets *in vivo* (Pamukcu *et al.*, 2011), as opposed to D1.1 cell derived CD40L, could be used to stimulate the HUVECs and confirm the specificity of the D1.1 cell activity. Fourthly, as mention previously, a time-course experiment, where VCAM-1 and IL-6 protein and mRNA levels are repeatedly measured over 24 h would provide additional information into the mechanisms by which anthocyanin metabolites reduce their production. Finally, the present study quantified the production of sVCAM-1, as opposed to membrane bound VCAM-1 following CD40L and TNF-α stimulation in HUVECs. Although this is a commonly utilised method (Zhu *et al.*, 2013) and a clinically relevant biomarker (Carter *et al.*, 2001), it would be informative to quantify membrane bound VCAM-1, in order explore the mechanisms by which the anthocyanin metabolites decreased sVCAM-1 production.

## 6.5. Conclusion

In summary, we demonstrate that recently identified, novel metabolites of anthocyanins reduce CD40L and TNF-α stimulated expression of the inflammatory markers, sVCAM-1 and IL-6. Furthermore, the metabolites are bioactive at concentrations that have recently been established as physiologically relevant following consumption of an anthocyanin rich bolus. Together, this data indicates that the anti-inflammatory effect of anthocyanins are likely attributed to their metabolites. This research provides an informative insight into understanding how the consumption of anthocyanins may contribute to optimising human health through diet.

# Chapter 7. General Discussion & Future Perspectives

Epidemiological evidence (Cassidy *et al.*, 2013; Cassidy *et al.*, 2011; McCullough *et al.*, 2012) and randomised control trials (Rodriguez-Mateos *et al.*, 2013; Zhu *et al.*, 2011) have indicated an association between the consumption of fruits and vegetables rich in anthocyanins and a decrease in cardiovascular disease (CVD) risk. However, the low bioavailability of anthocyanin glycosides (Manach *et al.*, 2005; Williamson *et al.*, 2005), in conjunction with their instability when exposed to physiological pH, suggests anthocyanin bioactivity *in vivo* may be mediated by the presence of their degradation products and metabolites.

Until recently, little was known concerning the bioavailability of anthocyanins metabolites, primarily due to five main deficiencies within the scientific literature. First, the majority of anthocyanin bioavailability studies to date exclusively focused on identifying parent anthocyanins and glucuronide, sulfate and methyl conjugates thereof (Bitsch *et al.*, 2004b; Mülleder *et al.*, 2002; Wu *et al.*, 2002). Second, there is a lack of intrinsic methods developed to identify a wide range of anthocyanin and anthocyanin metabolites. Third, in the few studies which aimed to identify phenolic acid metabolites of anthocyanins (Nurmi *et al.*, 2009; Russell *et al.*, 2009), their elucidation was complicated by use of a boluses containing complex anthocyanin and phenolic acid profiles, which often resulted in the failure of studies to identify phenolic acids that were not present in the original food source. Fourth, the absence of commercially available standards for glucuronide and sulfate conjugates limited the positive identification of anthocyanin metabolites. Finally, the lack of anthocyanin studies feeding a labelled anthocyanin bolus meant the origin of the identified metabolites could not be traced with certainty to the fed anthocyanin.

The present thesis sought to address some of these limitations by developing methods for the identification of possible anthocyanin metabolites (**Figure 7.1A**), and investigating their bioavailability in human samples from a study feeding an isotopically labelled ($^{13}$C-labelled cyanidin-3-glucoside) anthocyanin bolus and a study feeding a berry (elderberry) derived anthocyanin bolus (Figure 7.1B).

**Figure 7.1** Experimental scheme for the assessment of anthocyanin bioavailability and bioactivity

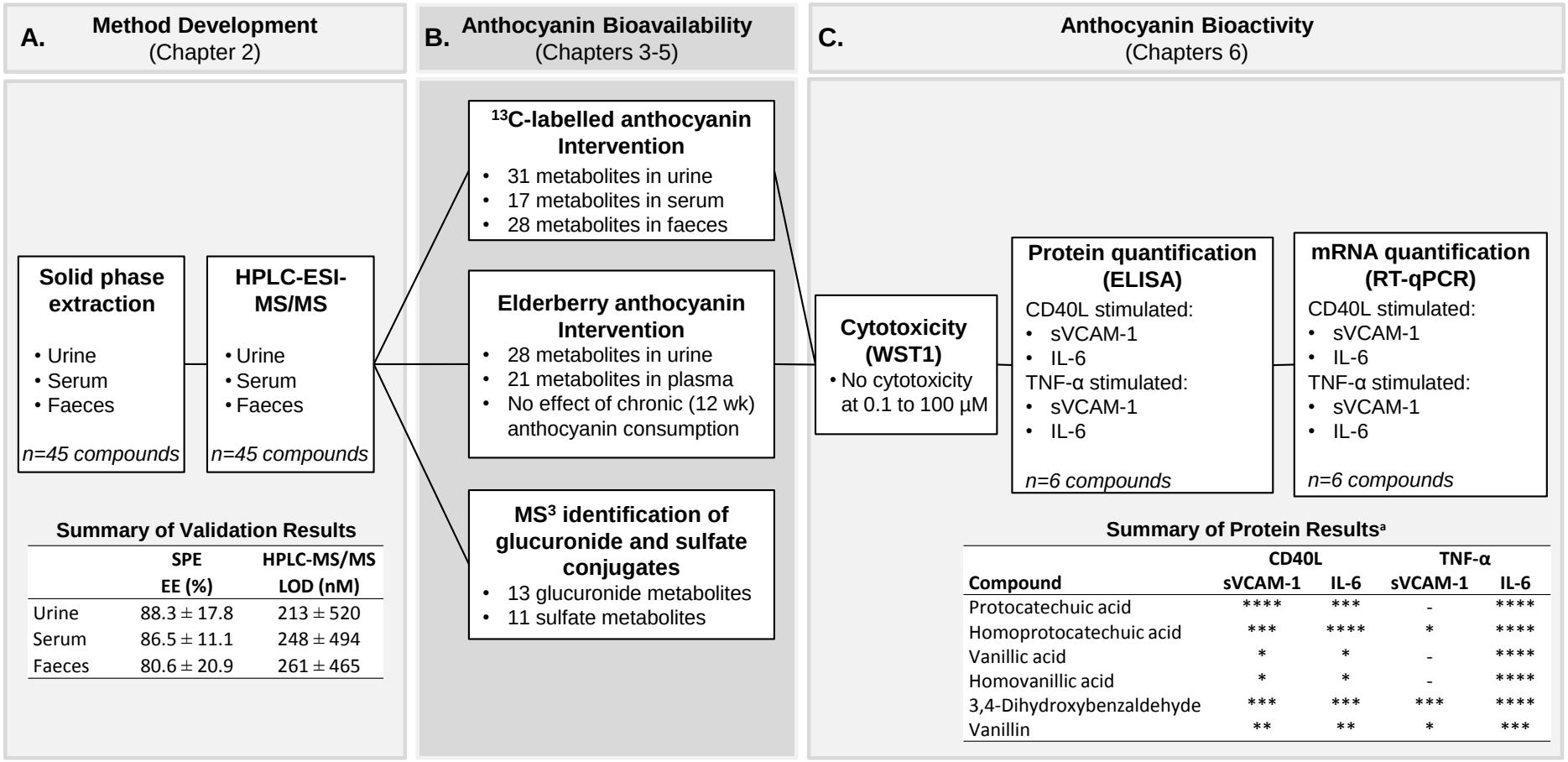


EE, extraction efficiency; IL-6, interleukin-6; LOD, limit of detection; SPE, solid phase extraction; sVCAM-1, soluble vascular cell adhesion molecule. [a]Significant ($p < 0.01$; ANOVA with Tukey post-hoc) decrease in biomarker expression at *one, **two, ***three, ****four of the concentrations examined.

Whilst a number of methods have previously been developed for the analysis of flavonoids and flavonoid derived phenolics (Kylli *et al.*, 2010; Plazonić *et al.*, 2009; Zhang *et al.*, 2004), the majority of reported methods for anthocyanin analysis have concentrated on quantification of parent anthocyanins and their respective metabolic conjugates. A major challenge associated with the development of methods for detecting anthocyanin metabolites *in vivo* relates to the formation of a large diversity of metabolic by-products, whose diversity and physicochemical properties make extraction and quantification in complex matrices problematic. The present study modelled 112 putative metabolites of anthocyanins based on the degradation, phase I, phase II and colonic metabolism of anthocyanins and other similarly structured flavonoids from previously published studies (Aura *et al.*, 2005; Cheminat *et al.*, 1986; Donovan *et al.*, 1999; Donovan *et al.*, 2002; Fernandes *et al.*, 2008; Forester *et al.*, 2008; Kay *et al.*, 2004; Mazza *et al.*, 1987; Mazza *et al.*, 2002; Moridani *et al.*, 2001; Williamson *et al.*, 2010; Woodward *et al.*, 2009). Analytical methods (SPE, HPLC and MS) were subsequently developed and validated to allow the quantification of 45 commercially available metabolites. The use of ten synthesised glucuronide and sulfate conjugates and structural elucidation using $MS^3$ enabled a more extensive search for anthocyanin metabolites than previously conducted.

Phenolic compounds are ubiquitous within plants (Dykes *et al.*, 2007; Schmitzer *et al.*, 2010), and can be formed following the consumption of a wide variety of compounds. For example, hippuric acid is formed from the reaction of benzoic acid with glycine, and is a common product of protein (Pero, 2010) or dietary polyphenol metabolism (Del Bo' *et al.*, 2012; Mulder *et al.*, 2005). Without the use of an isotope marker, previous studies could not confirm the origin of identified metabolites. Therefore, the labelled anthocyanin intervention (**Chapter 3**) enabled for the first time, confirmation of the degradation and metabolism of anthocyanins in humans into multiple phenolic compounds.

A total of 35 anthocyanin metabolites were identified with biological samples post consumption of 500 mg $^{13}$C-cyanidin-3-glucoside. These included methylated, sulfated and glucuronidated conjugates of the parent anthocyanin, anthocyanin degradation products and phase II metabolites. Taken together with previous studies investigating the stability and absorption of anthocyanins within the gastrointestinal tract (Aura *et al.*, 2005; Crozier *et al.*, 2010; Del Rio *et al.*, 2013; Fleschhut *et al.*, 2006; González-Barrio *et al.*, 2010; Hassimotto *et al.*, 2008; Keppler *et al.*, 2005), these results suggest that upon ingestion, a small proportion (~0.1%) of the anthocyanin dose is absorbed intact within the upper gastrointestinal tract and undergoes methylation, sulfation and glucuronidation to some

extent. The remaining bolus is likely degraded, followed by significant phase II conjugation, particularly methylation to form vanillic acid, sulfation to form protocatechuic acid sulfate, and conjugation with glycine to form hippuric acid. The absorption of many of the metabolites appeared to follow biphasic serum kinetics, displaying an initial serum peak between 0-5 h followed by a second peak after 6-48 h. This indicated that the metabolism and absorption likely occurs within different tissues and at different sites within the gastrointestinal tract, including the colon.

The elderberry intervention trial was conducted to investigate the bioavailability of anthocyanin metabolites following acute (1 x 500 mg) and chronic (500 mg x 12 wks) consumption of a food (elderberry) derived anthocyanin bolus. To the best of our knowledge, it was the first study to look at postprandial phenolic metabolite excretion following sustained anthocyanin dosing. No significant difference in the metabolism or clearance was identified following chronic anthocyanin consumption, suggesting there is no alteration in metabolic processing following 12 wks repeated dosing. However, the use of an elderberry bolus with a simple anthocyanin profile and $MS^3$ structural elucidation enabled the largest number of metabolic conjugates of elderberry anthocyanins to be identified to date.

To fully understand the bioactivity of anthocyanins, it was first necessary to gain a complete understanding of their absorption, distribution and metabolism *in vivo* and to subsequently integrate this understanding into establishing their bioactivity. Chronic inflammation is involved with the onset and development of pathological disturbances, including arteriosclerosis, diabetes and obesity (García-Lafuente *et al.*, 2009). Therefore, the final part of the current thesis aimed to establish the anti-inflammatory bioactivity of six anthocyanin metabolites via their effect on soluble vascular adhesion molecule-1 (sVCAM-1) and interleukin-6 (IL-6) production in stimulated endothelial cells. sVCAM-1 and IL-6 were selected for analysis as they play a pivotal role in inflammation and development of atherosclerosis. Their inhibition may prevent or attenuate the progression of atherosclerosis, through a decrease in the recruitment, differentiation and activation of a wide range of inflammatory mediators. The modulation of VCAM-1 and IL-6 production by anthocyanins has been the subject of many previous studies (Chao *et al.*, 2013; Kim *et al.*, 2006; Miyazaki *et al.*, 2008; Nizamutdinova *et al.*, 2009; Sen *et al.*, 2001; Zhu *et al.*, 2013), yet little is known concerning the bioactivity of the more bioavailable degradation products and metabolites. A key finding of the present thesis was that all metabolites tested significantly reduced the production of sVCAM-1 and IL-6 at one or more of the concentrations tested, following stimulation of HUVECs with CD40L. Furthermore, all compounds significantly

reduced the production of IL-6 and three metabolites significantly reduced the production of sVCAM-1 following stimulation of HUVECs with tumor necrosis factor-α (TNF-α) (Figure 7.1C). These results demonstrate that the degradation products and metabolites of anthocyanins appear to have anti-inflammatory properties. Metabolites containing a catechol group (*ortho* hydroxy) were significantly ($p<0.01$) bioactive over a greater number of concentrations than those containing a methylated catechol group, following stimulation with CD40L. The enhanced bioactivity of the compounds containing a catechol group over a methoxy group has been previously observed for flavonoids (Spencer *et al.*, 2003; Williams *et al.*, 2004).

## 7.1. Future perspectives

The main topics addressed in this thesis were the development and validation of methods for the detection of anthocyanin metabolites, the bioavailability and metabolism of anthocyanins in humans and the bioactivity of anthocyanin metabolites *in vitro* (Figure 7.1). In the authors opinion, the research topics discussed in the proceeding section must have a predominant position in future research.

The present thesis describes the development and validation of methods using solid phase extraction (SPE) and HPLC-ESI-MS/MS for the quantification of 45 anthocyanin metabolites. The validated methods achieved high extraction efficiencies using SPE in urine (88.3 ± 17.8%), serum (86.5 ± 11.1%) and faeces (80.6 ± 20.9%) and limits of detection below 100 nM for 34, 35 and 30 of the 45 compounds in urine, serum and faeces respectively (Figure 7.1). However, in common with the majority of analytical laboratories, the developed SPE method utilised individual cartridges, and was performed off-line, therefore making it time-consuming and costly in experiments were large number of samples need to be analysed. A further step in the development of analytical methods for anthocyanin metabolite analysis would be to optimise a 96 well SPE method or an automated on-line SPE method, suitable for the extraction of the metabolites of interest, to enable high throughput analysis of samples. Another limitation of the developed HPLC-MS/MS methods was that high (>100 nM) limits of detection were observed for 11, 10 and 15 of the compounds within the urine, serum and faecal matrices respectively. To improve the detection limits of these metabolites, future work should focus on developing methods for GCMS analysis, which can result in superior detection for the smaller, volatile phenolic acids, such as benzoic acid or benzaldehyde. Furthermore, the development of efficient derivatisation methods will improve the detection of analytes by increasing their volatility (Fiamegos *et al.*, 2004;

Robbins, 2003). The most common silylating reagents used for the derivatisation of phenolic acids are trimethylsilyl deratives (Rechner *et al.,* 2002). The development of these methods could ultimately enable the detection of anthocyanin metabolites present in samples below the detection limit of the current methodology and enable methods to be developed for potential anthocyanin metabolites not indicated in the current study.

Matrix effects, such as ion suppression are caused by the presence of co-eluting, residual matrix components competing or interfering with the ionisation of the analyte of interest. Matrix effects can alter the response and thus the measured concentration of an analyte of interest, leading to erroneous results. The analytical methods described in the present study (**Chapter 2**) corrected for this by utilising matrix matched calibration curves. The described methods are therefore more robust and more closely match the recommendations set out by the U.S. Department of Health and Human Services Food and Drug Administration (FDA) (FDA, 2001) than methods developed previously in the flavonoid field. In order to improve these methods further, it would be necessary to use labelled calibration standards within the sample to quantify unlabelled analytes.

The isotopically labelled study described in the present thesis (**Chapter 3**) was the first labelled anthocyanin bioavailability study to be conducted in humans and enabled the identification of 35 anthocyanin metabolites, which has not previously been possible. In addition, 11 sulfate and 13 glucuronide conjugates of these metabolites were putatively identified using $MS^3$ (Figure 7.1). In order to further this work, it would be necessary synthesise these novel metabolites. This would allow their retention time and fragmentation pattern to be confirmed with certainty and would enable accurate quantification to be performed.

Anthocyanins are speculated to undergo conjugation with glutathione (GSH), as the nucleophilic cysteinyl thiol group in GSH is easily added to activated double bonds, such as those found on aromatic rings (Levsen *et al.,* 2005). Moreover, the formation of quercetin GSH conjugates has been observed in murine hepatic suspensions and GSH related metabolites of quercetin degradation products have been observed in human urine (Hong *et al.,* 2006). Therefore, future work should additionally focus on identifying possible glutathione conjugates of anthocyanins and their metabolites.

A number of anthocyanin bioavailability studies conducted to date have investigated the dose response and metabolism of anthocyanins (Carkeet *et al.*, 2008; Charron *et al.*, 2007). However, the effect of anthocyanin dose on the bioavailability of anthocyanin metabolites is currently unknown. Future bioavailability studies should therefore focus on investigating the dose response of anthocyanins. For example, a randomised, double blind, crossover intervention trial could be conducted where participants are fed an isotopically labelled anthocyanin bolus, containing 250 mg, 500 mg and 1000 mg anthocyanins. Blood, urine, faecal and breath samples should be collected at baseline and for ≥72 h post bolus in order to ensure the concentrations of identified metabolites return to baseline values.

A key finding of this thesis revealed that all metabolites tested significantly reduced the production of sVCAM-1 and IL-6 in HUVECs following stimulation with CD40L. Moreover, all metabolites tested significantly reduced the production of IL-6 following stimulation with TNF-α. This indicates that the degradation products and metabolites of anthocyanins have anti-inflammatory properties and suggests they may be responsible for the perceived bioactivity of anthocyanins *in vivo*. The main challenge for future research is therefore to characterise the mechanisms by which anthocyanin metabolites act to reduce inflammation. Previous work indicates that anthocyanins and anthocyanin metabolites may act via the down regulation of nuclear factor- κB (NF-κB) (Karlsen *et al.*, 2007; Wang *et al.*, 2010) (Min *et al.*, 2010; Speciale *et al.*, 2010; Xia *et al.*, 2009). Alternatively, anthocyanins have been shown to reduce the production of pro-inflammatory molecules through interacting with the mitogen activated protein kinases (MAPK) family [extracellular signal regulated kinase (ERK), p38 and c-jun NH2-terminal kinase (JNK)] (Hirano *et al.*, 1996; Min *et al.*, 2010; Xia *et al.*, 2009). In order to deduce whether the six metabolites investigated in the present study reduce inflammation via similar mechanisms, it would be necessary to carry out a mechanistic study using a range of inhibitors, such as BAY-11-7082, an inhibitor of TNF-α induced phosphorylation of IκB-α, in conjunction with techniques such as immunoblotting and flow cytometry to investigate how the metabolites are regulating the inflammatory pathways.

In addition to characterising the bioactivity of anthocyanin metabolites *in vitro,* the activity of these compounds could be assessed in human intervention studies, to translate the identified effects observed in the cellular model to the human. To date, several randomised controlled trials with anthocyanins have been conducted describing decreased levels of pro-inflammatory cell adhesion molecules and cytokines (Karlsen *et al.*, 2007; Zhu *et al.*, 2013). To further investigate the bioactivity of anthocyanin metabolites compared to parent

anthocyanins, similar interventions could be performed using anthocyanin degradation products and metabolites. For example, an acute phase, randomised, double blind, placebo controlled, crossover intervention could be conducted where participants are fed a bolus dose (500 mg) of protocatechuic acid, vanillic acid, cyanidin-3-glucoside or placebo. Clinical vascular measures, such as endothelial vasodilator function and pulse wave analysis and biomarkers of inflammation such as plasma levels of nitric oxide metabolites (nitrite, nitrate and thionitrites) and pro-inflammatory cytokines could be investigated in such an intervention.

In conclusion, this thesis has contributed to the current literature on anthocyanin bioavailability and bioactivity by providing novel insights into the metabolism of anthocyanins and giving an indication of their bioactivity *in vitro*. However, further investigations into anthocyanin bioavailability and mechanisms of bioactivity are required to explain fully the observed cardioprotective effects of anthocyanins. A long-term goal of this work would be to supply nutritionist and clinicians with information on how the consumption of anthocyanins can be used to reduce risk factors associated with CVD.

# List of Abbreviations

| | |
|---|---|
| ADME | Absorption, distribution, metabolism and excretion |
| ANOVA | Analysis of variance |
| $BH_4$ | Tetrahydrobiopterin |
| CβG | Cytosolic-β-glucosidase |
| C3G | Cyanidin-3-*O*-glucoside |
| CAD | Collision-activated dissociation |
| CD40 | Cluster of differentiation 40 |
| CD40L | Cluster of differentiation 40 ligand |
| CE | Collision Energy |
| CEP | Collision cell entry potential |
| $C_{max}$ | Maximum concentration |
| COMT | Catechol-*O*-methyltransferase |
| CUR | Curtain gas |
| CV | Coefficient of variation |
| CVD | Cardiovascular disease |
| CXP | Collision cell exit potential |
| Cy | Cyanidin |
| DAD | Diode array detector |
| DMSO | Dimethyl sulfoxide |
| DP | Declustering potential |
| ELISA | Enzyme linked immunosorbent assay |
| ERK | Extracellular-signal-regulated kinases; |
| ESI | Electrospray ionisation |
| eNOS | Endothelial nitric oxide synthase |
| EP | Entrance potential |
| FMD | Flow mediated dilation |
| GIT | Gastrointestinal tract |
| GLUT2 | Glucose transporter 2 |
| GS1 | Gas 1 |
| GS2 | Gas 2 |
| GSH | Glutathione |
| HPLC | High performance liquid chromatography |
| HAEC | Human aortic endothelial cells |

| | |
|---|---|
| HCAEC | Human coronary artery endothelial cells |
| HUVEC | Human umbilical vein endothelial cells |
| ICAM | Intercellular adhesion molecules |
| IKK | Inhibitory-κB kinase |
| IL-6 | Interleukin-6 |
| iNOS | Inducible nitric oxide synthase |
| IRMS | Isotope ratio mass spectrometry |
| IS | Ion spray voltage |
| JAK | Janus kinase |
| JNK | c-Jun-N-terminal kinase |
| LDL | Low-density lipoprotein |
| LIT | Linear ion trap |
| LLE | Liquid-liquid extraction |
| LPH | Lactase phlorizin hydrolase |
| LPS | Lipopolysaccharide |
| NADPH | Nicotinamide adenine dinucleotide phosphate (reduced form) |
| NF-κB | Nuclear factor kappa B |
| $NH_2$ | Amine |
| NO | Nitric oxide |
| NOX | NADPH oxidase |
| $O_2^-$ | Superoxide |
| $ONOO^-$ | Peroxynitrite |
| oxLDL | Oxidised low-density lipoprotein |
| MAPK | Mitogen-activated protein kinase complex |
| MCP-1 | Monocyte chemoattractant protein-1 |
| MP | Mobile phase |
| mRNA | Messenger ribonucleic acid |
| MRP2 | multiresistant protein 2 |
| MS | Mass Spectrometry |
| m/z | Mass to charge ratio. |
| p38 | Mitogen-activated protein kinase subunit |
| p50 | NF-κB p50 subunit |
| p65 | NF-κB p65 subunit |
| PAPS | 3'-phosphoadenosine-5'-phosphosulfate |
| PCA | Protocatechuic acid |
| PCR | Polymerase chain reaction |

| | |
|---|---|
| PECAM-1 | Platelet endothelial cellular adhesion molecule-1 |
| PGA | Phloroglucinaldehyde |
| Pl3G | Pelargonidin-3-*O*-glucoside |
| PFP | Pentafluorophenyl |
| ROS | Reactive oxygen species |
| RP | Reverse phase |
| $R_t$ | Retention time |
| SD | Standard deviation |
| SGLT1 | Sodium dependent glucose transporter-1 |
| SOD | Superoxide dismutase |
| SPE | Solid Phase Extraction |
| STAT | signal transducer and activator of transcription |
| SULT | Sulfotransferase |
| $T_{msx}$ | Time at maximum concentration |
| TMS | Trimethylsilyl |
| TNF-α | Tumor necrosis factor alpha |
| TNFR1 | TNF receptor-1 |
| TOF | Time of flight |
| UDPDG | Uridine 5'-diphospho-glucuronosyl transferase |
| VCAM-1 | Vascular cell adhesion molecule-1 |
| WHO | World Health Organisation |

# Bibliography


Amaral S, Mira L, Nogueira J, Silva APd, Helena Florêncio M (2009). Plant extracts with anti-inflammatory properties—A new approach for characterization of their bioactive compounds and establishment of structure–antioxidant activity relationships. *Bioorganic & medicinal chemistry* **17**(5)**:** 1876-1883.

Arts IC, Sesink AL, Hollman PC (2002). Quercetin-3-glucoside is transported by the glucose carrier SGLT1 across the brush border membrane of rat small intestine. *J Nutr* **132**(9)**:** 2823; author reply 2824.

Arumugam M, Raes J, Pelletier E, Le Paslier D, Yamada T, Mende DR, *et al.* (2011). Enterotypes of the human gut microbiome. *Nature* **473**(7346)**:** 174-180.

Aura AM, Martin-Lopez P, O'Leary KA, Williamson G, Oksman-Caldentey KM, Poutanen K, *et al.* (2005). In vitro metabolism of anthocyanins by human gut microflora. *Eur J Nutr* **44**(3)**:** 133-142.

Aura AM, O'Leary KA, Williamson G, Ojala M, Bailey M, Puupponen-Pimiä R, *et al.* (2002). Quercetin derivatives are deconjugated and converted to hydroxyphenylacetic acids but not methylated by human fecal flora in vitro. *J. Agric. Food. Chem.* **50**(6)**:** 1725-1730.

Azzini E, Bugianesi R, Romano F, Di Venere D, Miccadei S, Durazzo A, *et al.* (2007). Absorption and metabolism of bioactive molecules after oral consumption of cooked edible heads of Cynara scolymus L. (cultivar Violetto di Provenza) in human subjects: a pilot study. *British Journal of Nutrition* **97**(05)**:** 963-969.

Azzini E, Vitaglione P, Intorre F, Napolitano A, Durazzo A, Foddai MS, *et al.* (2010). Bioavailability of strawberry antioxidants in human subjects. *Br. J. Nutr.* **104**(8)**:** 1165-1173.

Basu A, Du M, Leyva MJ, Sanchez K, Betts NM, Wu M, *et al.* (2010). Blueberries decrease cardiovascular risk factors in obese men and women with metabolic syndrome. *The Journal of Nutrition* **140**(9)**:** 1582-1587.

Baud V, Karin M (2001). Signal transduction by tumor necrosis factor and its relatives. *Trends in cell biology* **11**(9)**:** 372-377.

Baur JA, Pearson KJ, Price NL, Jamieson HA, Lerin C, Kalra A, *et al.* (2006). Resveratrol improves health and survival of mice on a high-calorie diet. *Nature* **444**(7117)**:** 337-342.

Bell DR, Gochenaur K (2006). Direct vasoactive and vasoprotective properties of anthocyanin-rich extracts. *Journal of Applied Physiology* **100**(4)**:** 1164-1170.

Berg RD (1996). The indigenous gastrointestinal microflora. *Trends in Microbiology* **4**(11)**:** 430-435.

Bermúdez-Soto M-J, Tomás-Barberán F-A, Garcia-Conesa M-T (2007). Stability of polyphenols in chokeberry (Aronia melanocarpa) subjected to in vitro gastric and pancreatic digestion. *Food Chemistry* **102**(3)**:** 865-874.

Bitsch R, Netzel M, Frank T, Strass G, Bitsch I (2004a). Bioavailability and biokinetics of anthocyanins from red grape juice and red wine. *Journal of Biomedicine and Biotechnology* **2004**(5)**:** 293-298.

Bitsch R, Netzel M, Sonntag S, Strass G, Frank T, Bitsch I (2004b). Urinary excretion of cyanidin glucosides and glucuronides in healthy humans after elderberry juice ingestion. *J. Biomed. Biotechnol.* **2004**(5)**:** 343-345.

Blankenberg S, Barbaux S, Tiret L (2003). Adhesion molecules and atherosclerosis. *Atherosclerosis* **170**(2)**:** 191-203.

Boss B, Richling E, Herderich M, Schreier P (1999). HPLC–ESI–MS/MS analysis of sulfated flavor compounds in plants. *Phytochemistry* **50**(2)**:** 219-225.

Bouïs D, Hospers GP, Meijer C, Molema G, Mulder N (2001). Endothelium in vitro: A review of human vascular endothelial cell lines for blood vessel-related research. *Angiogenesis* **4**(2)**:** 91-102.

Bremner P, Heinrich M (2002). Natural products as targeted modulators of the nuclear factor-KB pathway. *Journal of Pharmacy and Pharmacology* **54**(4)**:** 453-472.

Bub A, Watzl B, Heeb D, Rechkemmer G, Briviba K (2001). Malvidin-3-glucoside bioavailability in humans after ingestion of red wine, dealcoholized red wine and red grape juice. *European Journal of Nutrition* **40**(3)**:** 113.

Burton-Freeman B (2010). Postprandial metabolic events and fruit-derived phenolics: a review of the science. *Br J Nutr* **104 Suppl 3:** S1-14.

Cao G, Muccitelli HU, Sánchez-Moreno C, Prior RL (2001). Anthocyanins are absorbed in glycated forms in elderly women: a pharmacokinetic study. *Am. J. Clin. Nutr.* **73**(5)**:** 920-926.

Cao G, Sofic E, Prior RL (1997). Antioxidant and prooxidant behavior of flavonoids: structure-activity relationships. *Free Radical Biology and Medicine* **22**(5)**:** 749-760.

Cardona F, Andrés-Lacueva C, Tulipani S, Tinahones FJ, Queipo-Ortuño MI (2013). Benefits of polyphenols on gut microbiota and implications in human health. *The Journal of Nutritional Biochemistry* **24**(8)**:** 1415-1422.

Carkeet C, Clevidence BA, Novotny JA (2008). Anthocyanin excretion by humans increases linearly with increasing strawberry dose. *The Journal of Nutrition* **138**(5)**:** 897-902.

Carter RA, Wicks IP (2001). Vascular cell adhesion molecule 1 (CD106): a multifaceted regulator of joint inflammation. *Arthritis & Rheumatism* **44**(5)**:** 985-994.

Cassidy A, Mukamal KJ, Liu L, Franz M, Eliassen AH, Rimm EB (2013). High anthocyanin intake is associated with a reduced risk of myocardial infarction in young and middle-aged women. *Circulation* **127**(2)**:** 188-196.

Cassidy A, O'Reilly ÉJ, Kay CD, Sampson L, Franz M, Forman J, *et al.* (2011). Habitual intake of flavonoid subclasses and incident hypertension in adults. *Am J Clin Nutr* **93**(2)**:** 338-347.

Castañeda-Ovando A, Pacheco-Hernández MdL, Páez-Hernández ME, Rodríguez JA, Galán-Vidal CA (2009). Chemical studies of anthocyanins: A review. *Food Chemistry* **113**(4)**:** 859-871.

Chalker-Scott L (1999). Environmental significance of anthocyanins in plant stress responses. *Photochemistry and Photobiology* **70**(1)**:** 1-9.

Chao P-Y, Chen Y-L, Lin Y-C, Hsu J-I, Lin K-H, Lu Y-F, *et al.* (2013). Effects of black soybean on atherogenic prevention in hypercholesterolemic rabbits and on adhesion molecular expression in cultured HAECs. *Food and Nutrition* **4:** 9-21.

Charron CS, Clevidence BA, Britz SJ, Novotny JA (2007). Effect of dose size on bioavailability of acylated and nonacylated anthocyanins from red cabbage (Brassica oleracea L. Var. capitata). *J Agric Food Chem* **55**(13)**:** 5354-5362.

Cheminat A, Brouillard R (1986). PMR investigation of 3-O-([beta]-d-glucosyl)malvidin structural transformations in aqueous solutions. *Tetrahedron Letters* **27**(37)**:** 4457-4460.

Chun OK, Chung SJ, Song WO (2007). Estimated dietary flavonoid intake and major food sources of U.S. adults. *J Nutr* **137**(5)**:** 1244-1252.

Clark LC, Thompson HL (1949). Determination of creatine and creatinine in urine. *Analytical Chemistry* **21**(10)**:** 1218-1221.

Crozier A, Del Rio D, Clifford MN (2010). Bioavailability of dietary flavonoids and phenolic compounds. *Molecular Aspects of Medicine* **31**(6)**:** 446-467.

Crozier A, Jaganath IB, Clifford MN (2009). Dietary phenolics: chemistry, bioavailability and effects on health. *Natural product reports* **26**(8)**:** 1001-1043.

Curtis PJ, Kroon PA, Hollands WJ, Walls R, Jenkins G, Kay CD, *et al.* (2009). Cardiovascular disease risk biomarkers and liver and kidney function are not altered

in postmenopausal women after ingesting an elderberry extract rich in anthocyanins for 12 weeks. *J. Nutr.* **139**(12)**:** 2266-2271.

Czank C, Cassidy A, Zhang Q, Morrison DJ, Preston T, Kroon PA, *et al.* (2013). Human metabolism and elimination of the anthocyanin, cyanidin-3-glucoside: a 13C-tracer study. *Am. J. Clin. Nutr.* **97**(5)**:** 995-1003.

Dandona P, Aljada A, Bandyopadhyay A (2004). Inflammation: the link between insulin resistance, obesity and diabetes. *Trends in immunology* **25**(1)**:** 4-7.

Das NP, Griffiths LA (1969). Studies on flavonoid metabolism. Metabolism of (+)-[14C] catechin in the rat and guinea pig. *Biochem J* **115**(4)**:** 831-836.

Day AJ, Cañada FJ, Díaz JC, Kroon PA, McLauchlan R, Faulds CB, *et al.* (2000). Dietary flavonoid and isoflavone glycosides are hydrolysed by the lactase site of lactase phlorizin hydrolase. *FEBS Letters* **468**(2-3)**:** 166-170.

de Ferrars RM, Cassidy A, Curtis P, Kay CD (2013). Phenolic metabolites of anthocyanins following a dietary intervention study in postmenopausal women. *Mol Nutr Food Res*.

de Ferrars RM, Czank C, Zhang Q, Botting NP, Kroon PA, Cassidy A, *et al.* (2014). The pharmacokinetics of anthocyanins and their metabolites in humans *British Journal of Pharmacology***:** TBC.

de Pascual-Teresa S, Moreno DA, Garcia-Viguera C (2010). Flavanols and anthocyanins in cardiovascular health: a review of current evidence. *Int J Mol Sci* **11**(4)**:** 1679-1703.

Del Bo' C, Riso P, Brambilla A, Gardana C, Rizzolo A, Simonetti P, *et al.* (2012). Blanching improves anthocyanin absorption from highbush blueberry (Vaccinium corymbosum L.) purée in healthy human volunteers: A pilot study. *J. Agric. Food. Chem.* **60**(36)**:** 9298-9304.

Del Rio D, Borges G, Crozier A (2010). Berry flavonoids and phenolics: bioavailability and evidence of protective effects. *Br J Nutr* **104 Suppl 3:** S67-90.

Del Rio D, Rodriguez-Mateos A, Spencer JP, Tognolini M, Borges G, Crozier A (2013). Dietary (poly) phenolics in human health: structures, bioavailability, and evidence of protective effects against chronic diseases. *Antioxidants & redox signaling* **18**(14)**:** 1818-1892.

Donovan JL, Bell JR, Kasim-Karakas S, German JB, Walzem RL, Hansen RJ, *et al.* (1999). Catechin is present as metabolites in human plasma after consumption of red wine. *J Nutr* **129**(9)**:** 1662.

Donovan JL, Kasim-Karakas S, German JB, Waterhouse AL (2002). Urinary excretion of catechin metabolites by human subjects after red wine consumption. *Br J Nutr* **87**(1)**:** 31-37.

Dykes L, Rooney LW (2007). Phenolic compounds in cereal grains and their health benefits. *Cereal Foods Worldwide* **52**(3)**:** 105-111.

Edirisinghe I, Banaszewski K, Cappozzo J, McCarthy D, Burton-Freeman BM (2011). Effect of black currant anthocyanins on the activation of endothelial nitric oxide synthase (eNOS) in vitro in human endothelial cells. *J. Agric. Food. Chem.* **59**(16)**:** 8616-8624.

Egert S, Wolffram S, Bosy-Westphal A, Boesch-Saadatmandi C, Wagner AE, Frank J, *et al.* (2008). Daily quercetin supplementation dose-dependently increases plasma quercetin concentrations in healthy humans. *J. Nutr.* **138**(9)**:** 1615-1621.

Epstein FH, Ross R (1999). Atherosclerosis—an inflammatory disease. *New England journal of medicine* **340**(2)**:** 115-126.

Erdman JW, Jr., Balentine D, Arab L, Beecher G, Dwyer JT, Folts J, *et al.* (2007). Flavonoids and Heart Health: proceedings of the ILSI North America Flavonoids Workshop, May 31-June 1, 2005, Washington, DC. *J Nutr* **137**(3)**:** 718S-737S.

Fallingborg J (1999). Intraluminal pH of the human gastrointestinal tract. *Dan Med Bull* **46**(3)**:** 183-196.

Faria A, Pestana D, Azevedo J, Martel F, de Freitas V, Azevedo I, *et al.* (2009). Absorption of anthocyanins through intestinal epithelial cells – Putative involvement of GLUT2. *Mol Nutr Food Res* **53**(11)**:** 1430-1437.

Farrell T, Poquet L, Dionisi F, Barron D, Williamson G (2011). Characterization of hydroxycinnamic acid glucuronide and sulfate conjugates by HPLC-DAD-MS2: Enhancing chromatographic quantification and application in Caco-2 cell metabolism. *Journal of Pharmaceutical and Biomedical Analysis* **55**(5)**:** 1245-1254.

FDA (2001). Food and drug administration. Guidance for industry: bioanalytical method validation. In: *US Department of Health and Human Services, Food and Drug Administration, Center for Drug Evaluation and Research, Rockville, MD:* .

Feild TS, Lee DW, Holbrook NM (2001). Why leaves turn red in autumn. The role of anthocyanins in senescing leaves of red-osier dogwood. *Plant Physiology* **127**(2)**:** 566-574.

Felgines C, Krisa S, Mauray A, Besson C, Lamaison JL, Scalbert A, *et al.* (2010). Radiolabelled cyanidin 3-O-glucoside is poorly absorbed in the mouse. *Br J Nutr* **103**(12)**:** 1738-1745.

Felgines C, Talavera S, Gonthier MP, Texier O, Scalbert A, Lamaison JL, *et al.* (2003). Strawberry anthocyanins are recovered in urine as glucuro- and sulfoconjugates in humans. *J Nutr* **133**(5)**:** 1296-1301.

Felgines C, Talavera S, Texier O, Gil-Izquierdo A, Lamaison JL, Remesy C (2005). Blackberry anthocyanins are mainly recovered from urine as methylated and glucuronidated conjugates in humans. *J. Agric. Food. Chem.* **53**(20)**:** 7721-7727.

Feng R, Ni HM, Wang SY, Tourkova IL, Shurin MR, Harada H, *et al.* (2007). Cyanidin-3-rutinoside, a natural polyphenol antioxidant, selectively kills leukemic cells by induction of oxidative stress. *J Biol Chem* **282**(18)**:** 13468-13476.

Fernandes I, Azevedo J, Faria A, Calhau C, de Freitas V, Mateus N (2008). Enzymatic hemisynthesis of metabolites and conjugates of anthocyanins. *J Agric Food Chem* **57**(2)**:** 735-745.

Fiamegos YC, Nanos CG, Vervoort J, Stalikas CD (2004). Analytical procedure for the in-vial derivatization—extraction of phenolic acids and flavonoids in methanolic and aqueous plant extracts followed by gas chromatography with mass-selective detection. *Journal of Chromatography A* **1041**(1)**:** 11-18.

Fleschhut J, Kratzer F, Rechkemmer G, Kulling SE (2006). Stability and biotransformation of various dietary anthocyanins in vitro. *Eur J Nutr* **45**(1)**:** 7-18.

Forester SC, Waterhouse AL (2008). Identification of Cabernet Sauvignon Anthocyanin Gut Microflora Metabolites. *J. Agric. Food. Chem.* **56**(19)**:** 9299-9304.

Förstermann U, Sessa WC (2012). Nitric oxide synthases: regulation and function. *European Heart Journal* **33**(7)**:** 829-837.

Fossen T, Cabrita L, Andersen OM (1998). Colour and stability of pure anthocyanins influenced by pH including the alkaline region. *Food Chemistry* **63**(4)**:** 435-440.

Fotis L, Giannakopoulos D, Stamogiannou L, Xatzipsalti M (2012). Intercellular cell adhesion molecule-1 and vascular cell adhesion molecule-1 in children. Do they play a role in the progression of atherosclerosis. *Hormones* **11:** 140-146.

Freudenthaler S, Meineke I, Schreeb K, Boakye E, Gundert-Remy U, Gleiter C (1998). Influence of urine pH and urinary flow on the renal excretion of memantine. *British journal of clinical pharmacology* **46:** 541-546.

Gabay C (2006). Interleukin-6 and chronic inflammation. *Arthritis research and therapy* **8**(2)**:** S3.

Garcia-Alonso M, Minihane A-M, Rimbach G, Rivas-Gonzalo JC, de Pascual-Teresa S (2009). Red wine anthocyanins are rapidly absorbed in humans and affect monocyte chemoattractant protein 1 levels and antioxidant capacity of plasma. *J. Nutr. Biochem.* **20**(7)**:** 521-529.

García-Lafuente A, Guillamón E, Villares A, Rostagno M, Martínez J (2009). Flavonoids as anti-inflammatory agents: implications in cancer and cardiovascular disease. *Inflamm. Res.* **58**(9)**:** 537-552.

Gee JM, DuPont MS, Day AJ, Plumb GW, Williamson G, Johnson IT (2000). Intestinal transport of quercetin glycosides in rats involves both deglycosylation and interaction with the hexose transport pathway. *J Nutr* **130**(11)**:** 2765-2771.

Gee JM, DuPont MS, Rhodes MJ, Johnson IT (1998). Quercetin glucosides interact with the intestinal glucose transport pathway. *Free Radic Biol Med* **25**(1)**:** 19-25.

Gonzalez-Barrio R, Christine E, Crozier A (2011). Colonic Catabolism of Ellagitannins, Ellagic acid and Raspberry Anthocyanins: In Vivo and In Vitro Studies. *Drug Metab Dispos*.

González-Barrio Ro, Borges G, Mullen W, Crozier A (2010). Bioavailability of anthocyanins and ellagitannins following consumption of raspberries by healthy humans and subjects with an ileostomy. *J. Agric. Food. Chem.* **58**(7)**:** 3933-3939.

Gould KS (2004). Nature's swiss army knife: the diverse protective roles of anthocyanins in leaves. *Journal of Biomedicine and Biotechnology* **2004**(5)**:** 314-320.

Graf BA, Ameho C, Dolnikowski GG, Milbury PE, Chen CY, Blumberg JB (2006). Rat gastrointestinal tissues metabolize quercetin. *J Nutr* **136**(1)**:** 39.

Griffiths L, Barrow A (1972). Metabolism of flavonoid compounds in germ-free rats. *Biochemical Journal* **130**(4)**:** 1161-1162.

Hämäläinen M, Nieminen R, Vuorela P, Heinonen M, Moilanen E (2007). Anti-inflammatory effects of flavonoids: genistein, kaempferol, quercetin, and daidzein inhibit STAT-1 and NF-κ B activations, whereas flavone, isorhamnetin, naringenin, and pelargonidin inhibit only NF-κ B activation along with their inhibitory effect on iNOS expression and NO production in activated macrophages. *Mediators of inflammation* **2007**.

Harada K, Kano M, Takayanagi T, Yamakawa O, Ishikawa F (2004). Absorption of acylated anthocyanins in rats and humans after ingesting an extract of Ipomoea batatas purple sweet potato tuber. *Bioscience, biotechnology, and biochemistry* **68**(7)**:** 1500-1507.

Hassimotto NMA, Genovese MI, Lajolo FM (2008). Absorption and metabolism of cyanidin-3-glucoside and cyanidin-3-rutinoside extracted from wild mulberry (Morus nigra L.) in rats. *Nutr Res* **28**(3)**:** 198-207.

He J, Wallace TC, Keatley KE, Failla ML, Giusti MMn (2009). Stability of black raspberry anthocyanins in the digestive tract lumen and transport efficiency into gastric and small intestinal tissues in the rat. *J. Agric. Food. Chem.* **57**(8)**:** 3141-3148.

Heiss C, Jahn S, Taylor M, Real WM, Angeli FS, Wong ML, *et al.* (2010). Improvement of endothelial function with dietary flavanols is associated with

mobilization of circulating angiogenic cells in patients with coronary artery disease. *J Am Coll Cardiol* **56**(3)**:** 218-224.

Hertrampf R, Gundert-Remy U, Beckmann J, Hoppe U, Elsäßer W, Stein H (1991). Elimination of flecainide as a function of urinary flow rate and pH. *European journal of clinical pharmacology* **41**(1)**:** 61-63.

Hirano M, Osada S-i, Aoki T, Hirai S-i, Hosaka M, Inoue J-i, *et al.* (1996). MEK kinase is involved in tumor necrosis factor α-induced NF-κB activation and degradation of IκB-α. *Journal of Biological Chemistry* **271**(22)**:** 13234-13238.

Hollands W, Brett GM, Dainty JR, Teucher B, Kroon PA (2008). Urinary excretion of strawberry anthocyanins is dose dependent for physiological oral doses of fresh fruit. *Mol Nutr Food Res* **52**(10)**:** 1097-1105.

Hollman PC, Bijsman MN, van Gameren Y, Cnossen EP, de Vries JH, Katan MB (1999). The sugar moiety is a major determinant of the absorption of dietary flavonoid glycosides in man. *Free Radic Res* **31**(6)**:** 569-573.

Hollman PC, de Vries JH, van Leeuwen SD, Mengelers MJ, Katan MB (1995). Absorption of dietary quercetin glycosides and quercetin in healthy ileostomy volunteers. *Am J Clin Nutr* **62**(6)**:** 1276-1282.

Hollman PCH (2004). Absorption, bioavailability, and metabolism of flavonoids. *Pharmaceutical Biology* **42**(s1)**:** 74-83.

Hong Y-J, Mitchell AE (2006). Identification of glutathione-related quercetin metabolites in humans. *Chemical research in toxicology* **19**(11)**:** 1525-1532.

Hooper L, Kroon PA, Rimm EB, Cohn JS, Harvey I, Le Cornu KA, *et al.* (2008). Flavonoids, flavonoid-rich foods, and cardiovascular risk: a meta-analysis of randomized controlled trials. *Am. J. Clin. Nutr.* **88**(1)**:** 38-50.

Huang J, Bathena SPR, Alnouti Y (2010). Metabolite profiling of praziquantel and its analogs during the analysis of in vitro metabolic stability using information-dependent acquisition on a hybrid triple quadrupole linear ion trap mass spectrometer. *Drug metabolism and pharmacokinetics* **25**(5)**:** 487-499.

Ichiyanagi T, Rahman MM, Hatano Y, Konishi T, Ikeshiro Y (2007). Protocatechuic acid is not the major metabolite in rat blood plasma after oral administration of cyanidin 3-O-[beta]-d-glucopyranoside. *Food Chemistry* **105**(3)**:** 1032-1039.

Ichiyanagi T, Rahman MM, Kashiwada Y, Ikeshiro Y, Shida Y, Hatano Y, *et al.* (2004). Absorption and metabolism of delphinidin 3-O-β-d-glucopyranoside in rats. *Free Radical Biology and Medicine* **36**(7)**:** 930-937.

Ichiyanagi T, Shida Y, Rahman MM, Hatano Y, Konishi T (2006). Bioavailability and tissue distribution of anthocyanins in bilberry (Vaccinium myrtillus L.) extract in rats. *J. Agric. Food. Chem.* **54**(18)**:** 6578-6587.

Jennings A, Welch AA, Fairweather-Tait SJ, Kay C, Minihane A-M, Chowienczyk P, *et al.* (2012). Higher anthocyanin intake is associated with lower arterial stiffness and central blood pressure in women. *The American Journal of Clinical Nutrition* **96**(4)**:** 781-788.

Jeong J-W, Lee WS, Shin SC, Kim G-Y, Choi BT, Choi YH (2013). Anthocyanins downregulate lipopolysaccharide-induced inflammatory responses in BV2 microglial cells by suppressing the NF-κB and Akt/MAPKs signaling pathways. *International journal of molecular sciences* **14**(1)**:** 1502-1515.

Kahle K, Kraus M, Scheppach W, Ackermann M, Ridder F, Richling E (2006). Studies on apple and blueberry fruit constituents: Do the polyphenols reach the colon after ingestion? *Mol Nutr Food Res* **50**(4-5)**:** 418-423.

Karlsen A, Retterstøl L, Laake P, Paur I, Kjølsrud-Bøhn S, Sandvik L, *et al.* (2007). Anthocyanins inhibit nuclear factor-κB activation in monocytes and reduce plasma concentrations of pro-inflammatory mediators in healthy adults. *The Journal of Nutrition* **137**(8)**:** 1951-1954.

Kataoka H, Saito K, Yokoyama A (2010). Sampling and sample preparation for clinical and pharmaceutical analysis. In: Pawliszyn J, Lord HL (ed)^(eds). *Handbook of Sample Preparation*, edn. Veinheim Wiley-VCH Verlag. p^pp 285-313.

Kay CD (2010). The future of flavonoid research. *Br. J. Nutr.* **104**(SupplementS3)**:** S91-S95.

Kay CD, Hooper L, Kroon PA, Rimm EB, Cassidy A (2012). Relative impact of flavonoid composition, dose and structure on vascular function: A systematic review of randomised controlled trials of flavonoid-rich food products. *Mol Nutr Food Res* **56**(11)**:** 1605-1616.

Kay CD, Kroon PA, Cassidy A (2009). The bioactivity of dietary anthocyanins is likely to be mediated by their degradation products. *Mol Nutr Food Res* **53**(S1)**:** 92-101.

Kay CD, Mazza G, Holub BJ (2005). Anthocyanins exist in the circulation primarily as metabolites in adult men. *The Journal of Nutrition* **135**(11)**:** 2582-2588.

Kay CD, Mazza G, Holub BJ, Wang J (2004). Anthocyanin metabolites in human urine and serum. *Br. J. Nutr.* **91**(6)**:** 933-942.

Keppler K, Humpf HU (2005). Metabolism of anthocyanins and their phenolic degradation products by the intestinal microflora. *Bioorg Med Chem* **13**(17)**:** 5195-5205.

Keski-Hynnilä H, Kurkela M, Elovaara E, Antonio L, Magdalou J, Luukkanen L, *et al.* (2002). Comparison of electrospray, atmospheric pressure chemical ionization,

and atmospheric pressure photoionization in the identification of apomorphine, dobutamine, and entacapone phase II metabolites in biological samples. *Analytical Chemistry* **74**(14)**:** 3449-3457.

Kim DH, Jung EA, Sohng IS, Han JA, Kim TH, Han MJ (1998). Intestinal bacterial metabolism of flavonoids and its relation to some biological activities. *Archives of pharmacal research* **21**(1)**:** 17-23.

Kim HJ, Tsoy I, Park JM, Chung JI, Shin SC, Chang KC (2006). Anthocyanins from soybean seed coat inhibit the expression of TNF-α-induced genes associated with ischemia/reperfusion in endothelial cell by NF-κB-dependent pathway and reduce rat myocardial damages incurred by ischemia and reperfusion in vivo. *FEBS letters* **580**(5)**:** 1391-1397.

Kim S-J, Kim M-C, Um J-Y, Hong S-H (2010). The beneficial effect of vanillic acid on ulcerative colitis. *Molecules* **15**(10)**:** 7208-7217.

Kırca A, Özkan M, Cemeroğlu B (2007). Effects of temperature, solid content and pH on the stability of black carrot anthocyanins. *Food Chemistry* **101**(1)**:** 212-218.

Kodama DH, Gonçalves AEdSS, Lajolo FM, Genovese MI (2010). Flavonoids, total phenolics and antioxidant capacity: comparison between commercial green tea preparations. *Food Science and Technology (Campinas)* **30**(4)**:** 1077-1082.

Koli R, Erlund I, Jula A, Marniemi J, Mattila P, Alfthan G (2010). Bioavailability of various polyphenols from a diet containing moderate amounts of berries. *J. Agric. Food. Chem.* **58**(7)**:** 3927-3932.

Kottra G, Daniel H (2007). Flavonoid glycosides are not transported by the human Na+/glucose transporter when expressed in Xenopus laevis oocytes, but effectively inhibit electrogenic glucose uptake. *J Pharmacol Exp Ther* **322**(2)**:** 829-835.

Kraemer-Schafhalter A, Fuchs H, Pfannhauser W (1998). Solid-phase extraction (SPE)—a comparison of 16 materials for the purification of anthocyanins from aronia melanocarpa var Nero. *Journal of the Science of Food and Agriculture* **78**(3)**:** 435-440.

Kurilich AC, Clevidence BA, Britz SJ, Simon PW, Novotny JA (2005). Plasma and urine responses are lower for acylated vs nonacylated anthocyanins from raw and cooked purple carrots. *J. Agric. Food. Chem.* **53**(16)**:** 6537-6542.

Kylli P, Nohynek L, Puupponen-Pimiä R, Westerlund-Wikström B, McDougall G, Stewart D, *et al.* (2010). Rowanberry phenolics: Compositional analysis and bioactivities. *J Agric Food Chem.*

Lapidot T, Harel S, Granit R, Kanner J (1998). Bioavailability of red wine anthocyanins as detected in human urine. *J. Agric. Food. Chem.* **46**(10)**:** 4297-4302.

Lee J, Ebeler SE, Zweigenbaum JA, Mitchell AE (2012). UHPLC-(ESI)QTOF MS/MS profiling of quercetin metabolites in human plasma postconsumption of applesauce enriched with apple peel and onion. *J. Agric. Food. Chem.* **60**(34)**:** 8510-8520.

Levsen K, Schiebel HM, Behnke B, Dotzer R, Dreher W, Elend M, *et al.* (2005). Structure elucidation of phase II metabolites by tandem mass spectrometry: an overview. *J Chromatogr A* **1067**(1-2)**:** 55-72.

Libby P, Ridker PM, Maseri A (2002). Inflammation and atherosclerosis. *Circulation* **105**(9)**:** 1135-1143.

Lin S-J, Shyue S-K, Shih M-C, Chu T-H, Chen Y-H, Ku H-H, *et al.* (2007). Superoxide dismutase and catalase inhibit oxidized low-density lipoprotein-induced human aortic smooth muscle cell proliferation: Role of cell-cycle regulation, mitogen-activated protein kinases, and transcription factors. *Atherosclerosis* **190**(1)**:** 124-134.

Liu A-H, Guo H, Ye M, Lin Y-H, Sun J-H, Xu M, *et al.* (2007). Detection, characterization and identification of phenolic acids in Danshen using high-performance liquid chromatography with diode array detection and electrospray ionization mass spectrometry. *Journal of Chromatography A* **1161**(1–2)**:** 170-182.

Manach C, Williamson G, Morand C, Scalbert A, Remesy C (2005). Bioavailability and bioefficacy of polyphenols in humans. I. Review of 97 bioavailability studies. *Am. J. Clin. Nutr.* **81**(1 Suppl)**:** 230S-242S.

Manzano S, Williamson G (2010). Polyphenols and phenolic acids from strawberry and apple decrease glucose uptake and transport by human intestinal Caco-2 cells. *Mol Nutr Food Res* **54**(12)**:** 1773-1780.

Marks SC, Mullen W, Borges G, Crozier A (2009). Absorption, metabolism, and excretion of cider dihydrochalcones in healthy humans and subjects with an ileostomy. *J Agric Food Chem* **57**(5)**:** 2009-2015.

Matheny HE, Deem TL, Cook-Mills JM (2000). Lymphocyte migration through monolayers of endothelial cell lines involves VCAM-1 signaling via endothelial cell NADPH oxidase. *The Journal of Immunology* **164**(12)**:** 6550-6559.

Matsumoto H, Inaba H, Kishi M, Tominaga S, Hirayama M, Tsuda T (2001). Orally administered delphinidin 3-rutinoside and cyanidin 3-rutinoside are directly absorbed in rats and humans and appear in the blood as the intact forms. *J Agric Food Chem* **49**(3)**:** 1546-1551.

Mazza G, Brouillard R (1987). Recent developments in the stabilization of anthocyanins in food products. *Food Chemistry* **25**(3)**:** 207-225.

Mazza G, Cacace JE, Kay CD (2004). Methods of analysis for anthocyanins in plants and biological fluids. *J AOAC Int* **87**(1)**:** 129-145.

Mazza G, Kay CD, Cottrell T, Holub BJ (2002). Absorption of anthocyanins from blueberries and serum antioxidant status in human subjects. *J Agric Food Chem* **50**(26)**:** 7731-7737.

McCullough ML, Peterson JJ, Patel R, Jacques PF, Shah R, Dwyer JT (2012). Flavonoid intake and cardiovascular disease mortality in a prospective cohort of US adults. *Am J Clin Nutr* **95**(2)**:** 454-464.

McDougall GJ, Dobson P, Smith P, Blake A, Stewart D (2005a). Assessing potential bioavailability of raspberry anthocyanins using an in vitro digestion system. *J. Agric. Food. Chem.* **53**(15)**:** 5896-5904.

McDougall GJ, Fyffe S, Dobson P, Stewart D (2007). Anthocyanins from red cabbage - stability to simulated gastrointestinal digestion. *Phytochemistry* **68**(9)**:** 1285-1294.

McDougall GJ, Fyffe S, Dobson P, Stewart D (2005b). Anthocyanins from red wine - Their stability under simulated gastrointestinal digestion. *Phytochemistry* **66**(21)**:** 2540-2548.

McGhie TK, Ainge GD, Barnett LE, Cooney JM, Jensen DJ (2003). Anthocyanin glycosides from berry fruit are absorbed and excreted unmetabolized by both humans and rats. *J Agric Food Chem* **51**(16)**:** 4539-4548.

McGhie TK, Walton MC (2007). The bioavailability and absorption of anthocyanins: towards a better understanding. *Mol Nutr Food Res* **51**(6)**:** 702-713.

Milbury PE, Cao G, Prior RL, Blumberg J (2002). Bioavailablility of elderberry anthocyanins. *Mech. Ageing Dev.* **123**(8)**:** 997-1006.

Milbury PE, Vita JA, Blumberg JB (2010). Anthocyanins are bioavailable in humans following an acute dose of cranberry juice. *The Journal of Nutrition* **140**(6)**:** 1099-1104.

Millburn P, Smith R, Williams R (1967). Biliary excretion of foreign compounds. Biphenyl, stilboestrol and phenolphthalein in the rat: molecular weight, polarity and metabolism as factors in biliary excretion. *Biochem. J* **105:** 1275-1281.

Miller DL, Yaron R, Yellin MJ (1998). CD40L-CD40 interactions regulate endothelial cell surface tissue factor and thrombomodulin expression. *Journal of Leukocyte Biology* **63**(3)**:** 373-379.

Miller KC, Mack G, Knight KL (2009). Electrolyte and plasma changes after ingestion of pickle juice, water, and a common carbohydrate-electrolyte solution. *Journal of athletic training* **44**(5)**:** 454.

Min S-W, Ryu S-N, Kim D-H (2010). Anti-inflammatory effects of black rice, cyanidin-3-O-β-D-glycoside, and its metabolites, cyanidin and protocatechuic acid. *International immunopharmacology* **10**(8)**:** 959-966.

Mink PJ, Scrafford CG, Barraj LM, Harnack L, Hong CP, Nettleton JA, *et al.* (2007). Flavonoid intake and cardiovascular disease mortality: a prospective study in postmenopausal women. *Am. J. Clin. Nutr.* **85**(3)**:** 895-909.

Miyazaki K, Makino K, Iwadate E, Deguchi Y, Ishikawa F (2008). Anthocyanins from purple sweet potato Ipomoea batatas cultivar ayamurasaki suppress the development of atherosclerotic lesions and both enhancements of oxidative stress and soluble vascular cell adhesion molecule-1 in apolipoprotein E-deficient mice. *J. Agric. Food. Chem.* **56**(23)**:** 11485-11492.

Miyazawa T, Nakagawa K, Kudo M, Muraishi K, Someya K (1999). Direct intestinal absorption of red fruit anthocyanins, cyanidin-3-glucoside and cyanidin-3,5-diglucoside, into rats and humans. *J. Agric. Food. Chem.* **47**(3)**:** 1083-1091.

Mladěnka P, Zatloukalová L, Filipský T, Hrdina R (2010). Cardiovascular effects of flavonoids are not caused only by direct antioxidant activity. *Free Radical Biology and Medicine* **49**(6)**:** 963-975.

Moridani MY, Scobie H, Salehi P, O'Brien PJ (2001). Catechin metabolism: glutathione conjugate formation catalyzed by tyrosinase, peroxidase, and cytochrome p450. *Chem Res Toxicol* **14**(7)**:** 841-848.

Mulder TP, Rietveld AG, van Amelsvoort JM (2005). Consumption of both black tea and green tea results in an increase in the excretion of hippuric acid into urine. *Am. J. Clin. Nutr.* **81**(1)**:** 256S-260S.

Mülleder U, Murkovic M, Pfannhauser W (2002). Urinary excretion of cyanidin glycosides. *J. Biochem. Biophys. Methods* **53**(1-3)**:** 61-66.

Mullen W, Borges G, Donovan JL, Edwards CA, Serafini M, Lean MEJ, *et al.* (2009). Milk decreases urinary excretion but not plasma pharmacokinetics of cocoa flavan-3-ol metabolites in humans. *Am J Clin Nutr* **89**(6)**:** 1784.

Mullen W, Edwards CA, Serafini M, Crozier A (2008a). Bioavailability of pelargonidin-3-O-glucoside and Its metabolites in humans following the ingestion of strawberries with and without cream. *J. Agric. Food. Chem.* **56**(3)**:** 713-719.

Mullen W, Graf BA, Caldwell ST, Hartley RC, Duthie GG, Edwards CA, *et al.* (2002). Determination of flavonol metabolites in plasma and tissues of rats by HPLC-radiocounting and tandem mass spectrometry following oral ingestion of [2-14C] quercetin-4'-glucoside. *J Agric Food Chem* **50**(23)**:** 6902-6909.

Mullen W, Rouanet J-M, Auger C, Teissèdre P-L, Caldwell ST, Hartley RC, *et al.* (2008b). Bioavailability of [2-14C]quercetin-4′-glucoside in rats. *J. Agric. Food. Chem.* **56**(24)**:** 12127-12137.

Murkovic M, Mülleder U, Adam U, Pfannhauser W (2001). Detection of anthocyanins from elderberry juice in human urine. *J. Sci. Food Agric.* **81**(9)**:** 934-937.

Mutlib AE (2008). Application of stable isotope-labeled compounds in metabolism and in metabolism-mediated toxicity studies. *Chemical research in toxicology* **21**(9)**:** 1672-1689.

Nardini M, Forte M, Vrhovsek U, Mattivi F, Viola R, Scaccini C (2009). White wine phenolics are absorbed and extensively metabolized in humans. *Journal of Agricultural and Food Chemistry* **57**(7)**:** 2711-2718.

Nardini M, Natella F, Scaccini C, Ghiselli A (2006). Phenolic acids from beer are absorbed and extensively metabolized in humans. *The Journal of Nutritional Biochemistry* **17**(1)**:** 14-22.

Netzel M, Strass G, Herbst M, Dietrich H, Bitsch R, Bitsch I, *et al.* (2005). The excretion and biological antioxidant activity of elderberry antioxidants in healthy humans. *Food Research International* **38**(8)**:** 905-910.

Neveu V, Perez-Jiménez J, Vos F, Crespy V, du Chaffaut L, Mennen L, *et al.* (2010). Phenol-Explorer: an online comprehensive database on polyphenol contents in foods. *Database* **2010**.

Nizamutdinova IT, Kim YM, Chung JI, Shin SC, Jeong Y-K, Seo HG, *et al.* (2009). Anthocyanins from black soybean seed coats preferentially inhibit TNF-α-mediated induction of VCAM-1 over ICAM-1 through the regulation of GATAs and IRF-1. *J. Agric. Food. Chem.* **57**(16)**:** 7324-7330.

Nurmi T, Mursu J, Heinonen M, Nurmi A, Hiltunen R, Voutilainen S (2009). Metabolism of berry anthocyanins to phenolic acids in humans. *J. Agric. Food. Chem.* **57**(6)**:** 2274-2281.

Ohnishi R, Ito H, Kasajima N, Kaneda M, Kariyama R, Kumon H, *et al.* (2006). Urinary excretion of anthocyanins in humans after cranberry juice ingestion. *Bioscience, biotechnology, and biochemistry* **70**(7)**:** 1681-1687.

Ovaskainen M-L, Törrönen R, Koponen JM, Sinkko H, Hellström J, Reinivuo H, *et al.* (2008). Dietary intake and major food sources of polyphenols in finnish adults. *The Journal of Nutrition* **138**(3)**:** 562-566.

Pamukcu B, Lip GY, Snezhitskiy V, Shantsila E (2011). The CD40-CD40L system in cardiovascular disease. *Annals of medicine* **43**(5)**:** 331-340.

Passamonti S, Vrhovsek U, Mattivi F (2002). The interaction of anthocyanins with bilitranslocase. *Biochemical and Biophysical Research Communications* **296**(3)**:** 631-636.

Passamonti S, Vrhovsek U, Vanzo A, Mattivi F (2003). The stomach as a site for anthocyanins absorption from food. *FEBS Lett* **544**(1-3)**:** 210-213.

Patras A, Brunton NP, O'Donnell C, Tiwari BK (2010). Effect of thermal processing on anthocyanin stability in foods; mechanisms and kinetics of degradation. *Trends in Food Science & Technology* **21**(1)**:** 3-11.

Pereira D, Valentão P, Pereira J, Andrade P (2009). Phenolics: from chemistry to biology. *Molecules* **14**(6)**:** 2202-2211.

Pérez-Vicente A, Gil-Izquierdo A, García-Viguera C (2002). In vitro gastrointestinal digestion study of pomegranate juice phenolic compounds, anthocyanins, and bitamin C. *J. Agric. Food. Chem.* **50**(8)**:** 2308-2312.

Pergola C, Rossi A, Dugo P, Cuzzocrea S, Sautebin L (2006). Inhibition of nitric oxide biosynthesis by anthocyanin fraction of blackberry extract. *Nitric oxide* **15**(1)**:** 30-39.

Pero RW (2010). Health consequences of catabolic synthesis of hippuric acid in humans. *Current Clinical Pharmacology* **5**(1)**:** 67-73.

Piffaut B, Kader F, Girardin M, Metche M (1994). Comparative degradation pathways of malvidin 3,5-diglucoside after enzymatic and thermal treatments. *Food Chemistry* **50**(2)**:** 115-120.

Piskula MK, Terao J (1998). Accumulation of (−)-epicatechin metabolites in rat plasma after oral administration and distribution of conjugation enzymes in rat tissues. *The Journal of Nutrition* **128**(7)**:** 1172-1178.

Plazonić A, Bucar F, Maleš Ž, Mornar A, Nigović B, Kujundžić N (2009). Identification and quantification of flavonoids and phenolic acids in burr parsley (Caucalis platycarpos L.), using high-performance liquid chromatography with diode array detection and electrospray ionization mass spectrometry. *Molecules* **14**(7)**:** 2466-2490.

Proudfoot AT, Krenzelok EP, Brent J, Vale JA (2003). Does urine alkalinization increase salicylate elimination? If so, why? *Toxicological reviews* **22**(3)**:** 129-136.

Qin J, Li R, Raes J, Arumugam M, Burgdorf KS, Manichanh C, *et al.* (2010). A human gut microbial gene catalogue established by metagenomic sequencing. *Nature* **464**(7285)**:** 59-65.

Qu J, Wang Y, Luo G, Wu Z (2001). Identification and determination of glucuronides and their aglycones in Erigeron breviscapus by liquid chromatography–tandem mass spectrometry. *Journal of Chromatography A* **928**(2)**:** 155-162.

Ramassamy C (2006). Emerging role of polyphenolic compounds in the treatment of neurodegenerative diseases: A review of their intracellular targets. *European Journal of Pharmacology* **545**(1)**:** 51-64.

Rechner AR, Kuhnle G, Bremner P, Hubbard GP, Moore KP, Rice-Evans CA (2002). The metabolic fate of dietary polyphenols in humans. *Free Radical Biology and Medicine* **33**(2)**:** 220-235.

Riches Z, Stanley EL, Bloomer JC, Coughtrie MWH (2009). Quantitative evaluation of the expression and activity of five major sulfotransferases (SULTs) in human tissues: the SULT "pie". *Drug Metabolism and Disposition* **37**(11)**:** 2255-2261.

Rissanen TH, Voutilainen S, Virtanen JK, Venho B, Vanharanta M, Mursu J, *et al.* (2003). Low intake of fruits, berries and vegetables is associated with excess mortality in men: the Kuopio Ischaemic Heart Disease Risk Factor (KIHD) Study. *The Journal of Nutrition* **133**(1)**:** 199-204.

Robbins RJ (2003). Phenolic acids in foods: an overview of analytical methodology. *J. Agric. Food. Chem.* **51**(10)**:** 2866-2887.

Rodriguez-Mateos A, Rendeiro C, Bergillos-Meca T, Tabatabaee S, George TW, Heiss C, *et al.* (2013). Intake and time dependence of blueberry flavonoid–induced improvements in vascular function: a randomized, controlled, double-blind, crossover intervention study with mechanistic insights into biological activity. *Am. J. Clin. Nutr.*

Roy S, Hawes E, Midha K (1987). Influence of urinary pH on the disposition of methoxyphenamine and three metabolites in humans. *Journal of pharmaceutical sciences* **76**(6)**:** 427-432.

Russell WR, Scobbie L, Labat A, Duthie GG (2009). Selective bio-availability of phenolic acids from Scottish strawberries. *Mol. Nutr. Food Res.* **53**(S1)**:** S85-S91.

Santhanam U, Ghrayeb J, Sehgal PB, May LT (1989). Post-translational modifications of human interleukin-6. *Archives of Biochemistry and Biophysics* **274**(1)**:** 161-170.

Sasaki R, Nishimura N, Hoshino H, Isa Y, Kadowaki M, Ichi T, *et al.* (2007). Cyanidin 3-glucoside ameliorates hyperglycemia and insulin sensitivity due to downregulation of retinol binding protein 4 expression in diabetic mice. *Biochemical Pharmacology* **74**(11)**:** 1619-1627.

Saxholt E, Christensen AT, Møller A, Hartkopp HB, Hess Ygil K, Hels OH ( 2008). Danish food composition databank, revision 7. *Database*.

Schmitzer V, Veberic R, Slatnar A, Stampar F (2010). Elderberry (Sambucus nigra L.) wine: a product rich in health promoting compounds. *J. Agric. Food. Chem.* **58**(18)**:** 10143-10146.

Schuett H, Luchtefeld M, Grothusen C, Grote K, Schieffer B (2009). How much is too much? Interleukin-6 and its signalling in atherosclerosis. *Thromb Haemost* **102**(2)**:** 215-222.

Seeram NP, Bourquin LD, Nair MG (2001). Degradation products of cyanidin glycosides from tart cherries and their bioactivities. *J. Agric. Food. Chem.* **49**(10)**:** 4924-4929.

Selma MaV, Espín JC, Tomás-Barberán FA (2009). Interaction between phenolics and gut microbiota: role in human health. *J. Agric. Food. Chem.* **57**(15)**:** 6485-6501.

Sen CK, Bagchi D (2001). Regulation of inducible adhesion molecule expression in human endothelial cells by grape seed proanthocyanidin extract. *Molecular and cellular biochemistry* **216**(1-2)**:** 1-7.

Sesso HD, Gaziano JM, Jenkins DJ, Buring JE (2007). Strawberry intake, lipids, C-reactive protein, and the risk of cardiovascular disease in women. *J Am Coll Nutr* **26**(4)**:** 303-310.

Shaked-Sachray L, Weiss D, Reuveni M, Nissim-Levi A, Oren-Shamir M (2002). Increased anthocyanin accumulation in aster flowers at elevated temperatures due to magnesium treatment. *Physiologia Plantarum* **114**(4)**:** 559-565.

Shirley BW (1996). Flavonoid biosynthesis:'new'functions for an 'old'pathway. *Trends in Plant Science* **1**(11)**:** 377-382.

Speciale A, Canali R, Chirafisi J, Saija A, Virgili F, Cimino F (2010). Cyanidin-3-O-glucoside protection against TNF-α-induced endothelial dysfunction: involvement of nuclear factor-κB signaling. *J. Agric. Food. Chem.* **58**(22)**:** 12048-12054.

Spencer J, Kuhnle G, Williams R, Rice-Evans C (2003). Intracellular metabolism and bioactivity of quercetin and its in vivo metabolites. *Biochem. J* **372:** 173-181.

Stalmach A, Mullen W, Barron D, Uchida K, Yokota T, Cavin C, *et al.* (2009a). Metabolite profiling of hydroxycinnamate derivatives in plasma and urine after the ingestion of coffee by humans: identification of biomarkers of coffee consumption. *Drug Metab Disp* **37**(8)**:** 1749.

Stalmach A, Mullen W, Pecorari M, Serafini M, Crozier A (2009b). Bioavailability of C-linked dihydrochalcone and flavanone glucosides in humans following ingestion of unfermented and fermented rooibos teas. *J Agric Food Chem* **57**(15)**:** 7104-7111.

Sun J, Liang F, Bin Y, Li P, Duan C (2007). Screening non-colored phenolics in red wines using liquid chromatography/ultraviolet and mass spectrometry/mass spectrometry libraries. *Molecules* **12**(3)**:** 679-693.

Sun RX, Lu ZY, Wijdenes J, Brochier J, Hertog C, Rossi JF, *et al.* (1997). Large scale and clinical grade purification of syndecan-1+ malignant plasma cells. *J Immunol Methods* **205**(1)**:** 73-79.

Talavéra S, Felgines C, Texier O, Besson C, Gil-Izquierdo A, Lamaison J-L, *et al.* (2005). Anthocyanin metabolism in rats and their distribution to digestive area, kidney, and brain. *J. Agric. Food. Chem.* **53**(10)**:** 3902-3908.

Talavéra S, Felgines C, Texier O, Besson C, Lamaison JL, Remesy C (2003). Anthocyanins are efficiently absorbed from the stomach in anesthetized rats. *J Nutr* **133**(12)**:** 4178-4182.

Talavéra S, Felgines C, Texier O, Besson C, Manach C, Lamaison J-L, *et al.* (2004). Anthocyanins are efficiently absorbed from the small intestine in rats. *The Journal of Nutrition* **134**(9)**:** 2275-2279.

Tarozzi A, Morroni F, Hrelia S, Angeloni C, Marchesi A, Cantelli-Forti G, *et al.* (2007). Neuroprotective effects of anthocyanins and their in vivo metabolites in SH-SY5Y cells. *Neuroscience Letters* **424**(1)**:** 36-40.

Toromanović J, Kovač-Bešović E, Šapčanin A, Tahirović I, Rimpapa Z (2008). Urinary hippuric acid after ingestion of edible fruits. *Bosnian Journal of Basic Medical Sciences* **8**(1)**:** 38-43.

Tsuda T (2011). Dietary anthocyanin-rich plants: Biochemical basis and recent progress in health benefits studies. *Mol Nutr Food Res* **56**(1)**:** 159-170.

Tsuda T, Horio F, Osawa T (1999). Absorption and metabolism of cyanidin 3-O-beta-D-glucoside in rats. *FEBS Lett* **449**(2-3)**:** 179-182.

Valentova K, Stejskal D, Bednar P, Vostalova J, Cihalik C, Vecerova R, *et al.* (2007). Biosafety, antioxidant status, and metabolites in urine after consumption of dried cranberry juice in healthy women: a pilot double-blind placebo-controlled trial. *J. Agric. Food. Chem.* **55**(8)**:** 3217-3224.

Vauzour D, Vafeiadou K, Rodriguez-Mateos A, Rendeiro C, Spencer JP (2008). The neuroprotective potential of flavonoids: a multiplicity of effects. *Genes Nutr* **3**(3-4)**:** 115-126.

Veberic R, Jakopic J, Stampar F, Schmitzer V (2009). European elderberry (Sambucus nigra L.) rich in sugars, organic acids, anthocyanins and selected polyphenols. *Food Chemistry* **114**(2)**:** 511-515.

Vitaglione P, Donnarumma G, Napolitano A, Galvano F, Gallo A, Scalfi L, *et al.* (2007). Protocatechuic acid is the major human metabolite of cyanidin-glucosides. *J. Nutr.* **137**(9)**:** 2043-2048.

Walgren RA, Lin JT, Kinne RK, Walle T (2000). Cellular uptake of dietary flavonoid quercetin 4'-beta-glucoside by sodium-dependent glucose transporter SGLT1. *J Pharmacol Exp Ther* **294**(3)**:** 837-843.

Wallace TC (2011). Anthocyanins in cardiovascular disease. *Advances in Nutrition: An International Review Journal* **2**(1)**:** 1-7.

Walle T, Walle UK, Halushka PV (2001). Carbon dioxide is the major metabolite of quercetin in humans. *The Journal of Nutrition* **131**(10)**:** 2648-2652.

Wang D, Wei X, Yan X, Jin T, Ling W (2010). Protocatechuic acid, a metabolite of anthocyanins, inhibits monocyte adhesion and reduces atherosclerosis in apolipoprotein E-deficient mice. *J. Agric. Food. Chem.* **58**(24)**:** 12722-12728.

Wang D, Zou T, Yang Y, Yan X, Ling W (2011). Cyanidin-3-O-β-glucoside with the aid of its metabolite protocatechuic acid, reduces monocyte infiltration in apolipoprotein E-deficient mice. *Biochemical Pharmacology* **82**(7)**:** 713-719.

Wang Q, Xia M, Liu C, Guo H, Ye Q, Hu Y, *et al.* (2008). Cyanidin-3-O-β-glucoside inhibits iNOS and COX-2 expression by inducing liver X receptor alpha activation in THP-1 macrophages. *Life Sciences* **83**(5–6)**:** 176-184.

Wang Y, Ho CT (2009). Metabolism of flavonoids. *Forum Nutr* **61:** 64-74.

Weber J, Van Zanten A (1991). Interferences in current methods for measurements of creatinine. *Clinical chemistry* **37**(5)**:** 695-700.

Williams RJ, Spencer JPE, Rice-Evans C (2004). Flavonoids: antioxidants or signalling molecules? *Free Radical Biology and Medicine* **36**(7)**:** 838-849.

Williamson G, Clifford MN (2010). Colonic metabolites of berry polyphenols: the missing link to biological activity? *British Journal of Nutrition* **104**(S3)**:** S48-S66.

Williamson G, Manach C (2005). Bioavailability and bioefficacy of polyphenols in humans. II. Review of 93 intervention studies. *Am J Clin Nutr* **81**(1 Suppl)**:** 243S-255S.

Winter J, Moore L, Dowell V, Bokkenheuser V (1989). C-ring cleavage of flavonoids by human intestinal bacteria. *Applied and environmental microbiology* **55**(5)**:** 1203-1208.

Wittemer SM, Ploch M, Windeck T, Müller SC, Drewelow B, Derendorf H, *et al.* (2005). Bioavailability and pharmacokinetics of caffeoylquinic acids and flavonoids after oral administration of Artichoke leaf extracts in humans. *Phytomedicine* **12**(1–2)**:** 28-38.

Wolffram S, Block M, Ader P (2002). Quercetin-3-glucoside is transported by the glucose carrier SGLT1 across the brush border membrane of rat small intestine. *J Nutr* **132**(4)**:** 630-635.

Wong CC, Meinl W, Glatt H-R, Barron D, Stalmach A, Steiling H, *et al.* (2010). In vitro and in vivo conjugation of dietary hydroxycinnamic acids by UDP-glucuronosyltransferases and sulfotransferases in humans. *The Journal of Nutritional Biochemistry* **21**(11)**:** 1060-1068.

Woodward G, Kroon P, Cassidy A, Kay C (2009). Anthocyanin stability and recovery: Implications for the analysis of clinical and experimental samples. *J Agr Food Chem* **57**(12)**:** 5271-5278.

Woodward GM, Needs PW, Kay CD (2011). Anthocyanin derived phenolic acids form glucuronides following simulated gastrointestinal digestion and microsomal glucuronidation. *Mol Nutr Food Res* **55**(3)**:** 378-386.

Wu B, Basu S, Meng S, Wang X, Hu M (2011). Regioselective sulfation and glucuronidation of phenolics: Insights into the structural basis. *Current Drug Metabolism* **12**(9)**:** 900-916.

Wu X, Beecher GR, Holden JM, Haytowitz DB, Gebhardt SE, Prior RL (2006). Concentrations of anthocyanins in common foods in the United States and estimation of normal consumption. *J Agric Food Chem* **54**(11)**:** 4069-4075.

Wu X, Cao G, Prior RL (2002). Absorption and metabolism of anthocyanins in elderly women after consumption of elderberry or blueberry. *J. Nutr.* **132**(7)**:** 1865-1871.

Wu X, Gu L, Prior RL, McKay S (2004). Characterization of anthocyanins and proanthocyanidins in some cultivars of Ribes, Aronia, and Sambucus and their antioxidant capacity. *J Agric Food Chem* **52**(26)**:** 7846-7856.

Wu X, Pittman HE, Mckay S, Prior RL (2005). Aglycones and sugar moieties alter anthocyanin absorption and metabolism after berry consumption in weanling pigs. *The Journal of Nutrition* **135**(10)**:** 2417-2424.

Xia M, Ling W, Zhu H, Ma J, Wang Q, Hou M, *et al.* (2009). Anthocyanin attenuates CD40-mediated endothelial cell activation and apoptosis by inhibiting CD40-induced MAPK activation. *Atherosclerosis* **202**(1)**:** 41-47.

Xu J-W, Ikeda K, Yamori Y (2004a). Cyanidin-3-glucoside regulates phosphorylation of endothelial nitric oxide synthase. *FEBS Letters* **574**(1-3)**:** 176-180.

Xu J-W, Ikeda K, Yamori Y (2004b). Upregulation of enndothelial nitric oxide synthase by cyanidin-3-glucoside, a typical anthocyanin pigment. *Hypertension* **44**(2)**:** 217-222.

Yang J, Meyers KJ, van der Heide J, Liu RH (2004). Varietal differences in phenolic content and antioxidant and antiproliferative activities of onions. *Journal of Agricultural and Food Chemistry* **52**(22)**:** 6787-6793.

Yokozawa T, Chen CP, Dong E, Tanaka T, Nonaka G-I, Nishioka I (1998). Study on the inhibitory effect of tannins and flavonoids against the 1,1-diphenyl-2-picrylhydrazyl radical. *Biochemical Pharmacology* **56**(2)**:** 213-222.

Youdim KA, Martin A, Joseph JA (2000). Incorporation of the elderberry anthocyanins by endothelial cells increases protection against oxidative stress. *Free Radical Biology and Medicine* **29**(1)**:** 51-60.

Zamora-Ros R, Andres-Lacueva C, Lamuela-Raventos RM, Berenguer T, Jakszyn P, Barricarte A, *et al.* (2010). Estimation of dietary sources and flavonoid intake in a Spanish adult population (EPIC-Spain). *J Am Diet Assoc* **110**(3)**:** 390-398.

Zhang K, Zuo Y (2004). GC-MS determination of flavonoids and phenolic and benzoic acids in human plasma after consumption of cranberry juice. *J. Agric. Food. Chem.* **52**(2)**:** 222-227.

Zhang L, Zuo Z, Lin G (2007). Intestinal and hepatic glucuronidation of flavonoids. *Molecular Pharmaceutics* **4**(6)**:** 833-845.

Zhang Q, Botting NP, Kay CD (2011). A gram scale synthesis of a multi-13C-labelled anthocyanin, [6,8,10,3[prime or minute],5[prime or minute]-13C5]cyanidin-3-glucoside, for use in oral tracer studies in humans. *Chemical Communications* **47**(38)**:** 10596-10598.

Zhang Q, Raheem KS, Botting NP, Slawin AMZ, Kay CD, O'Hagan D (2012). Flavonoid metabolism: the synthesis of phenolic glucuronides and sulfates as candidate metabolites for bioactivity studies of dietary flavonoids. *Tetrahedron* **68**(22)**:** 4194-4201.

Zhang Y, Huo M, Zhou J, Xie S (2010). PKSolver: An add-in program for pharmacokinetic and pharmacodynamic data analysis in Microsoft Excel. *Computer Methods and Programs in Biomedicine* **99**(3)**:** 306-314.

Zhou-Stache J, Buettner R, Artmann G, Mittermayer C, Bosserhoff A (2002). Inhibition of TNF-α induced cell death in human umbilical vein endothelial cells and Jurkat cells by protocatechuic acid. *Medical and Biological Engineering and Computing* **40**(6)**:** 698-703.

Zhu Y, Ling W, Guo H, Song F, Ye Q, Zou T, *et al.* (2013). Anti-inflammatory effect of purified dietary anthocyanin in adults with hypercholesterolemia: A randomized controlled trial. *Nutrition, Metabolism and Cardiovascular Diseases* **23**(9)**:** 843-849.

Zhu Y, Xia M, Yang Y, Liu F, Li Z, Hao Y, *et al.* (2011). Purified anthocyanin supplementation improves endothelial function via NO-cGMP activation in hypercholesterolemic individuals. *Clin Chem* **57**(11)**:** 1524-1533.

# Appendix 1. Food exclusion list and suggested alternatives for $^{13}$C-cyanidin-3-glucoside intervention study.

For 7 days preceding the study day:

| Food to Exclude from the Diet | Foods to Limit (*Refer to note regarding amount of foods permitted) | Suggested alternatives (Unlimited intake) |
|---|---|---|
| **FRUITS** | | |
| **Blueberries**<br>**Blackcurrant**<br>**Bilberry**<br>**Redcurrant**<br>**Elderberry**<br>**Chokeberry**<br>**Blackberry**<br>**Raspberry**<br>**Cherry**<br>**Strawberry**<br>**Cranberry**<br>**Pomegranate**<br>**Red/purple/blue grape**<br>**Plum**<br>**Red or blood orange** | **Gooseberries**<br>**Orange**<br>**Red apples** | **Banana**<br>**Kiwi**<br>**Green apples**<br>**Grapefruit**<br>**Pear**<br>**Avocado**<br>**Melon**<br>**Pineapple**<br>**Apricots**<br>**Lemon**<br>**Clementine**<br>**Melon**<br>**Green grapes** |
| **VEGETABLES** | | |
| **Aubergine/Eggplant**<br>**Red onion**<br>**Red cabbage**<br>**Red/purple potato**<br>**Purple carrots** | **Black bean**<br>**Purple basil**<br>**Purple corn**<br>**Olives** | **White onion**<br>**Green / white cabbage**<br>**Broccoli**<br>**Carrots**<br>**Courgette** |
| **BEVERAGES** | | |
| **Juices derived from any above listed berries, fruits or vegetables**<br><br>**Red wine**<br>**Port**<br>**Sherry** | **Tea (green or black)**<br>**Coffee**<br>*Ideally, no more than a combined total of 2 drinks a day of tea and coffee.*<br>**Alcohol**<br>*-Ideally, no more than a combined total of 10 units per week of alcohol.* | **Fruit juices derived from non-berry sources e.g. Green apple juice etc.**<br>**White wine**<br><br>**Milk**<br>**Water**<br>**Carbonated drinks e.g. Coca-cola, Sprite** |
| **OTHER** | | |
| **Jams, sauces or dessert toppings derived from any above listed berries or fruits**<br>**Cheesecakes or desserts made from any above listed berries or fruits** | **Purple corn tortillas or crisps**<br>**Peanut skins**<br>**Rhubarb** | **Non-berry derived desserts, ice-creams and crisps** |

*Consume no more than a combined intake of 10 portions per week from the foods (berries, fruits, vegetables, and other) identified in the "FOODS TO LIMIT" category.
** If a rare food source in not on the list and you are not sure if you can eat it, a good rule of thumb is, "if it's red or blue, then it's not for you".